

IAEA-TECDOC-1401

# *Quantifying uncertainty in nuclear analytical measurements*



**IAEA**

International Atomic Energy Agency

July 2004

IAEA-TECDOC-1401

***Quantifying uncertainty in  
nuclear analytical measurements***



**IAEA**

International Atomic Energy Agency

July 2004

The originating Section of this publication in the IAEA was:

Agency's Laboratories, Seibersdorf  
International Atomic Energy Agency  
Wagramer Strasse 5  
P.O. Box 100  
A-1400 Vienna, Austria

QUANTIFYING UNCERTAINTY IN NUCLEAR ANALYTICAL MEASUREMENTS

IAEA, VIENNA, 2004  
IAEA-TECDOC-1401  
ISBN 92-0-108404-8  
ISSN 1011-4289

© IAEA, 2004

Printed by the IAEA in Austria  
July 2004

## FOREWORD

The lack of international consensus on the expression of uncertainty in measurements was recognised by the late 1970s and led, after the issuance of a series of rather generic recommendations, to the publication of a general publication, known as GUM, the Guide to the Expression of Uncertainty in Measurement. This publication, issued in 1993, was based on co-operation over several years by the Bureau International des Poids et Mesures, the International Electrotechnical Commission, the International Federation of Clinical Chemistry, the International Organization for Standardization (ISO), the International Union of Pure and Applied Chemistry, the International Union of Pure and Applied Physics and the Organisation internationale de métrologie légale. The purpose was to promote full information on how uncertainty statements are arrived at and to provide a basis for harmonized reporting and the international comparison of measurement results. The need to provide more specific guidance to different measurement disciplines was soon recognized and the field of analytical chemistry was addressed by EURACHEM in 1995 in the first edition of a guidance report on Quantifying Uncertainty in Analytical Measurements, produced by a group of experts from the field. That publication translated the general concepts of the GUM into specific applications for analytical laboratories and illustrated the principles with a series of selected examples as a didactic tool. Based on feedback from the actual practice, the EURACHEM publication was extensively reviewed in 1997–1999 under the auspices of the Co-operation on International Traceability in Analytical Chemistry (CITAC), and a second edition was published in 2000. Still, except for a single example on the measurement of radioactivity in GUM, the field of nuclear and radiochemical measurements was not covered. The explicit requirement of ISO standard 17025:1999, General Requirements for the Competence of Testing and Calibration Laboratories to quantify the uncertainty of measurement results, and the fact that this standard is used as a basis for the development and implementation of quality management systems in many laboratories performing nuclear analytical measurements, triggered the demand for specific guidance to cover uncertainty issues of nuclear analytical methods. The demand was recognized by the IAEA and a series of examples was worked out by a group of consultants in 1998. The diversity and complexity of the topics addressed delayed the publication of a technical guidance report, but the exchange of views among the experts was also beneficial and led to numerous improvements and additions with respect to the initial version.

This publication is intended to assist scientists using nuclear analytical methods in assessing and quantifying the sources of uncertainty of their measurements. The numerous examples provide a tool for applying the principles elaborated in the GUM and EURACHEM/CITAC publications to their specific fields of interest and for complying with the requirements of current quality management standards for testing and calibration laboratories. It also provides a means for the worldwide harmonization of approaches to uncertainty quantification and thereby contributes to enhanced comparability and competitiveness of nuclear analytical measurements.

The IAEA wishes to thank all the experts for their valuable contributions to the examples and the members of the EURACHEM/CITAC Working Group on Uncertainty in Chemical Measurement for their advice, input and recommendations as well as copyright release.

The IAEA officers responsible for this publication were R. Parr of the Division of Human Health, P. Povinec of the IAEA Marine Environment Laboratory in Monaco, and A. Fajgelj and P. De Regge of the Agency's Laboratories, Seibersdorf.

## *EDITORIAL NOTE*

*This publication has been prepared from the original material as submitted by the authors. The views expressed do not necessarily reflect those of the IAEA, the governments of the nominating Member States or the nominating organizations.*

*The use of particular designations of countries or territories does not imply any judgement by the publisher, the IAEA, as to the legal status of such countries or territories, of their authorities and institutions or of the delimitation of their boundaries.*

*The mention of names of specific companies or products (whether or not indicated as registered) does not imply any intention to infringe proprietary rights, nor should it be construed as an endorsement or recommendation on the part of the IAEA.*

*The authors are responsible for having obtained the necessary permission for the IAEA to reproduce, translate or use material from sources already protected by copyrights.*

## CONTENTS

SUMMARY .....	1
PAPERS ON QUANTIFYING UNCERTAINTY FOR SPECIFIC NUCLEAR ANALYTICAL METHODS	
Uncertainty in measurements close to detection limits: Detection and quantification capabilities .....	9
<i>L.A. Currie</i>	
XRF analysis of intermediate thickness samples .....	35
<i>A. Markowicz, N. Haselberger</i>	
EDXRF analysis of thin samples .....	45
<i>A. Tajani, A. Markowicz</i>	
EDXRF analysis of thick samples.....	53
<i>A. Tajani, A. Markowicz</i>	
PIXE analysis of aluminium in fine atmospheric aerosol particles collected on nuclepore polycarbonate filter.....	63
<i>W. Maenhaut</i>	
Uncertainty evaluation in instrumental and radio-chemical neutron activation analysis.....	77
<i>J. Kucera, P. Bode, V. Stepanek</i>	
Quantification of uncertainty in gamma-spectrometric analysis of environmental samples .....	103
<i>C. Dovlete, P.P. Povinec</i>	
Alpha-spectrometric analysis of environmental samples.....	127
<i>G. Kanisch</i>	
Alpha-spectrometric analysis of environmental samples — Spreadsheet approach.....	141
<i>L. Holmes</i>	
Determination of strontium-89 and strontium-90 in soils and sediments .....	149
<i>H. Janszen</i>	
Radiochemical determination of strontium-90 in environmental samples by liquid scintillation counting.....	167
<i>J. Moreno, N. Vajda, K. Burns, P.R. Danesi, P. De Regge, A. Fajgelj</i>	
Tritium assay in water samples using electrolytic enrichment and liquid scintillation spectrometry .....	195
<i>K. Rozanski, M. Gröning</i>	
Carbon-14 assay in water samples using benzene synthesis and liquid scintillation spectrometry .....	219
<i>K. Rozanski, M. Gröning</i>	
Determination of isotopic content and concentration of uranium by mass spectrometry .....	229
<i>A. Vian</i>	
LIST OF PARTICIPANTS .....	247

## SUMMARY

### 1. INTRODUCTION

#### 1.1. Background and scope

The confidence that can be attached to a measurement result and the degree to which the result is expected to agree with other results is provided by the measurement uncertainty. In 1993 the International Standardisation Organisation (ISO) published in collaboration with the Bureau International des Poids et Mesures (BIPM), the International Electrochemical Commission (IEC), the International Federation of Clinical Chemistry (IFCC), the International Union of Pure and Applied Chemistry (IUPAC), the International Union of Pure and Applied Physics (IUPAP) and the International Organisation of Legal Metrology (OIML), the “Guide to the Expression of Uncertainty in Measurement” (GUM) [1], establishes general rules for evaluating and expressing uncertainty across a broad spectrum of measurements. The application of the principles elaborated in the guide to quantitative analytical chemistry and the identification and quantification of uncertainty components in this field is a fairly complex issue, even for simple analytical procedures. A specific guide on “Quantifying Uncertainty in Analytical Measurement” was therefore published in 1995 by EURACHEM [2]. The report is based on the GUM and provides the theory, nomenclature and some practical examples of uncertainty evaluation in chemical analytical measurements. However, the examples given, cover only a few analytical techniques selected for the purpose of the publication. In the case of nuclear and nuclear-related analytical techniques, involving complex instrumentation, elaborated procedures and non-linear correction factors for the build up and decay of radionuclides, the process of identifying, quantifying and combining uncertainty components has to address the specific nature and variety of those uncertainty sources.

Within its mandate, the International Atomic Energy Agency is providing laboratories in its Member States with equipment, training and guidance on the use of nuclear analytical techniques. Through different programmes, for example the Analytical Quality Control Services, the IAEA is also assisting them to obtain analytical results of acceptable quality. It was realised that a guidance publication including practical examples is needed to assist laboratories in the identification and quantification of the uncertainty components in nuclear and related analytical measurements they perform. In co-operation with EURACHEM, the IAEA therefore invited a group of experts in the field in order to prepare and compile worked examples dedicated to illustrate the quantification of uncertainty components for the most common nuclear and nuclear related analytical methods. The examples were presented and discussed at a meeting in May 1998 and further refined and harmonized. The report of the consultants’ meeting, including a glossary of definitions is provided in the Annex. The current publication benefits from the revision of the EURACHEM guide, published in 2000 [3].

#### 1.2. Specific uncertainty features of nuclear analytical techniques

The term “nuclear analytical techniques” refers to techniques that provide the qualitative or quantitative determination of an element on the basis of characteristics and properties of the atomic nucleus. Actually, the application of nuclear techniques involves the measurement of isotopes rather than elements. The isotopes can be stable or radioactive and the radioactivity can be natural or induced. According to the above definition, the following analytical techniques are considered as nuclear techniques: mass spectrometry, ion beam analysis, nuclear magnetic resonance spectrometry, Mössbauer spectrometry, neutron scattering and diffraction, neutron activation analysis, isotopic dilution analysis, stable isotope and radiotracer studies, and direct radioactivity determinations [4]. Many of the nuclear analytical

techniques require an appropriate irradiation, either by particles or high energy electromagnetic radiation, and their use is therefore dependent on the availability of nuclear facilities (nuclear reactors, radioactive sources, accelerators, etc.)

Nuclear analytical techniques are in general independent of the chemical state of the element determined and therefore cannot be directly applied for the determination of chemical species. This represents a basic difference of nuclear analytical techniques in comparison to other analytical techniques, where in most cases the detection or determination is based on characteristics related to electron transitions (electric charge, oxidation state, stoichiometry, low energy electromagnetic radiation, etc.). Nuclear analytical techniques on the other hand are often very sensitive and specific and, because of the penetrating power of nuclear radiation, also nondestructive. A specific advantage is further that radioactive or stable isotopes different to the isotope of interest can be used as tracers to determine recovery factors or chemical yield. The uncertainty component associated to the recovery factor will then include a contribution from the quantity of tracer added and a contribution from the measurement of a ratio. Depending on the technique, either the ratio of the final to initial quantities of the tracer isotope, or the ratio of the tracer to the analysed isotope might provide the best accuracy. Nuclear analytical techniques in general are to be considered as relative rather than absolute analytical techniques. The measurement procedures therefore require calibration by appropriate calibration standards and the results should always be validated to be reliable and comparable. The uncertainty component associated with the calibration will therefore in most cases include an uncertainty contribution from the reference materials and an uncertainty contribution from the calibration line fitting or the scaling factor.

Data acquisition in nuclear analytical techniques frequently relies on the accumulation of counts resulting from a decay process from a higher energy level to a lower energy level by the emission of particles and/or radiation. Those processes are characterised by a Poisson distribution and therefore the uncertainty associated with those processes can be readily derived from the standard deviation of the Poisson distribution, thereby avoiding the need for sometimes tedious and lengthy repetitions of the measurements. This is a typical feature of the quantification of uncertainty in nuclear analytical techniques. For a sufficiently large number of counts the normal distribution can be used as a good approximation of the Poisson distribution. On the other hand, the observation of repetition data failing to comply with the expected distribution might provide an indication that the measurements are not under statistical control and that additional sources of uncertainty might be present and have to be taken into account.

Because of the radioactive decay, the measured quantities are not constant in time and useful information can only be extracted from the data when appropriate corrections for decay are applied. The correction factors for decay – and for build-up of the decay products, which sometimes are the measured quantities – are typically exponential functions of a single or several decay constants and time. The decay constant, governing the decay process, is a measured physical quantity and therefore subject to uncertainty and so is the measurement of time. The quantification of uncertainty in nuclear analytical techniques will therefore frequently involve non-linear components, whose contribution is not constant, but is a function of the time intervals between the different steps in the analytical procedure. This characteristic feature of nuclear analytical techniques might introduce a lot of complexity in the quantification of uncertainty, but on the other hand provides an opportunity for minimisation of the uncertainty by an adequate scaling of the time intervals.

The interaction of radiation, either particulate or electromagnetic, with matter is also a non-linear process and, therefore, the efficiency of nuclear radiation detectors is seldom described by a simple function. In general, the uncertainty component associated with the response of a detection device in nuclear analytical techniques will be composed of a contribution from the standards used for the calibration, a contribution from the curve fitting process and a contribution from the model used to describe the response function. In this respect the nuclear analytical techniques are quite similar to energy dispersive X ray techniques, where the induced radiation, although resulting from inner shell electron transitions rather than from the nucleus, is detected and measured by very similar detectors and data accumulation systems as used for gamma radiation. Energy dispersive X ray techniques have been promoted by the IAEA as a sensitive and selective technique for trace element analysis and more than one hundred laboratories world wide have been equipped and trained in this measurement technique with assistance of the IAEA. As no current guide provides examples on the quantification of uncertainty components for energy dispersive X ray techniques, it was felt useful to include them in the scope of this IAEA guide.

Radiation detection devices and associated electronics, although being very fast as a result of modern technologies, still might show saturation effects and dead-time at high count rates induced by high intensity radiation. The saturation and the dead-time effects are usually compensated by electronic circuitry or by counting clock pulses in parallel, but the compensation will still leave some uncertainty, which has to be accounted for in the evaluation.

Nuclear analytical techniques involve irradiation devices, such as nuclear reactors, accelerators, or radioactive sources, to induce the activated or excited states in the target material. They are complex devices, usually equipped with protective shielding and remotely operated components. Because of this complexity, reproducibility of the radiation field intensity, as well as its spectral and spatial distributions is not readily achieved and will introduce an uncertainty component to be accounted for in the overall evaluation.

The examples provided are an illustration of the general principles of GUM and the EURACHEM Guide [3] applied to nuclear and related analytical techniques and are typical for the measurement conditions and procedures of the laboratory of the author of the respective example. The examples are not intended and should not be used to define a generic uncertainty associated with a particular technique or measurement. The quantification and combination of uncertainty sources in an individual laboratory situation should be the result of a specific evaluation process, where the examples provided are used as guidance. In spite of considerable efforts to harmonise the examples, this compilation of examples from different authors still displays a certain variety in the conceptual and mathematical approach of the quantification of the uncertainties, and in the depth and detail of the mathematical derivations. Nevertheless it is felt that sufficient harmonisation and consistency with the GUM[1] and EURACHEM[3] guides has been achieved to provide useful guidance for the correct assessment and quantification of uncertainties in commonly used nuclear analytical techniques.

### **1.3. Approach and structure of the specific guidance**

The preparation of the specific guidance closely follows the approach and structure as suggested by the EURACHEM Guide [3] and is given in Figure 1. Each example starts with an introduction setting the background and framing the field of application of the nuclear analytical technique.

The second section provides the specification of the measurand, the measurement procedure and its various boundary conditions. It includes the equation(s) relating the measurand to the different input parameters. Uncertainties introduced by field sampling are not taken into account and the analytical process starts with the “sample as received”. The traceability chain to the unit in which the measurement result is reported has to be clearly described.

In the third section, the sources of uncertainty are identified and grouped with the help of a cause-and-effect (Ishikawa or fishbone) diagram. All potential sources of uncertainty are listed although they will not necessarily all be taken into account in the calculation of the combined uncertainty. However, when a potential source of uncertainty is identified but not further quantified, objective justification for neglecting this source is provided. The cause-and-effect diagram is an effective tool for identifying potential correlation between sources of uncertainty. Nevertheless, the effect of correlation has only been evaluated and quantified in very few cases and it usually turns out to have a negligible effect on the combined uncertainty. The combined uncertainty decreases in most cases when correlation is taken into account, but considerably augments the complexity of the calculations. A more conservative approach of neglecting the correlations altogether is preferred, bearing in mind essentially the didactic objective of the guide and its aim to promote the principles of uncertainty quantification.

The following section proceeds with the quantification of the uncertainty components according to the basic ways recommended in the EURACHEM Guide (dedicated measurements, suppliers data, quality control data, collaborative effort, expert judgment, etc.). Taking into account the source of the quantified uncertainty and its probability distribution, the uncertainties are converted to standard uncertainties and combined in the last section. In parallel with the uncertainty treatment, all examples also provide numerical values for the measured parameters and the calculation of the final result. The example is further documented by adding one or more summary tables listing the following items:

- (a) the description of the parameter whose uncertainty is being quantified, its symbol used in the equation and, where necessary, a reference to the detailed descriptive list;
- (b) the numerical value and the metrical unit of the parameter;
- (c) the uncertainty associated with the value of the parameter;
- (d) the conversion factor linking the uncertainty to the standard uncertainty;
- (e) the standard uncertainty  $u$ ;
- (f) the sensitivity factor;
- (g) the partial contribution of the parameter's uncertainty to the combined total uncertainty, expressed as a percentage.

The tables are intended to provide a summary of the worked examples and details of the calculation of the final combined uncertainty. Whereas the content of the items (a), (b) and (c) is self-explanatory, the other items might need some clarification.

According to the principles discussed in GUM [1], the combined uncertainty is obtained from the square root of the sum of the squares of the products of the standard uncertainties multiplied by their respective sensitivity factors. It is, therefore, necessary to derive the

standard uncertainties from the individual uncertainties associated with the different parameters. From the definition of those uncertainties and the assumptions made for the probability distribution within the uncertainty interval, a conversion factor is obtained, relating the stated uncertainty to the standard uncertainty  $u$ . Further, according to GUM [1], the sensitivity factor of a parameter is the partial derivative of the equation relating the measurand to the parameters with respect to that parameter. The sensitivity factor is an essential step in the calculation, but does not provide a good insight into the propagation of the parameter's uncertainty into the combined uncertainty, because it has to be multiplied by the uncertainty itself and squared to obtain the parameter partial contribution. The latter, expressed as a percentage of the sum of all partial contributions, is a much better indicator of the parameter's effect on the total uncertainty. The percentage clearly shows to which parameters efforts should be directed first in order to reduce the uncertainty associated with the measurement result.

Due to the nature of nuclear measurements, i.e. presence of background, and the fact that nuclear analytical techniques are often applied to measuring low activity samples, e.g. environmental radioactivity monitoring, the uncertainty quantification for the results close to detection limit requires special attention. This issue is covered in Part II, The Specific Guidance, under “Uncertainty in Measurements Close to Detection Limits”.

Twelve worked examples for nuclear and related analytical techniques have been prepared by experts in the field following the principles of the EURACHEM Guide [2] and the format as given in section 1.3

Some examples are further illustrated by an alternative approach using the spreadsheet method [5].

## REFERENCES

- [1] INTERNATIONAL ORGANISATION FOR STANDARDISATION, “Guide to the Expression of Uncertainty in Measurement”, First Edition, Geneva (1993).
- [2] EURACHEM, “Quantifying Uncertainty in Analytical Measurement”, First Edition, Editor: Laboratory of the Government Chemist Information Services, Teddington (Middlesex) & London (1995). ISBN 0-948926-08-2.
- [3] ELLISON, S.L.R., ROSSLEIN, M., WILLIAMS, A., BERGLUND, M., HAESSELBARTH, W., HEDEGAARD, K., KARLS, R., MANSSON, M., STEPHANY, R., VAN DER VEEN, A., WEGSCHEIDER, W., VAN DE WIEL, H., WOOD, R., PAN XIU RONG, SALIT, M., SQUIRRELL, A., YUSUSDA, K., JOHNSON, R., JUNG-KEUN LEE, MOWREY, M., DE REGGE, P., FAJGELJ, A., GALSWORTHY, D., EURACHEM/CITAC Guide “Quantifying Uncertainty in Analytical Measurement”, Second Edition, Editors: S. L. R. Ellison, M. Rosslein, A Williams, (2000), ISBN 0-948926-15-5.
- [4] DE GOEIJ, J.J., BODE, P., “Nuclear Analytical Techniques: Strong and Weak Points, Threats and Opportunities”, Int. Symp. on Harmonisation of Health Related Environmental Measurements Using Nuclear and Isotopic Techniques, Hyderabad, India, 4-7 November (1996).
- [5] KRAGTEN, J., Calculating Standard Deviations and Confidence Intervals with a Universally Applicable Spreadsheet Technique, *Analyst*, Vol. 119 (1994) 2161-2165.

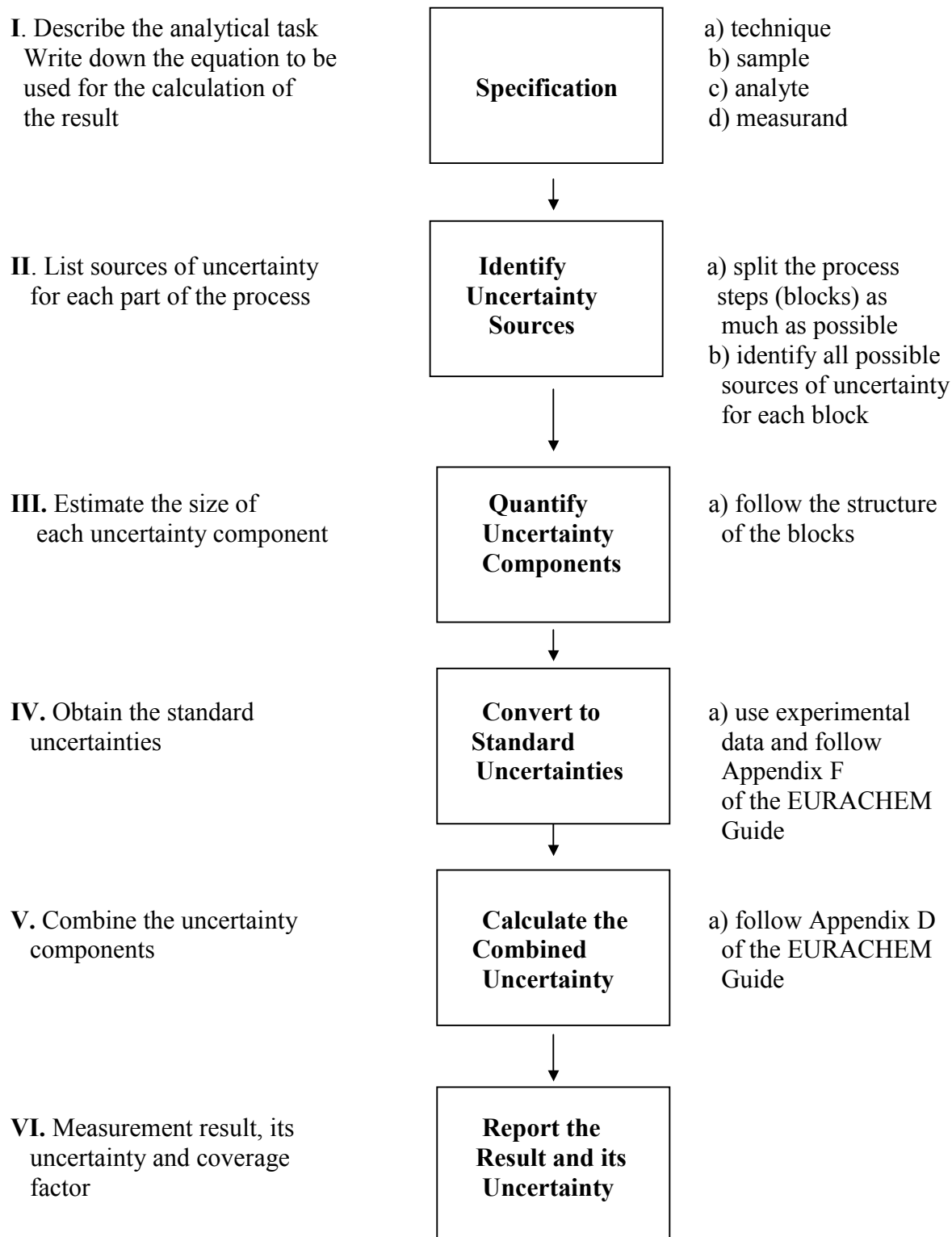


*FIG. 1. Approach and structure of the worked examples nuclear and related analytical techniques in the IAEA Guide.*

**PAPERS ON QUANTIFYING UNCERTAINTY FOR SPECIFIC  
NUCLEAR ANALYTICAL METHODS**

# UNCERTAINTY IN MEASUREMENTS CLOSE TO DETECTION LIMITS: DETECTION AND QUANTIFICATION CAPABILITIES

L.A. CURRIE

National Institute of Standards and Technology, Gaithersburg, United States of America

## Abstract

The contribution is divided into two parts. First the theoretical part of the “close to detection limit” issue is discussed. An overview is given over the basic concepts and nomenclature related to the limits of the analytical measurement process: detection decision (critical value), detection limit (minimum detectable value) and quantification limit (minimum quantifiable value). Terms and definitions used reflect the latest IUPAC and ISO recommendations regarding the detection and quantification capabilities as fundamental performance characteristics of the analytical measurement process. Statistical features of the measured signal obtained in nuclear measurements are discussed in detail in this part covering the Poisson and normal distribution and the determination of the standard deviation  $\sigma_0$  or its estimate  $s_0$ . Also the role of the blank is extensively discussed. Three types of blank are identified: instrumental background, which is obtained in the absence of the analyte; the spectrum baseline, which is the sum of the instrumental background and any signal due to interfering species observed in the region of interest for the analyte; and finally the blank which arises from contamination from reagents, sampling procedure, or sample preparation steps, introducing unwanted quantities of the very analyte being sought. It is recommended that, regarding the reporting of low-level data, “Experimental results should not be censored, and should always include quantitative estimates of uncertainty. When the result is indistinguishable from the blank, based on comparison of the result ( $\hat{L}$ ) with the critical value ( $L_C$ ), then it is important also to appropriately indicate that fact. Such a result should not be interpreted as “zero” and should also not be reported without the accompanying uncertainty. The second part elaborates on two examples dealing with low-level counting of  $^{39}\text{Ar}$  and peak detection in gamma ray spectrometry. Both examples are supported with real measurement data.

## 1. INTRODUCTORY REMARKS

*Uncertainty* in measurement results (MR) and *detection and quantification limits* for the measurement process (MP) are intimately linked through the error structure of the latter. Knowledge of the detailed organization of the MP and its error components is as essential for the assessment of its detection and quantification performance characteristics as it is to derive meaningful uncertainty estimates for results of the MP. The MP-MR dichotomy is especially prominent in the case of “low-level” measurements -- i.e., those close to detection limits. Here, one faces the matter of making *detection decisions*, based on a *critical level*, which itself is an inherent part of the detection capability paradigm, where in addition to the “detected”/“not detected” decision, it is still essential to provide an estimated value and uncertainty for the measured quantity.

Although it has been stated that “the approach of reporting results of chemical measurements together with measurement uncertainty is relatively new” [1], already 35 years ago that was policy for *all* measurements at the National Bureau of Standards (NBS), precursor of the National Institute of Standards and Technology (NIST). Quoting Churchill Eisenhart in NBS Handbook 91 [2], “A certified or reported value whose accuracy is entirely unknown is worthless.” Recognition of the importance of detection capabilities in chemical metrology took place also quite early in this Century. In the very first volume of *Mikrochemie* 75 years ago, Fritz Feigl of the University of Vienna proposed a system for quantifying this capability as the *Erfassungsgrenze* [3]. Meanwhile we have enjoyed several decades of miscommunication and confusion, as chemists employed different terminology in connection with the same concept, and similar terminology for quite different concepts — representing a special sort of “errors of the first and second kinds”!

Just as the uncertainty efforts of the International Organization for Standardization (ISO) offered a resolution to the diverse approaches to measurement uncertainty [4], the detection capability harmonization efforts of ISO and IUPAC offered a resolution to the long standing conceptual and communication problems surrounding detection and quantification capabilities. The need for a harmonized international position was recognized in 1993, when members of IUPAC and ISO met, with the objective of developing such a position from documents then in draft stage. These efforts culminated in 1995, with the publication of IUPAC Recommendations for the international chemical community [5], and the preparation of an ISO document for metrology in general [6]. While not identical, the documents are based on the same fundamental concepts, and compatible formulations and terminology. In the following text, we present these concepts, together with their application to chemical metrology as developed in the IUPAC document. A brief review of the relevant history of the topic, and discussions of critical approaches and open questions in the application of the basic concepts which follow are drawn, in part, from Currie [7,8]. The literature cited in the foregoing references provides detailed information on the statistical and chemical aspects of the topic.

The final portion of this text consists of an overview of specific applications plus detailed numerical examples. Here, a second critical link between uncertainty and detection/quantification limits becomes apparent: that is, uncertainty of the limits, themselves. Like all parameters in scientific metrology, those characterizing detection/quantification measurement capabilities can only be estimated, where the estimates perforce must be characterized by uncertainties.

## 2. BASIC CONCEPTS AND NOMENCLATURE

### 2.1. A very brief history

Early papers on chemical detection limits were published by Kaiser [9] and Currie [10]. In the latter, which treated the hypothesis testing approach to detection decisions and limits in chemistry, it was shown that the then current meanings attached to the expression "detection limit" led to numerical values that spanned three orders of magnitude, when applied to the *same* specific measurement process. Differing concepts are but one side of the problem. A review of the history of detection and quantification limits in chemistry published in 1988 [7] gives a partial compilation of terms, all referring to the same, detection limit concept -- ranging from "Identification Limit" to "Limiting Detectable Concentration" to "Limit of Guarantee for Purity," for example. Perhaps the most serious terminological trap has been the use of the expression "detection limit" (a) by some to indicate the critical value ( $L_C$ ) of the estimated amount or concentration above which the decision "detected" is made; but (b) by others, to indicate the inherent "true" detection capability ( $L_D$ ) of the measurement process in question. The first, "signal/noise" school, explicitly recognizes only the false positive ( $\alpha$ , Type-1 error), which in effect makes the probability of the false negative ( $\beta$ , Type-2 error) equal to 50%. The second, "hypothesis testing" school employs independent values for  $\alpha$  and  $\beta$ , commonly each equal to 0.05 or perhaps 0.01. In the most extreme case, the same numerical value of the "detection limit" is employed, e.g.,  $3.3\sigma_o$ , where  $\sigma_o$  is the standard deviation of the estimated net signal ( $\hat{S}$ ) when its true value ( $S$ ) is zero. The ratio  $\beta/\alpha$  for the first (single/noise) group, assuming normality, is thus 0.50/0.0005 or one thousand, far in excess of the unit ratio of the second group!<sup>2</sup>

Unfortunately, many are unaware of the above subtle differences in concepts and terminology, or of the care and attention to assumptions required for calculating meaningful

detection limits; but these become manifest when difficult, low-level laboratory intercomparisons are made. By way of illustration, in the International Atomic Energy Agency's interlaboratory comparison of arsenic in horse kidney ( $\mu\text{g/g}$  level), several laboratories failed to detect the As, yet their reported "detection limits" lay far below quantitative results reported by others; and the range of reported values spanned nearly five orders of magnitude [11].

*Stimuli for the recent IUPAC<sup>1</sup> and ISO efforts.* Early guidance on detection limits, strongly influenced by the work of Kaiser, was given by IUPAC. Resulting "official" recommendations appeared in the early editions of the *Compendium of Analytical Nomenclature*, where the "limit of detection ... is derived from the smallest measure that can be detected with reasonable certainty for a given analytical procedure." This quantity was then related to a multiple  $k$  of the standard deviation of the blank "according to the confidence level desired," with the general recommendation of  $k = 3$ . Hypothesis testing was not mentioned, nor was the issue of false negatives, nor the quantification limit [12]. Deficiencies in the "IUPAC definition" have been recognized by many [13], and are responsible, in part, for the new IUPAC effort [5]. The IUPAC Recommendations of 1995 for detection and quantification capabilities now constitute the "new IUPAC definition"; discussion of these fundamental performance characteristics forms much of the substance of chapter 18 of the latest (3rd) edition of the IUPAC *Compendium of Analytical Nomenclature*, which has just been published [14].

A second important factor in the new IUPAC effort to develop a proper treatment of both detection and quantification limits, and a parallel effort by ISO, were formal requests by CODEX<sup>3</sup> in 1990 to each of the organizations for guidance on the terms "Limit of Detection" and "Limit of Determination," because of the urgency of endorsing methods of analysis based on their capabilities to reliably measure essential and toxic elements in foods -- a problem that CODEX had been attempting to resolve since 1982.

## 2.2. Summary of the 1995 international recommendations

Detection and Quantification capabilities are considered by IUPAC as fundamental performance characteristics of the Chemical Measurement Process (CMP). As such, they require a fully defined, and controlled measurement process, taking into account such matters as types and levels of interference, and even the data reduction algorithm. Perhaps the most important purposes of these performance characteristics is for planning — ie, for the selection or development of CMPs to meet a specific scientific or regulatory need. In the new IUPAC and ISO documents, detection limits (minimum detectable amounts) are derived from the theory of hypothesis testing and the probabilities of false positives  $\alpha$ , and false negatives  $\beta$  [5,6]. Quantification limits [5] are defined in terms of a specified value for the relative standard deviation (RSD). Default values for  $\alpha$  and  $\beta$  are 0.05, each; and the default RSD for Quantification is taken as 10%.

As CMP Performance Characteristics, both Detection and Quantification Limits are associated with underlying *true values* of the quantity of interest; they are *not* associated with any particular outcome or result. The *detection decision*, on the other hand, is result-specific. It is made by comparing the experimental result with the Critical Value, which is the minimum significant *estimated value* of the quantity of interest. For presentation of the defining relations,  $L$  is used as the generic symbol for the quantity of interest. This is replaced by  $S$  when treating net analyte signals; and  $x$ , when treating analyte concentrations or amounts. The symbol  $A$  is used by IUPAC to represent the Sensitivity, or slope of the

calibration curve; it is noted that  $A$  is not necessarily independent of  $x$ , nor even a simple function of  $x$ . Subscripts  $C$ ,  $D$ , and  $Q$  are used to denote the Critical Value, Detection Limit, and Quantification Limit, respectively.

### 2.2.1. Defining relations

The basic concepts are given as mathematical expression below. Each case requires parameter specification:  $\alpha$  and  $\beta$ , for the probabilities of the errors of the first and second kinds (false positives and false negatives); and  $RSD_Q$ , for the relative standard deviation at the Quantification Limit. Mandatory values of these parameters are *not* incorporated in the defining expressions; recommended default values are shown in parentheses.

*Detection Decision (Critical Value) ( $L_C, \alpha = 0.05$ )*

$$\Pr(\hat{L} > L_C \mid L=0) \leq \alpha \quad (1)$$

*Detection Limit (Minimum Detectable Value) ( $L_D, \beta = 0.05$ )*

$$\Pr(\hat{L} \leq L_C \mid L=L_D) = \beta \quad (2)$$

*Quantification Limit (Minimum Quantifiable Value) ( $L_Q, RSD_Q = 0.10$ )*

$$L_Q = k_Q \sigma_Q \quad \text{where } k_Q = 1/RSD_Q \quad (3)$$

Note that  $L_D$ ,  $L_Q$ , and  $\sigma_Q$  denote CMP "true" parameter values. In practice they may be derived from estimates (or assumptions), such that calculated values themselves will be characterized by uncertainties. Also, for  $L_D$  and  $\beta$  to be meaningful,  $L_C(\alpha)$  must be employed for detection decision making. The relation,  $\beta$  vs  $L_D$  is known as the "Operating Characteristic" (OC) of the (detection) significance test performed at significance level  $\alpha$ ;  $(1-\beta)$  is the "power" of the test. Eq. (1) is given as an inequality, because not all values of  $\alpha$  are possible for discrete distributions, such as the Poisson. Note that the values of  $\alpha$ ,  $\beta$ , and  $k_Q$  given above are IUPAC recommended default values, which serve as a common basis for measurement process assessment. They may be adjusted appropriately in particular applications where detection or quantification needs are more or less stringent.

Also addressed in the IUPAC document is the issue of reporting. The recommendation is *always* to report both the estimated value of the measured quantity ( $L$ ) and its uncertainty, *even* when  $\hat{L} < L_C$  results in the decision "not detected." Otherwise, there is needless information loss, and, of course, the impossibility of averaging a series of results. The practice of quoting upper limits for "non-detects" can be helpful, but this still impairs future uses of the data. Quoting  $L_D$  as an *a posteriori* upper limit is not recommended, as this is really an *a priori* performance characteristic. Although it can be viewed as the "maximum upper limit" in the case of the null hypothesis,  $L_D$  does not reflect the new information contained in the experimental result. (See also §3.5.)

### 2.2.2. Simplified Relations

Under the very special circumstances where the distribution of  $\hat{L}$  can be taken as Normal, with constant standard deviation  $\sigma_o$  (homoscedastic) and the default parameter values, the foregoing defining relations yield the following expressions.

$$L_C = z_{1-\alpha} \sigma_o \rightarrow 1.645 \sigma_o \quad (4a)$$

$$L_C = t_{1-\alpha, \nu} s_o \rightarrow 2.132 s_o \text{ [4 df]} \quad (4b)$$

$$L_D = L_C + z_{1-\beta} \sigma_D \rightarrow 2L_C = 3.29 \sigma_o. \quad (5a)$$

$$L_D = \delta_{\alpha, \beta, \nu} \sigma_o \quad (5b)$$

$$\approx 2t_{1-\alpha, \nu} \sigma_o \rightarrow 4.26 \sigma_o \text{ [4 df]}$$

$$L_Q = k_Q \sigma_Q \rightarrow 10 \sigma_o \quad (6)$$

where:

$\sigma_o$ ,  $\sigma_D$ , and  $\sigma_Q$  represent the standard deviation of the estimator  $\hat{L}$ : under the null hypothesis, at the Detection Limit, and at the Quantification Limit, respectively;  $s_o^2$  represents an estimate of  $\sigma_o^2$ , based on  $\nu$  degrees of freedom;  $z$  and  $t$  represent the appropriate 1-sided critical values of the standard normal variate and Students-t, respectively; and  $\delta$  represents the non-centrality parameter of the non-central-t distribution. The actual value for  $\delta(.05, .05, 4)$  appearing above (Eq. 5b) is 4.07.

The above relations represent the simplest possible case, based on restrictive assumptions; they should in no way be taken, however, as the defining relations for detection and quantification capabilities. Some interesting complications arise when the simplifying assumptions do not apply. These will be discussed below. It should be noted, in the second expressions for LC and LD given above, that although so may be used for a rigorous detection test<sup>4</sup>,  $\sigma_o$  is required to calculate the detection limit. If so is used for this purpose, the calculated detection limit must be viewed as an estimate with an uncertainty derived from that of  $\sigma/s$ .<sup>5</sup> Finally, for chemical measurements the fundamental contributing factor to  $\sigma_o$ , and hence to the detection and quantification performance characteristics, is the variability of the blank. This is introduced formally below, together with the influence of heteroscedasticity.

### 2.2.3. Heteroscedasticity

In the case of heteroscedasticity, which occurs when the variance of the estimated quantity is not constant, its variation must be taken into account in computing detection and quantification limits. The critical level is unaffected, since it reflects the variance of the null signal only. Two types of  $\sigma$  variation are common in chemical and physical metrology: (a)  $\sigma^2$  (variance) proportionate to response, as with shot noise and Poisson counting processes; and (b)  $\sigma$  (standard deviation) increasing in a linear fashion. Detailed treatment of this issue is beyond the scope of this document, but further information may be found in [7, ch. 1]. To illustrate, given normality, negligible uncertainty in the mean value of the blank (such that  $\sigma_o \gg \sigma_B$ ), and  $\sigma(\hat{S})$  increasing with a constant slope ( $d\sigma/dS$ ) of 0.04 -- equivalent to an asymptotic relative standard deviation (RSD) of 4%, we find the following,

$$L_C = 1.645 \sigma_B \quad (7)$$

$$L_D = L_C + 1.645 \sigma_D, \quad (8)$$

$$\text{with } \sigma_D = \sigma_B + 0.04 L_D$$

$$L_Q = 10 \sigma_Q, \quad (9)$$

with  $\sigma_Q = \sigma_B + 0.04 L_Q$

Solutions to equations 8 and 9 are  $L_D = 3.52 \sigma_B$ , and  $L_Q = 16.67 \sigma_B$ , respectively. Thus, with a linear relation for  $\sigma(\hat{S})$ , with intercept  $\sigma_B$  and a 4% asymptotic RSD, the ratio of the quantification limit to the detection limit is increased from 3.04 to 4.73. If  $\sigma$  increases too sharply,  $L_D$  and/or  $L_Q$  may not be attainable for the CMP in question. This problem may be attacked through replication, giving  $\sigma$  reduction by  $1/\sqrt{n}$ , but caution should be exercised since unsuspected systematic error will *not* be correspondingly reduced!

### 2.3. The earthquake metaphor, and links with the outside world

Detection or quantification capabilities are generally of interest because of an external driving force  $L_R$ , which we take as an external value that the CMP must be able to detect (or quantify). To illustrate such a relationship, as well as most of the foregoing principles, an hypothetical example from [5] is given in the Appendix.

Among the links to public needs and perceptions that are implied in this diagram, is what might be called "The Zero Myth." In many cases the lay public believes, given sufficient effort or funding, that a concentration of zero may be detected and/or achieved. Not unlike the Third Law of Thermodynamics, however, neither is possible, even in concept. A policy of reporting "zero" when  $\hat{L} < L_C$ , yielding the decision "Not Detected," compounds this lack of understanding. These are issues of major national and international importance, especially in the context of legislation and regulation, where necessarily, and appropriately, many of the policy makers have critical sociopolitical expertise, but not necessarily scientific or technical expertise. The solution to this sociotechnical dilemma is, once again, very careful communication; and, beyond that, mutual understanding and education among the complementary disciplines.

One possible (partial) solution to this dilemma is the substitution of a non-zero value  $L_o$  for characterizing the null hypothesis. Eq. (1) would then take the form

$$\Pr(\hat{L} > L_C \text{ } L=L_o) \leq \alpha \quad (10)$$

Further discussion of such a non-zero null is given in [7, ch. 1 (§3.3.1)] in connection with discrimination limits.

## 3. TRANS-DEFINITIONAL ISSUES

### 3.1. Signal and concentration domains

Derived expressions for signal and concentration detection and quantification limits are given in §3.7.4 and §3.7.5 of [5], and extended in [8]. The treatment in the signal domain, yielding  $S_C$ ,  $S_D$ , and  $S_Q$ , is relatively straightforward; but some interesting problems arise in making the transition to the concentration domain ( $x_C$ ,  $x_D$ ,  $x_Q$ ), particularly when there is non-negligible uncertainty in the "sensitivity"  $A$  (slope of the calibration curve). For the simplest (single component, straight line) calibration function the estimated concentration  $\hat{x}$  is given by

$$\hat{x} = (y - \hat{B}) / \hat{A} \quad (11)$$

Although this is the simplest case, it nonetheless offers challenges, for example in the application of error propagation for the estimation of the  $\hat{x}$  distribution if  $e_y$  is non-normal,

and for the non-linear parts of the transformation (denominator of Eq. 11). In [8], which treats a normal response only, three cases for error in the estimated slope of the calibration curve are considered: (1) negligible ( $A$  known), (2) systematic ( $e^{\hat{A}}$  fixed), and (3) random ( $e^{\hat{A}} \sim N(0, V^{\hat{A}})$ ). The first alternative is transparent; one simply applies a constant divisor ( $A$ ) to convert signal detection and quantification limits to the corresponding values in the concentration domain. The second is the simplest to apply if  $A$  is not redetermined with each measurement. In this case, the detection decision is made in the signal domain, but concentration estimates, and concentration detection and quantification limits are estimated with the use of  $\hat{A}$ , taking into account its uncertainty.

The last of the above alternatives is commonly employed to obtain "calibration" or "regression" based detection limits, using a technique introduced by Hubaux and Vos [15]. This method, however, has a drawback in that it yields "detection limits" that are *random variables*, as acknowledged in the original publication of the method [15, p. 850]; different results being obtained for each realization of the calibration curve, even though the underlying measurement process is fixed. IUPAC [5] suggests dealing with this problem by considering the median of the distribution of such "detection limits." (The expected value is infinity.) An alternative, suggested in [5] and developed in [8], treats the exact, non-normal distribution of  $\hat{x}$  in developing concentration detection limits.

A problem may arise with calibration based detection limits if the magnitude and variability of the intercept are not equivalent to the corresponding quantities for the actual blank. This can occur under extrapolation and model error. That is, if the calibration process does not include a real blank, and the model is non-linear near the origin, then the computed intercept will be biased with respect to the blank, leading to an erroneous Critical Level. The intercept-derived critical level will be wrong also if the calibration operation fails to represent the full measurement process, including replication of the blank with *each* calibration point. In that case, the computed residual standard deviation from the fit will be too small, as it does not include the variability of the blank. To guard against these problems it is advisable always to estimate the blank variance directly through replication.

### 3.2. Specification of the measurement process

This is *absolutely essential*. Quoting §3.7.2 of [5]: "Just as with other Performance Characteristics,  $L_D$  and  $L_Q$  cannot be specified in the absence of a fully defined measurement process, including such matters as types and levels of interference *as well as* the data reduction algorithm. 'Interference free detection limits' and 'Instrument detection limits', for example, are perfectly valid within their respective domains; but if detection or quantification characteristics are sought for a more complex chemical measurement process, involving for example sampling, analyte separation and purification, and interference and matrix effects, then it is mandatory that all of these factors be considered in deriving values for  $L_D$  and  $L_Q$  for that process. Otherwise the actual performance of the CMP (detection, quantification capabilities) may fall far short of the requisite performance."

### 3.3. What is sigma?

Beyond the conceptual framework for detection and quantification limits, there is probably no more difficult or controversial issue, than deciding just what to use for  $\sigma_o$  or its estimate  $s_o$ . Though often ignored, the matter of heteroscedasticity must obviously be taken into account. But it is crucial also to take into account the *complete error budget* of the specified measurement process. If this is done successfully, and if all assumptions are satisfied, the

apparent dichotomy between the intra-laboratory approach and the inter-laboratory approach to detection and quantification limits essentially vanishes.<sup>6</sup> Some perspective on this issue is given in [5, §4.1, quoted below], in terms of Sampled and Target Populations.

*Sampled Population [S] vs Target Population [T].* The above concept has been captured by Natrella [2] by reference to two populations that represent, respectively, the population (of potential measurements) actually sampled, and that which would be sampled in the ideal, bias-free case. The corresponding **S** and **T** populations are shown schematically in Fig. 1, for a two-step measurement process. When only the **S**-population is randomly sampled (left side of the figure), the error  $e_1$  from the first step is systematic while  $e_2$  is random. In this case, the estimated uncertainty is likely to be wrong, because a) the apparent imprecision ( $\sigma_S$ ) is too small, and b) an unmeasured bias ( $e_1$ ) has been introduced. Realization of the **T**-Population (right side of the figure) requires that all steps of the CMP be random -- ie,  $e_1$  and  $e_2$  in the figure behave as random, independent errors; **T** thus represents a Compound Probability Distribution. If the contributing errors combine linearly and are themselves normal, then the **T**-distribution also is normal. The concept of the **S** and **T** populations is absolutely central to all hierarchical measurement processes (Compound CMPs), whether intralaboratory or interlaboratory. Strict attention to the concept is essential if one is to obtain consistent uncertainty estimates for Compound CMPs involving different samples, different instruments, different operators, or even different methods. In the context of (material) sampling, an excellent exposition of the nature and importance of the hierarchical structure has been presented by Horwitz [16].

"From the interlaboratory perspective, the first population in Fig. 1 ( $e_1$ ) would represent the distribution of errors among laboratories; the second [**S**] would reflect intralaboratory variation ('repeatability'); and the third [**T**], overall variation ('reproducibility'). If the sample of collaborating laboratories can be taken as unbiased, representative, and homogeneous, then the interlaboratory 'process' can be treated as a compound CMP. In this fortunate (at best, asymptotic) situation, results from individual laboratories are considered random, independent variates from the compound CMP population. For parameter estimation (means, variances) in the interlaboratory environment it may be appropriate to use *weights* -- for example, when member laboratories employ different numbers of replicates [17]."

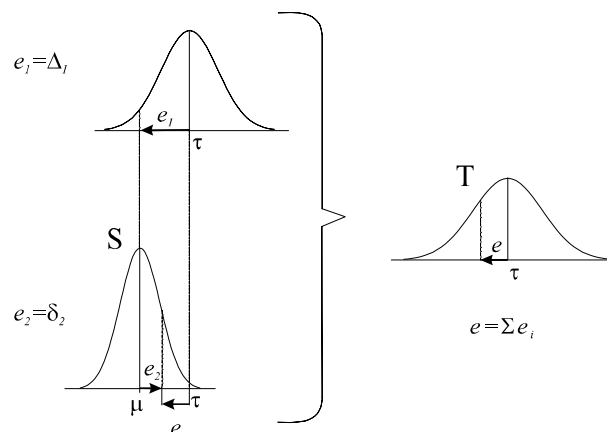


Fig. 1. Sampled [**S**] and Target [**T**] Populations.

### 3.4. The central role of the blank

The blank ( $B$ ) is one of the most crucial quantities in trace analysis, especially in the region of the Detection Limit. In fact, as shown above, the distribution and standard deviation of the blank are intrinsic to calculating the Detection Limit of any CMP. Standard deviations are difficult to estimate with any precision (ca. 50 observations required for 10% RSD for the Standard Deviation). Distributions (*cdfs*) are harder! It follows that extreme care must be given to the minimization and estimation of realistic blanks for the over-all CMP, and that an adequate number of full scale blanks must be assayed, to generate some confidence in the nature of the blank distribution and some precision in the estimate of the blank RSD.

Provided that the assumption of normality is justified, an imprecise estimate for the Blank standard deviation is taken into account without difficulty in Detection Decisions, through the use of Student's- $t$ . Detection Limits, however, are themselves rendered imprecise if  $\sigma_B$  is not well known. (See Ref. 5, §3.7.3.2)

Blanks or null effects may be described by three different terms, depending upon their origin: the *Instrumental Background* is the null signal (which for certain instruments may be set to zero, on the average) obtained in the absence of any analyte- or interference-derived signal; the (spectrum or chromatogram) *Baseline* comprises the summation of the instrumental background plus signals in the analyte (peak) region of interest due to interfering species; the *Chemical (or Analyte) Blank* is that which arises from contamination from the reagents, sampling procedure, or sample preparation steps, which corresponds to the very analyte being sought. A fourth, "pseudo-blank" is the intercept of the calibration curve, as estimated by ordinary least squares (OLS) or weighted least squares (WLS) applied to a calibration model. The intercept-blank and its variance offers certain pitfalls, however, as noted in §3.1. (See §5.3 for a detailed numerical example that treats the "3 B's" -- Background, Baseline, Blank.)

Assessment of the blank (and its variability) may be approached by an "external" or "internal" route, in close analogy to the assessment of random and systematic error components [11]. The "external" approach consists of the generation and direct evaluation of a series of ideal or surrogate blanks for the overall measurement process, using samples that are identical or closely similar to those being taken for analysis -- but containing none of the analyte of interest. The CMP and matrix and interfering species should be unchanged. (The surrogate is simply the best available approximation to the ideal blank -- ie, one having a similar matrix and similar levels of interferants.) The "internal" approach has been described as "Propagation of the Blank". This means that each step of the CMP is examined with respect to contamination and interference contributions, and the whole is then estimated as the sum of its parts -- with due attention to differential recoveries and variance propagation. This is an important point: that the blank introduced at one stage of the CMP will be attenuated by subsequent partial recoveries. Neither the internal nor the external approach to blank assessment is easy, but one or the other is mandatory for accurate low-level measurements; and consistency (internal, external) is requisite for quality. Both approaches require expert chemical knowledge concerning the CMP in question.

Special care must be taken when the blank has large relative standard deviation (RSD). This invariably means that the blank is not normal, for the negative values that must occur with a normally distributed variable with large RSD, such as a net signal near the detection limit, cannot be obtained, and conventional error propagation can be misleading. Non-normal blank distributions have their greatest impact on the Critical Level and Detection Limit because of the one-sided character of the false positive and false negative probabilities. Clearly, if the

gross signal ( $y$ ) is normal and the blank ( $B$ ), lognormal, for example, then the distributional character of the net signal ( $S=y-B$ ) will change with its magnitude.

### 3.5. Reporting of low-level data

Quantifying measurement uncertainty for low-level results -- i.e., those that are close to detection limits -- deserves very careful attention: (a) because of the impact of the blank and its variability, and (b) because of the tendency of some to report such data simply as "non-detects" [18] or "zeroes" or "less thans" (upper limits). The recommendations of IUPAC [5,14] in such cases are unambiguous: experimental results should not be censored, and they should *always* include quantitative estimates of uncertainty, following the guidelines of *GUM* [4]. When a result is indistinguishable from the blank, based on comparison of the result ( $\hat{L}$ ) with the critical level ( $L_C$ ), then it is important also to indicate that fact, perhaps with an asterisk or "ND" for not detected. But "ND" should never be used alone. Otherwise there will be information loss, and possibly bias if "ND" is interpreted as "zero."

Data from an early IAEA intercomparison exercise on radioactivity in seawater illustrates the point [19]. Results obtained from fifteen laboratories for the fission products Zr-Nb-95 in low-level sample SW-1-1, consisted of eight "values" and seven "non-values" as follows. (The data are expressed as reported, in pCi/L; multiplication by 0.037 yields Bq/L.)

VALUES:

2.2±0.3 9.5 9.2±8.6 77±11 0.38±0.23 84±7 14.1 0.44±0.06

NON-VALUES:

<0.1 ND <7.3 ND <40 <20.9 <26.8

The data as a whole are uninterpretable, particularly the "non-values." A simple mean and standard uncertainty calculated from the "values" is  $25 \pm 12$ . Because of missing information, a weighted mean of the "values" cannot be calculated. In many cases the meanings of the stated uncertainties or upper limits were not made clear. Ironically, for this particular sample, the true value of the activity concentration for the radionuclide pair was negligible because of unintended shipment delays that were long compared to the longer half-life [ $^{95}\text{Zr}$ , 65 d].

## 4. SOME FUTURE CHALLENGES

The "real world" holds many complexities and challenges beyond the preceding, relatively straightforward univariate, linear, and monotonic perspective. Very real detection and quantification capability issues in the environmental and physical sciences, for example, include: (1) multiple univariate and multivariate detection decisions and limits as found, for example, in chemical and nuclear monitoring programs when the null hypothesis dominates, and in the analysis of multicomponent spectra and chromatograms; (2) multivariate environmental blanks, especially in the measurement and source apportionment of multi-isotopic chemical species, such as tropospheric aerosols and atmospheric carbon monoxide; and (3) the appropriate treatment of detection and quantification limits for archaeological or geophysical artifacts or events that are governed by discrete, non-linear, and non-monotonic calibration curves, as in the case of radiocarbon ( $^{14}\text{C}$ ) dating [20].

In contrast to the future challenges, one of those from the past is fast disappearing. That is the estimation of detection and quantification capabilities for complex functional and distributional models. The broad availability of rapid computational and statistical graphics

tools has made possible rapid iterative, graphical solutions to previously daunting analytical problems, and Monte Carlo approaches for the treatment of intricate error and distributional systems. A brief introduction and references to some of the problems in the physical and environmental sciences may be found in Ref. 8.

## 5. EXAMPLES OF APPLICATIONS

The following subsections give an overview of selected applications, illustrating some critical issues arising in the estimation of detection and quantification limits, together references to source or closely related literature. For the first two cases, based on actual data for "simple" low-level counting and gamma-ray peak detection, respectively, expanded treatments showing numerical details ("worked examples"), are given in §5.2 and §5.3.

*Special note:* Because of the tutorial, numerical intent of the examples in §5.2 and §5.3, all calculated results are given to at least one decimal digit. The objective is to preserve computational (numerical) accuracy even though the convention concerning significant figures may be violated. By contrast, observed counts will always be integers because of the discrete nature of the Poisson process. In practice, of course, final results should *always* be reported to the correct number of significant figures.

### 5.1. Overview

#### *Low-Level Counting of $^{39}\text{Ar}$*

Ref: Currie, L.A., Eijgenhuijsen, E.M., and Klouda, G.A., "On the validity of the Poisson Hypothesis for low-level counting; investigation of the distributional characteristics of background radiation with the NIST Individual Pulse Counting System," *Radiocarbon* 40 (1998) 113-127.

Issues: Normal background (small RSD)

Tests of Poisson hypothesis, randomness

Heteroscedasticity, non-central-t

Combined uncertainty (concentration domain)

Two cases are presented using anticoincidence data (Set I) and coincidence data (Set II) from the above reference. For Set I data the background variance is found to be consistent with that of a Poisson Process and the observed counts are sufficiently large that the Poisson-Normal approximation can be used for detection decisions and for the calculation of detection and quantification limits. The Set II data illustrate the contrasting situation where there is an extra variance component, requiring the use of the replication variance estimate  $s^2$  and information drawn from the  $t$  (central and non-central) and  $\chi^2$  distributions. This is a common occurrence for non-anticoincidence, background limited, low-level counting where the primary background component derives from an external process such as cosmic ray interactions. For the Set II data, the background variance was primarily due to cosmic ray variations, which in the short term (intervals of a few days) are *not even random*, reflecting short term trends in barometric pressure.

#### *Peak detection [ $\gamma$ -ray spectrometry]*

Ref: Currie, L.A., "Detection: International Update, and Some Emerging di-Lemmas involving Calibration, the Blank, and Multiple Detection Decisions," *Chemometrics and Intell. Lab. Systems* 37 (1997) 151-181. (See §4.1.).

Issues: Algorithm dependence

Background, baseline, blank

Null hypothesis dominance

Multiple detection decisions

Low-level data reporting

Several of the above issues are illustrated in the numerical example given in §5.3. Multiple detection decisions, mentioned but not covered in the example, require an adjustment of  $z$  or  $t$  to take into account the number of null hypothesis tests, because the overall probability for one or more false positives when  $k$ -tests are made is

$$1 - (1-\alpha)^k \approx k\alpha \quad (\alpha \ll 1) \quad (12)$$

Thus, to maintain an overall false positive probability of 0.05, one must use 1-sided  $z(\alpha')$  or  $t(v, \alpha')$ , where  $\alpha' \approx 0.05/k$ . For  $k=5$  independent tests, for example,  $z(0.01) = 2.326$ , and  $t(9, 0.01) = 2.821$ . In the latter case, it is also necessary to obtain an independent estimate of  $\sigma_o$  for each application of the  $t$ -test.<sup>4</sup> (See Ref. 8, §4.1 for an extended discussion of alternative approaches to multiple and collective detection decisions.)

### *Extensions*

The applications discussed above highlight some of the more common issues involving detection, quantification, and data reporting for low-level, nuclear-related measurements as found in the "simple" scalar, sample - background situation (§5.2) and simple peak detection, including multiple detection decisions and the treatment of background vs baseline vs blank (§5.3). Although the influence of interfering components is illustrated by the effect of an elevated baseline on isolated peaks, this latter example does not address more complicated cases such as overlapping peaks, where the impact of interference is amplified by a "variance inflation factor" due a poorly conditioned inverse matrix. Some discussion of this topic may be found in Ref. 5 (§3.7.6) and Ref. 8 (§4).

Other noteworthy situations which will not be illustrated here include: (1) *calibration-based detection limits*, which capture the covariance between the estimated blank (as intercept) and sensitivity (as calibration factor or slope) as well as the variance function (dependence of  $\sigma^2$  on concentration); and (2) *more complicated functional and blank models*, which arise in environmental isotope ratio measurements such as accelerator and stable isotope mass spectrometry, where non-linear blank correction functions are the rule, and multivariate and non-normal blanks are often encountered. Some discussion of these advanced topics is given in Ref. 8. Numerical examples for calibration-based detection limits, based on real experimental data, may be found in references 6 and 21.

### **5.2. Example-1: low-level counting [<sup>39</sup>Ar]**

The first example illustrates the treatment of simple counting data for making detection decisions and the estimation of detection and quantification limits in the signal (counts) and radioactivity concentration (Bq/mol) domains. Two sets of actual background counting data, drawn from Ref. 22, are used to illustrate the Poisson-Normal case, where the standard deviation is (1) well represented by the square root of the mean number of counts (Set 1 data) and (2) based on replication, due to the presence of non-Poisson variance components (Set 2 data). Set 1 data are in fact the observed number of anticoincident counts in ten, 1000 minute counting periods; set 2 are the corresponding cosmic ray induced coincidence counts.

**5.2.1. The data** [counts; t = 1000 min]

Set 1: 265 305 277 277 263 312 310 318 286 270

$$\text{Mean } (\bar{B}) = 288.3$$

$$\text{Poisson-}\sigma_B = \sqrt{288.3} = 17.0$$

$$\text{Replication-}s_B = 21.0$$

Using the  $\chi^2$  test, we find  $(s/\sigma)^2$  to be non-significant ( $p=0.13$ ), so the Poisson value for  $\sigma_B$  will be used.

Set 2: 18730 19310 19100 19250 19350 19210 19490 19190 19640 18780

$$\text{Mean } (\bar{B}) = 19205.0$$

$$\text{Poisson-}\sigma_B = \sqrt{19205.0} = 138.6$$

$$\text{Replication-}s_B = 283.2$$

Using the  $\chi^2$  test, we find  $(s/\sigma)^2$  to be very significant ( $p<0.0001$ ), so the replication value  $s_B$  must be used as an estimate for  $\sigma_B$ .

**5.2.2. Equations for Poisson-normal variables [counts]**

$$\hat{S} = y - \hat{B} \tag{13}$$

$$V(\hat{S}) = V(y) + V(\hat{B}) = S + B + B/n = S + B\eta \tag{14}$$

$$\sigma_o = \sqrt{B\eta} \dots \text{OR} \dots s_o = s_B \sqrt{\eta} \text{ [TEST: } \chi^2] \tag{15}$$

$$L_C = z_C \sigma_o \dots \text{OR} \dots L_C = t_C s_o \tag{16}$$

$$L_D = L_C + z \sigma_D = L_C + z(z + \sigma_o) \tag{17a}$$

$$L_D = z^2 + 2z \sigma_o \dots \text{OR} \dots L_D \approx \delta \sigma_o \approx 2L_C \tag{17b}$$

$$\text{where: } \delta \approx 2t(4\sqrt{4v+1}) \approx 2t \quad v = n-1$$

$$L_Q = k_Q \sigma_Q = k_Q \{ (k_Q/2) [1 + \text{SQRT}(1 + (2\sigma_o/k_Q)^2)] \} \tag{18a}$$

$$L_Q = 10 \sigma_Q = 10 \{ 5 [1 + \text{SQRT}(1 + (\sigma_o/5)^2)] \} \tag{18b}$$

Note that the facts that  $\sigma_D > \sigma_o$  (Eq. 17) and  $\sigma_Q > \sigma_o$  (Eq. 18) derive from the variance function for Poisson counting data given in Eq. (14). Also, when Eq. (14) is applied to actual counting data, a subtle but necessary approximation is made by calculating the Poisson variances from observed counts which serve as estimates for the (unobservable) population means,  $S$  and  $B$ .

Parameter values for the current example are:

$$n = 10, v = n-1 = 9, \eta = (1 + 1/n) = 11/10 = 1.10$$

$$\alpha = \beta = 0.05, k_Q = 10.$$

$$z = 1.645$$

$$t = 1.833, \delta = 3.57$$

$$\sigma_o = \sigma_B \sqrt{\eta} = \sigma_B \sqrt{1.10}, s_o = s_B \sqrt{\eta} = s_B \sqrt{1.10}$$

Note that  $L_D$  and  $L_Q$  require information on the dependence of the variance  $\sigma^2$  on signal (or concentration) level (variance function). For the Set-1 data, this is given directly from Poisson "counting statistics" where the variance is equal to the (true) mean number of counts. For the Set-2 data, where we must use  $s^2$  to estimate  $\sigma^2$ , one really needs full replication data as a function of signal (or concentration) level. For the purpose of this example, however, we shall assume that the variance is approximately independent of concentration over the range of interest -- i.e.,  $\sigma \approx \sigma_o$  for  $L \leq L_Q$ . In practice, such an assumption should always be tested. See §2.2.3 for further discussion of this topic (heteroscedasticity).

### 5.2.3. Signal domain (all units are counts)

#### Set-1 Data

$$\sigma_B = \sqrt{288.3} = 17.0 \quad s_B = 21.0 [\chi^2: \text{NS}]$$

$$\text{therefore: } \sigma_o = \sigma_B \sqrt{\eta} = 17.0 \sqrt{(11/10)} = 17.8$$

$$S_C = 1.645 \sigma_o = 29.3$$

$$S_D = 2.71 + 3.29 \sigma_o = 61.3$$

$$S_Q = 10 \sigma_Q = 10(5)[1 + \text{SQRT}(1 + (\sigma_o/5)^2)] = 10(23.49) = 234.9$$

(In the case of  $S_Q$ , we see that the variance function for this particular Poisson process yields a ratio ( $\sigma_Q/\sigma_o$ ) of 1.32.)

$$\text{New observation: } y = 814; \text{ then } \hat{S} = 814 - 288.3 = 525.7$$

$\hat{S}$  exceeds  $S_C$ , so "detected"

$$\text{Report: } \hat{S} = 525.7, u = (814 + [288.3/10])^{1/2} = 29.0 [\text{relative } u = 5.5\%]$$

#### Set-2 Data

$$\sigma_B = \sqrt{19205.0} = 138.6 \quad s_B = 283.2 [\chi^2: \text{Significant } (p < 0.00001)]$$

$$\text{therefore: } s_o = s_B \sqrt{\eta} = 283.2 \sqrt{(11/10)} = 297.0$$

( $\sigma$  assumed constant for  $S \leq S_Q$ ; homoscedastic)

$$S_C = 1.833 s_o = 544.4$$

$$S_D = \delta \sigma_o = 3.57 \sigma_o$$

$$\hat{S}_D = 3.57 s_o = 1060.3$$

$$S_Q = 10\sigma_Q \approx 10\sigma_o$$

$$\hat{S}_Q = 10s_o = 2970.0$$

The relative (standard) uncertainty for  $\hat{S}_D$  and  $\hat{S}_Q$  derive from that for  $s_o/\sigma_o$ . Rigorous bounds for the latter can be obtained from the  $\chi^2$  distribution, but a good approximation for  $v > 5$  is given by  $u(s_o/\sigma_o) \approx 1/\sqrt{2v}$ ; for 9 degrees of freedom, this gives  $u = 23.6\%$ . The minimum possible value for  $\sigma_o$ , of course, is the Poisson value [23].

New observation:  $y = 19004$ ; then  $\hat{S} = 19004 - 19205.0 = -201.0$

$\hat{S}$  does not exceed  $S_C$ , so "not detected"

Report:  $\hat{S} = -201.0$ ,  $u = s_o = 297.0$

#### 5.2.4. Concentration domain (Bq/mol)<sup>7</sup>

$$\hat{x} = (y - \hat{B}) / \hat{A} = \hat{S} / \hat{A}$$

$$\hat{A} = t\hat{V}\hat{E} = (60000 \text{ s}) (0.000252 \text{ mol}) (0.939) = 14.19 \text{ mol/Bq}$$

where:  $t$  is the counting time;  $V$ , the moles of Ar in the counting tube; and  $E$ , the counting efficiency for <sup>39</sup>Ar.

$$\begin{aligned} u_c(A)/A &= \text{SQRT} \{ [u(V)/V]^2 + [u(E)/E]^2 \} \\ &= \text{SQRT} \{ [0.52\%]^2 + [1.28\%]^2 \} = 1.4\% \end{aligned}$$

##### Set 1 Data

$$\hat{x}_D = 61.3/14.19 = 4.32 \quad (u_c = 1.4\%)$$

$$\hat{x}_Q = 234.9/14.19 = 16.55 \quad (u_c = 1.4\%)$$

New observation:

$$\hat{x} = 525.7/14.19 = 37.0$$

$$u_c = \text{SQRT} \{ [5.5\%]^2 + [1.4\%]^2 \} = 5.7\% \text{ or } 2.1 \text{ Bq/mol}$$

##### Set 2 Data<sup>8</sup>

$$\hat{x}_D = 1060.3/14.19 = 74.7$$

$$\hat{x}_Q = 2970.0/14.19 = 209.3$$

Uncertainties above dominated by  $u(\sigma_o)$ , which has a relative uncertainty of approximately  $1/\sqrt{2v} = 1/\sqrt{18}$ , or 23.6%. Combining this with the 1.4% relative uncertainty for  $A$ , as above, has little effect; the combined relative uncertainty for the concentration detection and quantification limits is still about 23.6%. (See the report of Working Group 2 for a discussion of additional error components that must be considered for low-level  $\beta$  counting.)

New observation:

$$\hat{x} = -201.0/14.19 = -14.2$$

$$u_c = 297.0/14.19 = 20.9$$

### 5.3. Example-2: gamma-ray peak detection

The second example treats detection and quantification capabilities for isolated ("baseline resolved") gamma ray peaks. The data were derived from a one hour measurement of the gamma ray spectrum of NIST Mixed Emission Source Gamma Ray Standard Reference Material (SRM) 4215F. The full spectrum for this SRM contains several major pure radionuclide peaks used for calibration of the energy scale. For the purposes of this example, however, we consider only the high energy region dominated by the Compton baseline plus  $^{60}\text{Co}$  peaks at 1173 keV and 1332 keV and the  $^{88}\text{Y}$  peak at 1836 keV. Within this region, shown in Fig. 2, is a small impurity peak at 1460 keV due to  $^{40}\text{K}$ , the subject of this example. The ordinate in Fig. 2 uses the Poisson variance stabilizing transformation,  $\text{counts}^{1/2}$ , corresponding to a constant y-standard deviation of 0.50, which is 5% of the smallest y-axis interval (tic mark) shown. (In the figure, the y-axis ranges from 0 to 200, corresponding to a count range of 0 to 40,000 counts; and the x-axis ranges from channel 1100 to 2100, with the last datum in channel 2048.) Peak channel gross counts are 26184 (1173 keV), 20918 (1332 keV), 581 (1460 keV), and 8881 (1836 keV). The baseline in the region of the  $^{40}\text{K}$  peak is ca. 265 counts/channel.

The data shown in Fig. 2 will be used to estimate detection and quantification limits for  $^{40}\text{K}$  under the three "B" limiting conditions (background, baseline, blank), and to illustrate the reporting of low-level peak area data. To focus on these issues we limit the discussion here to the signal domain (peak area detection, quantification, and estimation). (See other worked examples for a discussion of additional error components that must be considered in radionuclide or element uncertainty estimation for gamma-ray spectrometry and neutron activation analysis.)

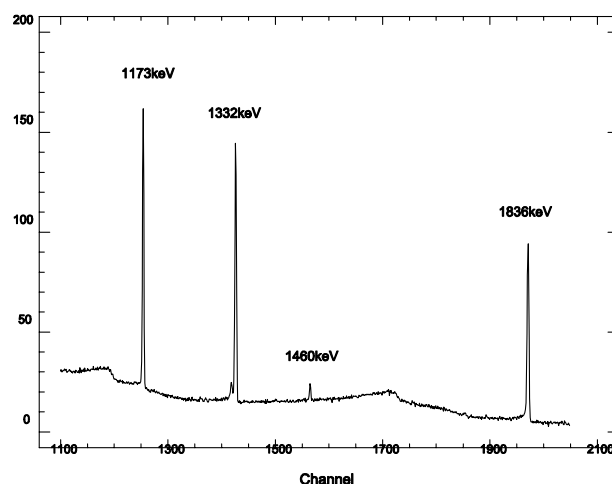


Fig. 2. SRM 4215F:  $\gamma$ -ray spectrum segment showing energy calibration ( $^{60}\text{Co}$  [1173, 1332 keV],  $^{88}\text{Y}$  [1836 keV]) and impurity ( $^{40}\text{K}$  [1460 keV]) peaks.

### 5.3.1. Background limiting

This case is exactly analogous to the low-level counting example above, except that signal and background are here based on the summation of counts over a  $k$ -channel spectrum window. Given the approximate peak width of 3.5 channels (FWHM) in this region of the spectrum, we take a 6-channel window centered at the  $^{40}\text{K}$  peak location for background and net peak area estimation. For a 60 minute counting period, this gives a long-term average  $B=3.6$  counts for the 6-channel window. For the purposes of this example, we take this to be the "well-known" background case, where  $B$  has negligible uncertainty.

Unlike the first example, the expected value of the background is so small that the Normal approximation to the Poisson distribution is inadequate. Also, because of the discrete nature of the Poisson distribution, we must use the inequality relationship indicated in Eq. (1), such that  $\alpha \leq 0.05$ . For a mean of 3.6 counts, this gives a critical (integer) value for the gross counts of 7, for which  $\alpha=0.031$ . (For 6 counts,  $\alpha=0.073$ .) Using 7 counts for the gross counts critical value, Eq. (2) gives 13.15 as the gross counts detection limit, for which  $\beta=0.05$ . Subtracting the background of 3.6 gives the corresponding net signal (peak area) values for  $S_C$  (3.4 counts) and  $S_D$  (9.55 counts). Had the normal approximation to the Poisson distribution been used, we would have obtained  $1.645\sqrt{3.6} = 3.12$  counts for  $S_C$ , and  $2.71 + 3.29\sqrt{3.6} = 8.95$  counts for  $S_D$ . The net count quantification limit  $S_Q$  is given by  $50[1+(1+B/25)^{1/2}] = 103.5$  counts. In this case  $B$  is sufficiently small that it has little influence on the value of  $S_Q$ .

### 5.3.2. Baseline limiting

Detection and Quantification capabilities under background limiting conditions tend to be overly optimistic, reflecting interference-free conditions. When the Compton baseline is non-negligible, we get the situation depicted in Fig. 2. Here, the limits are governed by both the baseline noise and the peak estimation algorithm and its estimated parameters. To illustrate, we take the simplest of estimation algorithms, the 3/6/3 square wave filter, for the estimation of the net peak area. This carries the assumption that the peak is located entirely within the central 6 channels, and that two 3-channel tails can serve as a reliable correction for a linear baseline. The channel count data for the  $^{40}\text{K}$  peak in Fig. 2 are:

Baseline counts,  $B_i = 266 \ 270 \ 266$  [left tail],  $279 \ 258 \ 250$  [right tail]; Sum,  $B = 1589$

Peak counts,  $P_i = 328 \ 473 \ 581 \ 501 \ 301 \ 244$ ; Sum,  $P = 2428$

Net peak area (counts),  $\hat{S} = P - B = 839$ ;  $u(\hat{S}) = (2438+1589)^{1/2} = 63.5$  (Poisson)

#### 5.3.2.1. DETECTION, QUANTIFICATION LIMITS (Poisson variance)

$S_C$ ,  $S_D$  and  $S_Q$  can be calculated using the equations given in §5.2, using  $\eta=2$  for the paired signal-background case, since the baseline is estimated with the same number of channels as the gross peak. Thus, in units of counts,

$$\sigma_B = \sqrt{1589} = 39.9 \quad \sigma_o = \sigma_B \sqrt{2} = 56.4$$

$$S_C = z\sigma_o = 1.645 * 56.4 = 92.8$$

$$S_D = z^2 + 2S_C = 2.71 + 2(92.8) = 188.3$$

$$S_Q = 50(1 + [1+(\sigma_0/5)^2]^{1/2}) = 616.2 \text{ net counts [ca. } 10\sigma_0\text{]}$$

Since  $\hat{S}$  (839) exceeds  $S_C$  (92.8), we conclude "detected."

A significance test can be applied also to  $\hat{S}$  in comparison with  $S_Q$ . Since the lower (0.05) tail of the 90% confidence interval, which equals  $839 - 1.645*63.5 = 734.5$ , exceeds  $S_Q$ , we conclude that the "true" (expected) value of  $S$  exceeds the quantification limit.

*Algorithm Dependence.* The above calculations apply to the simplest of all peak estimation algorithms, one that works reliably with isolated peaks supported by linear baselines. The same data, however, could be evaluated with far more sophisticated algorithms, based, for example, on a non-linear fit to a 3 or 4 parameter peak function (gaussian-exponential, or gaussian-lorentzian). In such cases, the detection and quantification limits would be different, as they depend upon the entire measurement process, including data reduction algorithms. These performance characteristics would be further altered, of course, if the level or nature of the interference were greater or more complex, as with the case of overlapping peaks.

*Influence of the background.* If the background spectrum is linear over the peak+baseline spectral region used for the above estimate, its influence is automatically taken into account by the baseline correction algorithm. If the background, itself, contains a significant  $^{40}\text{K}$  peak, however, the magnitude and uncertainty of that peak must be considered in the estimation of  $S$  and its uncertainty, and in the calculation of  $S_{C,D,Q}$ . It is not a problem for the present example, however, because of the relative magnitude of the Compton interference. That is, even if the entire 3.6 count background in the six channel peak window were  $^{40}\text{K}$ , it would be equivalent to less than 0.5% of the baseline correction and less than 10% of the uncertainty for that correction.

### 5.3.2.2. DETECTION, QUANTIFICATION LIMITS (Replication variance)

Alternatively, the detection decisions and detection and quantification limits may be based on the replication variance  $s^2$ . Comparison of the Poisson- $\sigma$  to the replication- $s$  is accomplished by taking the sum of the Poisson weighted squared residuals from fitting the baseline model. The sum should be distributed as chi-square if there is no extra (non-Poisson) variance component. The result of such a fit, using the 3 left and 3 right tail  $B_i$ 's gives a non-significant slope ( $p=0.45$ ) and  $s_i=10.28$  counts per channel with 4 degrees of freedom. (Again, extra, non-significant digits are shown in the interest of numerical accuracy.) The same conclusion follows from calculating the difference between the means of the 3 left and 3 right  $B_i$ 's compared to the Poisson- $\sigma$  for that difference, which is  $5.0\pm 23.0$  counts. We can gain a degree of freedom, therefore, by computing  $s$  from the mean (per channel) background; this gives  $s_i=9.97$  counts per channel with 5 degrees of freedom. The estimated replication standard deviation for the 6-channel background sum is therefore  $s=9.97\sqrt{6}=24.4$  counts. Comparing this with the Poisson- $\sigma$  ( $\sqrt{1589}$ ) from §5.3.2.1, we get  $(s/\sigma)=(24.4/39.9)=0.61$ , for which  $p(\chi^2)=0.87$ , consistent with Poisson variance only. That conclusion for this particular set of experimental observations could be the end of this example, but we continue because of the important tutorial value of illustrating the treatment of replication variance.

When we choose to use the replication variance<sup>9</sup>, which would be necessary if  $p(\chi^2)<.05$ , we get the following results (units of counts).

$$s_B = 24.4 \quad s_0 = s_B\sqrt{2} = 34.4$$

$$S_C = t(5 \text{ df})s_o = 2.015*34.4 = 69.3$$

$$S_D = \delta\sigma_o; \delta \approx 2t(4\text{df}/[4\text{df}+1]) = 2t(20/21) = 1.905t [5 \text{ df}]$$

$\hat{\sigma}_o = s_o$ ; Bounds are given by Chisquare

For 5 df,  $(s/\sigma)\text{min} = 0.48$ ,  $(s/\sigma)\text{max} = 1.49$  [90% interval]

Thus,  $\hat{S}_D = 1.905*2.015*34.4 = 132.0$  net counts

90% interval: 88.6 to 275.1 net counts

$S_Q = 10\sigma_Q \approx 10\sigma_o$ ;  $\hat{S}_Q = 344.0$ ; 90% interval: 230.9 to 716.7 counts

The approximation assumes  $\sigma(\hat{S})$  to be constant. In practice the variance function should be determined.

CONCLUSIONS: Since  $\hat{S} > S_C$ ,  $^{40}\text{K}$  has been detected. Since the lower (0.05) limit for  $S$  (769.7 counts) exceeds the upper limit for  $S_Q$  (716.7 counts), we conclude that  $S$  exceeds the quantification limit.

### 5.3.3. Blank limiting

This represents the most difficult case, where the very component of interest is present as a blank component<sup>10</sup> of the reference spectrum. That, in fact, was the case for SRM 4215F, where the unintended  $^{40}\text{K}$  peak was present as a blank contaminant. Calculation of  $S_C$ ,  $S_D$ , and  $S_Q$  then requires an estimate of  $\sigma_B$  for  $^{40}\text{K}$  which must be obtained by replication of the blank. The distribution of the blank, and the magnitude of  $\sigma_B$  depend on the sources of the blank. For the particular SRM 4215F, it is believed that  $^{40}\text{K}$  arose from background potassium in the detector system and a chemical impurity in the master solution for the standard, possibly derived from leaching of potassium from the glass container [8]. In more complicated cases of sample preparation, trace levels of potassium can be derived from the sampling and sample handling environment. Since  $^{40}\text{K}$  is a natural radionuclide having a half-life of ca.  $1.2 \times 10^9$  years, it is therefore present in all potassium, and in favorable cases it can be used for the non-destructive analysis of potassium. In fact, such an application is relevant to research on atmospheric aerosol in remote regions, where it is of great practical importance to determine the minimum quantifiable amount of potassium by a non-destructive technique, such as the direct measurement of  $^{40}\text{K}$ .

Although  $\sigma_B$  can be determined only through blank replication of the actual measurement process, some observations can be offered in relation to the above mentioned sources of the blank. The detection system component, which likely represents a fixed contamination level of this long-lived radionuclide, is expected to exhibit a Poisson distribution, with a gross (peak + baseline) blank variance equal to the expected number of counts. If the blank derives from processing reagents and if its relative standard deviation is rather small (e.g., <10 %), it is likely to exhibit normal behavior. On the other hand, if it comes primarily from low-level environmental contamination sources, experience shows that the relative standard deviation is frequently quite large (e.g., >20 %), and the distribution, asymmetric and non-normal, since negative blank contributions cannot occur.

To offer a brief numerical treatment, let us suppose that 10 replicates of the potassium blank gave an average net peak area of 620 counts with an estimated standard deviation  $s_B$  of 75 counts. Since the ratio  $s/\sigma = 75/\sqrt{620} = 3.01$  exceeds the 0.95 critical value  $((s/\sigma)_C = \sqrt{1.88} = 1.37$  for 9 df) from the chi-square distribution, we conclude that non-Poisson error components (chemical blank variations) are present; so we shall use the  $s_B$  for estimation of detection and quantification limits. For this particular example, we take measurements of gross signal and blank to be paired.<sup>11</sup> Thus,  $n = 2$  and  $s_o = s_B \sqrt{2} = 106.1$  counts. Values for  $S_C$ ,  $S_D$ , and  $S_Q$  (units of counts) are calculated as follows.

t-statistics:

For  $v=9$  degrees of freedom,  $t(v, \alpha) = t(9, .05) = 1.833$

non-central-t,  $\delta(v, \alpha, \beta) = \delta(9, .05, .05) = 3.575$

$\delta$ -approximation:  $2t(4v/(v+1)) = 1.946t = 3.567$

$$S_C = ts_o = 1.833 (106.1) = 194.5 \text{ counts}$$

Note that  $S_C$  calculated in this way is a "single use" statistic. Repeated detection decisions require independent estimates of  $\sigma_o$ , as well as an adjustment of  $t$  as discussed in §5.1.

$$S_D = \delta\sigma_o \text{ provided that } \sigma \text{ is constant between } S=0 \text{ and } S=S_D$$

If  $\sigma(\hat{S})$  is not constant, the variance function must be determined. (See the discussion in §2.2.3.) For the present illustration, we shall treat  $\sigma$  as constant (homoscedastic).

Not knowing  $\sigma_o$ , we use  $s_o$  as an estimate, and set bounds from bounds for  $(s/\sigma)$  from the  $\chi^2$  distribution.

Thus,

$$\hat{S}_D = \delta s_o = 3.575(106.1) = 379.3 \text{ counts}$$

$$(s/\sigma)_{.05} = 0.607, (s/\sigma)_{.95} = 1.37 \text{ (from } \chi^2 \text{ with } v=9)$$

$$276.9 < S_D < 624.9 \text{ (90\% confidence interval)}$$

$$S_Q = k_Q \sigma_Q = 10 \sigma_o \text{ provided that } \sigma \text{ is constant between } S=0 \text{ and } S=S_Q$$

(See the above note, concerning the variance function.)

Thus,

$$\hat{S}_Q = 10s_o = 1061.0 \text{ counts}$$

$$774.4 < S_Q < 1747.9 \text{ (90\% confidence interval)}$$

If  $\sigma$  is an increasing function of signal level, the above estimates will be biased low, but they can be viewed as lower bounds. The ultimate lower bounds, for counting data, are given by the Poisson-based values for  $S_D$  and  $S_Q$ . For the present example, taking  $\sigma_B = \sqrt{620}$  (negligible baseline and/or background case) these are

$$S_D \text{ (Poisson)} = 2.71 + 3.29\sqrt{2B} = 118.6 \text{ counts}$$

$$S_Q \text{ (Poisson)} = 50(1 + [1 + (35.2/5)^2]^{1/2}) = 405.7 \text{ counts}$$

### 5.3.4. Summary

The comparative results for the  $^{40}\text{K}$  detection and quantification capabilities as limited by the three B's (background, baseline, blank), expressed in terms of the 1460 keV peak area counts are as follows.

Background limiting:	$S_D = 9.55$	$S_Q = 103.5$
Baseline limiting:	$S_D = 188.3$	$S_Q = 616.2$
Blank limiting:	$\hat{S}_D = 379.3$	$\hat{S}_Q = 1061.0$

For the blank limiting case, *estimated* values for  $S_D$  and  $S_Q$  are given, because (non-Poisson) blank variability made it necessary to use a statistical estimate ( $s_o$ ) for  $\sigma_o$ . As shown in §5.3.3,  $S_D$  and  $S_Q$  are consequently uncertain by about a factor of 1.5.

Although this example was purposely limited to the signal (peak area) domain, it is interesting to consider the results in terms of radioactivity (Bq) for  $^{40}\text{K}$ , and mass (mg) for naturally radioactive potassium. Conversion factors (Sensitivities), taking into account the 1460 keV gamma counting efficiency,  $^{40}\text{K}$  gamma branching ratio, and K radioactivity concentration (specific activity) are 42.2 peak area counts/Bq, and 1.26 counts/mg, respectively. Detection limits for  $^{40}\text{K}$  for the three cases are thus 0.23 Bq (background limiting), 4.46 Bq (baseline limiting), and 8.99 Bq (blank limiting). The corresponding detection limit for potassium in the background limiting case is 7.58 mg. Uncertainties in the estimated sensitivities would introduce equivalent relative uncertainties in the estimated detection and quantification limits.<sup>10</sup>

Because of the applicability of  $^{40}\text{K}$  counting to the direct, non-destructive assay of potassium, it is interesting also to compare the last result with what could be obtained by low-level  $\beta$  counting. For the measurement process discussed in §5.2 the corresponding sensitivity is 1.62 counts/ $\mu\text{g}$ ; since  $S_D$  in that case was 61.3 counts, the mass detection limit for potassium would be (61.3/1.62) or 37.8  $\mu\text{g}$ . The gain of more than a factor of one thousand in sensitivity came about because of major increases in branching ratio, counting efficiency, and counting time for the low-level  $\beta$  counting technique. Because  $\beta$ -particles are far more readily absorbed than gamma rays, this latter technique is most attractive for inherently thin samples (such as air particulate matter) or potassium that has been concentrated chemically, as opposed to the non-destructive analysis of large samples by gamma spectrometry. For selected applications, therefore, low-level  $\beta$  counting can be useful for the assay of natural levels of  $^{40}\text{K}$ , as it is for  $^{14}\text{C}$  and  $^3\text{H}$ .

### 5.4 Detection of Earthquake Precursors

This example is adapted directly from §3.7.3 of Ref. 5. A graphical representation of these concepts is given in Fig. 3, where the "driving force" in this hypothetical example is the ability to detect the release of specific chemical precursors of earthquakes (e.g., radon) at levels corresponding to earthquakes of magnitude  $L_R$  and above. Thus  $L_R$  is the "requisite limit" or maximum acceptable limit for undetected earthquakes; this is driven, in turn, by a maximum acceptable loss to society. (Derivation of  $L_R$  values for sociotechnical problems, of course, is far more complex than the subject of this report!) The lower part of the figure shows the minimum detectable value for the chemical precursor  $L_D$ , that must not exceed  $L_R$ , and its relation to the probability density functions (pdf) at  $L = 0$  and at  $L = L_D$  together with  $\alpha$  and  $\beta$ , and the decision point (Critical Value)  $L_C$ . The figure has been purposely constructed to

illustrate heteroscedasticity -- in this case, variance increasing with signal level, and unequal  $\alpha$  and  $\beta$ . The point of the latter construct is that, although 0.05 is the recommended default value for these parameters, particular circumstances may dictate more stringent control of the one or the other. Instructive implicit issues in this example are that (1) a major factor governing the detection capability could be the natural variation of the radon background (blank variance) in the environment sampled, and (2) a calibration factor or function is needed in order to couple the two abscissae in the diagram. In principle, the response of a sensing instrument could be calibrated directly to the Richter scale (earthquake magnitude); alternatively, there could be a two-stage calibration: instrument response-radon concentration, and radon concentration-Richter scale.

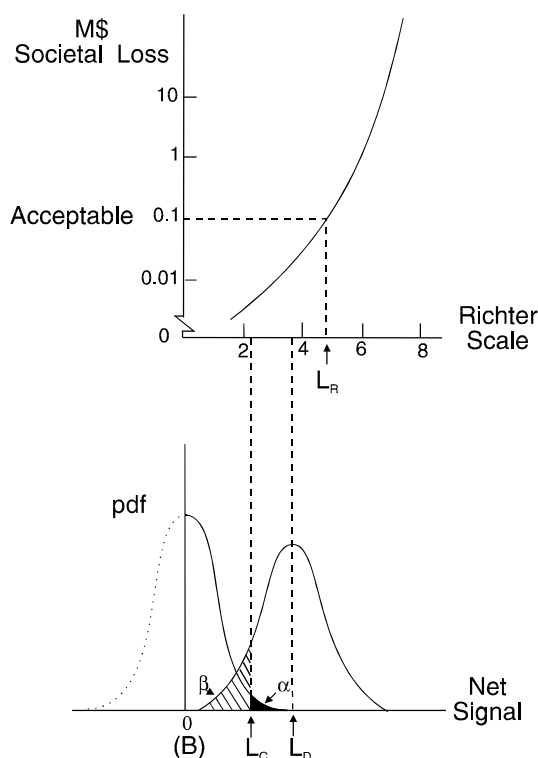


Fig. 3. *Detection: needs and capabilities.*

*Top portion shows the requisite limit  $L_R$ ; bottom shows detection capability  $L_D$ .*

## REFERENCES

- [1] INTERNATIONAL ATOMIC ENERGY AGENCY, Information sheet, consultants meeting on quantifying uncertainty in nuclear analytical measurements, IAEA, Vienna (Jan. 1998). See also guideline documents cited by the IAEA: EURACHEM Guide, Quantifying uncertainty in analytical measurements, LGC Information Services, Teddington, Middlesex, UK (1995); and TAYLOR, B.N., KUYATT, C.E., Guidelines for evaluating and expressing uncertainty of NIST measurement results, NIST Technical Note 1297, National Institute of Standards and Technology, Gaithersburg, MD 20899, USA (1993).
- [2] NATRELLA, M., EXPERIMENTAL STATISTICS, NBS Handbook 91, U.S. Government Printing Office, Washington DC (1963). (Chapt. 23: "Expression of the Uncertainties of Final Results.")
- [3] FEIGL, F., Tüpfel- und Farbreaktionen als mikrochemische Arbeitsmethoden, MIKROCHEMIE **1** (1923) 4.
- [4] INTERNATIONAL ORGANIZATION FOR STANDARDIZATION, Guide to the expression of uncertainty in measurement, Geneva, Switzerland (1993).

- [5] INTERNATIONAL UNION OF PURE AND APPLIED CHEMISTRY, Recommendations in evaluation of analytical methods including detection and quantification capabilities, IUPAC Commission on Analytical Nomenclature, *Pure and Appl. Chem.* **67** (1995) 1699-1723 (prepared by L.A. Currie).
- [6] INTERNATIONAL ORGANIZATION FOR STANDARDIZATION, ISO/TC69/SC6 (P. Wilrich, chairman), Standard 11843-1,2 Capability of Detection, Part 1 (Standard): Terms and definitions (1997); Part-2 (Draft Standard): Methodology in the linear calibration case (1998).
- [7] CURRIE, L.A., Ed., DETECTION IN ANALYTICAL CHEMISTRY: Importance, Theory, and Practice, ACS Sympos. Series 361, American Chemical Society, Washington, DC (1988).
- [8] CURRIE, L.A., Detection: international update, and some emerging dilemmas involving calibration, the blank, and multiple detection decisions," *Chemometrics and Intelligent Laboratory Systems* **37** (1997) 151-181.
- [9] KAISER, H., Die Berechnung der Nachweisempfindlichkeit, *Spectrochim. Acta*, **3** (1947) 40-67.
- [10] CURRIE, L.A., Limits for qualitative detection and quantitative determination, *Analyt. Chem.* **40** (1968) 586-593.
- [11] CURRIE, L.A., PARR, R.M., Perspectives on detection limits for nuclear measurements in selected national and international programs, Ch. 9, in Currie, L.A., Ed., *Detection in Analytical Chemistry: Importance, Theory, and Practice*, ACS Sympos. Series 361, American Chemical Society, Washington DC (1988).
- [12] INTERNATIONAL UNION OF PURE AND APPLIED CHEMISTRY, H. Freiser, G.H. Nancollas, Ed., *Compendium of Analytical Nomenclature*, 2nd edition, Blackwell Scientific Publ., Oxford, UK (1987); 1st edition (1978).
- [13] LONG, G.L., WINEFORDNER, J.D., Limit of detection: a closer look at the IUPAC definition *Analyt. Chem.* **55** [7] (1983) 713A-724A.
- [14] INTERNATIONAL UNION OF PURE AND APPLIED CHEMISTRY, *Compendium of Analytical Nomenclature*, 3rd edition; Presentation of the results of chemical analysis (ch. 2); Performance characteristics of analytical processes (ch. 18, §18.4); J. Inczédy, A.M. Ure, T. Lengyel, A. Gelencsér, Eds., Blackwell Scientific Publ., Oxford UK (1998).
- [15] HUBAUX, A., VOS, G., Decision and detection limits for linear calibration curves, *Analyt. Chem.*, **42** (1970) 849-855.
- [16] INTERNATIONAL UNION OF PURE AND APPLIED CHEMISTRY, IUPAC Commission on Analytical Nomenclature, *Nomenclature for sampling in analytical chemistry*, *Pure and Appl. Chem.*, **62** (1990) 1193 (prepared by W. Horwitz).
- [17] MANDEL, J., PAULE, R.C., Interlaboratory evaluation of a material with unequal numbers of replicates, *Analyt. Chem.*, **42** (1970) 1194.
- [18] LAMBERT, D., PETERSON, B., TERPENNING, I., Nondetects, detection limits, and the probability of detection, *J. Amer. Stat. Assoc.* **86** (1991) 266-277.
- [19] FUKAI, R., BALLESTRA, S., MURRAY, C.N., Intercalibration of methods for measuring fission products in seawater samples, *Radioact. Sea* **35** (1973).
- [20] STUIVER, M., LONG, A., KRA, R.S., eds., *Calibration 1993*, *Radiocarbon* **35** (1993).
- [21] CURRIE, L.A., The many dimensions of detection in chemical analysis, in: *Chemometrics in Pesticide/Environmental Residue Analytical Determination*, D. Kurtz, Ed., (American Chemical Society), ACS SYMPOSIUM SERIES **284**, Chapter 5 (1984) 49-81. (See also §3.2 in Ref. 8.)
- [22] CURRIE, L.A., EIJGENHUIJSEN, E.M., KLOUDA, G.A., On the validity of the Poisson hypothesis for low-level counting; investigation of the distributional characteristics of background radiation with the NIST individual pulse counting system, *Radiocarbon* **40** (1998) 113-127.
- [23] CURRIE, L.A., Optimal estimation of uncertainty in reporting of accelerator mass spectrometry results, *Nucl. Instr. Meth. Phys. Res.* **92** (1994) 188-93.
- [24] KAISER, H., Zum Problem der Nachweisgrenze, *Z. Analyt. Chim.* **209** (1965) 1-18.
- [25] GIBBONS, R.D., Some statistical and conceptual issues in the detection of low-level environmental pollutants, *Environmental and Ecological Statistics*, **2** (1995) 125-167. [Discussants: K. Campbell; W.A. Huber; C.E. White and H.D. Kahn; B.K. Sinha, W.P. Smith and H. Lacayo; W.A. Telliard; and C.B. Davis.]

## NOTES

1. The primary source for material presented in this paper is the IUPAC document prepared for the Commission on Analytical Nomenclature, "Recommendations in Evaluation of Analytical Methods including Detection and Quantification Capabilities" [5]. An *Index of Terms* is given at the end of that document. Further technical issues, identified in the IUPAC document and developed in a more comprehensive study [8], are also noted in this review. Of special importance in the latter work are alternative approaches to calibration-based detection limits, MP design considerations, parameter estimation, and multiple, extended, and "collective" (multivariate) detection decisions. The text of this overview paper has been adapted in part from an invited paper at the 1996 Joint Statistical Meetings (American Statistical Association). Original title: "Foundations and future of detection and quantification limits." Contribution of the National Institute of Standards and Technology; not subject to copyright.
2. Some confusion between the two types of "detection limits" arose in part from an oversight in Kaiser's first publication on the topic in 1947 [9] which ignored the idea of the false negative. False negatives nevertheless occur, and when ignored (equivalent to equating  $L_C$  and  $L_D$ ) their *defacto* probability becomes 50%, at least for symmetric distributions. Kaiser addressed this problem by offering a new term in 1965, "Limit of Guarantee for Purity" [24], but this term has scarcely ever appeared in the literature.
3. Codex Alimentarius Commission, Committee on Methods of Analysis and Sampling, Food and Agricultural Organization, World Health Organization.
4. The use of  $ts_o$  for multiple detection decisions is valid only if a new estimate  $s_o$  is obtained for each decision. In the case of a large or unlimited number of null hypothesis tests, it is advantageous to substitute the tolerance interval factor  $K$  for Student's- $t$ . See Ref. 8 for an extended discussion of this issue.
5. Uncertainty of the ratio  $s_o/\sigma_o$  derives from percentage points of the chisquare distribution. Alternatively, if  $\nu$  is not too small, it is possible to use an asymptotic expression for the relative standard deviation of  $s_o$ :  $\text{rsd}(s_o) \approx 1/\sqrt{2\nu}$ . Thus, 8 degrees of freedom are required for an estimate of  $\sigma$  with an  $\text{rsd}$  of 25%. If  $\sigma$  varies with concentration, one needs to estimate the variance function ( $\sigma^2$  vs concentration) in order to derive  $L_D$  and  $L_Q$ . This must be done with iterative weighted least squares, using  $(2\nu/\sigma^2)$  as weights. See Ref. 6 (ISO Standard 11843-2, example 2) for an illustration of this procedure.
6. In practical application, the complexity of defining and estimating " $\sigma$ " goes considerably deeper. For a recent informative and provocative discussion of this and related regulatory-detection issues, the reader may consult Ref. 25.
7. The transformation from the signal domain (observed response, in the present case, counts) to the concentration domain is fraught with subtle "error propagation" difficulties, especially for calibration factors having large relative uncertainties. Following the discussion of §3.1 we take the simplest approach in this example, estimating the uncertainty in detection and quantification limits from the uncertainty in the calibration factor  $A$ . For small relative uncertainty in  $A$ , the result differs little from more sophisticated approaches employing "calibration-based" limits [8, §3.2]. When the relative uncertainty of  $A$  is large (e.g., >20%) there is a further complication due to increasing non-normality of the  $\hat{x}$  distribution.

For the special case where the background and standard, and therefore  $x$ , are measured for each sample, the simplified expressions in §2.2.2 can be applied directly to the observed series, with  $x_i = S_i/A_i = ((y-B)/A)_i$ , provided that the relative standard deviation of the  $A_i$  is not so large that the normality assumption for the  $x_i$  is seriously violated.

8. Set 2 data illustrate a special  $\hat{x}$  error propagation problem that arises for low-level data, when the net signal is at or near zero. The simplified form of the Taylor expansion doesn't work, because of (implicit) division by zero. The simplified form gives the relative variance of the estimated concentration  $\hat{x}$  as the sum of the relative variances of the net signal (numerator,  $\hat{S}$ ) and the calibration factor (denominator,  $\hat{A}$ ):

$$(\sigma_{\hat{x}}/x)^2 = (\sigma_{\hat{A}}/A)^2 + (\sigma_{\hat{S}}/S)^2$$

The  $S=0$  problem can be avoided by using the proper expression for the uncertainty of a ratio of random variables [8, Eq 21, for independent  $\hat{S}$ ,  $\hat{A}$ ]

$$V_{\hat{x}} = (1/A^2) [V_{\hat{S}}(1 + \phi_{\hat{A}}^2) + S^2 \phi_{\hat{A}}^2]$$

where  $\phi_{\hat{A}}$  is the relative standard deviation of  $\hat{A}$

If  $S=0$ , the last term in the brackets vanishes. If, in addition  $\phi_{\hat{A}}^2 \ll 1$ , the result becomes  $\sigma_{\hat{x}} \approx \sigma_{\hat{S}}/A$ , as with the final result for the Set-2 data.

9. The replication variance  $s^2$  may always be selected as the variance estimator, but it is quite imprecise when  $v$  is small.  $\sigma^2$  [Poisson] is more precise and sets the lower bound for the true variance, but it underestimates the true variance if extra, non-Poisson components are present. A conservative but potentially biased approach, generally applied in low-level counting and accelerator mass spectrometry, is to use the larger of  $s^2$  or  $\sigma^2$  (Poisson) [23].
10. In keeping with the peak area (signal domain) treatment for the background and baseline parts of this example, we continue with the reference to the blank expressed as counts, and the symbols  $S_{C,D,Q}$ . If the replications of the blank were expressed directly in x-units (radioactivity, Bq for  $^{40}\text{K}$ ; or mass, kg for K) the appropriate symbol set would be  $x_{C,D,Q}$ . For a comprehensive treatment of all significant uncertainty components in the measurement of  $^{40}\text{K}$ , see the worked example on *Radionuclides in Marine Sediment Samples*, in the contribution of Dovlete and Povinec to this TECDOC.
11. Paired measurements are always advisable, to offset possible errors from a drifting or changing blank. (For a drifting blank,  $s_o$  may be calculated directly from paired blank observations; alternatively,  $s_B$  may be calculated from "local"  $B_i$  replicates, or from the dispersion about a fitted trend line.) Furthermore, if a non-normal blank distribution is likely, paired observations will force a symmetric distribution for  $\hat{S}_{\text{null}}$  ( $S=0$ ), but in such a case it is advantageous also to estimate the net signal from k-replicate pairs. That brings about approximate normality as a result of the central limit theorem. In the present example, the estimated relative standard deviation of the blank (75/620) is 0.12, so the assumption of normality may be considered acceptable.

# XRF ANALYSIS OF INTERMEDIATE THICKNESS SAMPLES

A. MARKOWICZ, N. HASELBERGER

Agency's Laboratories, International Atomic Energy Agency, Seibersdorf

## Abstract

X ray fluorescence (XRF) analysis refers to the measurements of characteristic X rays resulting from electrons filling the inner shell vacancies produced in the sample by means of a suitable source of radiation. Energy dispersive XRF (EDXRF) measures the energy of the emitted X rays by collecting the ionisation products induced in a solid state semiconductor detector. On their pathway through the sample, the exciting radiation and the emitted radiation are attenuated. The samples are categorised in thin, intermediate and thin samples by their attenuation factor. Common sources of uncertainty are discussed and quantified for each category, including the subsampling, the sample preparation and the degree of homogeneity of the sample, the calibration and the stability of the EDXRF spectrometer, the evaluation of the spectra, and the absorption correction factor. For samples of intermediate thickness additional uncertainty sources have to be taken into account for the determination of the total mass per unit area and the potential non-uniform thickness of the sample. The absorption factor is obtained from a set of transmission measurements of each individual sample and a reference target and the associated uncertainty is obtained from the measurement uncertainties.

## 1. INTRODUCTION

A number of approaches have been developed for quantification in X ray fluorescence (XRF) analysis of intermediate-thickness samples whose total mass per unit area  $m$  fulfils the relation [1]

$$m_{thin} < m < m_{thick} \quad (1)$$

where  $m_{thin}$  and  $m_{thick}$  are the values of mass per unit area for thin and thick samples, defined by

$$m_{thin} \leq \frac{0.1}{\mu(E_0)\csc\Psi_1 + \mu(E_i)\csc\Psi_2} \quad (2)$$

where  $\mu(E_0)$  and  $\mu(E_i)$  are the total mass attenuation coefficients for the whole specimen at the energy of incident radiation ( $E_0$ ) and characteristic radiation ( $E_i$ );  $\Psi_1$  and  $\Psi_2$  are the effective incident and take off angles,

$$m_{thick} \geq \frac{4.61}{\mu(E_0)\csc\Psi_1 + \mu(E_i)\csc\Psi_2} \quad (3)$$

One of the most commonly used methods in quantitative XRF analysis of intermediate-thickness samples is the emission-transmission (E-T) method in which the specific X ray intensities from a sample are measured successively with and without a multielement target positioned adjacent to the back of the sample in a fixed geometry [1]. In the absence of enhancement effects and assuming monochromatic excitation, the mass per unit area of the  $i$ -th element,  $m_i$ , for homogeneous intermediate thickness samples, can be calculated from the following equation:

$$m_i = \frac{I_{i,s}}{B_i} Ab_{corr} \quad (4)$$

where  $B_i$  is the calibration factor which can be determined either experimentally as the slope of the straight calibration line for the  $i$ -th element obtained with thin homogeneous samples or semi-empirically based on both an experimentally determined coefficient and the relevant fundamental parameters;  $Ab_{corr}$  is the absorption correction factor given by

$$Ab_{corr} = \frac{-\ln H}{1-H} \quad (5)$$

$$\text{with } H = \frac{I_{i,T} - I_{i,S}}{I_{i,0}} \quad (5a)$$

The absorption correction factor  $Ab_{corr}$  represents the combined attenuation of the primary and fluorescent radiations in the whole specimen and can be determined individually for each sample by transmission experiments, as shown in Figure 1.

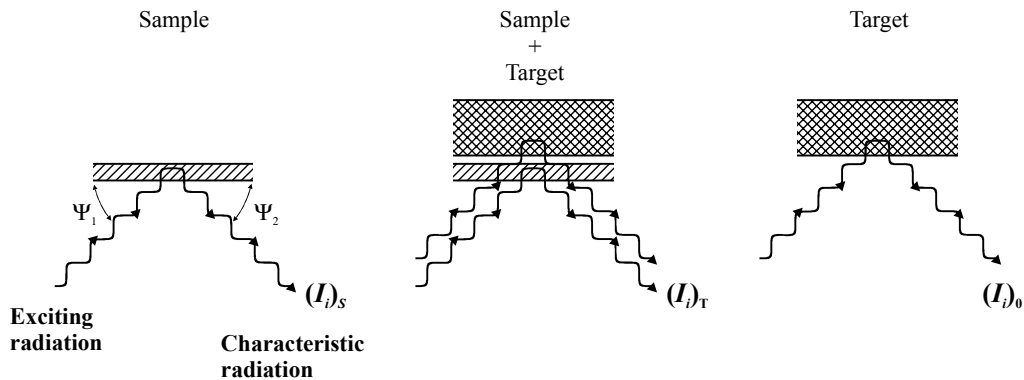


Fig. 1. Experimental procedure used in the emission-transmission method.

Finally, the concentration of the  $i$ -th element  $W_i$  is calculated from

$$W_i = \frac{I_{i,S} (-\ln H)}{B_i m (1-H)} \quad (6)$$

The emission-transmission method can be applied for quantitative XRF analysis of various materials, including samples of environmental, biological and geological origin (e.g., soil, sediments, plants, air particulates collected on filters, etc.).

## 2. EXAMPLE

### 2.1. Specification

#### (a) Technique

The example is related to the emission-transmission method applied in radioisotope excited XRF analysis (Cd-109 excitation source, measurement time=1000 s). XRF measurements were carried out with an energy-dispersive (ED) spectrometer consisting of a Si/Li solid state detector and a Canberra multichannel analyzer. For the E-T experiments an infinitely thick multielement target was used. Spectrum evaluation was performed using the AXIL routine [2].

*(b) Specimen*

A pellet of geological material (total mass per unit area  $m=0.0866\text{g/cm}^2$ ) was prepared and analyzed.

*(c) Analyte: Sr*

*(d) Measurand:*

Concentration of Sr in the geological sample. The concentration of Sr was determined from Equation 6 (see Introduction).

## **2.2. Sources of uncertainty**

1. Calibration of the EDXRF spectrometer (performed by using pure element foils, e.g. from Advent Research Materials Ltd. or pellets prepared from pure compounds).
2. Instability of the EDXRF spectrometer including both detector and electronics.
3. Sample preparation
  - 3a. Heterogeneity of the material to be analyzed
  - 3b. Non-uniformity of sample thickness
4. Spectral data processing with fitting programme
5. Quantification
  - 5a. Determination of the absorption correction factor
6. Uncertainty in determination of total mass per unit area

## **2.3. Quantification of uncertainty components**

### *2.3.1. Calibration of the EDXRF spectrometer*

The calibration is performed by using single element foils or intermediate thickness pellets prepared from pure compounds. Based on the measurements the sensitivity factors were calculated for 7-15 elements as the ratio of the intensity of the characteristic X rays of the element of interest to the mass per unit area of that element in the calibration sample, corrected (if necessary) for the matrix absorption effects. The uncertainties of the experimental values for the sensitivity factors are calculated including the uncertainties of the characteristic X rays intensities, uncertainties of the mass per unit area of the element in the calibration sample and uncertainties of the absorption correction factor. For each experimental point the uncertainty was smaller than 1% relative. In the next step, a calibration curve for the factor vs. atomic number of the element was defined, based on the least squares fitting procedure. Finally, the uncertainty of the calibration of the EDXRF spectrometer is calculated as the root mean square (rms) - 2%

### *2.3.2. Instability of the EDXRF spectrometer*

(including the following sources of uncertainty:  $I_0$ ,  $\varepsilon(E_i)$ , electronics).

The instability was evaluated from the results of 18 repetitive measurements of an Fe metal foil performed during 9 hours in a day at fixed time intervals. The mean value of the peak area for the Fe- $K_\alpha$  line and its uncertainty (standard deviation) were calculated. After subtraction of the contribution of counting statistics, the uncertainty due to the instability of the EDXRF spectrometer was found to be 0.025% (relatively very small and neglected in further calculations).

### *2.3.3. Sample preparation*

(a). Uncertainty due to heterogeneity of the geological material was evaluated experimentally for 6 sub-samples taken at random from the geological material - 5%.

(b) Uncertainty due to non-uniformity of sample thickness negligible (see Ref. 3 for details).

### 2.3.4. Spectral data processing with fitting programme

Least-squares fitting procedure (AXIL) gives net peak areas and their uncertainties (both in counts) which in the case of the geological material were as follows:

$$I_{i,s} = 2974; u(I_{i,s}) = 70; I_{i,T} = 105984; u(I_{i,T}) = 352; I_{i,0} = 286684; u(I_{i,0}) = 567$$

### 2.3.5. Quantification

Uncertainty in determination of the absorption correction factor  $Ab_{corr}$  is due to the uncertainties of the intensities of the characteristic X rays  $I_{i,s}$ ,  $I_{i,T}$ , and  $I_{i,0}$ . The uncertainty of  $Ab_{corr}$  is calculated based on the law of uncertainty propagation applied to Eqs. 5 and 5a.

$$u(Ab_{corr}) = \frac{A-1-\ln A}{(A-1)^2} u(A) \quad (7)$$

with  $A = H^{-1}$

$$u(A) = \sqrt{\frac{[u(I_{i,0})]^2}{[(I_{i,T}) - (I_{i,s})]^2} + \frac{[u(I_{i,T})]^2 [(I_{i,0})]^2}{[(I_{i,T}) - (I_{i,s})]^4} + \frac{[u(I_{i,s})]^2 [(I_{i,0})]^2}{[(I_{i,T}) - (I_{i,s})]^4}} \quad (7a)$$

$$\text{Finally,} \quad Ab_{corr} = 1.6; u(Ab_{corr}) = 0.0028$$

2.3.6. Uncertainty in determination of total mass per unit area  $m$  - 0.02% (negligible).

## 2.4. Conversion of uncertainties to standard uncertainties (standard deviations)

- (a) Calibration of the EDXRF spectrometer,  $u(B_i) = 2\%$
- (b) Instability of the EDXRF spectrometer,  $u(inst) \approx 0\%$
- (c) Sample preparation,  $u(F_{prep}) = 5\%$
- (d) Spectral data processing with fitting programme
  - $I_{i,s} - u(I_{i,s}) = 2.4\%$
  - $I_{i,T} - u(I_{i,T}) = 0.3\%$
  - $I_{i,0} - u(I_{i,0}) = 0.2\%$
- (e) Quantification
  - $Ab_{corr} - u(Ab_{corr}) = 0.7\%$
- (f) Determination of total mass per unit area  $m$  -  $u(m) \approx 0\%$

## 2.5. Calculation of combined uncertainty

By using the law of uncertainty propagation to the modified Eq. 4, which includes the correction factor  $F_{prep}$  related to sample preparation step ( $F_{prep} = 1$ )

$$W_i = \frac{I_{i,s}}{B_i m} Ab_{corr} F_{prep} \quad (8)$$

the combined relative uncertainty  $u_c$  is calculated [4]

$$u_c = \frac{u(W_i)}{W_i} = \sqrt{\left(\frac{u(I_{i,S})}{I_{o,s}}\right)^2 + \left(\frac{u(Ab_{corr})}{Ab_{corr}}\right)^2 + \left(\frac{u(B_i)}{B_i}\right)^2 + \left(\frac{u(F_{prep})}{F_{prep}}\right)^2} \quad (9)$$

The correlation between the first term related to  $I_{i,S}$  and the second one describing the contribution of  $Ab_{corr}$  (which also requires  $I_{i,S}$  in the calculation) was not considered.

## 2.6. Sensitivity factors

The sensitivity factors, defined as the partial derivatives, are as follows:

$$a) \quad \text{for } B_i: -\frac{I_{i,S}}{B_i^2 m} Ab_{corr} F_{prep}$$

$$b) \quad \text{for } F_{prep}: -\frac{I_{i,S}}{B_i m} Ab_{corr}$$

$$c) \quad \text{for } I_{i,S}: -\frac{1}{B_i m} Ab_{corr}$$

$$d) \quad \text{for } Ab_{corr}: -\frac{I_{i,S}}{B_i m} F_{prep}$$

## 2.7. Results

$$W_i = \frac{2974 [\text{counts}]}{5.494 \times 10^5 \frac{\text{counts}}{\text{mg/cm}^2} \times 86.6 \frac{\text{mg}}{\text{cm}^2}} \times 1.6 \times 1.0 \times 10^6 = 100 \mu\text{g/g}$$

$$u_c = \frac{u(W_i)}{W_i} = \sqrt{\left(\frac{70}{2974}\right)^2 + \left(\frac{0.0028}{1.6}\right)^2 + \left(\frac{9.017 \times 10^3}{5.494 \times 10^5}\right)^2 + \left(\frac{0.05}{1}\right)^2}$$

$$= \sqrt{0.0006 + 3.0625 \times 10^{-6} + 0.0003 + 0.0025} = 0.0583$$

Since the uncertainty of sample preparation is a major contribution to the combined uncertainty, the coverage factor  $k = 2.57$  was taken from t distribution at the degree of freedom = 5 and  $\alpha = 0.05$ . The expanded combined uncertainty is calculated, and the final result is obtained

$$W_i = 100 \pm 15 \mu\text{g} \cdot \text{g}^{-1}$$

Summary Table

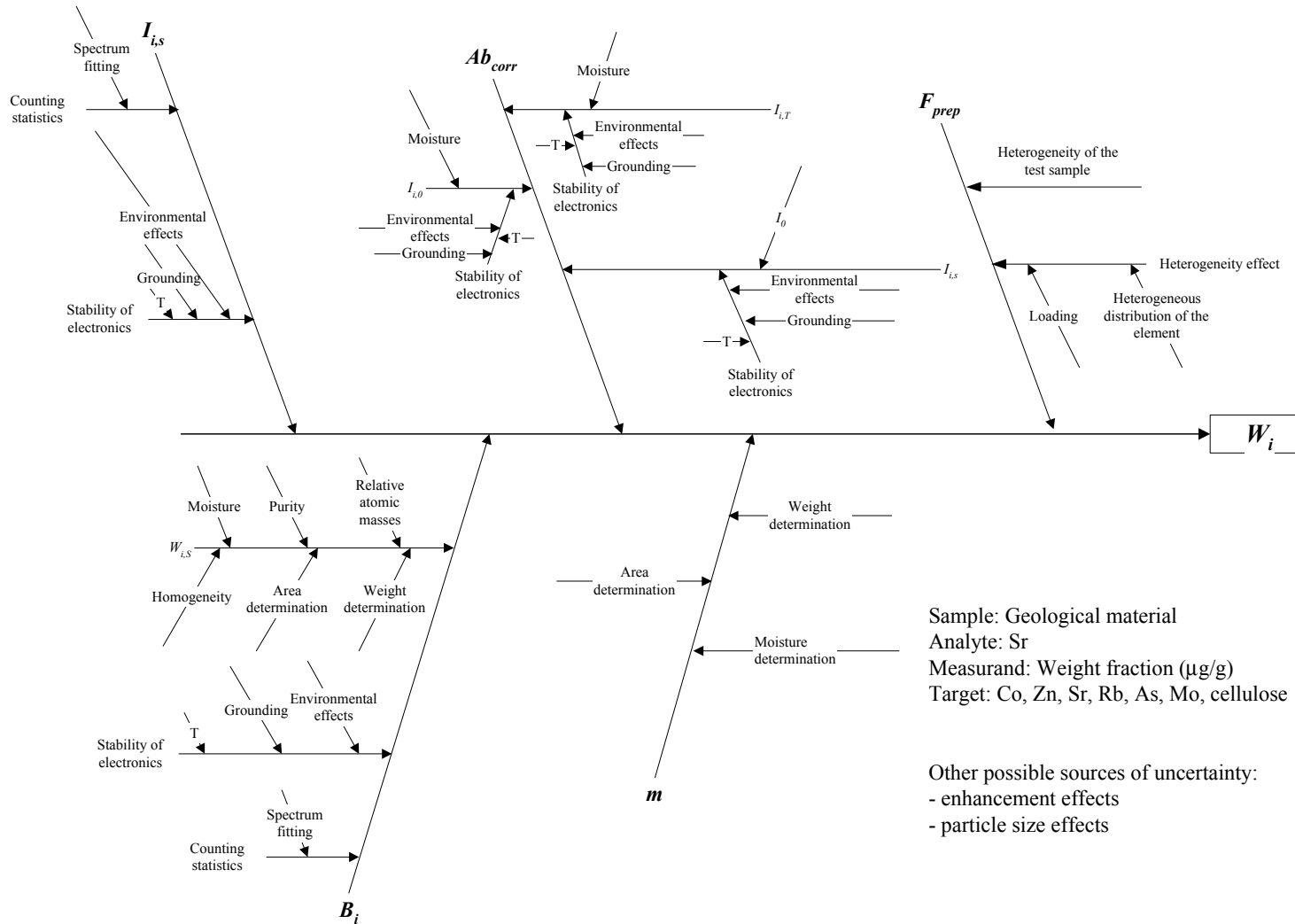
Symbol/ Reference to list	Value of variable	Uncer- tainty	Conversion factor to standard uncertainty	Stan- dard Uncer- tainty ( <i>u</i> )	Sensi- tivity Factor	Percent contri- bution to ( <i>u<sub>c</sub></i> ) <sup>2</sup>
$B_i$ (see 2.3.1)	$5.494 \times 10^5$ [c/mg/cm <sup>2</sup> ]	$9.017 \times 10^3$ [c/mg/cm <sup>2</sup> ]	1	0.0164	$-1.82 \times 10^{-10}$	8.8
$F_{prep}$ (see 2/3/3)	1	0.05	1	0.05	$10^{-4}$	73.5
$I_{i,s}$ (see 2.3.4)	2974 [counts]	70 [counts]	1	0.0235	$3.36 \times 10^{-8}$	17.6
$Ab_{corr}$ (see 2.3.4)	1.6	0.0028	1	0.0028	$6.25 \times 10^{-5}$	0.1

### REFERENCES

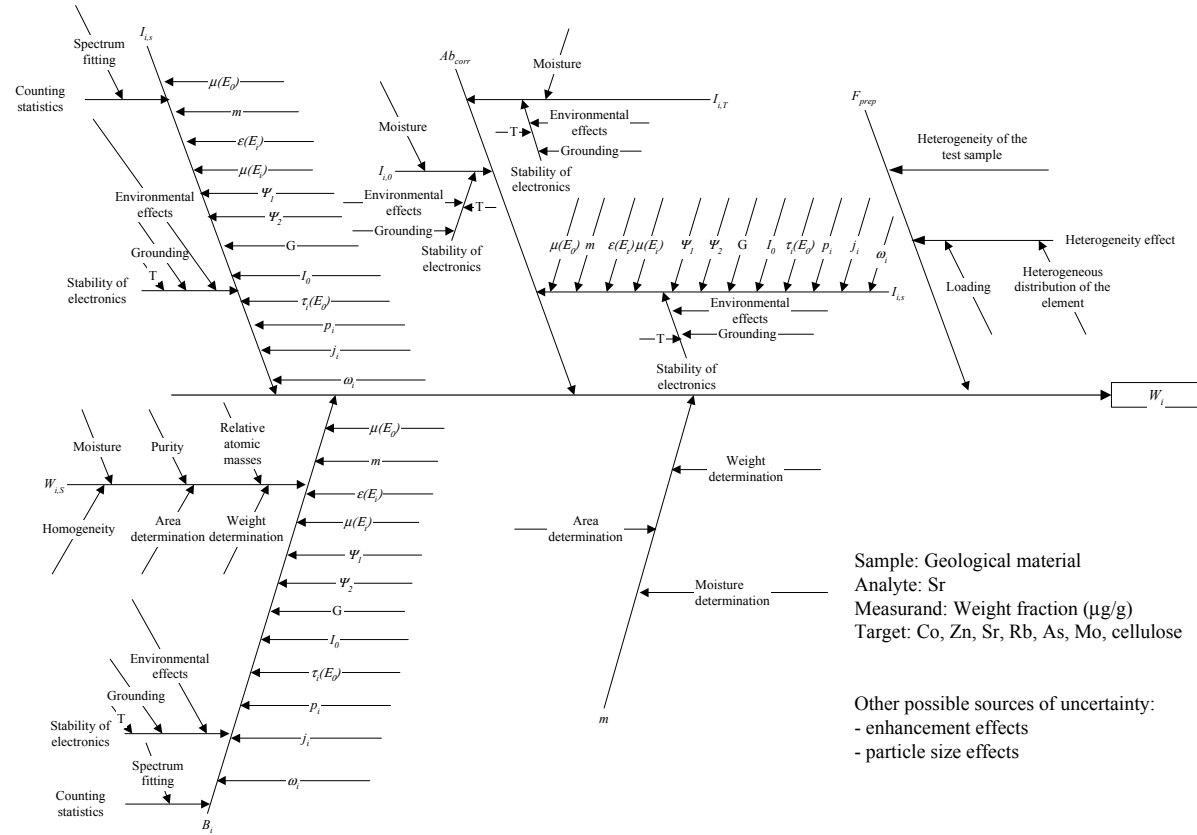
- [1] MARKOWICZ, A.A., VAN GRIEKEN, R.E., Quantification in XRF analysis of intermediate thickness samples, in: Handbook of X ray Spectrometry, VAN GRIEKEN, R.E., MARKOWICZ, A.A., Eds., Marcel Dekker, Inc., New York (1993) 339-358.
- [2] VAN ESPEN, P., JANSSENS, K., SWENTERS, I., AXIL X ray Analysis Software. Canberra Packard, Benelux.
- [3] MARKOWICZ, A., ABDUNNABI, A.A., Study of the effect of sample loading heterogeneity in the energy-dispersive X ray fluorescence analysis of specimens of intermediate thickness, X ray Spectrometry **20** (1991) 97-101.
- [4] MARKOWICZ, A., HASELBERGER, N., EL HASSAN, H.S., SEWANDO, M.S.A., Accuracy of the emission-transmission method applied in XRF analysis of intermediate thickness samples, J. Radioanal. Nucl. Chemistry, **158** 2 (1992) 409-415

# INTERMEDIATE THICKNESS EDXRF

Simplified cause and effect diagram



### INTERMEDIATE THICKNESS EDXRF Cause and effect diagram



## SYMBOLS AND ABBREVIATIONS

$Ab_{corr}$	Absorption correction factor
AXIL	Software package for spectrum fitting
$B_i$	Calibration factor
EDXRF	Energy Dispersive X ray Fluorescence
$E_i$	Energy of the characteristic X rays of the $i$ -th element
$E_0$	Energy of the primary radiation
$\varepsilon(E_i)$	Detector efficiency
$F_{prep}$	Correction factor for sample preparation
G	Geometrical constant
$I_0$	Intensity of the primary radiation
$I_{i,s}$	Intensity of the characteristic X rays of the $i$ -th element in the analysed sample
$j_i$	Absorption jump factor
k	Coverage factor
$m$	Total mass of a sample per unit area
$m_i$	Mass per unit area for the $i$ -th element in the analysed sample
$m_{thin}$	Total mass per unit area for the so-called thin samples
$p_i$	Transition probability for a given spectra line in an X ray series for the $i$ -th element
$u(Ab_{corr})$	Standard uncertainty of the absorption correction factor
$u(B_i)$	Standard uncertainty of the calibration factor for the $i$ -th element
$u(F_{prep})$	Standard uncertainty of the correction for sample preparation
$u(inst)$	Standard uncertainty for instability of the EDXRF spectrometer
$u(I_{i,s})$	Standard uncertainty of the intensity of the characteristic X rays of the $i$ -th element in the analysed sample
$u(m)$	Standard uncertainty of the total mass per unit area for the analysed sample
$u(W_i)$	Standard uncertainty of the elemental concentration
$u_c$	Combined relative uncertainty of the elemental concentration
$\mu(E_0)$	Total mass attenuation coefficient for the primary radiation of energy $E_0$ in the whole sample
$\mu(E_i)$	Total mass attenuation coefficient for the characteristic X rays of the $i$ -th in the whole sample
$\tau_i(E_0)$	Photo - electric mass absorption coefficient of the primary radiation in the $i$ -th element
$\omega_i$	Fluorescence yield for the $i$ -th element
$\Psi_1$	Effective incident angle for the primary radiation
$\Psi_2$	Effective take-off angle for the characteristic X rays
$W_i$	Concentration of the $i$ -th element in the analysed sample expressed as weightfraction (or $\mu\text{g g}^{-1}$ )
$W_{i,s}$	Concentration of the $i$ -th element in the calibration sample expressed as weight fraction (or $\mu\text{g g}^{-1}$ )

# EDXRF ANALYSIS OF THIN SAMPLES

A. TAJANI, A. MARKOWICZ

Agency's Laboratories, International Atomic Energy Agency, Seibersdorf

## Abstract

X ray fluorescence (XRF) analysis refers to the measurements of characteristic X rays resulting from electrons filling the inner shell vacancies produced in the sample by means of a suitable source of radiation. Energy dispersive XRF (EDXRF) measures the energy of the emitted X rays by collecting the ionisation products induced in a solid state semiconductor detector. On their pathway through the sample, the exciting radiation and the emitted radiation are attenuated. The samples are categorised in thin, intermediate and thin samples by their attenuation factor. Common sources of uncertainty are discussed and quantified for each category, including the subsampling, the sample preparation and the degree of homogeneity of the sample, the calibration and the stability of the EDXRF spectrometer, the evaluation of the spectra, and the absorption correction factor. For thin samples with a low attenuation factor, a single absorption correction factor and its associated uncertainty is estimated.

## 1. INTRODUCTION

X ray Fluorescence (XRF) analysis is based on the measurements of the characteristic X rays resulting from the deexcitation of inner shells vacancy produced in the sample by means of suitable source of electromagnetic radiation. Energy-dispersive XRF analysis (EDXRF) employs detectors that directly measure the energy of the X rays by collecting the ionisation products in a suitable detecting medium (nowadays semiconductor materials). In this example EDXRF is used to analyse samples which total mass per unit area satisfies the condition [1]

$$m_{thin} \leq \frac{0.1}{\mu(E_0) \csc \Psi_1 + \mu(E_i) \csc \Psi_2} \quad (1)$$

where  $\mu(E_0)$  and  $\mu(E_i)$  are the total mass attenuation coefficients for the whole specimen at the energy of incident radiation,  $E_0$ , and characteristic radiation,  $E_i$ ;  $\Psi_1$  and  $\Psi_2$  are the effective incident and take-off angles.

In the absence of enhancement effects and assuming monochromatic excitation, the mass per unit area of the  $i$ -th element,  $m_i$ , for homogeneous samples, can be calculated from the following equation

$$m_i = \frac{I_{i,s}}{B_i} Ab_{corr} \quad (2)$$

where  $I_{i,s}$  is the intensity of the characteristic X rays of the  $i$ -th element,  $B_i$  is the calibration factor, and  $Ab_{corr}$  is the absorption correction factor which represents the combined attenuation of the primary and fluorescent radiations in the whole specimen [1]. The value of the calibration factor  $B_i$  can be determined either experimentally as the slope of the straight calibration line for the  $i$ -th element obtained with thin homogeneous samples or semi-empirically based on both an experimentally determined coefficient and the relevant fundamental parameters. The thin-sample technique can be applied for quantitative XRF analysis of various materials, including samples of environmental, biological and geological origin (e.g., soil, sediments, plants, filters loaded with air particulates, Millipore filters with precipitate etc.).

The concentration, in weight fraction, of the  $i$ -th element,  $W_i$ , is calculated from

$$W_i = \frac{I_{i,s}}{B_i m} Ab_{corr} \quad (3)$$

## 2. EXAMPLE

### 2.1. Specification

#### (a) *Technique*

An energy-dispersive spectrometer based on a secondary target excitation system (Mo-anode tube, 5 mA, 50 kV, measurement time = 2000 s) was used to analyse a thin-sample. The detection system consisted of a Si(Li) detector with resolution of 180 eV at 5.9 keV. Spectrum evaluation was performed by using the AXIL program [2].

#### (b) *Specimen*

A pellet with mass per unit area  $m = 0.0204 \text{ g/cm}^2$  was prepared by mixing 95 % of  $\text{C}_6\text{H}_{10}\text{O}_5$  and 5 % of  $\text{SrCO}_3$

#### (c) *Analyte*: Sr

#### (d) *Measurand*:

Concentration of Sr in the mixture of  $\text{SrCO}_3$  and  $\text{C}_6\text{H}_{10}\text{O}_5$ . The concentration of Sr was determined from Equation 3 (see Introduction).

### 2.2. Sources of uncertainty

1. Spectrum evaluation: Uncertainty in spectrum fitting
2. Calibration of the EDXRF spectrometer
3. Quantification: Absorption correction factor
4. Sample preparation:
  - 4.a Degree of homogeneity of the material
  - 4.b Purity of the material
5. Instability of the EDXRF spectrometer
6. Uncertainty in the sample mass to be analysed (weighing)

### 2.3. Quantification of uncertainty components

#### 2.3.1. *Spectrum evaluation*:

The fitting program is based on the least squares fitting procedure which provides the values of the net peak areas together with the associated uncertainties. In this example the values were:

$$I_{i,s} \pm u(I_{i,s}) = (147700 \pm 3000) \text{ counts}$$

#### 2.3.2. *Calibration of the EDXRF spectrometer*:

The calibration was performed by using single element foils or intermediate thickness pellets prepared from pure compounds. Based on the measurements the calibration factors,  $B_i$ , were calculated for 14 samples as the ratio of the intensity of the characteristic X rays of the

element of interest to the mass per unit area of that element in the calibration sample corrected ( if necessary) for the matrix absorption effects. The uncertainties of the experimental values for the calibration factors are calculated including the uncertainties of the characteristic X rays intensities, uncertainties of the mass per unit area of the element in the calibration sample and the uncertainties of the absorption correction factor. For each experimental point the uncertainty was smaller than 1 % relative. In the next step, a calibration curve for the factor vs. atomic number of the element was defined based on the least squares fitting procedure. Finally the uncertainty of the calibration of the EDXRF spectrometer was calculated as the root mean square of the differences between the experimental and fitted values (circa 5 %) [1].

### 2.3.3. Quantification:

Absorption correction factor. In the case of thin samples the value of  $Ab_{corr}$  is [1]

$$1 \leq Ab_{corr} \leq 1.0526$$

Considering  $Ab_{corr} = 1.0263$ , the uncertainty associated with the absorption correction factor is 0.0263.

### 2.3.4. Sample preparation:

- (a) The uncertainty due to the heterogeneity of the material was calculated as the standard deviation of the results from repetitive measurements of 10 subsamples randomly taken from the bottle and analysed under the same experimental conditions. It was estimated to be equal to 5%.
- (b) Uncertainty due to the purity of the sample analysed is equal to 0.1 % (negligible and ignored in further calculations).

### 2.3.5 Instability of the EDXRF spectrometer (including the detector efficiency, $\varepsilon(E_i)$ , the intensity of the primary radiation, $I_0$ , and the instability of electronics).

It was calculated from the results of 18 repetitive measurements of an Fe metal foil during 9 hours in a day at fixed time intervals. The mean value of the peak area of the Fe- $K_\alpha$  line and its uncertainty were calculated. After subtraction of the contribution of counting statistics, the uncertainty due to the instability of the EDXRF spectrometer was found to be 0.025 %

### 2.3.6. Uncertainty in weighing the sample to be analysed is about $10^{-4}$ g (negligible)

## 2.4. Conversion of uncertainties to standard deviations

- (a) Spectrum evaluation,  $u(I_{i,s})/I_{i,s} \approx 2\%$
- (b) Calibration of the EDXRF spectrometer,  $u(B_i) = 5\%$
- (c) Quantification,  $u(Ab_{corr}) = 1.5\%$  (assuming a rectangular distribution)
- (d) Sample preparation,  $u(F_{prep}) = 5\%$
- (e) Instability of the EDXRF spectrometer,  $u(inst) = 0.025\%$  (negligible and ignored in further calculations)

- (f) Weighing of sample mass,  $u(m) = 0.001\%$  (negligible and ignored in further calculations)

## 2.5. Sensitivity factors

Including a correction factor for the sample preparation,  $F_{prep}$ , ( $F_{prep} = 1$ ), Equation 3 becomes

$$W_i = \frac{I_{i,s}}{B_i m} Ab_{corr} F_{prep} \quad (4)$$

According to this equation the following sensitivity factors have been calculated:

$$\frac{\partial W_i}{\partial I_{i,s}} = \frac{Ab_{corr}}{B_i m} F_{prep} = 2.21 \times 10^{-4}$$

$$\frac{\partial W_i}{\partial B_i} = -\frac{I_{i,s}}{B_i^2 m} Ab_{corr} F_{prep} = -1.43 \times 10^{-4}$$

$$\frac{\partial W_i}{\partial Ab_{corr}} = \frac{I_{i,s}}{B_i m} F_{prep} = 31.76$$

$$\frac{\partial W_i}{\partial F_{prep}} = \frac{I_{i,s}}{B_i m} Ab_{corr} = 32.6$$

## 2.6. Calculation of combined uncertainty

The combined uncertainty  $u_c$  is calculated by applying the law of uncertainty propagation to Equation 4

$$u_c = \frac{u(W_i)}{W_i} = \sqrt{\left[\frac{u(I_{i,s})}{I_{i,s}}\right]^2 + \left[\frac{u(B_i)}{B_i}\right]^2 + \left[\frac{u(Ab_{corr})}{Ab_{corr}}\right]^2 + \left[\frac{u(F_{prep})}{F_{prep}}\right]^2} \quad (5)$$

## 2.7. Results

$$W_i = \frac{147700 \text{ counts}}{2.28 \times 10^5 \frac{\text{counts}}{\text{mg/cm}^2} \times 20.4 \frac{\text{mg}}{\text{cm}^2}} \times 1.0263 \times 1 \times 10^3 = 32.6 \text{ mg g}^{-1} \quad (6)$$

$$u_c = \frac{u(W_i)}{W_i} = \sqrt{\left(\frac{3000}{147700}\right)^2 + \left(\frac{1.14 \times 10^4}{2.28 \times 10^5}\right)^2 + \left(\frac{0.0152}{1.0263}\right)^2 + \left(\frac{0.05}{1}\right)^2 =$$

$$= \sqrt{4.12 \times 10^{-4} + 0.0025 + 0.0002 + 0.0025} = 0.075 \quad (7)$$

## 2.8. Expanded combined uncertainty

The expanded combined uncertainty is calculated by multiplying the combined uncertainty,  $u_c$ , by the coverage factor  $k = 2$ . This value for the coverage factor was chosen due to the fact that the two major sources of uncertainty,  $B_i$  and  $F_{prep}$  have enough degrees of freedom (10 and 9 respectively) to justify the use of the normal distribution. The final result is then

$$W_i = (33 \pm 5) \text{ mg g}^{-1}$$

Summary table

Symbol/ Reference to list	Value of variable	Uncer- tainty	Conversion factor to standard uncertainty	Standard uncertainty ( $u$ )	Sensitivity factor	Percent contribution to $u_c^2$
$I_{i,s}/2.3.1$	147700	3000	1	0.0203	$2.21 \times 10^{-4}$	7.3
$B_i/2.3.2$	$2.28 \times 10^5$	$1.14 \times 10^4$	1	0.05	$-1.43 \times 10^{-4}$	44.4
$Ab_{corr}/2.3.3$	1.0263	0.0263	$\frac{1}{\sqrt{3}}$	0.0152	31.76	3.9
$F_{prep}/2.3.4$	1	0.05	1	0.05	32.6	44.4

## REFERENCES

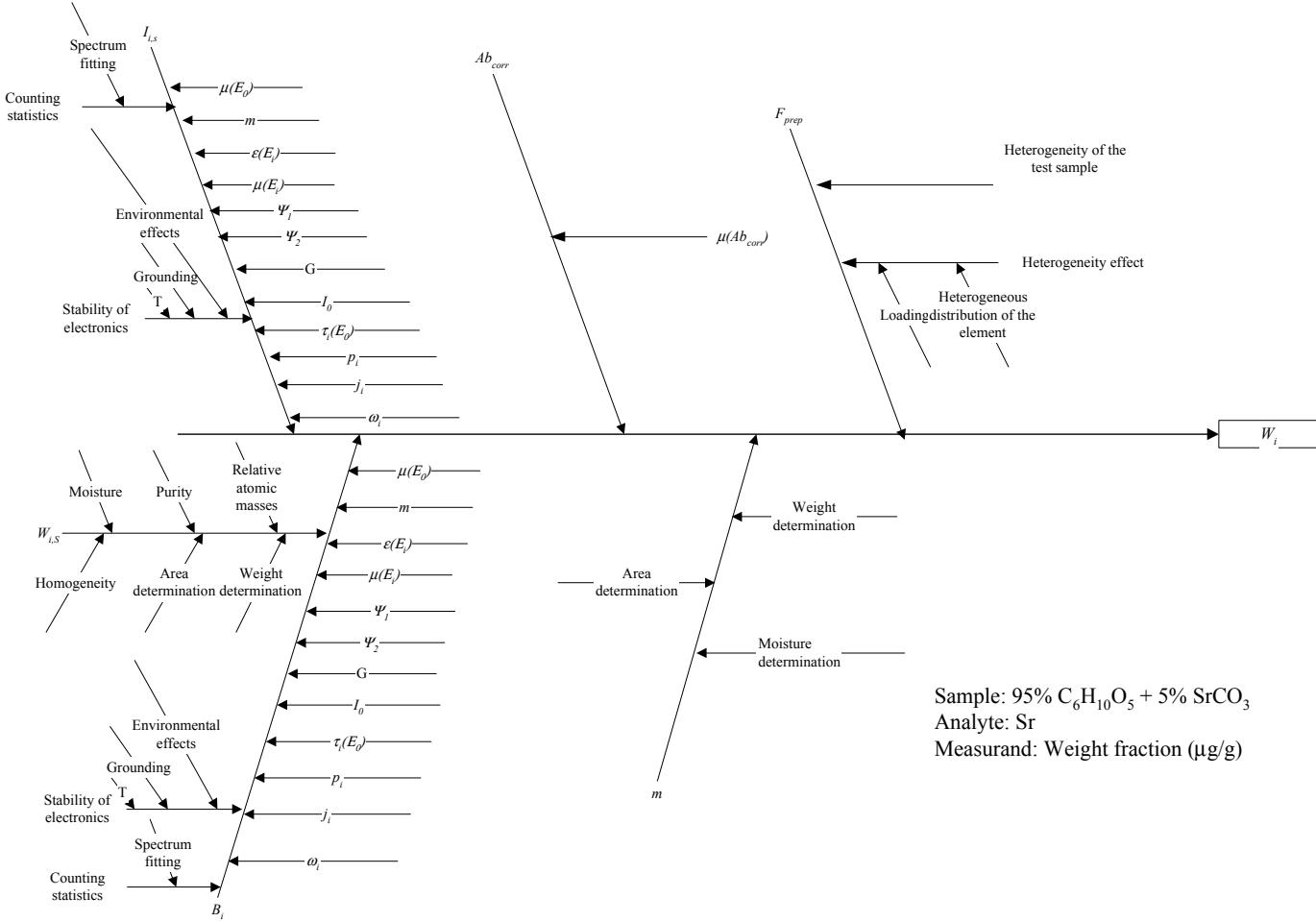
- [1] MARKOWICZ, A.A., VAN GRIEKEN, R.E., Handbook of X ray Spectrometry, Eds., Marcel Dekker, Inc., New York (1993).
- [2] VAN ESPEN, P., JANSSEN, K., SWENTERS, I., AXIL X ray Analysis Software, Canberra Packard, Benelux.

## SYMBOLS AND ABBREVIATIONS

$Ab_{corr}$	Absorption correction factor
AXIL	Software package for spectrum fitting
$B_i$	Calibration factor
EDXRF	Energy Dispersive X ray Fluorescence
$E_i$	Energy of the characteristic X rays of the $i$ -th element
$E_0$	Energy of the primary radiation
$\varepsilon(E_i)$	Detector efficiency
$F_{prep}$	Correction factor for sample preparation
G	Geometrical constant
$I_0$	Intensity of the primary radiation
$I_{i,s}$	Intensity of the characteristic X rays of the $i$ -th element in the analysed sample
$j_i$	Absorption jump factor
k	Coverage factor
$m$	Total mass of a sample per unit area
$m_i$	Mass per unit area for the $i$ -th element in the analysed sample
$m_{thin}$	Total mass per unit area for the so-called thin samples
$p_i$	Transition probability for a given spectra line in an X ray series for the $i$ -th element
$u(Ab_{corr})$	Standard uncertainty of the absorption correction factor
$u(B_i)$	Standard uncertainty of the calibration factor for the $i$ -th element
$u(F_{prep})$	Standard uncertainty of the correction for sample preparation
$u(inst)$	Standard uncertainty for instability of the EDXRF spectrometer
$u(I_{i,s})$	Standard uncertainty of the intensity of the characteristic X rays of the $i$ -th element in the analysed sample
$u(m)$	Standard uncertainty of the total mass per unit area for the analysed sample
$u(W_i)$	Standard uncertainty of the elemental concentration
$u_c$	Combined relative uncertainty of the elemental concentration
$\mu(E_0)$	Total mass attenuation coefficient for the primary radiation of energy $E_0$ in the whole sample
$\mu(E_i)$	Total mass attenuation coefficient for the characteristic X rays of the $i$ -th in the whole sample
$\tau_i(E_0)$	Photo-electric mass absorption coefficient of the primary radiation in the $i$ -th element
$\omega_i$	Fluorescence yield for the $i$ -th element
$\Psi_1$	Effective incident angle for the primary radiation
$\Psi_2$	Effective take-off angle for the characteristic X rays
$W_i$	Concentration of the $i$ -th element in the analysed sample expressed as weightfraction (or $\mu\text{g g}^{-1}$ )
$W_{i,s}$	Concentration of the $i$ -th element in the calibration sample expressed as weight fraction (or $\mu\text{g g}^{-1}$ )

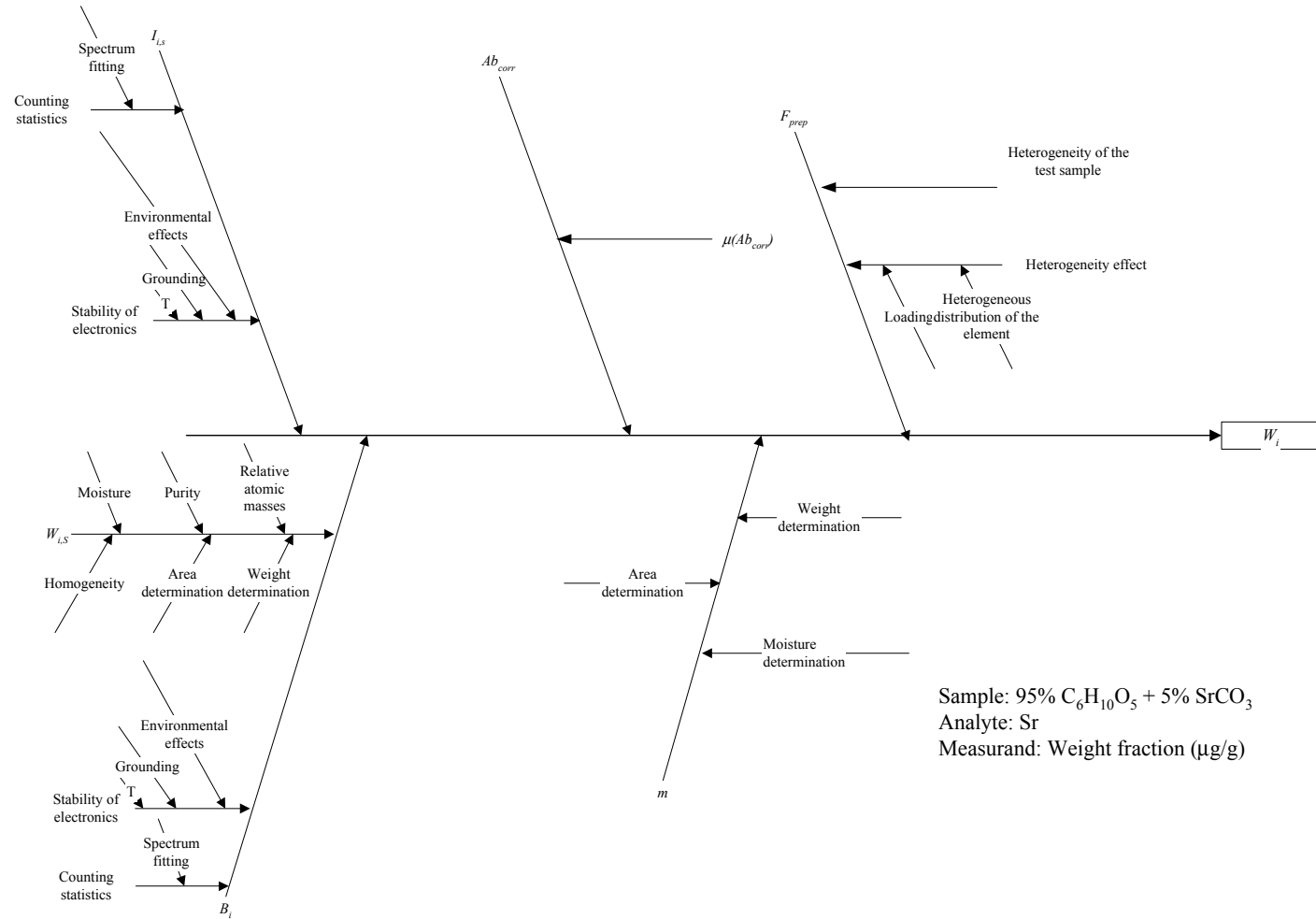
# EDXRF - THIN SAMPLE

Cause and effect diagram



## EDXRF - THIN SAMPLE

### Simplified cause and effect diagram



# EDXRF ANALYSIS OF THICK SAMPLES

A. TAJANI, A. MARKOWICZ

Agency's Laboratories, International Atomic Energy Agency, Seibersdorf

## Abstract

X ray fluorescence (XRF) analysis refers to the measurements of characteristic X rays resulting from electrons filling the inner shell vacancies produced in the sample by means of a suitable source of radiation. Energy dispersive XRF (EDXRF) measures the energy of the emitted X rays by collecting the ionisation products induced in a solid state semiconductor detector. On their pathway through the sample, the exciting radiation and the emitted radiation are attenuated. The samples are categorised in thin, intermediate and thin samples by their attenuation factor. Common sources of uncertainty are discussed and quantified for each category, including the subsampling, the sample preparation and the degree of homogeneity of the sample, the calibration and the stability of the EDXRF spectrometer, the evaluation of the spectra, and the absorption correction factor. Quantitative analysis of thick samples is based on the ratio of the fluorescent peak to the scattered (Compton) peak. The concentration of a particular element is calculated from a calibration line obtained by measuring a set of standards with known composition and fitting a least squares regression line through the data. Furthermore a matrix correction factor, obtained from another set of measurements, has to be applied. The example given for thick samples includes the quantification of the uncertainties associated with the least squares regression and with the matrix correction factor.

## 1. INTRODUCTION

The thick-sample technique is applied for quantitative EDXRF analysis of various materials, including samples of environmental, biological and geological origin which mass per unit area satisfies the condition [1]:

$$m_{thick} \geq \frac{4.61}{\mu(E_0) \csc \Psi_1 + \mu(E_i) \csc \Psi_2} \quad (1)$$

where  $\mu(E_0)$  and  $\mu(E_i)$  are the total mass attenuation coefficients for the whole specimen at the energy of incident radiation,  $E_0$ , and characteristic radiation,  $E_i$ ;  $\Psi_1$  and  $\Psi_2$  are the effective incident and take-off angles.

In this example the unknown concentration of the  $i$ -th analyte,  $W_{i, obs}$ , is calculated based on the ratio of the net fluorescent peak area  $I_{i,s}$  to the scattered Compton peak area  $I_C$  according to the formula:

$$W_{i, obs} = \frac{\left( \frac{I_{i,s}}{I_C} \right)_{obs} - c}{s} \quad (2)$$

$s$  and  $c$  are respectively the slope and the intercept of the calibration curve for the  $i$ -th element, determined by least squares regression for the results obtained for a set of standards of known concentration. The following expression is applied to calculate the coefficients  $s$  and  $c$ :

$$\frac{I_{i,s}}{I_C} = sW_i + c \quad (3)$$

## 2. EXAMPLE

### 2.1. Specification

(a) *Technique*:

An energy-dispersive spectrometer based on a radioisotope excitation source (Cd-109, measurement time = 2000 s) was used to analyse a thick-sample. The detection system consisted of a Si(Li) solid state detector with resolution (FWHM) of 180 eV at 5.9 keV. Spectrum evaluation was performed by using the AXIL program [2].

(b) *Specimen*:

A pellet of geological material with mass per unit area,  $m=1.02 \text{ g/cm}^2$ , was prepared and analysed.

(c) *Analyte*: Pb.

(d) *Measurand*:

Concentration of Pb in a soil sample (see Equation 2).

### 2.2. Sources of uncertainty

The main sources of uncertainties which contribute to the uncertainty of the concentration  $W_{i,obs}$  are the following:

- (a) Uncertainty from linear least squares calibration (see Equation 3)
- (b) Sample preparation
- (c) Quantification
- (d) Instability of the EDXRF spectrometer

[6]

### 2.3. Quantification of uncertainty components

2.3.1. The uncertainty from linear least squares calibration is given by the root mean square

(RMS) of the residuals  $\left(\frac{I_{i,s}}{I_C}\right)_{obs,j} - \left(\frac{I_{i,s}}{I_C}\right)_{fit,j}$  (3)

$$RMS\ uncertainty = \frac{\sqrt{\sum_{j=1}^n \left[ \left(\frac{I_{i,s}}{I_C}\right)_{obs,j} - \left(\frac{I_{i,s}}{I_C}\right)_{fit,j} \right]^2}}{\sqrt{n}} \quad (4)$$

where  $\left(\frac{I_{i,s}}{I_C}\right)_{obs,j}$  are the measured values while  $\left(\frac{I_{i,s}}{I_C}\right)_{fit,j}$  are the values found from

Equation 3.

In the current example four standards with different matrices and various known concentrations of Pb were used to find the calibration curve and determine the parameters  $s$  and  $c$ .

In Table 1 the values of  $\left(\frac{I_{i,s}}{I_C}\right)_{obs,j}$ ,  $\left(\frac{I_{i,s}}{I_C}\right)_{fit,j}$  and  $W_i$  are listed. The slope  $s = 0.00013$ , the intercept  $c = -0.0011$  and the root mean square  $RMS = 7.2 \times 10^{-3}$  were found.

**Table 1: Parameters used for calibration**

$\left(\frac{I_{i,s}}{I_C}\right)_{obs,j}$	$\left(\frac{I_{i,s}}{I_C}\right)_{fit,j}$	$W_i$ ( $\mu\text{g g}^{-1}$ )
0.0164	0.0140	116
0.0697	0.0653	511
0.1302	0.1302	1010
0.2200	0.2065	1597

### 2.3.2. Sample preparation:

The uncertainty due to the heterogeneity of the material was calculated as the standard deviation of the results from repetitive measurements of 10 subsamples randomly taken from the bottle and analysed under the same experimental conditions. It was estimated to be equal to 5%

### 2.3.3. Quantification:

The uncertainty due to the incomplete correction for the matrix absorption effect was experimentally estimated and found less than 5 %

### 2.3.4. Instability of the EDXRF spectrometer (including the detector efficiency, $\epsilon(E_i)$ , the intensity of the primary radiation, $I_0$ , and the instability of electronics).

It was calculated from the results of 18 repetitive measurements of an Fe metal foil during 9 hours in a day at fixed time intervals. The mean peak area of the Fe- $K_{\alpha}$  line and its uncertainty (standard deviation) were calculated. After subtraction of the contribution of counting statistics, the instability of the EDXRF spectrometer was found to be 0.025 %.

## 2.4. Conversion of uncertainties to standard deviations

- Linear least squares calibration,  $u(cal) = \frac{RMS}{s} \times \sqrt{\frac{n}{n-2}} = 78$  (see Ref. 3)
- Sample preparation,  $u(F_{prep}) = 5\%$
- Quantification,  $u(F_{matrix}) = 5\%$
- Instability of the EDXRF spectrometer,  $u(inst) = 0.025\%$  (negligible)

## 2.5. Sensitivity factors

Including the correction factors  $F_{prep}$ , related to the sample preparation step, and  $F_{matrix}$ , due to the incomplete correction for the matrix absorption effect, both equal to 1, Equation 2 becomes

$$W_{i,obs} = \left[ \frac{\left( \frac{I_{i,s}}{I_C} \right)_{obs} - c}{s} \right] F_{prep} F_{matrix} \quad (5)$$

Assuming that  $\frac{\left( \frac{I_{i,s}}{I_C} \right) - c}{s} = Y$ , the following sensitivity factors were calculated:

$$\frac{\partial W_{i,obs}}{\partial Y} = F_{prep} F_{matrix} = 1$$

$$\frac{\partial W_{i,obs}}{\partial F_{matrix}} = \frac{\left( \frac{I_{i,s}}{I_C} - c \right)}{s} F_{prep} = 986$$

$$\frac{\partial W_{i,obs}}{\partial F_{prep}} = \frac{\left( \frac{I_{i,s}}{I_C} - c \right)}{s} F_{matrix} = 986$$

## 2.6. Calculation of combined uncertainty

By applying the law of uncertainty propagation to the modified equation 5, the combined relative uncertainty  $u_c$  is calculated [3]

$$u_c = \frac{u(W_{i,obs})}{W_{i,obs}} = \sqrt{\frac{[u(cal)]^2 s^2}{\left[ \left( \frac{I_{i,s}}{I_C} \right)_{obs} - c \right]^2} + \left[ \frac{u(F_{prep})}{F_{prep}} \right]^2 + \left[ \frac{u(F_{matrix})}{F_{matrix}} \right]^2} \quad (6)$$

## 2.7. Results

For the unknown sample:

$$\left( \frac{I_{i,s}}{I_C} \right)_{obs,j} = 0.1271 \quad \text{and} \quad W_{i,obs} = \frac{0.1271 + 0.0011}{0.00013} = 986 \mu\text{g g}^{-1}$$

$$u_c = \sqrt{\frac{(7.2 \times 10^{-3})^2 \times 4}{2 \times (0.1271 + 0.0011)^2} + \left(\frac{0.05}{1}\right)^2 + \left(\frac{0.05}{1}\right)^2} = \sqrt{0.0063 + 0.0025 + 0.0025} = 0.1063$$

## 2.8. Expanded combined uncertainty

The expanded combined uncertainty is calculated by multiplying the combined uncertainty,  $u_c$ , by the coverage factor  $k = 4.3$  (from the Student's  $t$  distribution for 2 degrees of freedom and  $\alpha = 0.05$ ). The final result is then

$$W_i = (986 \pm 450) \mu\text{g g}^{-1}$$

Summary table

<i>Symbol/ Reference to list</i>	<i>Value of variable</i>	<i>Uncer- tainty</i>	<i>Conversion factor to standard uncertainty</i>	<i>Standard uncertainty (u)</i>	<i>Sensiti- vity factor</i>	<i>Percent contribu- tion to <math>u_c^2</math></i>
<i>RMS/ III.3</i>	986	78	1	78	1	55.8
<i>F<sub>prep</sub> / III.2</i>	1	0.05	1	0.05	986	22.1
<i>F<sub>matrix</sub> / III.4</i>	1	0.05	1	0.05	986	22.1

## REFERENCES

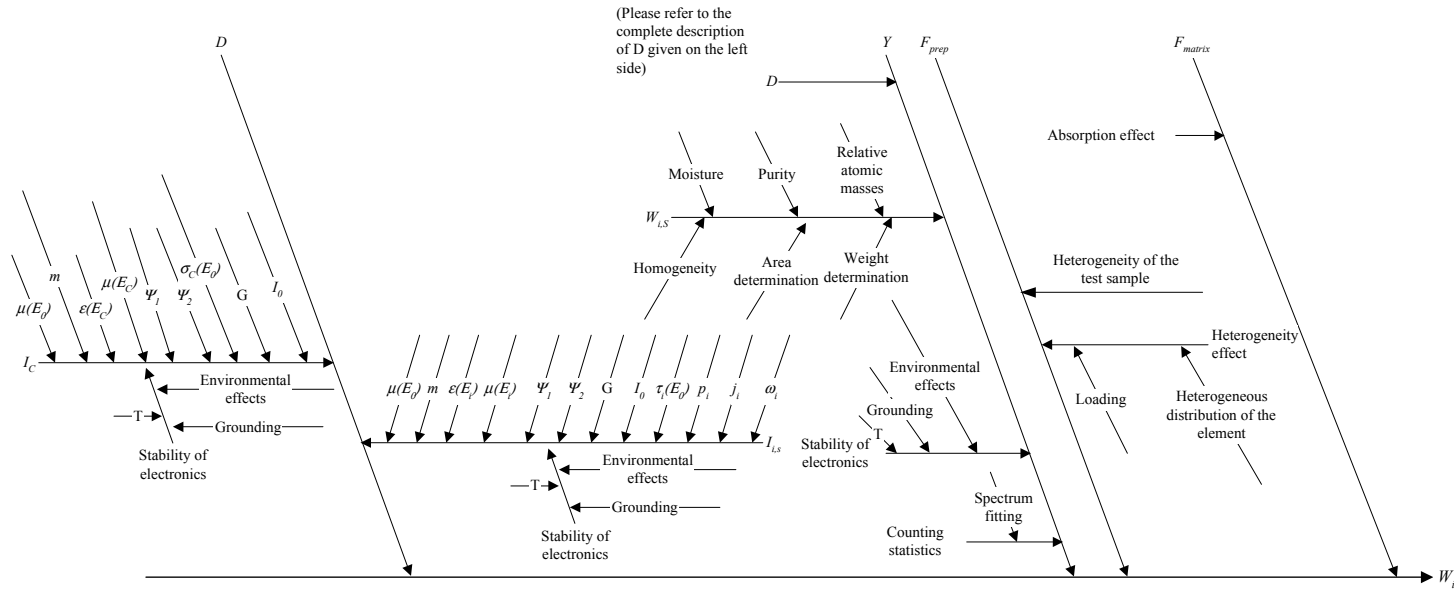
- [1] MARKOWICZ, A.A., VAN GRIEKEN, R.E., Handbook of X ray Spectrometry, Eds., Marcel Dekker, Inc., New York (1993).
- [2] VAN ESPEN, P., JANSSEN, K., SWENTERS, I., AXIL X ray Analysis Software, Canberra Packard, Benelux.
- [3] EURACHEM, "Quantifying Uncertainty in Analytical Measurement", Editor: Laboratory of the Government Chemist Information Services, Teddington (Middlesex) & London (1995). ISBN 0-948926-08-2.

## SYMBOLS AND ABBREVIATIONS

AXIL	Software package for spectrum fitting
$C$	Intercept of the calibration curve
EDXRF	Energy Dispersive X ray Fluorescence
$E_i$	Energy of the characteristic X rays of the $i$ -th element
$E_0$	Energy of the primary radiation
$\varepsilon(E_i)$	Detector efficiency at the energy of the characteristic X rays of the $i$ -th element
$\varepsilon(E_C)$	Detector efficiency at the Compton scattered radiation
$F_{prep}$	Correction factor for sample preparation
$F_{matrix}$	Correction factor for matrix absorption
$G$	Geometrical constant
$I_0$	Intensity of the primary radiation
$I_{i,s}$	Intensity of the characteristic X rays of the $i$ -th element in the analysed sample
$I_C$	Intensity of the Compton scattered radiation
$j_i$	Absorption jump factor
$k$	Coverage factor
$m$	Total mass of a sample per unit area
$m_i$	Mass per unit area for the $i$ -th element in the analysed sample
$m_{thick}$	Total mass per unit area for the so called thick samples
$n$	Number of calibration samples
$p_i$	Transition probability for a given fluorescence line for the $i$ -th element
$RMS$	Root mean square
$s$	Slope of the calibration curve
$c$	Intercept of the calibration curve
$u(cal)$	Standard uncertainty due to the linear least squares calibration
$u(F_{prep})$	Standard uncertainty of the correction for sample preparation
$u(F_{matrix})$	Standard uncertainty of the correction for matrix absorption
$u(inst)$	Standard uncertainty for instability of the EDXRF spectrometer
$u(m)$	Standard uncertainty of the total mass per unit area for the analysed sample
$u(W_i)$	Standard uncertainty of the elemental concentration
$u_c$	Combined relative uncertainty of the elemental concentration
$\mu(E_0)$	Total mass attenuation coefficient for the primary radiation of energy $E_0$ in the whole sample
$\mu(E_C)$	Total mass attenuation coefficient for the Compton scattered radiation in the whole sample
$\mu(E_i)$	Total mass attenuation coefficient for the characteristic X rays of the $i$ -th element in the whole sample
$\sigma_C(E_0)$	Compton mass-scattering coefficient of the sample material for the primary radiation
$\tau_i(E_0)$	Photo-electric mass absorption coefficient of the primary radiation in the $i$ -th element

$\omega_i$	Fluorescence yield for the $i$ -th element
$\Psi_1$	Effective incident angle for the primary radiation
$\Psi_2$	Effective take-off angle for the characteristic X rays
$W_i$	Concentration of the $i$ -th element in the analysed sample expressed as weight fraction (or $\mu\text{g g}^{-1}$ )
$W_{i,S}$	Concentration of the $i$ -th element in the calibration sample expressed as weight fraction (or $\mu\text{g g}^{-1}$ )

### EDXRF - THICK SAMPLE Cause and effect diagram



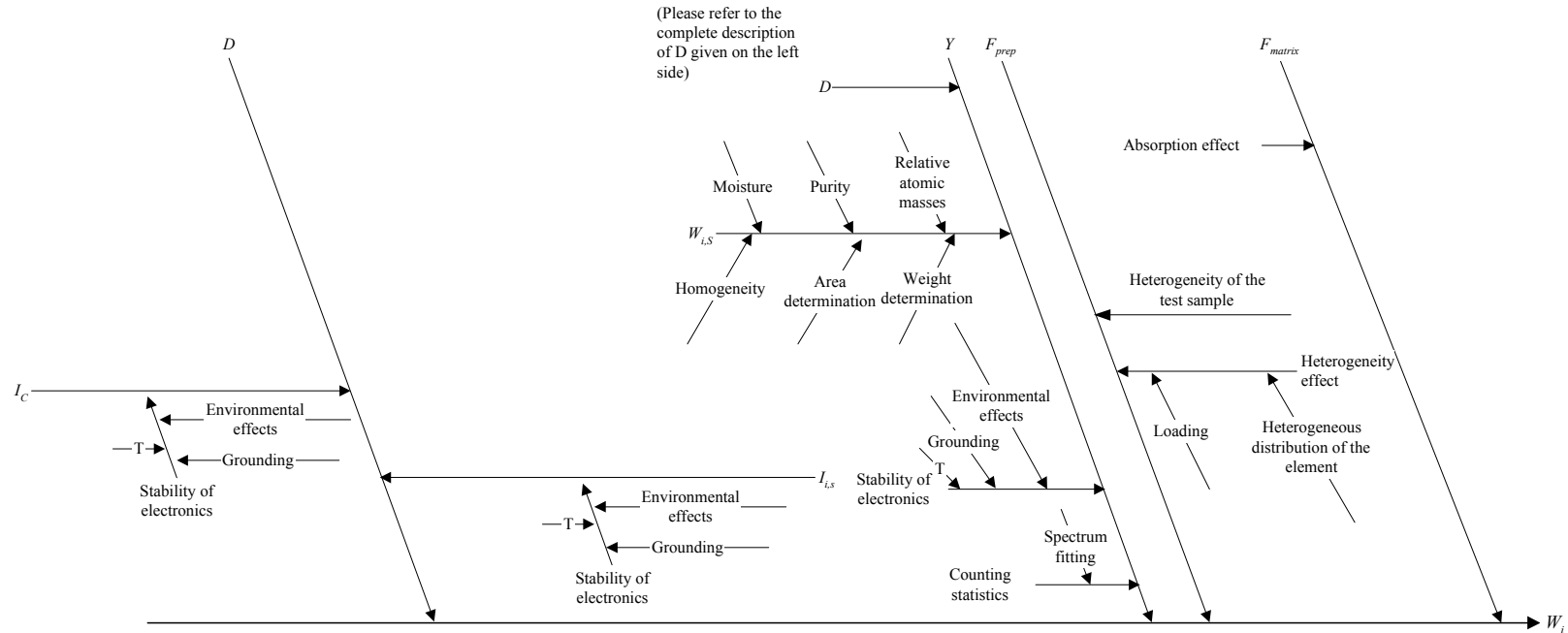
$$Y = \frac{I_{i,s}}{I_c} - c$$

$$\frac{I_{i,s}}{I_c} = D$$

Sample: Geological material  
 Analyte: Pb  
 Measurand: weight fraction ( $\mu\text{g/g}$ )  
 Other possible sources of uncertainty:  
 - Enhancement effects  
 - Particle size effects

# EDXRF - THICK SAMPLE

## Simplified cause and effect diagram



$$Y = \frac{I_{i,s} - c}{I_c} \quad \frac{I_{i,s}}{I_c} = D$$

Sample: Geological material  
 Analyte: Pb  
 Measurand: weight fraction ( $\mu\text{g/g}$ )  
 Other possible sources of uncertainty:  
 - Enhancement effects  
 - Particle size effects

# PIXE ANALYSIS OF ALUMINIUM IN FINE ATMOSPHERIC AEROSOL PARTICLES COLLECTED ON NUCLEPORE POLYCARBONATE FILTER

W. MAENHAUT

University of Gent, Department of Analytical Chemistry, Institute for Nuclear Sciences,  
Gent, Belgium

## Abstract

Particle induced X ray emission (PIXE) is an analytical technique based on the bombardment of the sample with high energy protons, which gives rise to the emission of characteristic X rays. PIXE is often the technique of choice for multi-element analysis of atmospheric aerosol samples and the example deals with such an application. The sources of uncertainty are grouped into six categories. First, sources associated with the instrumentation, e.g. the accelerator energy, the beam intensity and homogeneity, the X ray detector, etc. are discussed and quantified. A second category addresses the uniformity, purity and mass per unit area of the calibration standard. The third category concerns uncertainty sources associated with the aerosol filter, including the effective particle diameter, the volume of air sampled, the lateral uniformity, the depth profile and the blank values. The fourth category deals with the bombardment of the specimen and the acquisition of the X ray spectrum and evaluates the effects of deterioration of the deposit and the filter, induced changes in matrix composition and losses in the X ray detector and associated electronics. The fifth and sixth categories address respectively the uncertainties introduced by the data processing and spectrum fitting procedures, and the correction factors for matrix effects.

## 1. INTRODUCTION

Particle-induced X ray emission (PIXE) is an analytical technique which is based on the fact that the bombardment of a sample with protons (or heavier ions) of a few MeV gives rise to the emission of characteristic X rays. Protons with energies in the range of 1-4 MeV are usually employed for the excitation and the X rays emerging from the sample are normally measured with an energy-dispersive Si(Li) detection system. The major advantages of PIXE are its multielement character (as in other X ray emission techniques, all elements from Na to U can in principle be measured), the high sensitivity (relative detection limits down to 0.1  $\mu\text{g/g}$ , absolute detection limits down to  $10^{-12}$  g in normal macro-PIXE and down to  $10^{-15}$  g in micro-PIXE), the smooth variation of the relative detection limit with atomic number of the analyte element, the ability to analyze tiny samples (1 mg or less), the speed of the analysis (1-10 min bombardment time per sample), the possibility for automation, and the fact that it is often non-destructive. Limitations of the technique are that it suffers from spectral interferences, that matrix effects have to be accounted for, that the sample mass actually probed in the analysis is at most 10 mg, and that it does not allow the direct measurement of ultra-trace elements that are present at ng per g levels. A comprehensive coverage of PIXE can be found in two textbooks [1,2] and in book chapters [e.g. 3].

PIXE is often the technique of choice for the multielemental analysis of atmospheric aerosol samples. The example chosen here deals with such application. It presents the determination of aluminium in fine atmospheric aerosol particles collected on Nuclepore polycarbonate filter. Nuclepore polycarbonate filter is the most suitable aerosol filter for subsequent PIXE analysis. It has the advantage that the aerosol particles are essentially collected on the surface of the filter, so that no matrix effects are caused by the filter itself. Such effects may be important with fiber filters or membrane filters, and appropriate corrections are needed with such filter types [4]. On the other hand, the use of Nuclepore polycarbonate filter for the aerosol collection does not imply that matrix effects are then nonexistent in PIXE. So-called "particle size" effects [5] still remain. These effects are usually negligible for the elements

from K upward, but not for the lighter elements (Na to Cl). PIXE of these light elements (that is in the energy region 1-3 keV) is also complicated by the fact that their peaks are superimposed on an intense background and that the discrimination between both is not easy in this region of the PIXE spectrum [6]. Consequently, for the analyte element Al chosen here, the sources of uncertainty are much larger than when for example Fe or Zn would have been selected.

## 2. SPECIFICATION

### 2.1. Technique

All PIXE bombardments in the example are performed with a 2.5 MeV proton beam which is provided by an electrostatic accelerator. The specimens (sample, standard) are irradiated in vacuum, and the beam size at the specimen is 0.5 cm<sup>2</sup>. The beam is laterally uniform. A Faraday cup and current integrator are used for measuring the beam current and the integrated charge (proton dose). The X rays are measured with a Si(Li) detector, which has its entrance window inside the vacuum chamber. A thin Be foil is placed in front of Si(Li) in order to stop the protons scattered from the specimen. Pile-up rejection and live-time correction are applied in the pulse processing and spectrum acquisition. The count rate is below 3000 counts per s in all measurements. The angles between the incident proton beam and the specimen surface ( $\theta$ ) and between the specimen surface and the specimen detector axis ( $\varphi$ ) are each 67.5°. The PIXE spectra are analyzed with the nonlinear least-squares fitting program AXIL-84 [7], which provides net peak areas and associated standard deviations (essentially due to counting statistics) for the X ray lines in the spectrum. The Al  $K\alpha$  line is used for the quantification, and the amount of Al in the sample is derived from a comparison with a standard (relative method of quantification [8]).

### 2.2. Specimens

The unknown sample consists of fine (that is <2  $\mu\text{m}$  equivalent aerodynamic diameter (EAD)) aerosol particles, which are collected on a 47-mm diameter Nuclepore polycarbonate filter (of 0.4  $\mu\text{m}$  pore size) with a Gent PM10 stacked filter unit (SFU) sampler [9]. The aerosol deposit on the filter does not comprise more than one monolayer of particles and the surface area of this deposit is 12.88 cm<sup>2</sup>. The aerosol deposit is laterally uniform, when considering areas on the filter of 0.5 cm<sup>2</sup> or larger.

The standard is a so-called thin-film standard. It consists of a uniform layer of Al metal (50  $\mu\text{g}/\text{cm}^2$ ) on a thin Mylar backing film and was obtained from MicroMatter Corporation (Deer Harbor, WA, USA) [10].

### 2.3. Analyte

The element Al is the analyte.

### 2.4. Measurand

The concentration of fine (<2  $\mu\text{m}$  EAD) particulate Al in the air is the measurand, and it is calculated as follows:

$$C_{Al,air} = \frac{Y_{K\alpha(Al),sample} F_{matr,sample} Q_{stand} (C_{Al} \rho t)_{stand} 1000 A_{filter}}{Q_{sample} Y_{K\alpha(Al),stand} F_{matr,stand} V_{air}}$$

where

$C_{Al,air}$	=	concentration of fine Al in the air (ng/m <sup>3</sup> )
$Y_{K\alpha(Al),sample}$	=	net peak area (in counts) for Al $K\alpha$ in the PIXE spectrum from the sample
$F_{matr,sample}$	=	PIXE matrix correction factor for Al in the sample
$Q_{sample}$	=	preset proton charge for the PIXE bombardment of the sample ( $\mu\text{C}$ )
$Y_{K\alpha(Al),stand}$	=	net peak area (in counts) for Al $K\alpha$ in the PIXE spectrum from the standard
$F_{matr,stand}$	=	PIXE matrix correction factor for Al in the standard
$Q_{stand}$	=	preset proton charge for the PIXE bombardment of the standard ( $\mu\text{C}$ )
$(C_{Al}\rho t)_{stand}$	=	mass thickness of Al in the standard ( $\mu\text{g}/\text{cm}^2$ ); $C_{Al}$ denotes the concentration of Al in the standard and $\rho t$ the mass thickness of the standard
$A_{filter}$	=	area of the aerosol deposit on the filter sample ( $\text{cm}^2$ )
$V_{air}$	=	volume of air passed through the filter sample ( $\text{m}^3$ )

When the specimen has a uniform thickness and composition and is larger than the size of the PIXE beam, the matrix correction factor can be calculated as follows (using fundamental parameters):

$$F_{matr}(X_{pZ}) = \frac{\sigma(E_0) \rho t / \sin \theta}{\int_{E_0}^{E_f} \frac{\sigma(E) T_p(E)}{S(E)} dE}$$

where  $X_{pZ}$  represents the X ray line used for analysis (characteristic line  $p$  of analyte element with atomic number  $Z$ ),  $\sigma(E)$  the  $K$  ionization cross-section for the analyte element at proton energy  $E$ ,  $\rho t$  the mass thickness of the specimen, and  $\theta$  the angle between the incident proton beam and the specimen surface;  $E_0$  and  $E_f$  are respectively the incident proton energy and the energy of the protons after passage through the specimen ( $E_f = 0$  for an infinitely thick specimen);  $T_p(E)$  denotes the transmission of the X rays from successive depths in the specimen, and  $S(E)$  is the matrix stopping power.  $T_p(E)$  is itself given by:

$$T_p(E) = \exp \left( - \frac{\mu_p \sin \theta}{\sin \phi} \int_{E_0}^E \frac{dE}{S(E)} \right)$$

with  $\mu_p$  the mass attenuation coefficient for line  $p$  in the sample matrix, and  $\phi$  the angle between the specimen surface and the specimen-detector axis (i.e., the X ray take-off angle). It should be noted here that the matrix correction factor, as expressed by Equations (2) and (3), does not include secondary or tertiary fluorescence enhancement effects.

Prior to the PIXE bombardments of the aerosol filter sample and the thin-film standard, the following data needed for the calculation of the measurand are available:

$(C_{Al}\rho t)_{stand}$	=	50 $\mu\text{g}/\text{cm}^2$
$A_{filter}$	=	12.88 $\text{cm}^2$
$V_{air}$	=	21.5 $\text{m}^3$

The preset charges used in PIXE and the net peak areas obtained by the spectrum analysis are the following:

$Q_{stand}$	=	1 $\mu\text{C}$
$Q_{sample}$	=	100 $\mu\text{C}$

$$\begin{aligned}
Y_{K\alpha(Al),stand} &= 35272 \pm 303 \\
Y_{K\alpha(Al),sample} &= 3153 \pm 342
\end{aligned}$$

The uncertainties associated with the Al  $K\alpha$  peak areas are standard uncertainties (**u**) which are obtained from the spectrum fitting, and they only include the uncertainty from counting statistics.

### 3. SOURCES OF UNCERTAINTY

The sources of uncertainty can be grouped in 6 categories: (1) those associated with the instrumentation (experimental PIXE set-up), (2) those related to the thin-film Al standard (as received), (3) uncertainties associated with the aerosol filter sample (as received), (4) uncertainties in the PIXE bombardment and spectrum acquisition, (5) uncertainties from the PIXE spectrum processing with the fitting program, and (6) uncertainties in the correction for matrix effects. In each of these categories, the uncertainty sources are numbered (e.g., for category (1) from 1.a through 1.f), and these numbers are used throughout the following sections and in Table 1.

#### 3.1. Instrumentation

1.a. The energy of the proton beam provided by the accelerator can change with time, and be different in the bombardments of the different specimens (samples and standards). Changes in beam energy lead to changes in ionization cross-sections, and thus also to changes in X ray yields.

1.b. The intensity across the beam at the specimen may not be perfectly uniform. For PIXE of non-uniform samples, one needs to have a uniform beam. Uniformity of the beam is, however, not required in case the specimen is uniform and larger than the beam size [1,2].

1.c. Measurement of the integrated beam charge with a Faraday cup and current digitizer is not that trivial [1,2]. The problems are, however, much less severe with thin specimens than with intermediately or infinitely thick specimens.

1.d. Characteristic X rays are not only generated in the bombarded area of the specimen. They may also be produced in the specimen holder and in the walls and other parts of the PIXE chamber (by protons scattered from the beam collimators in directions outside of the beam path) and these extraneous X rays may be seen by the Si(Li) detector. The extent of the interference depends on the design of the PIXE chamber. It can be significantly reduced by placing an X ray collimator in front of the Si(Li), so that the effective view of the detector is restricted to the bombarded specimen area.

1.e. The X ray absorber, which is placed between the specimen and detector, and the entrance window(s) of the Si(Li) may change or deteriorate with time. A deposit of organic material (or carbon) may accumulate on the absorber or entrance window(s) which are inside the vacuum of the PIXE chamber. Changes in such absorbers (or windows) lead to changes in the detection efficiency. Depending on the speed with which the alterations take place and the duration of the PIXE bombardments, the detection efficiency may be different for the different specimens (samples, standards).

1.f. The X ray detector itself may change with time. For example, ice may build up on the detector crystal [1,2]. As for 1.e, this leads to an alteration in detection efficiency.

### **3.2. Thin-film Al standard**

2.a. There is an inherent uncertainty in the Al mass thickness of the thin-film standard, as indicated by the manufacturer.

2.b. There may be problems with the purity and stoichiometry of the standard. The mass thickness of MicroMatter standards is obtained by weighing of a thin layer evaporated on a substrate film (e.g., Mylar) [10]. During the production of the Al standard (prior to weighing), impurities may be introduced or some oxidation may take place, so that the reported mass thickness does not apply to pure aluminium.

2.c. The lateral uniformity of the mass thickness of the thin-film standard is limited. For the PIXE bombardment ( $0.5 \text{ cm}^2$  beam size) in the present example, uniformity down to a  $0.5 \text{ cm}^2$  area is important.

### **3.3. Aerosol filter sample**

3.a. The air volume passed through the filter sample has an associated uncertainty.

3.b. There is an uncertainty associated with the diameter and thus area of the aerosol deposit on the filter sample (the area of the deposit in the present example is  $12.88 \text{ cm}^2$ ).

3.c. The lateral uniformity of the aerosol deposit on the filter sample is limited. For the PIXE bombardment ( $0.5 \text{ cm}^2$  beam size) in the present example, uniformity down to a  $0.5 \text{ cm}^2$  area is important.

3.d. The collection of particles on a Nuclepore polycarbonate filter does not only occur on the surface of the filter, but also inside the pores (by diffusion of very small particles from the air stream to the pore walls) [11]. The PIXE matrix correction factors for particles collected inside these pores are different from those collected on the filter surface. In the current example it is therefore important to know what are the relative fractions of Al-containing particles that were collected on the filter surface and within the pores.

3.e. The analyte element (Al) may not only be present in the aerosol, but also in the filter material itself (blank value). Normally, a correction for the blank value has to be made. There is an uncertainty associated with blank corrections because of inherent blank variability (Variations of blank values from filter to filter or even within a single filter).

### **3.4. Specimen bombardment and spectrum acquisition**

4.a. In the course of the PIXE bombardment, aerosol particles may fall off from the filter (in case the aerosol and/or filter are not sticky enough). Also, the matrix composition of the aerosol particles may change (because of radiation- or heat-induced losses of the elements H, C, N, O, S [12]).

4.b. Volatilization of analyte elements may occur during the bombardment. (The analyte in the present example is Al).

4.c. In the spectrum acquisition for the current example, pile-up pulses are rejected. Correction for the lost pulses is made by extending the duration of the measurement (live-time correction). There is an uncertainty associated with this live-time correction.

### 3.5. Spectral data processing with fitting program

5.a. As indicated in the Introduction, the extraction of the net peak areas for the characteristic X rays in the low-energy region (1-3 keV) of the PIXE spectrum is no easy task. In the current example, the Al  $K\alpha$  peak has to be resolved from the neighboring  $K$  lines (and their low-energy tails), from escape peaks (from  $K K\alpha$ ), from interfering  $L$  lines (Br  $L\alpha$ ), and especially from the underlying background. The uncertainty associated with resolving the Al  $K\alpha$  peak is particularly important for the spectrum from the sample. Al is not present in large concentrations in the fine size fraction of the aerosol; in contrast, S is normally the dominant element in the PIXE spectrum of such samples.

5.b. As in any radiation counting experiment, there is the inherent uncertainty arising from counting statistics.

### 3.6. Correction for matrix effects

The matrix correction factor for the Al standard (or any homogeneous specimen larger than the beam size) can be calculated using Equations (2) and (3). Such calculation requires knowledge of the mass thickness and composition of the specimen and of a number of fundamental parameters (stopping powers, ionization cross-sections, X ray mass attenuation coefficients). For the Al standard, uncertainties in the calculated correction factor arise from:

- 6.a. Uncertainty in the mass thickness of the Al layer,
- 6.b. Uncertainty in the stopping power  $S_{Al}(E)$ ,
- 6.c. Uncertainty in the  $K$  ionization cross-section  $\sigma_{Al}$ ,
- 6.d. Uncertainty in the mass attenuation coefficient  $\mu_p$  for the Al  $K\alpha$  X ray s.

Accurate calculation of the matrix correction factor (particle size effects) for Al in the aerosol sample is virtually impossible. This is due to the great variability in size and composition of the Al-containing particles. Furthermore, even the composition of an individual particle may not be uniform; e.g., a surface layer of different composition may be present. In the current example, empirical matrix correction factors are employed for the aerosol sample. These empirical correction factors were derived from comparison of PIXE with instrumental neutron activation analysis (INAA) for subsections of Nuclepore polycarbonate filter samples of fine (<2  $\mu\text{m}$  EAD) continental aerosols [13].

6.e. It is, however, uncertain to which extent these empirical correction factors apply to the actual filter sample analyzed.

## 4. QUANTIFICATION OF UNCERTAINTY COMPONENTS

*Note:* When the word uncertainty in this section is followed by (u), it means that the uncertainty is considered to be a standard uncertainty.

### 4.1. Instrumentation

1.a. The variation in proton beam energy (difference between irradiation of sample and standard) is estimated at 10 keV maximum. A change of 10 keV at the incident proton energy ( $E_0 = 2.5$  MeV) leads to change of 0.05% in  $\sigma_{Al}$ .

1.b. The variation in beam intensity across the specimen is assumed to be smaller than 5%. The uncertainty transmission from this variation to the final result is neglected; both standard and filter sample are essentially considered as laterally uniform specimens.

1.c. The uncertainty (**u**) in the integrated beam charge is estimated at 1% for thin specimens. This is based on repetitive PIXE measurements of thin film standards for a constant preset charge.

1.d. The contribution from extraneous Al X rays is assumed to be negligible. This was deduced from bombardments (a) with no specimen in the target position and (b) of thin non-Al containing specimens (see also 3.e in subsection 4.3 below).

1.e and 1.f. are neglected, because of the short time lapse (less than one hour) between bombardment of standard and filter sample.

#### **4.2. Thin-film Al standard**

2.a. The uncertainty in the mass thickness of the standard is 5%, as specified by the manufacturer [10].

2.b. This uncertainty is neglected, as the pure element was used for production of the Al standard.

2.c. For the uncertainty arising from the non-uniformity in the mass thickness of the Al standard (at the 0.5 cm<sup>2</sup> area level), a conservative guess of 5% is adopted.

#### **4.3. Aerosol filter sample**

3.a. This example is prepared for the sample as received in laboratory. For this reason the uncertainty in the air volume is not retained for calculating the combined uncertainty.

3.b. The uncertainty (**u**) in the area of the aerosol deposit is estimated at 1%.

3.c. For the uncertainty arising from the non-uniformity in the mass thickness of the aerosol deposit (at the 0.5 cm<sup>2</sup> area level), a conservative guess of 5% is adopted. This is based on stepping a 0.5 cm<sup>2</sup> beam over several aerosol filter samples, which were collected with the same sampler as used for the sample of the current example.

3.d. This uncertainty is neglected. With the air flow-rate and filter pore size used for sampling, only very fine particles (<0.1 μm) are collected inside the pores. The great majority of Al-containing particles should be collected on the surface.

3.e. There is no blank value for Al. This is deduced from the bombardment of blank Nuclepore polycarbonate filters from the same lot as used for the actual sampling (Al was present at levels below the PIXE detection limit in these blank filters).

#### **4.4. Specimen bombardment and spectrum acquisition**

4.a. The loss of particles from the aerosol filter during the PIXE bombardment is neglected. Possible changes in aerosol matrix composition during the bombardment affect the matrix effects, but the latter are treated empirically (see under 6.e below).

4.b. This uncertainty is neglected. The Al metal layer in the standard and the Al compounds present in the aerosol sample are not expected to be volatilized during the PIXE bombardment in vacuum.

4.c. The uncertainty in the live-time correction is 5%, both for standard and sample. This is based on extensive testing of the spectrum acquisition system used. These tests involved repeated measurements of the same samples for a constant preset charge, but at widely varying beam intensities. The large variation in beam intensities led to large differences in count rates and in the number of rejected pile-up pulses, and thus also to large differences in the extent of live-time correction applied. The peak areas of the characteristic X rays (for which the error from counting statistics was less than 1%) remained within a range of 5% over a wide range of beam intensities (up to count rates of 5000 counts per s).

#### 4.5. Spectral data processing with fitting program

5.a. The uncertainty in resolving the Al  $K\alpha$  peak from neighboring and interfering lines and especially from the background is estimated at 1% for the standard. In contrast, for the filter sample, the uncertainty is estimated at 20%. This is mainly due to the high background under the Al  $K\alpha$  peak in the PIXE spectrum of the sample. Although the S  $K\alpha$  / Al  $K\alpha$  ratio in this spectrum was of the order of 100/1, the S  $K\alpha$  tail contributed very little to the uncertainty in the Al  $K\alpha$  peak area. The estimated uncertainties in the peak resolving are based on experience gained from an intercomparison of different PIXE spectrum fitting programs, including the program used here (AXIL-84) [6]. The intercomparison was done on spectra from several samples and standards, including spectra similar to those of the current example.

5.b. The uncertainties (**u**) arising from counting statistics are calculated and reported by the fitting program used [10].

#### 4.6. Correction for matrix effects

For the standard:

6.a through 6.d. The calculated matrix correction factor  $F_{matr,stand} = 1.0109$ .

Thus, the correction is only 1%. The attenuation of the Al  $K\alpha$  X rays provides the major contribution in this correction [Note: the average decrease of the proton energy  $E$  in the standard is only 2.5 keV; this leads to a change of only 0.025% in  $\sigma_{Al}$ ]. The uncertainty in the calculated attenuation of the Al  $K\alpha$  X rays arises from the uncertainties in  $\mu_p$  and in the mass thickness of the standard (which are estimated at 5% each, see also subsection 4.2). These uncertainties lead to an uncertainty of less than 0.1% in  $F_{matr,stand}$ . This small uncertainty is neglected.

For the sample:

6.e. The empirical matrix correction factor for Al in typical fine continental aerosol particles is 1.2. Thus the correction amounts to 20%. The uncertainty in applying this value for the filter sample analyzed is estimated at a factor of 2. This means that the range in  $F_{matr,sample}$  is from 1.1 to 1.4 and that the uncertainty range for  $F_{matr,sample}$  is  $1.4 - 1.1 = 0.3$ .

## 5. CONVERSION OF UNCERTAINTIES TO STANDARD UNCERTAINTIES

### 5.1. Instrumentation

1.c.

$\frac{u(Q_{stand})}{Q_{stand}}$  and  $\frac{u(Q_{sample})}{Q_{sample}}$  for the integrated beam charge is 0.01 for both standard and sample respectively.

### 5.2. Thin-film Al standard

2.a.

$\frac{u(C_{Al} \rho t)_{stand}}{(C_{Al} \rho t)_{stand}}$  for the mass thickness of the standard is  $0.05/\sqrt{6} = 0.020$  [A triangular distribution function is assumed to convert the uncertainty to standard uncertainty].

2.c.

$\frac{u(f_{uniform,stand})}{f_{uniform,stand}}$  arising from non-uniformity of the mass thickness of the Al metal layer is  $0.05/\sqrt{3} = 0.029$  [A rectangular distribution function is assumed to convert the uncertainty to standard uncertainty].

### 5.3. Aerosol filter sample

3.b.

$\frac{u(A_{filter})}{A_{filter}}$  for the area of the aerosol deposit is 0.01.

3.c.

$\frac{u(f_{uniform,sample})}{f_{uniform,sample}}$  arising from non-uniformity of the mass thickness of the aerosol deposit is  $0.05/\sqrt{3} = 0.029$  [A rectangular distribution function is assumed].

### 5.4. Specimen bombardment and spectrum acquisition

4.c.

$\frac{u(f_{live-time-corr,stand})}{f_{live-time-corr,stand}}$  and  $\frac{u(f_{live-time-corr,sample})}{f_{live-time-corr,sample}}$  for the live-time correction, both for standard and sample respectively, is  $0.05/\sqrt{6} = 0.020$  [A triangular distribution function is assumed].

## 5.5. Spectral data processing with fitting program

5.a.

$\frac{u(Y_{K\alpha(AI),stand})}{Y_{K\alpha(AI),stand}}$  arising from the uncertainty in resolving the Al  $K\alpha$  peak is for the standard:  $0.01/\sqrt{6} = 0.0041$  [A triangular distribution is assumed]; and for the filter sample  $\frac{u(Y_{K\alpha(AI),sample})}{Y_{K\alpha(AI),sample}}$  is  $0.20/\sqrt{6} = 0.082$  [A triangular distribution is assumed].

5.b.

The Al  $K\alpha$  peak areas and associated standard uncertainties from counting statistics, as reported by the fitting program are:

- for the standard:  $35272 \pm 303$ ; thus  $\frac{u(Y_{K\alpha(AI),stand})}{Y_{K\alpha(AI),stand}} = 0.0086$ ; and

- for the filter sample:  $3153 \pm 342$ ; thus  $\frac{u(Y_{K\alpha(AI),sample})}{Y_{K\alpha(AI),sample}} = 0.109$ .

## 5.6. Correction for matrix effects

For the sample:

6.e. The standard uncertainty  $u$  for the matrix correction factor is  $0.3/\sqrt{6} = 0.122$  [A triangular distribution function is assumed].

Thus,  $\frac{u(F_{matr,sample})}{F_{matr,sample}}$  is  $0.122/1.2 = 0.102$ .

## 6. CALCULATION OF COMBINED STANDARD UNCERTAINTY

Although Equation (1) is the basic equation for the calculation of the measurand, it does not show explicitly how the various uncertainty components contribute to the combined uncertainty  $u_c$ . To show the effects of the various uncertainties clearly, it is useful to rewrite Equation (1) as follows:

$$C_{Al,air} = \frac{Y_{K\alpha(AI),sample} F_{matr,sample} Q_{stand} (C_{Al} \rho t)_{stand} 1000 A_{filter}}{Q_{sample} Y_{K\alpha(AI),stand} F_{matr,stand} V_{air}}$$

$$x \frac{f_{uniform,sample} f_{life-time-corr,sample}}{f_{uniform,standard} f_{life-time-corr,standard}}$$

where  $f_{uniform,sample}$ ,  $f_{life-time-corr,sample}$ ,  $f_{uniform,standard}$ , and  $f_{life-time-corr,standard}$  are correction factors assumed to be unity in the original calculation. In writing Equation (4), no correction factors were introduced which are related to those uncertainties which were considered negligible.

Taking equation (4) into account, the combined uncertainty  $u_c$  can be calculated as follows:

$$\begin{aligned}
\frac{u^2(C_{Al,air})}{C_{Al,air}^2} &= \frac{u^2(Q_{stand})}{Q_{stand}^2} + \frac{u^2(Q_{sample})}{Q_{sample}^2} + \frac{u^2(C_{Al}\rho t)_{stand}}{(C_{Al}\rho t)_{stand}^2} + \frac{u^2(f_{uniform,stand})}{f_{uniform,stand}^2} + \frac{u^2(A_{filter})}{A_{filter}^2} + \\
&\frac{u^2(f_{uniform,sample})}{f_{uniform,sample}^2} + \frac{u^2(f_{life-time-corr,stand})}{f_{life-time-corr,stand}^2} + \frac{u^2(f_{life-time-corr,sample})}{f_{life-time-corr,sample}^2} + \frac{u^2(f_{K\alpha(Al),stand,peak-resolv})}{f_{K\alpha(Al),stand,peak-resolv}^2} + \\
&\frac{u^2(f_{K\alpha(Al),stand,count.stat})}{f_{K\alpha(Al),stand,count.stat}^2} + \frac{u^2(f_{K\alpha(Al),sample,count.stat})}{f_{K\alpha(Al),sample,count.stat}^2} + \frac{u^2(f_{K\alpha(Al),sample,peak-resolv})}{f_{K\alpha(Al),sample,peak-resolv}^2} + \frac{u^2(F_{matr,sample})}{F_{matr,sample}^2} \quad (5) \\
&= 0.01^2 + 0.01^2 + 0.020^2 + 0.029^2 + 0.01^2 + 0.029^2 + 0.020^2 + 0.020^2 + \\
&0.0041^2 + 0.0086^2 + 0.082^2 + 0.109^2 + 0.102^2 \\
&= 0.032282
\end{aligned}$$

## 7. RESULT AND ASSOCIATED COMBINED STANDARD UNCERTAINTY

The value of the measurand  $C_{Al,air}$  is calculated by entering the values of the variables in Equation (1):

$$C_{Al,air} = \frac{3153 \times 1.0109 \times 1 \times 50 \times 1000}{100 \times 35272 \times 1.2} \frac{12.88}{21.5} = 22.6 \text{ ng/m}^3$$

The associated combined standard uncertainty  $u_c(C_{Al,air})$ , is derived from  $\frac{u^2(C_{Al,air})}{C_{Al,air}^2}$ , which itself was obtained using Equation (5). Thus:

$$\begin{aligned}
u_c(C_{Al,air}) &= C_{Al,air} \sqrt{\frac{u^2(C_{Al,air})}{C_{Al,air}^2}} \\
&= 22.6 \text{ ng/m}^3 \times \sqrt{0.032282} \\
&= 4.1 \text{ ng/m}^3
\end{aligned}$$

To convert this combined standard uncertainty into an expanded uncertainty  $U$ , it has to be multiplied by a coverage factor  $k$ . The coverage factor used here is 2. Thus:

$$\begin{aligned}
U(C_{Al,air}) &= k u_c(C_{Al,air}) \\
&= 2 \times 4.1 \text{ ng/m}^3 \\
&= 8.2 \text{ ng/m}^3
\end{aligned}$$

An overview of the various uncertainty components, the numeric values of the uncertainties and the standard uncertainties, and how the latter contribute to the combined standard uncertainty  $u_c$  is presented in Table 1. In the first column of the Table reference numbers are given for all identified uncertainty components of section 3 above, even for those components which were considered to be negligible in section 4, so that no numeric uncertainty values for them are given in Table 1. The sensitivity factor in the last but one column of the Table indicates how the standard uncertainty in a variable (or parameter) is propagated into the combined standard uncertainty. Here, all sensitivity factors are equal to 1. However, this is

not necessarily always the case. For example, if the uncertainty for the calculated matrix correction factor  $F_{matr,stand}$  would not have been negligible, then the sensitivity factors for the uncertainties of  $\mu_p$  and  $(C_{Alpt})_{stand}$  in the calculation of the uncertainty of  $F_{matr,stand}$  would have been included in Table 1, and these sensitivity factors would not have been equal to 1, but much smaller. Note that the relationship between  $F_{matr,stand}$  and  $\mu_p$  and  $(C_{Alpt})_{stand}$  is not linear [See Equations (2) and (3)]. The last column of Table 1 indicates what is the percent contribution from each uncertainty component to the variance ( $u_c$ )<sup>2</sup>. Clearly, only 3 uncertainty components provide large contributions. These components are the uncertainties related to the determination of the Al  $K\alpha$  peak area in the PIXE spectrum from the sample (both the uncertainties from resolving the peak from the background and from counting statistics are important here) and the uncertainty in the matrix correction factor for Al in the sample.

## REFERENCES

- [1] JOHANSSON, S.A.E., CAMPBELL, J.L., PIXE: A Novel Technique for Elemental Analysis, Wiley, Chichester (1988).
- [2] JOHANSSON, S.A.E., CAMPBELL, J.L., MALMQVIST, K. (Eds.), Particle-induced X ray emission spectrometry (PIXE), Wiley, Chichester (1995).
- [3] MAENHAUT, W., MALMQVIST, K.G., "Particle-induced X ray emission analysis", Handbook on X ray Spectrometry: Methods and Techniques, in: VAN GRIEKEN, R., MARKOWICZ, A.A. (Eds.), Marcel Dekker, Inc., New York (1993) 517-581.
- [4] KEMP, K., "Matrix corrections for PIXE analysis of urban aerosols on Whatman 41 filters", X ray fluorescence analysis of environmental samples (DZUBAY, T.G., Ed.), Ann Arbor Science, Michigan, MI (1977) 203-208.
- [5] JEX, D.G., HILL, M.W., MANGELSON, N.F., Proton induced X ray emission of spherical particles: corrections for X ray attenuation, Nucl. Instr. and Meth. **B49** (1990) 141-145.
- [6] CAMPBELL, J.L., MAENHAUT, W., BOMBELKA, E., CLAYTON, E., MALMQVIST, K., MAXWELL, J.A., PALLON, J., VANDENHAUTE, J., An intercomparison of spectral data processing techniques in PIXE, Nucl. Instr. and Meth. **B14** (1986) 204-220.
- [7] MAENHAUT, W., VANDENHAUTE, J., Accurate analytic fitting of PIXE spectra, Bull. Soc. Chim. Belg. **95** (1986) 407-418.
- [8] MAENHAUT, W., RAEMDONCK, H., Accurate calibration of a Si(Li) detector for PIXE analysis, Nucl. Instr. and Meth. **B1** (1984) 123-136.
- [9] MAENHAUT, W., FRANÇOIS, F., CAFMEYER, J., "The "Gent" stacked filter unit (SFU) sampler for the collection of aerosols in two size fractions: Description and instructions for installation and use", Applied Research on Air Pollution using Nuclear-Related Analytical Techniques, Report on the First Research Co-ordination Meeting, Vienna, Austria, 30 March - 2 April 1993, NAHRES-19, IAEA, Vienna (1994) 249-263.
- [10] HEAGNEY, J.M., HEAGNEY, J.S., Thin film X ray fluorescence calibration standards, Nucl. Instr. and Meth. **167** (1979) 137-138.
- [11] HEIDAM, N.Z., Review: Aerosol fractionation by sequential filtration with Nuclepore filters, Atmos. Environ. **15** (1981) 891-904.
- [12] MAENHAUT, W., Multielement analysis of biological materials by PIXE, Scanning Microsc. **4** (1990) 43-62.
- [13] CORNILLE, P., MAENHAUT, W., PACYNA, J.M., Sources and characteristics of the atmospheric aerosol near Damascus, Syria, Atmos. Environ. **24A** (1990) 1083-1093.

**Table 1. Summary table on the uncertainty components for the current example on PIXE.**

Reference to uncertainty source	Symbol for variable (unit) or for correction factor	Value of variable or of correction factor	Uncertainty	Conversion factor to standard uncertainty	Standard uncertainty (u)	Sensitivity factor	Percent contribution to $(u_c)^2$
1.a, 1.b							
1.c - standard	$Q_{stand} (\mu C)$	1	0.01	1	0.01	1	0.3
- sample	$Q_{sample} (\mu C)$	100	1	1	1	1	0.3
1.d to 1.fs							
2.a	$(C_{Al\rho t})_{stand} (\mu g/cm^2)$	50	2.5	$1/\sqrt{6}$	1.02	1	1.2
2.b							
2.c	$f_{uniform,stand}$	1	0.05	$1/\sqrt{3}$	0.029	1	2.6
3.1	$V_{air} (m^3)$	21.5					
3.b	$A_{filter} (cm^2)$	12.88	0.13	1	0.13	1	0.3
3.c	$f_{uniform,sample}$	1	0.05	$1/\sqrt{3}$	0.029	1	2.6
3.d, 3.e							
4/a. 4/b							
4.c - standard	$f_{live-time-corr,stand}$	1	0.05	$1/\sqrt{6}$	0.020	1	1.2
- sample	$f_{live-time-corr,sample}$	1	0.05	$1/\sqrt{6}$	0.020	1	1.2
5.a - standard	$Y_{K\alpha(Al),stand}$	35272	1%	$1/\sqrt{6}$	1444	1	0.05
- sample	$Y_{K\alpha(Al),sample}$	3153	20%	$1/\sqrt{6}$	257	1	21
5.b - standard	$Y_{K\alpha(Al),stand}$	35272	303	1	303	1	0.25
- sample	$Y_{K\alpha(Al),sample}$	3153	342	1	342	1	37
6.a to 6.d	$F_{matr,standard}$	1.0109					
6.e	$F_{matr,sample}$	1.2	0.3	$1/\sqrt{6}$	0.122	1	32

Value of the measurand  $C_{Al,air} = 22.6 \text{ ng/m}^3$

Associated combined standard uncertainty  $u_c(C_{Al,air}) = 4.1 \text{ ng/m}^3$ ; Expanded uncertainty  $U_c(C_{Al,air}) = 8.2 \text{ ng/m}^3$

# UNCERTAINTY EVALUATION IN INSTRUMENTAL AND RADIO-CHEMICAL NEUTRON ACTIVATION ANALYSIS

J. KUCERA\*, P. BODE\*\*, V. ŠTEPÁNEK\*

\*Nuclear Physics Institute, Academy of Sciences of the Czech Republic, Rez near Prague, Czech Republic

\*\*Delft University of Technology, Interfaculty Reactor Institute, Delft, Netherlands

## Abstract

Neutron activation analysis is a multi-element analysis method based on irradiation of the sample with a powerful neutron source, e.g. a nuclear reactor, and subsequent measurement of the induced radioactivity. The measurement is done either without any chemical processing of the sample by gamma spectrometric analysis or after chemical decomposition and treatment to isolate the radionuclides of interest and eliminate the matrix and interfering radionuclides. A particular feature of NAA is the use of a single comparator rather than a set of calibration standards for each single element to be determined. The concept involves the use of a composite nuclear constant relating the gamma emission rate observed for the comparator to the gamma emission rate of a standard quantity of an individual element. The uncertainty sources of INAA are evaluated in three groups: 1) the preparation of the sample, the calibration standards, the comparator and the neutron fluence monitors; 2) the irradiation characteristics, the neutron spatial and spectral variations, the absorption effects and interfering nuclear reactions; 3) the gamma spectrometric measurement, including the counting geometry and statistics, the decay-time and live-time corrections, the radiation background, the spectrum fitting and spectral interferences. For the case of RNAA the uncertainty sources associated with the radiochemical separation procedure and yield determination using stable or radioactive tracers are evaluated.

## 1. INTRODUCTION

Neutron activation analysis (NAA) is based on irradiation of the sample to be analyzed with neutrons, most frequently in the most powerful neutron source - a nuclear reactor, and subsequent counting of the induced radioactivity, most frequently employing  $\gamma$ -ray spectrometric measurement with a HPGe detector. In its non-destructive mode, the so called instrumental NAA (INAA), the irradiated sample is counted without any chemical treatment after various decay times depending on half-lives of the induced radionuclides, while in its destructive mode, the so called radiochemical NAA (RNAA), sample decomposition and radiochemical separation is employed prior to counting to eliminate matrix activity or to isolate the radionuclide(s) of interest. Chemical separation can also be performed prior to irradiation. This approach is especially useful for the determination of elements forming radionuclides with short half-lives and in speciation studies (this analysis mode is sometimes called molecular activation analysis - MAA). However, pre-irradiation separation may result in introducing an analytical blank (like in other trace analytical techniques) which is virtually absent when INAA or RNAA is used.

The basic principles and major applications of NAA have been described in detail in several monographs [e.g. 1-4] and also the advantageous features of NAA have already been reviewed [5]. Nevertheless, it is worthwhile mentioning some of the most favourable features of NAA as follows:

- sensitivity and applicability for minor and trace elements in a wide range of matrices
- the virtual absence of an analytical blank
- the relative freedom from matrix and interference effects
- the capability of INAA for multi-element determination, often allowing 30 to 40 elements to be determined in many matrices

- an inherent potential for accuracy compared to other analytical techniques. Since the theoretical basis of NAA is simple and well understood, the sources of uncertainty can be modelled and well estimated
- the isotopic basis which often offers a choice of analytically independent routes for element determination.

In RNAA the technique has other advantageous features:

- trace and ultra-trace (radio) chemistry can be performed under controlled conditions by inactive carrier additions
- the chemical yield of the separation can be obtained simply using carrier budgeting or the radiotracer method.

Due to its favourable features, NAA has found extensive applications in many fields, such as the biomedicine, environmental and nutritional sciences, geology and geochemistry, industrial and forensic applications, and quality assurance of analysis and the preparation of reference materials. A review of uncertainty sources in reactor NAA in general is given in the present work, followed by two examples to demonstrate evaluation of the uncertainty of results obtained by INAA and RNAA for V and Mn, respectively, in two reference materials of environmental and biological origin.

## 2. BASIC CONSIDERATIONS

### 2.1. Analyte

The element to be determined is the analyte, which is, however, assayed using a nuclear reaction of its stable isotope (or one of its stable isotopes, if several exist) by its conversion, mostly by the  $(n,\gamma)$  reaction, to the radioactive indicator with suitable properties for measurement. For both stable and radioactive isotopes an index  $a$  is used.

### 2.2. Measurand

The mass fractions of the element to be determined related, e.g., either to the dry or wet matter of a sample, is the measurand - index  $m$ .

### 2.3. Irradiation with reactor neutrons

Reactor neutrons can be divided, according to their energies, into three basic components: subcadmium ("thermal") neutrons with the most probable energy of 0.025 eV, i.e., with the most probable velocity  $v_0 = 2200 \text{ m s}^{-1}$  (at  $20.44^\circ\text{C}$ ), epicalcium (epithermal) neutrons with energies ranging from the cadmium cut-off (0.55 eV for a 1 mm thick Cd-cylinder in an isotropic neutron flux) up to approximately 1 MeV, and fast neutrons with energies  $E_n > 1 \text{ MeV}$ . These components are characterized by the respective neutron fluence rates (flux densities),  $\Phi_{\text{th}}$ ,  $\Phi_{\text{e}}$ , and  $\Phi_{\text{f}}$  ( $\text{cm}^{-2} \text{ s}^{-1}$ ). The thermal and epithermal neutrons induce  $(n,\gamma)$  reactions with many target nuclei and thus are most important in NAA. Therefore, only  $(n,\gamma)$  reactions will be considered in the present report in detail, while the use of reactions with fast neutron will be only briefly mentioned, although determination of some elements using various reactions with fast neutrons, such as  $(n,p)$ ,  $(n,\alpha)$ , and  $(n,2n)$ , is also possible or even more advantageous than employing reactions with thermal or epithermal neutrons.

Considering only reactions of thermal and epithermal neutrons, the reaction rate per nucleus  $R$  can be written as

$$R = \Phi_0 \sigma_0 + \Phi_e I_0$$

where  $\Phi_0$  = conventional thermal neutron fluence rate;

$\sigma_0$  = activation cross section for neutrons with the energy of 0.025 eV;

$\Phi_e$  = epithermal neutron fluence rate;

$I_0$  = resonance integral including the  $1/v$  tail.

In (n, $\gamma$ ) activation analysis, when the sample is irradiated in the whole reactor spectrum, the mass fraction  $c$  of the element to be determined is given by the equation:

$$c_m = \frac{M_a}{N_A \theta_a \gamma_a} \frac{\left( \frac{N_p / t_c}{SDCW} \right)_a}{\left( G_{th,a} \Phi_0 \sigma_{0,a} + G_{e,a} \Phi_e I_{0,a}(\alpha) \right) \varepsilon_{p,a} Y_a} \quad (1)$$

where  $M$  = molar mass

$N_A$  = Avogadro's number

$\theta$  = relative isotopic abundance of the target isotope

$\gamma$  = absolute gamma-intensity (emission probability) of the particular radioisotope

$N_p$  = net number of counts in the full-energy peak corrected for pulse losses

$t_c$  = counting time

$W$  = sample mass

$G_{th}$  = correction factor for thermal neutron self-shielding

$G_e$  = correction factor for epithermal neutron self-shielding

$\alpha$  = measure for the deviation of the epithermal neutron fluence rate distribution from the  $1/E$  shape, approximated by a  $1/E^{1+\alpha}$  function

$\varepsilon_p$  = full-energy peak detection efficiency, including correction for gamma-attenuation

$Y_a$  = chemical yield of separation (if pre-irradiation or radiochemical separation is carried out)

and S,D,C are saturation, decay and counting factors, respectively, given as

$$S = 1 - e^{-\lambda t_i} \quad D = e^{-\lambda t_d} \quad C = (1 - e^{-\lambda t_c}) / \lambda t_c$$

where  $\lambda$  = decay constant =  $\ln 2 / T_{1/2}$

and  $t_i$ ,  $t_d$ , and  $t_c$  are irradiation, decay and counting times, respectively, and  $T_{1/2}$  is the half-life of the radionuclide.

The equation (1) is valid provided that no significant changes of the number of atoms of the target nuclide occur on irradiation (no burn-up) and that the neutron fluence rate remains constant during irradiation.

When the sample is irradiated with epithermal neutrons (under a Cd cover formed by a cylindrical box with 1 mm thick walls), in the so called epithermal neutron activation analysis (ENAA), the following equation holds:

$$c_m = \frac{M_a}{N_A \theta_a \gamma_a} \frac{\left[ \left( \frac{N_p / t_c}{SDCW} \right)_{Cd} \right]_a}{G_{e,a} F_{Cd,a} \Phi_e I_{0,a}(\alpha) \varepsilon_{p,a} Y_a} \quad (2)$$

where  $F_{Cd}$  = Cd-transmission factor for epithermal neutrons.

The term  $SDC$  in Eqs (1) and (2) should be modified in case of branching activation and mother-daughter decay according to the generalized Bateman-Rubinson equation [1, p.143]. A good overview of these calculations has also been given by De Corte et al. [6].

For reactions with fast neutrons, the term  $\Phi_0 \sigma_0$  in the denominator of equation (1) is replaced by  $\Phi_f \sigma_f$

where  $\Phi_f$  = fast neutron fluence rate;  
 $\sigma_f$  = activation cross section for reactor fast neutron spectrum,

the terms  $G_{th}$  and  $G_e$  equal to unity, and the term  $\Phi_e I_0(\alpha)$  can be left out, because it is negligible.

## 2.4. Standardization modes in NAA

For the actual determination of  $c_m$  in INAA, ENAA, and RNAA, three types of standardization can be used:

- relative (using synthetic element standards or primary matrix reference materials)
- single-comparator, most frequently employing the  $k_0$ -standardization
- absolute (parametric)

Since unacceptable uncertainties are still associated with the values of nuclear parameters, such as  $\sigma_0$ ,  $I_0$ ,  $\gamma$ ,  $\theta$ ,  $\lambda$  (in order of decreasing importance), the absolute standardization is used only rarely and will not be dealt with in the present report.

### 2.4.1. Relative standardization

In the relative standardization method, a chemical standard (index  $st$ ) with known mass  $w$  of the element is coirradiated with the sample of known mass  $W$  (or especially when short-lived radionuclides are employed both the standard and sample are irradiated separately under the same conditions, usually with a monitor of the neutron fluence rate) and both are counted in the same geometrical arrangements with respect to the HPGe detector. Since  $M_a = M_{st}$ ,  $\theta_a = \theta_{st}$ ,  $\gamma_a = \gamma_{st}$ ,  $S_a = S_{st}$ ,  $\sigma_{0,a} = \sigma_{0, st}$ , and  $\varepsilon_a = \varepsilon_{st}$  (provided that gamma-attenuation in sample and standard does not differ, i.e.  $F_{att, a} = F_{att, st} = 1$ , ( $F_{att}$  = attenuation factor, which is usually fulfilled for  $\gamma$  ray energies  $E_\gamma > 100$  keV, small source dimensions, and large source-to-detector distances), the well known simple expressions (for NAA and ENAA, respectively) are obtained:

$$c_m = \frac{\left(\frac{N_p / t_c}{DCW}\right)_a}{\left(\frac{N_p / t_c}{DCW}\right)_{st}} \quad (3)$$

$$c_m = \frac{\left[\left(\frac{N_p / t_c}{DCW}\right)_{Cd}\right]_a}{\left[\left(\frac{N_p / t_c}{DCW}\right)_{Cd}\right]_{st}} \quad (4)$$

Equations (3) and (4) are valid provided that the neutron flux gradient between the sample and standard position in the irradiation container is negligible or corrected for (for instance, using coirradiation of suitable neutron flux monitors) and that  $G_{th,a} = G_{th,st} = G_{e,a} = G_{e,st} = 1$ . With the relative standardization, it is not even necessary to presume that the neutron fluence rate is constant during irradiation and that no burn-up occurs, because these effects would have the same influence on the sample and standard in the case of simultaneous irradiation. It appears straightforward that equation (3) is also valid for irradiation with fast neutrons.

#### 2.4.2. $k_0$ -standardization

The concept of the  $k_0$ -standardization in NAA, one of the most frequently used single-comparator (monostandard) method, is based on coirradiation of the sample and of a neutron fluence rate monitor (index  $n$ ) and on using an experimentally determined composite nuclear constant  $k_{0,n}(a)$

$$k_{0,n}(a) = \frac{M_n \theta_a \sigma_{0,a} \gamma_a}{M_a \theta_n \sigma_{0,n} \gamma_n} \quad (5)$$

The gold comparator is most frequently used as the neutron fluence rate monitor, versus which the  $k_0$ -factors ( $k_{0,Au}$ ) were determined in independent experiments for the most important (n, $\gamma$ ) reactions and  $\gamma$ -ray energies of the resulting radioisotopes by DE CORTE and SIMONITS [7,8]. However, the use of the  $k_0$ -standardization is not restricted to the gold comparator, because it holds, by definition,

$$k_{0,n}(a) = k_{0,Au}(a)/k_{0,Au}(n) \quad (6)$$

and these  $k_{0,n}(a)$  can be replaced accordingly in the following equations (7) and (8).

The mass fraction of an element in INAA when irradiation in the whole reactor spectrum is performed is given by

$$c_m = \frac{\left(\frac{N_p / t_c}{SDCW}\right)_a}{A_{sp,n}} \cdot \frac{1}{k_{0,n}(a)} \cdot \frac{G_{th,n} f + G_{e,n} Q_{0,n}(\alpha)}{G_{th,a} f + G_{e,a} Q_{0,a}(\alpha)} \cdot \frac{\varepsilon_{p,n}}{\varepsilon_{p,a}} \quad (7)$$

while in ENAA

$$c_m = \left[ \frac{\left( \frac{N_p / t_c}{SDCW} \right)_a}{A_{sp,n}} \right]_{Cd} \cdot \frac{1}{k_{0,n}(a)} \cdot \frac{F_{Cd,n} G_{e,n} Q_{0,n}(\alpha)}{F_{Cd,a} G_{e,a} Q_{0,a}(\alpha)} \cdot \frac{\varepsilon_{p,n}}{\varepsilon_{p,a}} \quad (8)$$

where  $N_p$  = measured net peak area, corrected for pulse losses [dead time, random coincidence (pulse pile-up), true coincidence (cascade summing)]  
 $A_{sp} = (N_p/t_c)/SDCW$ , the specific count rate, with  $w$  - mass of the monitor element  
 $f = \Phi_{th}/\Phi_e$ , the thermal (subcadmium) to epithermal neutron fluence rate ratio  
 $Q_0 = I_0/\sigma_0$ .

Further details of the  $k_0$ -standardization have already been described elsewhere [9,10].

### 2.4.3. Special aspects of standardization in RNAA

Both the relative and  $k_0$ -standardization can be used in RNAA based on  $(n,\gamma)$  reactions provided that a chemical yield of analyte  $Y_a$  is determined to take into account the possible incomplete recovery of the analyte on sample decomposition and subsequent separation ( $Y_a \leq 1$ ). In these cases, the right hand sides of Eqs (3), (4), (7) and (8) are to be divided by the value of  $Y_a$ . A special case may arise in the relative standardization if both the sample and standard are subject to the same decomposition and separation procedure which may result in approximately the same chemical yield of the analyte in the sample and standard. Under these circumstances, no correction for  $Y_a$  would be needed in equations (3) and (4). However, the same value of  $Y_a$  for the sample and standard should never be taken for granted, even if the same decomposition and separation procedure is applied, because, in general, the chemical composition of the sample and standard differ and thus a different chemical behaviour should be expected, especially on decomposition. Therefore, determining the  $Y_a$  value for the sample should be preferred whenever possible, while the standard should not be subjected to any chemical treatment. In this way, one of the possible sources of uncertainty (that resulting from the chemical treatment of the standard) is excluded.

There are basically three methods of the chemical yield determination, of which two are based on radioactivity measurements, that are listed below in order of decreasing preference:

- (i) use of a radioactive tracer of the measurand, different from that one originating on neutron irradiation (indicator of the analyte), with suitable parameters ( $E_\gamma$  of the radiotracer  $< E_\gamma$  of the indicator radioisotope, sufficiently long half-life of the radiotracer to allow simultaneous counting of both the radiotracer and indicator radioisotope or counting of the radiotracer after the decay of the indicator radioisotope - in such a case the fulfillment of the above requirement for  $E_\gamma$  is not needed)
- (ii) reactivation of a stable carrier of the analyte added to the sample prior to decomposition and subsequent separation and counting of the induced radioactivity;
- (iii) determination of the amount of the stable carrier added to the sample prior to decomposition and subsequent separation by any suitable analytical technique, such as spectrophotometry, atomic absorption spectrometry, gravimetry, etc. Although there are numerous ways to determine the chemical yield using this approach, another analytical technique (and the necessary equipment) should be available in a laboratory for this purpose.

In the last two approaches, it must be ensured that a sufficient amount of the stable carrier is added to the sample to make the amount of the originally present analyte negligible.

### 3. SOURCES OF UNCERTAINTY

In general, the sources of standard uncertainty  $u_i$  can be grouped according to the individual steps of analysis into four categories: (1) preparation of the sample and comparator (standard,  $k_0$ -factors, neutron fluence rate monitor); (2) irradiation; (3)  $\gamma$ -ray spectrometry measurement; and (4) radiochemical separation, if performed. Most of the sources of uncertainty within the above categories have been discussed by GREENBERG et al. [11]. In the present work, some additional sources of uncertainty are identified as follows:

1. Sample and comparator preparation,  $u_1$ 
  - 1.a. Mass determination of a sample,  $u_{1a}$
  - 1.b. Mass determination of comparators,  $u_{1b}$
  - 1.c. Mass changes of samples due to moisture uptake during weighing,  $u_{1c}$
  - 1.d. Concentration of comparators (standards), purity and stoichiometry of chemicals used for the preparation of standards and/or the uncertainty of  $k_0$ -values,  $u_{1d}$
  - 1.e. Variation of isotopic abundance,  $u_{1e}$
  - 1.f. Blank variation and the necessary correction (due to analyte content in an irradiation vial and/or capsule),  $u_{1f}$
2. Irradiation,  $u_2$ 
  - 2.a. Irradiation geometry differences,  $u_{2a}$
  - 2.b. Neutron self-shielding/scattering differences,  $u_{2b}$
  - 2.c. Duration (timing) of irradiation,  $u_{2c}$
  - 2.d. Nuclear reaction interferences,  $u_{2d}$
  - 2.e. Neutron spectrum variations in time and space,  $u_{2e}$
  - 2.f. Volatilization losses during irradiation,  $u_{2f}$
3.  $\gamma$ -ray spectrometry measurement,  $u_3$ 
  - 3.a. Counting statistics,  $u_{3a}$
  - 3.b. Counting geometry differences,  $u_{3b}$
  - 3.c. Pulse-pileup losses (random coincidences),  $u_{3c}$
  - 3.d. True coincidences (cascade summing),  $u_{3d}$
  - 3.e. Dead-time effects,  $u_{3e}$
  - 3.f. Decay timing effects,  $u_{3f}$
  - 3.g. Duration (timing) of counting,  $u_{3g}$
  - 3.h.  $\gamma$ -ray self-shielding,  $u_{3h}$
  - 3.i.  $\gamma$ -ray interferences,  $u_{3i}$
  - 3.j. Peak integration method,  $u_{3j}$
  - 3.k. Blank correction (due to counting room/shielding background),  $u_{3k}$
4. Radiochemical separation,  $u_4$ 
  - 4.a. Mass determination of stable carrier and/or radiotracer,  $u_{4a}$
  - 4.b. Yield determination,  $u_{4b}$
  - 4.c. Isotopic exchange between the radioindicator and radiotracer and/or stable carrier,  $u_{4c}$

Obviously, from the standard uncertainties within an  $i$ -th category, the combined uncertainty of the category,  $u_{c,i}$  can be calculated and from these values the combined uncertainty of the

whole analytical procedure,  $u_c$ , can be evaluated using the rules for calculating combined uncertainty according to Ref. [12].

#### 4. QUANTIFICATION OF UNCERTAINTY COMPONENTS

The origin of the individual uncertainty components, the possible ways of their evaluation, as well as typical ranges of relative standard uncertainties are given in Table 1. Using the outlined or altered procedures, every laboratory should quantify the uncertainty components that are adequate for various matrices and analytes in the laboratory's specific conditions and not to rely upon the values given in Table 1, because they are given for illustration only.

#### 5. EXAMPLES

##### 5.1. Example 1: Vanadium determination by INAA

###### 5.1.1. Introduction

This example deals with the determination of the uncertainty budget in INAA using the relative standardization for the vanadium determination in BCR CRM 038 Coal Fly Ash.

###### 5.1.2. Specification

Vanadium is determined in about 100 mg aliquots of BCR CRM 038 Coal Fly Ash heat sealed in acid-cleaned polyethylene (PE) disc capsules using the following procedure:

Standards of vanadium are prepared by weighing out about 20 mg aliquots of a solution containing  $1.0675 \text{ mg g}^{-1}$  of vanadium, which was obtained by dissolution of  $\text{NH}_4\text{VO}_3$  (puriss., p.a. grade) in demineralized water, onto discs of Whatman-2 chromatographic paper which are heat sealed after air-drying into PE disc capsules. Thus, samples and standards of almost identical geometrical shapes are obtained. The comparison standard makes a direct link to SI when all sources of uncertainty are quantified, because  $\text{NH}_4\text{VO}_3$  is a compound with a well defined stoichiometry.

The samples and standards are irradiated simultaneously for 1 min. at a thermal neutron fluence rate of  $8.10^{13} \text{ cm}^{-2} \text{ s}^{-1}$  with the aid of a pneumatic facility. Blank PE capsules and PE capsules with blank chromatographic paper discs are also irradiated. To control the effect of the neutron flux gradient in a 10 cm long irradiation PE container (rabbit), the PE capsules with the samples and standards are closely attached to each other and held rigidly in place with polystyrene blocks.

Measurement of the 1434 keV  $\gamma$ -rays of the radioisotope  $^{52}\text{V}$  ( $T_{1/2}=3.75 \text{ min.}$ ) is carried out in a 12 cm distance from the top of a HPGe detector (rel. efficiency 11%, resolution FWHM 1.8 keV for the 1332.4 keV photons of  $^{60}\text{Co}$ ) for 7 min. after a decay time of 7 min. and 15 min. for the samples and standards, respectively. The dead time is about 25% and 15% for the samples and standards, respectively. The detector is coupled to a computer controlled  $\gamma$ -ray spectrometric system through a chain of associated linear electronics which contains a Nuclear Data (ND) 599 Loss Free Counting module for a dynamic correction of high and variable counting rates according to Westphal [17]. An adapted ND software for NAA is employed for on-line spectra evaluation. In all measurements the samples and standards are fixed towards the detector by compressing in a holder made of perspex plates to minimize variations of the counting geometry and differences of the thickness of the samples and

standards. No  $^{52}\text{V}$  activity is found in the measurement of the blank PE capsules and chromatographic paper discs.

### Calculation

Since the same irradiation and counting times were used for the samples and standards, the equation (3) can further be simplified as

$$c_m = \frac{(N_p)_a D_{st} w}{(N_p)_{st} D_a W} \quad (9)$$

### 5.1.3. Identifying and analysing uncertainty sources

The relevant uncertainty sources are listed in Table 1 and their influence on the measurand is shown in a cause and effect diagram in Fig. 1. Obviously, not all uncertainty sources as identified in Table 1 and/or Fig. 1 appear directly in Eq. 9. However, it should be realized that the individual components of the uncertainties of irradiation and counting can be projected into the uncertainties of  $N_p$  values (and/or sample and comparator masses) as if the peak area values were fluctuating, as schematically depicted in Fig.1. Therefore, it is useful to identify the individual uncertainty sources in the consecutive steps of analysis, i.e. sample and standard preparation, irradiation and counting (Cf. Table 1).

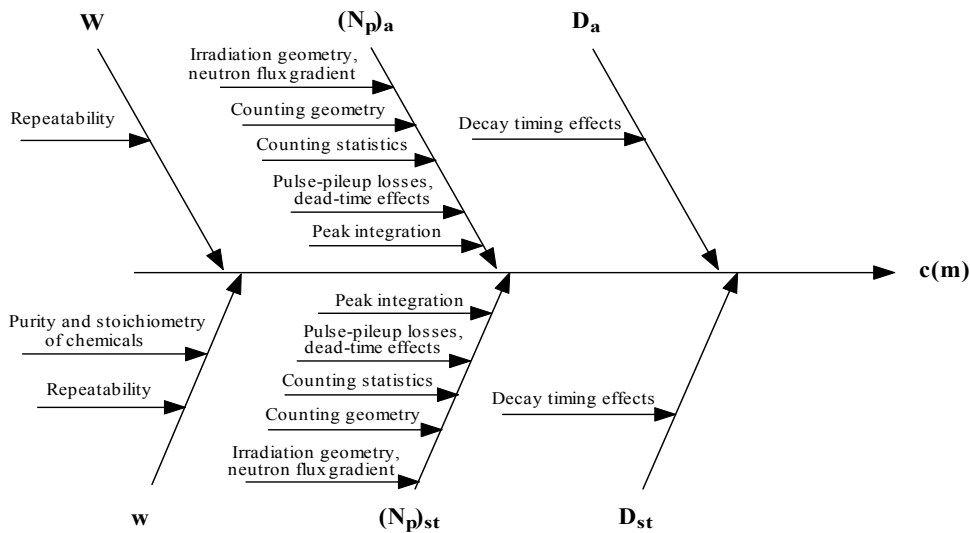


Fig. 1. Cause and effect diagram for INAA (example 5.1.).

#### Sample and standard preparation.

Sources of uncertainty occur in the determination of the mass of the sample and standard (uncertainty sources 1a, 1b) and in the purity of the standard material (1d). With the discussed type of material, no effects of moisture uptake during weighing could be detected; therefore uncertainty source 1c is negligible. No natural variation of the abundance of vanadium stable

isotopes is reported and no detectable blank values in both PE capsules and chromatographic paper are found, therefore uncertainty sources 1e and 1f, respectively, can be neglected.

### *Irradiation*

The uncertainties from differences in the irradiation position (uncertainty source 2a) for the sample and standard are derived from the neutron flux gradient, evaluated from the measurement results of the standards. Self shielding and scattering effects (uncertainty source 2b) are not expected to occur in this type of material. The uncertainty in the timing of the irradiation (uncertainty source 2c) depends mainly on the precision of the timing of the start and stop of the irradiation. The uncertainty due to interfering nuclear reactions (uncertainty source 2d) follows from the reaction rates of the analytical reaction  $^{52}\text{V}: ^{51}\text{V}(\text{n}, \gamma)^{52}\text{V}$  with thermal neutrons ( $\sigma_{\text{th}} = 4.8 \text{ b}$ ) and two interfering reactions with fast neutrons:  $^{51}\text{Cr}(\text{n}, \text{p})^{52}\text{V}$  ( $\sigma_{\text{f}} = 1.09 \text{ mb}$ ) and  $^{55}\text{Mn}(\text{n}, \alpha)^{52}\text{V}$  ( $\sigma_{\text{f}} = 0.11 \text{ mb}$ ). It can be neglected beforehand on basis of the cross sections, element contents in the material analyzed, and the difference in the thermal and fast neutron fluxes. The uncertainty due to variations of the neutron spectrum in time and space (uncertainty source 2e) can be neglected beforehand, because the samples and standards are irradiated simultaneously, and because the analytical reaction  $^{51}\text{V}(\text{n}, \gamma)^{52}\text{V}$  has a  $Q_0 = 0.6$ , indicating hardly any influence from the shape of the neutron spectrum in the epithermal/fast energy region. The uncertainty due to volatilization losses (uncertainty source 2f) can be neglected in advance, since vanadium is not volatile and does not form easily volatile compounds.

### *Gamma-ray spectrometry measurement*

The uncertainty from the measurement of the induced radioactivity follows directly from the counting statistics (uncertainty sources 3a) for both the samples and standards. The uncertainty introduced by differences in the counting geometry (uncertainty source 3b) has been derived from repeated measurements of a source at the given geometry with repositioning after each measurement (control chart evaluation). The uncertainty due to pulse pile-up losses (uncertainty source 3c) is derived from repeated measurements of the sources, measured at different dead times (control chart evaluation).  $^{52}\text{V}$  emits  $\gamma$ -rays of only one energy; therefore true coincidences do not occur (uncertainty source 3d). The uncertainties, introduced due to differences in dead time (uncertainty source 3e) between sample and standard are largely eliminated by using the loss-free counting module. The timing uncertainties (uncertainty source 3f) have effects upon the uncertainty of the correction for decay and should be considered due to the relative short half life of  $^{52}\text{V}$  (together with its uncertainty evaluated from various nuclear data sources). The effect of the uncertainty of the counting period (uncertainty source 3g) upon the correction for decay during counting can be neglected given the duration of the counting (7 minutes) and the half life of the radionuclide (3.75 min.). The self-shielding of the 1434 keV photons by the paper filter discs and PE capsules can be neglected (uncertainty source 3h). The uncertainty in the peak area integration (uncertainty source 3j) was derived from a comparison using several peak evaluation software packages and/or by hand integration. The uncertainty due to the  $^{52}\text{V}$  activity present as a background activity (uncertainty source 3k, not the blank value) can be left out since only the sample to be counted was present in the counting room.

#### 5.1.4. Quantifying uncertainty components

##### *Sample and standard preparation*

A 100-mg sample of BCR CRM 038 was weighed on a calibrated analytical balance. In the balance specification, the uncertainty (repeatability,  $s$ ) for the total load of 0 g to 50 g is specified as 0.015 mg ( $u_{1a}$ ).

The uncertainty in the mass of the vanadium standard ( $u_{1b}$ ) comes from combining the uncertainty in the weighed mass (21.35 mg of a stock solution weighed out; uncertainty 0.015 mg) with the uncertainty of the concentration of 1 mg g<sup>-1</sup> of the stock solution of NH<sub>4</sub>VO<sub>3</sub>. Since, however, about 100 g of the stock solution was weighed with the uncertainty of 0.03 mg for the total load of 50 g to 200 g as given in the balance specification, the latter uncertainty (a relative value of 0.00004 %) can be neglected. For the calculation of both uncertainties  $u_{1a}$  and  $u_{1b}$ , a normal distribution is assumed.

The uncertainty in the purity of the NH<sub>4</sub>VO<sub>3</sub> follows from the manufacturer's specifications. In this example, the purity "Puriss., p.a. grade" is specified as better than 99.7 %. Assuming a rectangular distribution with a range  $2a = 0.3$  %, the uncertainty  $u_{1d}$  is taken as 0.15 % (a semi range).

##### *Irradiation*

The uncertainty introduced due to differences in the position of the sample and standard has been derived from the uncertainty in the polynomial fitting of the gradient through the specific peak areas found by counting the standards. The neutron flux gradient varies between 0.9975 and 1.0025 around the mean value of the standards; the associated uncertainty  $u_{2a}$  is taken as 0.25 (the semi range of a triangular distribution). The uncertainty resulting from the variation of the duration of irradiation was evaluated from the response of a pneumatic sensor in the irradiation position. It amounted to 0.2 s assuming a Gaussian distribution, i.e., 0.33 % relative for the irradiation time of 1 min. An alternative way to estimate this uncertainty may be to analyse the sound of the rabbit in the irradiation channel or to irradiate suitable neutron flux monitors with precisely known element mass, which can subsequently be counted with a very low uncertainty. However, in this example the uncertainty  $u_{2c}$  could be left out, because the sample and standard were irradiated simultaneously. Other uncertainties related to irradiation could be neglected as well, as was explained in 5.1.3.

##### *Gamma-ray spectroscopy measurement*

The number of counts in the peak area of the 1434 keV line for the sample and standard are 36794 and 10342, respectively. Their respective uncertainties ( $u_{3a}$ )<sub>sample, standard</sub> are 442 and 83, assuming a normal distribution. The uncertainty related to differences in the counting geometry was derived from repeated measurements, indicating that the results differed between 99.8 % and 100.2 % of the mean value. Thus, the relative uncertainty  $u_{3b}$  is equal to 0.2 %, provided that a rectangular distribution is assumed. Similarly, the results related to the assessment of the pile-up effects varied between 99.4 % and 100.6 % around the mean value, and the uncertainty  $u_{3c}$  of 0.6% was evaluated employing a rectangular distribution.

The samples and standards were measured after a 7 min. and 15 min. decay, respectively. The uncertainty of the <sup>52</sup>V half life was evaluated from two values of 3.751 min. and 3.743 min. given in the well known nuclear data sources [18] and [19], respectively, as  $3.747 \pm 0.004$  min. (a relative value of 0.11 %) using a rectangular distribution. The uncertainty in the decay

determination, resulting from the imprecise measurement of the decay time, is 1 s (i.e., relative values of 0.24 % and 0.11 % for the sample and standard, respectively). Both uncertainties enter into the standard uncertainty of the decay correction D, which can also be written as

$$D = 2^{-\frac{t_d}{T_{1/2}}},$$

$$\text{yielding } u_D = \frac{D}{T_{1/2}} \sqrt{u_{t_d}^2 + \left(\frac{t_d}{T_{1/2}}\right)^2 u_{T_{1/2}}^2} \quad (10)$$

$$\text{or in the relative form } \frac{u_D}{D} = \frac{1}{T_{1/2}} \sqrt{u_{t_d}^2 + \left(\frac{t_d}{T_{1/2}}\right)^2 u_{T_{1/2}}^2} \quad (11)$$

After substitution into Eq (11), the uncertainty  $u_{3f}$  results in 0.49 % and 0.62 % for the sample and standard, respectively.

The uncertainty introduced by the peak integration method  $u_{3j}$  was derived from a comparison of several software packages, namely Nuclear Data, Hyperment for PC [20] and Deimos [21]. Assuming a rectangular distribution the semi range was 0.1 % relative for both the sample and standard.

#### 5.1.5. Calculating the combined standard uncertainty

Since Eq (9) involves only multiplication and division of quantities, the combined standard uncertainty  $u_c(c_m)$  can be calculated according to the equation [13]

$$u_c(c_m) = c_m \sqrt{u_1^2 + u_2^2 + u_3^2} \quad (12)$$

where the individual components of  $u_c(c_m)$  are expressed as relative standard uncertainties of the uncertainty sources in particular analytical steps entering into the variables in Eq (9) (see Table 2 and Fig. 1).

For this example, the following uncertainty components of sample and comparator preparation are taken into consideration:

$$u_1 = \sqrt{u_{1a}^2 + u_{1b}^2 + u_{1d}^2} \quad (13)$$

Most of the uncertainty components of the irradiation stage were found to be negligible, so that

$$u_2 = \sqrt{u_{2a}^2} \quad (14)$$

Of the various uncertainty components in  $\gamma$ -ray spectrometry measurement the following ones are considered significant

$$u_3 = \sqrt{u_{3a}^2(s) + u_{3a}^2(st) + u_{3b}^2(s) + u_{3b}^2(st) + u_{3c}^2(s) + u_{3c}^2(st) + u_{3f}^2(s) + u_{3f}^2(st) + u_{3j}^2(s) + u_{3j}^2(st)} \quad (15)$$

where  $(s)$  and  $(st)$  mean sample and standard, respectively.

Numerical values of variables, uncertainties and their conversion to the relative standard uncertainties, and other parameters are summarized in Table 2 together with calculation of the expanded uncertainty.

The mass fraction of vanadium determined was  $339 \text{ mg kg}^{-1}$  and the associated expanded uncertainty amounted to  $10.9 \text{ mg kg}^{-1}$  (i.e., 3.22 %). Obviously, the latter value was mostly influenced by contributions of counting statistics of the  $^{52}\text{V}$  activities in the sample and standard. The vanadium value determined [22] compares very well with the BCR noncertified value of  $334 \text{ mg kg}^{-1}$  within the uncertainty margins.

## 5.2. Example 2: Manganese determination by RNAA

### 5.2.1. Introduction

This example deals with the determination of the uncertainty budget in RNAA using the relative standardization for the manganese determination in IAEA RM A-13 Animal Freeze Dried Blood.

### 5.2.2. Specification

The procedure for the preparation of samples and standards and their irradiation was performed mostly as in Example 1 with the following changes: the sample mass amounted to 150 mg, standards were prepared by weighing out 100 mg aliquots of a stock solution with a Mn concentration of  $0.100 \text{ mg g}^{-1}$ . The stock solution was prepared by dissolution of 99.99 % manganese metal, Koch Light, Ltd. (a comparison standard which makes a direct link to SI when all sources of uncertainty are quantified) into PE irradiation vials and the duration of irradiation amounted to 3 min.

After irradiation, the samples were removed from PE irradiation vials and decomposed in a mixture of 5 mL of 65%  $\text{HNO}_3$  + 2 mL of 70%  $\text{HClO}_4$  by heating at  $230^\circ\text{C}$  for 10 min. in the presence of 1 mg of  $\text{Mn}^{2+}$  inactive carrier which was added as a 50 mg aliquot of the carrier solution. The solution resulting after decomposition was diluted with about 100 mL of water and neutralized with  $\text{NH}_4\text{OH}$  to pH 6-9. Then,  $\text{MnO}_2$  was precipitated by addition of 3 mL of a 5%  $(\text{NH}_4)_2\text{S}_2\text{O}_8$  solution and boiling for 2-3 min. The precipitate was filtered off with the aid of a membrane filter with a pore diameter of 1  $\mu\text{m}$  and washed with dilute  $\text{HNO}_3$  (1:10). A thin and homogeneously distributed deposit of the precipitate was obtained well suitable for reproducible counting close to a HPGe detector. The whole procedure was completed within 20-25 min. The chemical yield of the separation varied in the range of 90-95% as was ascertained by reactivation of the inactive carrier using the above irradiation procedure after the induced activity of the  $^{56}\text{Mn}$  radionuclide originating from the originally present Mn in the sample had decayed [23].

The irradiated Mn standard solution was only 100 times gravimetrically diluted and 10 mg aliquots were weighed out onto the membrane filter and air dried to obtain the geometrical shape of the standards for counting matching that of the samples.

Counting of the 846.8 keV  $\gamma$ -rays of  $^{56}\text{Mn}$  (the interfering activity of the 843.8 keV photons of  $^{27}\text{Mg}$  was completely removed by the radiochemical procedure employed) for 30 min. was performed after decay times of 30 min. and 35 min. for the samples and standards, respectively, directly on the cap of the HPGe detector mentioned in Example 1. The dead time for both samples and standards did not exceed 3 %.

The  $^{56}\text{Mn}$  activity originates not only from the analytical reaction  $^{55}\text{Mn}(n, \gamma)$  with thermal neutrons but also from two interfering reactions with fast neutrons  $^{56}\text{Fe}(n,p)^{56}\text{Mn}$  and  $^{59}\text{Co}(n,\alpha)^{56}\text{Mn}$ . The interference contributions of these reactions were measured by irradiation of about 100 mg of high purity Fe and Co metals in a cadmium box with the wall thickness of 1 mm. Apparent manganese values of  $39.1 \pm 0.6 \mu\text{g Mn/g Fe}$  and  $5.9 \pm 0.1 \mu\text{g Mn/g Co}$  were found for the former and latter interfering reactions from repeated irradiations of the respective high purity metals behind a 1 mm Cd shielding.

### *Calculation*

Since the same irradiation and counting times were used as in the previous example, Eq (9) is to be modified only to take into account the chemical yield of separation as follows

$$c_m = \frac{(N_p)_a D_{st} w}{(N_p)_{st} D_a W Y_a} \quad (16)$$

### **5.2.3. Identifying and analysing uncertainty sources**

Similarly to Example 1, the relevant uncertainty sources are those listed in Table 1. Their influence on the measurand is depicted in the cause and effect diagram in Fig. 2. The individual components of the uncertainties of irradiation and counting are projected into the uncertainties of  $N_p$  values as illustrated in Fig.2. Thus, the individual uncertainty sources are the same as in Example 1 with addition of the uncertainty of the chemical yield determination and will again be discussed for the consecutive steps of analysis.

### **5.2.4. Quantifying uncertainty components**

#### *Sample and standard preparation*

A 150-mg sample of IAEA RM A-13 Freeze Dried Animal Blood was weighed using a calibrated analytical microbalance with the uncertainty (repeatability,  $s$ ) of 0.015 mg for the total load of 0 g to 50 g ( $u_{1a}$ ).

The uncertainty in the mass of the manganese standard ( $u_{1b}$ ) is obtained by combining the uncertainty in the weighted mass (100 mg of a stock solution, uncertainty 0.015 mg) with the uncertainty of the concentration of  $0.100 \text{ mg g}^{-1}$  of the stock solution, which can be neglected (see Example 1).

The relative uncertainty of the chemical composition of the starting material (99.99 % Mn) for the standard preparation  $u_{1d}$  is 0.005 % (a semi range of a rectangular distribution).

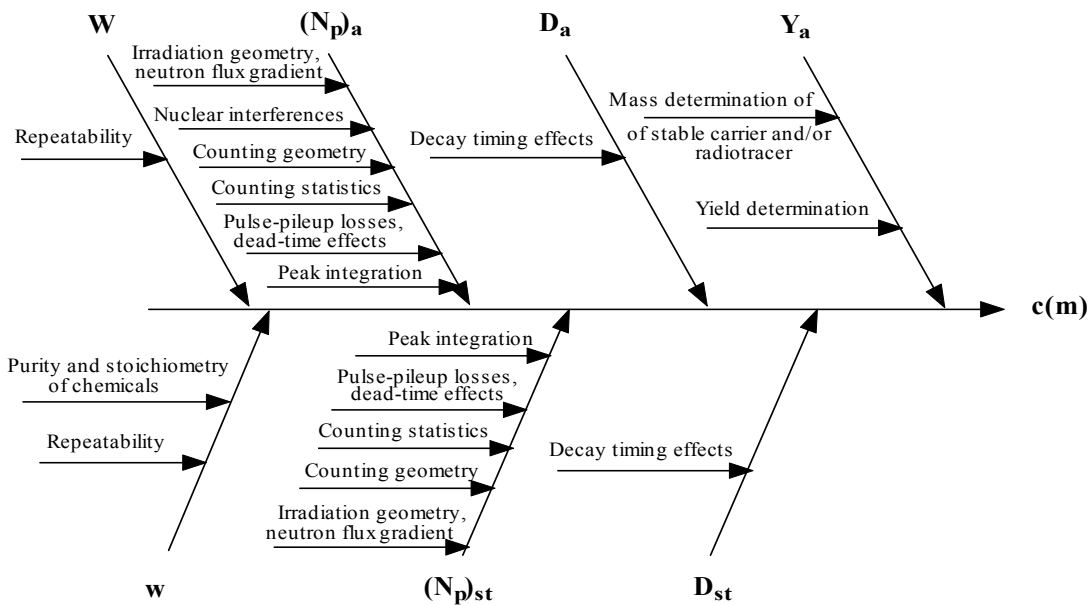


Fig. 2. Cause and effect diagram for RNAA (example 5.2.2).

### Irradiation

The relative uncertainty  $u_{2a}$  due to differences in the position of the sample and standard is the same as in Example 1, i.e. 0.25 %, while other uncertainties in this analysis step can be neglected except of those resulting from interfering nuclear reactions. Of these, the influence of the interfering reaction  $^{59}\text{Co}(n,\alpha)^{56}\text{Mn}$  ( $\sigma_f = 0.16 \mu\text{b}$ ) is negligible due to a very low concentration of Co in the material analyzed (no information has been obtained in the IAEA certification campaign, however, in analogy with similar materials of this kind, a value below  $1 \text{ mg kg}^{-1}$  can be expected). On the other hand, the correction for the interfering reaction  $^{56}\text{Fe}(n,p)^{56}\text{Mn}$  ( $\sigma_f = 1.07 \text{ mb}$ ) is significant (the content of Fe in this material amounts to  $2.4 \text{ mg g}^{-1}$ ). Thus, the uncertainty of the correction  $39.1 \pm 0.6 \mu\text{g Mn/g Fe}$  should be taken into account. For this value of  $u_{2d}$  a Gaussian distribution is assumed, because it was evaluated from repeated measurements.

### Gamma-ray spectroscopy measurement

The number of counts in the peak area of the 846.8 keV line for the standard and sample are 1449 and 5342, respectively. Their respective uncertainties  $(u_{3a})_{\text{sample, standard}}$  are 65 and 59, assuming a normal distribution. The relative uncertainty  $u_{3b}$  (due to differences in the counting geometry) is equal to 0.5 %, assuming a rectangular distribution. It is somewhat higher compared to Example 1, but still reasonably low even for counting on the top of the HPGe detector due to the almost identical shape of the sample and standard and the positioning system employed. On the other hand, a lower relative uncertainty  $u_{3c}$  of 0.1 % (the assessment of the pile-up effects) was evaluated employing a rectangular distribution due to very low dead times of both the sample and standard.

The samples and standards were counted after 30-min. and 35-min decay times, respectively, for 30 min. The uncertainty of the  $^{56}\text{Mn}$  half life was evaluated from reliable literature data ( $2.579 \text{ h}$  [18] and  $2.5785 \text{ h}$  [19]) as  $2.57875 \pm 0.00025 \text{ h}$  (a relative value of 0.01 %) using a rectangular distribution. The uncertainty in the decay determination was again 1 s, i.e., 0.06 % and 0.05 % relative for the sample and standard, respectively. Thus, the relative uncertainties

due to decay effects calculated according to Eq (11) are 0.0041 % and 0.0029 % for the sample and standard, respectively, and can be neglected.

The relative uncertainty introduced by the peak integration method  $u_{3j}$  derived as in Example 1 was 0.3 % and 0.2 % for the sample and standard, respectively.

### *Radiochemical separation*

The uncertainty  $u_{4a}$  of the mass of the inactive Mn carrier added at the beginning of decomposition as a 50 mg aliquot of the carrier solution is 0.015 mg. The uncertainty of the yield determination  $u_{4b}$  is composed from the contributions arising from the reactivation and subsequent counting of the Mn carrier which will be denoted here as  $u_2$  and  $u_3$ , respectively. The uncertainty of  $u_2$  is equal to only  $u_{2a}$ , i.e., 0.25 % relative, because simultaneous irradiation of the standard (the aliquot of the carrier solution) and sample with the separated carrier was carried out and the aforementioned interfering reactions can be neglected (see "Irradiation" above). Counting of the reactivated carrier was performed in a 10 cm distance from the top of the HPGe detector. Hence, a lower relative uncertainty due to positioning against the detector was obtained compared to that of the samples and standards amounting to 0.1 %, while the other sources of uncertainty of this step could be neglected. Since complete decomposition of the samples was achieved, the uncertainty source due to the establishing the isotopic exchange between the  $^{56}\text{Mn}$  radioindicator and the stable carrier could be neglected as well.

#### **5.2.5. Calculating the combined standard uncertainty**

Since Eq (16) contains again only multiplication and division of quantities, the combined standard uncertainty  $u_c(c_{Mn})$  can be calculated according to the equation

$$u_c(c_{Mn}) = c_{Mn} \sqrt{u_1^2 + u_2^2 + u_3^2 + u_4^2} \quad (17)$$

where the individual components are again expressed as relative standard deviations of the uncertainty sources in particular analytical steps entering into the variables in Eq (16) (see Table 3 and Fig. 2).

The uncertainty components of sample and standard preparation are the same as in Example 1, i.e.,

$$u_1 = \sqrt{u_{1a}^2 + u_{1b}^2 + u_{1d}^2} \quad (18)$$

while those of irradiation are as follows

$$u_2 = \sqrt{u_{2a}^2 + u_{2d}^2} \quad (19)$$

The number of the uncertainty components in  $\gamma$ -ray spectrometry measurement is reduced compared to Example 1 as

$$u_3 = \sqrt{u_{3a}^2(s) + u_{3a}^2(st) + u_{3b}^2(s) + u_{3b}^2(st) + u_{3j}^2(s) + u_{3j}^2(st)} \quad (20)$$

The uncertainty components of radiochemical separation are given by

$$u_4 = \sqrt{u_{4a}^2 + u_{4b}^2} = \sqrt{u_{4a}^2 + u_{2a}'^2 + u_{3a}'^2 + u_{3b}'^2} \quad (21)$$

Numerical values of variables, uncertainties and their conversion to the relative standard uncertainties, and other parameters are summarized in Table 3 together with calculation of the expanded uncertainty. The mass fraction of manganese determined was  $31 \mu\text{g kg}^{-1}$  and the associated expanded uncertainty amounted to  $3.0 \mu\text{g kg}^{-1}$  (i.e., 9.8 %). This example again demonstrates that the value of the combined uncertainty consisted mostly of counting statistics of the  $^{56}\text{Mn}$  activities in the sample and standard. It also shows that if the yield determination is performed for each sample, the additional uncertainty  $u_4$  introduced by radiochemical separation is rather small. It may be presumed that a somewhat lower uncertainty would be obtained by using the  $^{54}\text{Mn}$  radiotracer for the determination of the yield of chemical separation for each sample, because the term  $u_{2a}'$  in Eq (21) would be left out. However, when we would rely only on the fact that the yield of chemical separation varies in the range 90-95% (as found, for instance, in preliminary experiments), then another way of evaluation of the  $u_4$  value should be used. Presuming that all values within the above range  $2a = 5$  have the same probability (a rectangular distribution), the standard uncertainty  $u_4$  is to be calculated as  $a/\sqrt{3} = 1.44$ . This value exceeds significantly that one obtained when the yield of chemical separation is determined for each sample.

### 5.3. Uncertainty budget in the $k_0$ -NAA standardization

Evaluating combined uncertainty in the  $k_0$ -standardization, disregarding whether in INAA, ENAA or RNAA, is much more complex as obvious from Eqs 5, 7, 8 and was dealt with in detail by De Corte et al. [9,10,24-26]. Instead of uncertainties associated with the standard preparation in the relative standardization, uncertainties of  $k_0$ -factors come into consideration and other uncertainties of the parameters  $Q_0$ ,  $\alpha$ ,  $f$ ,  $\varepsilon_p$ , and of coincidence corrections should be taken into account as well.

For sake of simplicity, only the final account of uncertainties in the  $k_0$ -standardization is presented here as given by De Corte et al. [9,10].

Table 2. Relative standard uncertainties of parameters in the  $k_0$ -NAA standardization

Parameter	Contribution
$k_0$	~ 1 %
$Q_0$	~ 1 %
$\alpha$	~ 1.5 %
$F$	~ 1 %
$\varepsilon_p$ -measurement and conversion	~ 2 %
true-coincidence correction	~ 1.5 %
Overall (quadratic summation)	~ 3.5 %

For calculation of the combined uncertainty of results obtained using the  $k_0$ -NAA standardization, the individual uncertainty components in Table 2 are to be combined with those of counting statistics of the samples and neutron flux monitors.

## REFERENCES

- [1] DE SOETE, D., GIJBELS, R., HOSTE, J., Neutron Activation Analysis, Wiley- Interscience, London/New York/Sydney/Toronto, 1972.
- [2] KRUGER, P., Principles of Activation Analysis, Wiley-Interscience, New York, 1971.
- [3] AMIEL, S., Nondestructive Activation Analysis, Elsevier, Amsterdam, 1981.
- [4] PARRY, S.J., Activation Spectrometry in Chemical Analysis, John Wiley&Sons, New York, 1991.
- [5] BYRNE, A.R., Review of neutron activation analysis in the standardization and study of reference materials, including its application to radionuclide reference materials, Fresenius J. Anal. Chem., 345 (1993) 144-151.
- [6] DE CORTE, F., SIMONITS, A., DE WISPELAERE, A., ELEK, A.,  $k_0$ -measurement and related nuclear data compilation for (n,gamma) reactor neutron activation analysis Pt. 3a. Experimental, J. Radioanal. Chem., 133 (1989) 3-41.
- [7] DE CORTE, F., SIMONITS, A.,  $k_0$ -measurement and related nuclear data compilation for (n,gamma) reactor neutron activation analysis Pt. 3b. Tabulation, J. Radioanal. Nucl. Chem., Articles 133 (1989) 43-130.
- [8] DE CORTE, F., SIMONITS, A., BELLEMANS, F., FREITAS, M.C., JOVANOVIĆ, S., SMODIS, B., ERDTMANN, G., PETRI, H., DE WISPELAERE, A., Recent advances in the  $k_0$ -standardization of neutron activation analysis. Extensions, applications, prospects, J. Radioanal. Nucl. Chem., 169 (1993) 125-158.
- [9] DE CORTE, F., The  $k_0$ -standardization method: a move to the optimization of neutron activation analysis, Habilitation Thesis, University of Gent, 1987.
- [10] DE CORTE, F., SIMONITS, A., Vade Mecum for  $k_0$ -Users, Addendum to the KAYZERO/SOLCOI software package, DSM Research, Gellen (NL), R94/11492, December 1994.
- [11] GREENBERG, R.R., LINDSTROM, R.M., BECKER, D.A., Presented at the 9th Int. Conf. Modern Trends in Activation Analysis (MTAA-9), Seoul, September 24-30, 1995.
- [12] ELLISON, S.L.R., ROSSLEIN, M., WILLIAMS, A., BERGLUND, M., HAESSELBARTH, W., HEDEGAARD, K., KARLS, R., MANSSON, M., STEPHANY, R., VAN DER VEEN, A., WEGSCHEIDER, W., VAN DE WIEL, H., WOOD, R., PAN XIU RONG, SALIT, M., SQUIRRELL, A., YUSUSDA, K., JOHNSON, R., JUNG-KEUN LEE, MOWREY, M., DE REGGE, P., FAJGELJ, A., GALSWORTHY, D., EURACHEM/CITAC Guide "Quantifying Uncertainty in Analytical Measurement", Second Edition, Editors: S. L. R. Ellison, M. Rosslein, A Williams, (2000) ,ISBN 0-948926-15-5.
- [13] BODE, P., BLAAUW, M., OBRUSNIK, I., Variation of neutron flux and related parameters in an irradiation container, in use with  $k_0$ -based neutron activation analysis, J. Radioanal. Nucl. Chem. 157 (1992) 301-312.
- [14] INTERNATIONAL ATOMIC ENERGY AGENCY, IAEA TECDOC 564, "Practical aspects of operating a neutron activation analysis laboratory", IAEA Vienna, 1990.
- [15] BLAAUW, M., AMMERLAAN, M.J.J., BODE, P., Quantification of some sources of variation in neutron activation analysis, J. Appl. Radiat. Isotop. 44 (1993) 547-551.
- [16] INTERNATIONAL ATOMIC ENERGY AGENCY, IAEA TECDOC 1011, "Intercomparison on gamma-ray analysis software packages", IAEA Vienna, 1998.
- [17] WESTPHAL, G.P., Instrumental correction of counting losses in nuclear pulse spectroscopy Nucl. Instr. Methods B10/11 (1985) 1047-1050.
- [18] BROWN, E., FIRESTONE, R.B., Table of Isotopes, John Wiley & Sons, New York, Chichester, Brisbane, Toronto, Sydney, 1986.
- [19] FIRESTONE, R.B., BAGLIN, C.M., CHU, S.Y.F., Table of Isotopes, 8<sup>th</sup> Edition, 1998 Update, John Wiley & Sons, New York, Chichester, Brisbane, Toronto, Sydney, 1998.
- [20] FAZEKAS, B., MOLNAR, G., BELGYA, I., DABOLCZI, L., SIMONITS, A., Introducing HYPERMET-PC for automatic analysis of complex gamma-ray spectra, J. Radioanal. Nucl. Chem., 215 (1997) 271-277.

- [21] FRANA, J., Unpublished results.
- [22] KUCERA, J., SOUKAL, L., Low uncertainty determination of manganese and vanadium in environmental and biological reference materials by instrumental neutron activation analysis. *Fresenius J. Anal. Chem.* 360 (1998) 415-418.
- [23] KUCERA, J., SOUKAL, L., FALTEJSEK, J., Low level determination of manganese in biological reference materials by neutron activation analysis, *J. Radioanal. Nucl. Chem., Letters* 107 (1986) 361-369.
- [24] DE CORTE, F., SORDO-EL HAMMAMI, K., MOENS, L., SIMONITS, A., DE WISPELAERE, A., HOSTE, J., The accuracy and precision of the experimental alpha-determination in the  $1/E_{\text{sup}}(1+\alpha)$  epithermal reactor-neutron spectrum, *J. Radioanal. Chem.*, 62 (1981) 209.
- [25] MOENS, L., DE CORTE, F., SIMONITS, A., XILEI, L., DE WISPELAERE, A., DE DONDER, J., HOSTE, J., Calculation of the absolute peak efficiency of Ge and Ge(Li) detectors for different counting geometries, *J. Radioanal. Chem.*, 70 (1982) 539.
- [26] SIMONITS, A., JOVANOVIĆ, S., DE CORTE, F., EL NIMR, T., MOENS, L., HOSTE, J., A method for experimental determination of effective resonance energies related to (n, gamma) reactions, *J. Radioanal. Nucl. Chem.*, 82 (1984) 169-179.

Table 1. Origin, evaluation, and typical magnitude of uncertainties in NAA

Uncertainty component	Comments on the origin and evaluation of uncertainty components	Typical rel. stand. uncertainty
$u_l$	<i>Sample and comparator preparation</i>	
$u_{1a}$	A 5-decimal place balance can produce uncertainty of 0.015 mg for 0-50 g samples, while a 4-decimal place balance can produce uncertainty of 0.1mg for 0-110 g samples (can be found in the balance specification as repeatability or reproducibility). Alternatively, this can be evaluated from control charts of repetitive measurements of a range of amounts of increasing mass, and depending on the tarr mass. Then a Gaussian distribution is to be used for evaluation of the standard uncertainty.	0.015- 0.1 % (for a 100 mg sample)
$u_{1b}$	As above, however usually approx. 20 mg comparator foils or standard aliquots are weighed. A rectangular or a Gaussian distribution is to be used, see above. For $k_0$ -values uncertainties see chapter 5.3	0.075 - 0.5 %
$u_{1c}$	Depends on a sample type (a very high moisture uptake is to be expected for freeze dried urine, while almost no uptake occurs on weighing of fly ash). Can be evaluated for every type of sample via repetitive measurements whilst the sample remains on the balance and extrapolation is carried out towards a reference point. A Gaussian or triangular distribution can be recommended for the evaluation of the standard uncertainty.	negligible - 1 %
$u_{1d}$	The purity of the starting material is crucial in the preparation of synthetic standards (a rectangular distribution is to be used for the evaluation of the standard uncertainty). The quality of certificates of vendors is often doubtful since not all impurities are mentioned. Sometimes also detection limits are to be included to determine the minimum purity by using a rectangular distribution. If matrix CRM are used instead of synthetic standards, the uncertainty of the certified value, which usually amounts to several per cent, must be taken into account..	0.1 - several %
$u_{1e}$	May be important for elements whose $\theta$ varies in nature (Li, B, S), for elements for which the abundance of certain isotopes is not well established (Ca) or if man-made variability was introduced (Li, U). It can be considered negligible for most other elements. Doubts may be evaluated via mass spectrometry. A Gaussian or triangular distribution can then be used for evaluation of the standard uncertainty, depending on information available.	negligible for most elements

$u_2$	<i>Irradiation</i>	
$u_{2a}$	Depends on the construction of irradiation position (rotation facilities, "flipping" midway through the irradiation, etc.) and on a neutron flux gradient present. By carefully placing comparators next to samples in a sandwich-type configuration and polynomial interpretation it can be kept below 0.1%. A Gaussian or triangular distribution is to be used for evaluation of the standard uncertainty.	< 0.1 - 0.5 %
$u_{2b}$	Self-shielding is in most cases negligible, a need for correction may arise for elements with high absorption cross sections and high density materials (metals). Self-shielding can be accurately measured by dilution with non-absorbing materials or calculated [1, p. 457]. Elastic scattering may be important for elements with low Z. A Gaussian or triangular distribution seems to be appropriate for evaluation of the standard uncertainty.	~ 0.1 % in most cases
$u_{2c}$	Mostly negligible when samples and standards are irradiated together and when the start and stop times can be measured accurately. Uncertainties involving the length of irradiation are important when samples and standards are irradiated separately. Their importance depends upon the half-life of the particular radioisotope and the length of irradiation. If the flux monitoring approach is used to control the length of irradiation, uncertainty is limited to $u_{3a}$ achieved for the monitor. Usually type A. Negligible when samples and standards are irradiated together and when start and stop times can be measured accurately.	negligible - 0.3 %
$u_{2d}$	Depends upon the nuclide being measured, and is insignificant in many cases. Corrections for fast neutron interferences can be made by irradiating in two or more facilities with different neutron energy spectra and/or by calculation, if the relevant parameters (fast neutron cross section, and fast neutron fluence rate and spectrum shape) are sufficiently well known. A Gaussian distribution is to be used for evaluation of the standard uncertainty.	negligible - ~ 1 %
$u_{2e}$	Evaluation of neutron spectrum variations in time and space may be derived from repeated irradiations and measurements of the appropriate foils (Zr+Au). The gradients of a fluence rate, $f$ and $\alpha$ can thus be derived as a function of reactor operating time, Xe-poisoning and position of the foils (monitors) in the rabbit. A Gaussian or triangular distribution should be used for evaluation of the standard uncertainty [13].	negligible - ~ 1 %
$u_{2f}$	This is applicable to a number of elements of which the halogens and Hg are the most well-known. The degree of this effect does not depend only on an element, but also on its chemical speciation (chemical form), temperature, radiation dose, and type of irradiation container. Quantification can only be done by irradiation in various types of irradiation containers, e.g., polyethylene and sealed quartz tubes, and by comparison of the differences obtained. A rectangular distribution is recommended for estimation of the standard uncertainty.	negligible - several %

$U_3$		$\gamma$ ray spectrometry measurement
$U_{3a}$	The most important component in this category, instantly available from the measurement result ( $u_{3a} = \sqrt{2N_p + B}$ , B-background) which may vary in a wide range (from 0.2 % up to 40 % for small peaks close to detection limit). A Poisson distribution is to be used for evaluation of the standard uncertainty.	usually 0.2 - 30 %
$U_{3b}$	To minimize this component, the samples and standards should have a well defined shape (discs, columns, pellets of similar thickness) and should be counted at least 5 cm from the detector. It can be quantified from repeated measurements of an identical sample, especially in case of long-lived radionuclides using a Gaussian or triangular distribution. However, frequently, there is a need to count on the end-cap of the detector. In such a case, evaluation should be done according to [14].	~ 0.1 - 20 %
$U_{3c}$	Can be accurately corrected for by the appropriate setting of the electronic chain (amplifier shaping time, etc.) and by using the appropriate correction method (pulser, Westphal's Loss Free Counting module, etc.). Can be evaluated from repeated measurements of a sample, especially at different dead times, using a Gaussian or triangular distribution.	~ 0.1 - 0.5 %
$U_{3d}$	Irrelevant in the relative standardization. A correction needed in the $k_0$ -standardization can be associated with a reasonably low uncertainty. A Gaussian or triangular distribution is recommended for evaluation of the standard uncertainty.	~ 1%
$U_{3e}$	Important only when the measurement time is close to the half-life of a radionuclide being measured. In most cases the uncertainty due to dead time correction can be considered negligible if appropriate care is taken in experimental design. In case of a pulser-peak dead-time correction, software may often have difficulties in fitting the pulser peak in the spectrum due to excessive tailing. In this approach, the precision associated with the missing counts should be taken into account rather than the peak area (Cf. [15]). A Poisson distribution should be used for evaluation of the standard uncertainty.	negligible in most cases
$U_{3f}$	Should be considered only for radionuclides with very short half-lives (< 1 min.). Timing uncertainties would be entirely negligible for radionuclides with much greater half-lives.	negligible in most cases
$U_{3g}$	Imprecision in the counting time affects the correction for decay during the measurement of short-lived radionuclides and is usually negligible for medium- and long-lived radionuclides. Uncertainty of 1 s may result from the way the analyzer is started (hard start or clock pulse start). Might therefore be applicable to the short-lived radionuclides and counting times in the order of the half-life of the radionuclide only. In such a case, a rectangular distribution is recommended for evaluation of the standard uncertainty.	negligible in most cases
$u_{3h}$	May be important for measuring $E_\gamma < 100$ keV. Can be calculated or accurately measured by counting a sample (or standard) directly, and again with a nonirradiated sample inserted between the counted sample and the detector (without changing the counting geometry). The uncertainty evaluation is usually limited by counting statistics which	~ 0.1 - ~ 0.5 %

follows a Poisson distribution.

$u_{3i}$  Although many of the radionuclides measured in NAA are susceptible to  $\gamma$ -ray interferences, such interferences, if significant, can usually be evaluated by one of the three methods: ~ 0.3 - ~ 1 %

1) comparing results from multiple  $\gamma$ -rays of a single radionuclide;

2) recounting samples after significant decay, since interfering radionuclides rarely have similar half-lives;

3) looking for additional  $\gamma$ -rays from known interferences. Uncertainties will be determined from counting statistics of the various measurements which follow a Poisson distribution.

$u_{3j}$  Various intercomparison of different peak area evaluation programmes yielded usually insignificant differences for single peaks ( $u_{3j} < 0.1\%$ ). Larger uncertainties are to be expected for a number of counts close to detection limit and especially for multiplets. Can be evaluated by comparing results of several peak area evaluation programmes and/or hand integration. See also [16]. Note that in case of small peaks, this component would not be completely independent of the uncertainty due to counting statistics  $u_{3a}$ . The larger value of  $u_{3a}$ , the larger value of  $u_{3i}$  is to be expected. A Gaussian or triangular distribution can be used for evaluation of the standard uncertainty. ~ 0.5 - several %  
(for multiplets)

$U_{3k}$  Various shielding of the counting room and/or detector results in various background in the spectra of samples with a low activity, especially in RNAA. This affects counting statistics which follows a Poisson distribution. Control charts are useful to evaluate the variability in the background of the counting room due to variations in radon levels and/or insufficiently shielded other activities present. Mostly negligible in INAA. negligible in most cases

$u_4$

*Radiochemical separation*

$u_{4a}$  See  $u_{1a}$ ,  $u_{1b}$ . Larger uncertainties are to be expected when pipetted aliquots of an inactive carrier and/or radiotracer are added instead of weighed aliquots. 0.02 - 0.5 %

$u_{4b}$  Depends on the way of the yield determination. When use is made of a radiotracer or reactivation, uncertainties of counting statistics of the radiotracer or of the reactivated carrier are to be taken into account (a Poisson distribution). When another analytical technique is employed, its uncertainty is to be included. Can be evaluated by repeating the decomposition and separation procedure. In the latter case, a rectangular distribution is mostly applicable for evaluation of the standard uncertainty. ~ 0.3 - ~ 0.5 %

$u_{4c}$  Negligible when a homogeneous system is obtained by the sample decomposition (i.e., by the total destruction and mineralization). On the other hand, larger uncertainties are to be expected, if, e.g., chelating organic compounds or rests of the solid phase remain undestroyed after sample decomposition negligible in most cases

Table 2. Summary table on the uncertainty components of the vanadium determination in BCR CRM 038 by INAA with the relative standardization

Reference [7]	Symbol for variable*	Value of variable (unit)	Uncertainty	Conversion factor to standard uncertainty	Relative standard uncertainty $u_i$ , %	Sensitivity factor	Percent contribution to combined uncertainty $u_c$
1.a	W	100 (mg)	0.015	1	0.015	1	0.01
1.b	W	21.35 (mg)	0.015	1	0.07	1	0.19
1.d	[w]	99.85 (%)	0.15	$1/\sqrt{3}$	0.087	1	0.29
2.a	[ $N_{p,a}$ , $N_{p,st}$ ]	100 (%)	0.25	$1/\sqrt{6}$	0.10	1	0.38
3.a (sample)	[ $N_{p,a}$ ]	36794 (counts)	442	1	1.2	1	55.29
3.a (standard)	[ $N_{p,st}$ ]	10342 (counts)	83	1	0.8	1	24.57
3.b (sample)	[ $N_{p,a}$ ]	100 (%)	0.2	$1/\sqrt{3}$	0.1	1	0.38
3.b (standard)	[ $N_{p,st}$ ]	100 (%)	0.2	$1/\sqrt{3}$	0.1	1	0.38
3.c (sample)	[ $N_{p,a}$ ]	100 (%)	0.6	$1/\sqrt{3}$	0.35	1	4.70
3.c (standard)	[ $N_{p,st}$ ]	100 (%)	0.6	$1/\sqrt{3}$	0.35	1	4.70
3.f (sample)	[ $D_a$ ] (%)	100 (%)	0.49	$1/\sqrt{3}$	0.28	1	3.01
3.f (standard)	[ $D_{st}$ ]	100 (%)	0.62	$1/\sqrt{3}$	0.36	1	4.98
3.j (sample)	[ $N_{p,a}$ ]	100 (%)	0.2	$1/\sqrt{3}$	0.12	1	0.55
3.j (standard)	[ $N_{p,st}$ ] (%)	100 (%)	0.2	$1/\sqrt{3}$	0.12	1	0.55

Value of the measurand  $c_V = 339 \text{ mg kg}^{-1}$

Combined standard uncertainty  $u_c(c_V) = 5.47 \text{ mg kg}^{-1}$ ; Expanded uncertainty =  $339 \pm 10.9 \text{ mg kg}^{-1}$  (Coverage factor =2)

\* - projected in variable in brackets

Table 3. Summary table on the uncertainty components of the manganese determination in IAEA RM A-13 by in RNAA with the relative standardization

Reference to uncertainty source	Symbol for variable*	Value of variable (unit)	Uncertainty	Conversion factor to standard uncertainty	Relative standard uncertainty $u_i$ , %	Sensitivity factor	Percent contribution to combined uncertainty $u_c$
1.a	W	150 (mg)	0.015	1	0.010	1	0.0004
1.b	W	100 (mg)	0.015	1	0.15	1	0.0009
1.d	[w]	99.99 (%)	0.005	1/√3	0.003	1	0.00005
2.a	[N <sub>p,a</sub> , N <sub>p,st</sub> ]	100 (%)	0.25	1/√6	0.10	1	0.04
2.d	[N <sub>p,a</sub> ]	39.1 (µg Mn/g Fe)	0.6	1	1.53	1	9.80
3.a (sample)	N <sub>p,a</sub>	1449 (counts)	65	1	4.48	1	84.00
3.a (standard)	N <sub>p,st</sub>	5342 (counts)	59	1	1.10	1	5.06
3.b (sample)	[N <sub>p,a</sub> ]	100 (%)	0.5	1/√3	0.29	1	0.35
3.b (standard)	[N <sub>p,st</sub> ]	100 (%)	0.5	1/√3	0.29	1	0.35
3.j (sample)	[N <sub>p,a</sub> , ]	100 (%)	0.3	1/√3	0.17	1	0.12
3.j (standard)	[N <sub>p,st</sub> ]	100 (%)	0.2	1/√3	0.11	1	0.05
4.a	[Y <sub>a</sub> ]	100 (mg)	0.015	1	0.015	1	0.0009
4.b (2.a')	[Y <sub>a</sub> ]	100 (%)	0.25	1/√6	0.10	1	0.04
4.b (3.a')	[Y <sub>a</sub> ]	579605 (counts)	1159	1	0.20	1	0.17
4.b (3.b')	[Y <sub>a</sub> ]	100 (%)	0.1	1/√3	0.06	1	0.015

Value of the measurand  $c_{Mn} = 31.0 \mu\text{g kg}^{-1}$

Combined standard uncertainty  $u_c(c_{Mn}) = 1.51 \mu\text{g kg}^{-1}$ ; Expanded uncertainty =  $31.0 \pm 3.03 \mu\text{g kg}^{-1}$  (coverage factor =2)

\* - projected in variable in brackets

# QUANTIFICATION OF UNCERTAINTY IN GAMMA-SPECTROMETRIC ANALYSIS OF ENVIRONMENTAL SAMPLES

C. DOVLETE, P.P. POVINEC

Marine Environment Laboratory, International Atomic Energy Agency, Monaco

## Abstract

The example given discusses and quantifies the uncertainty sources for the determination of radionuclides in environmental samples by gamma ray spectrometry. The method usually involves the nondestructive measurement of a large sample with a high efficiency and high resolution detector. In addition to the usual sources of uncertainty, this analysis method has particular uncertainties related to the self-absorption of radiation in the sample and the coincidences of radiation detection due to the high angular efficiency. The example distinguishes between *a-priori* quantifiable sources of uncertainty related to the instrumentation and the nuclear parameters of the radionuclides and the uncertainties to be quantified from the measurement results. The latter include differences in counting geometry and self-absorption between calibration standards and samples, counting statistics, decay- and life-time correction factors, and several types of coincidences. An interesting feature of this example is the evaluation of the uncertainty on the detection efficiency by Monte Carlo simulation of individual photon histories, rather than from experimental measurement.

## 1. SCOPE AND DEFINITIONS

### 1.1. Gamma-ray spectrometry

#### 1.1.1 Introduction

The aim of gamma-spectrometric analysis of environmental samples is to determine the activity concentration of gamma-ray emitting radionuclides and the associated uncertainty of the results. The method is usually applied to non-destructive analysis of environmental samples. However, it can also be applied to destructive analysis, e.g. following extraction of the analyte from the sample, if there is a need to pre-concentrate the analyte.

Gamma-spectrometry is recognized as a wide-purpose multi-nuclide method of analysis presently based mainly on the use of high resolution semiconductor detectors of planar, coaxial or well type [1, 2].

#### 1.1.2. Method

The activity concentration of natural and anthropogenic gamma-emitters in environmental samples is determined by gamma-spectrometry. The method includes:

- (i) Sample preparation
- (ii) Calibration and measurement
- (iii) Data evaluation
- (iv) Reporting of results

Similar procedures can be applied for other samples e.g. biological samples, metallic or plastic materials, liquids, etc.

### 1.1.2.1. Calibration and measurement

The energy calibration includes the calculation of two sets of parameters: the energy versus the channel number, and the peak shape or FWHM (Full Width at Half Maximum) versus the energy.

The efficiency calibration includes the calculation of the efficiency of the semiconductor detector system as a function of energy. This includes effects from the intrinsic detector crystal, the detector-source geometry, the materials surrounding the detector and absorption in the source matrix. The efficiency calibration is needed for each source-detector combination (e.g. for a disk source, for a Marinelli container, etc.).

After the efficiency calibration with secondary standards, in most cases prepared in the same geometry and matrix as an unknown sample, the sample is counted, usually for one or more days, to meet the required statistical uncertainty. The counting period depends on the activity of the sample. The stability of the spectrometer is checked during the measurements, as well as at the end with a standard source. If there is a shift in the spectra, the best way is to identify the problem and to measure the sample again. Usually, with present day electronics, no shifts are observed in the spectra.

### 1.1.2.2. Data evaluation

Data reduction and evaluation are done usually using a commercial software, checked for performance using standard sources or certified reference materials.

### 1.1.2.3. Reporting of results

Results of measurements are reported on the basis of evaluation sheets, after careful evaluation of the full analytical procedure, including uncertainty analysis.

### 1.1.2.4. Calculation of the activity concentration

The activity concentration  $A$  of a gamma-emitting radionuclide in the sample is calculated as:

$$A = \frac{N}{\varepsilon \gamma t_s m K_1 K_2 K_3 K_4 K_5},$$

where:  $N$  is the corrected net peak area of the corresponding photopeak given as

$$N = N_s \frac{t_s}{t_b} N_b$$

$N_s$  is the net peak area in the sample spectrum,

$N_b$  is the corresponding net peak area in the background spectrum,

$\varepsilon$  is the efficiency at photopeak energy,

$t_s$  is the live time of the sample spectrum collection in seconds,

$t_b$  is the live time of the background spectrum collection in seconds,

$m$  is the mass [kg] of the measured sample,

$\gamma$  is the emission probability of the gamma line corresponding to the peak energy,

$K_1$  is the correction factor for the nuclide decay from the time the sample was collected to the start of the measurement given as

$$K_1 = \exp\left(-\frac{\ln 2 \cdot \Delta t}{T_{1/2}}\right),$$

where  $\Delta t$  is the elapsed time from the time the sample was taken to the beginning of the measurement and  $T_{1/2}$  is the radionuclide half life.

$K_2$  is the correction factor for the nuclide decay during counting period given as

$$K_2 = \frac{T_{1/2}}{\ln 2 \cdot t_r} \left(1 - \exp\left(-\frac{\ln 2 \cdot t_r}{T_{1/2}}\right)\right),$$

where  $t_r$  is the elapsed real clock time during the measurement.

$K_3$  is the correction factor for a self-attenuation in the measured sample compared with the calibration sample.

The self-attenuation factor  $K_3$  is defined as the ratio of the full energy peak efficiency  $\varepsilon(\mu, E)$  for a sample with the linear attenuation coefficient  $\mu$  and the full energy peak efficiency  $\varepsilon(\mu_{ref}, E)$  for a sample with linear attenuation  $\mu_{ref}$ :

$$K_3 = \frac{\varepsilon(\mu, E)}{\varepsilon(\mu_{ref}, E)}$$

Evidently, if the matrix of both the calibration sample and the measured sample is the same, then  $K_3 = 1$ .

If more than one photon is absorbed by the detector during a pulse sampling cycle, the sum of the energies of two (or more) is recorded in the spectrum instead of two (or more) different signals. Any full-energy photon that is summed with another pulse is not recorded in the single photon peak and represents a loss of counts or efficiency. This loss is count rate dependent.

$K_4$  is the correction factor for pulses loss due to random summing [2]:

$$K_4 = \exp(-2 R \tau),$$

where  $\tau$  is the resolution time of the measurement system and  $R$  is the mean count rate. For low count rates this correction factor could be taken as 1.

$K_5$  is the coincidence correction factor for those nuclides decaying through a cascade of successive photon emissions. If the nuclide has no cascade of gamma-rays then  $K_5 = 1$ . Also if the calibration sample and measured sample contain the same nuclide, then there is no need for this correction ( $K_5 = 1$ ). The coincidence correction factor  $K_5$  for the line with energy  $E$  of the nuclide having cascading radiations is defined as the ratio of the corresponding

apparent efficiency  $\varepsilon_{\text{ap}}(E)$  to the full energy peak efficiency,  $\varepsilon(E)$ , at the same energy obtained from the energy curve (or Monte-Carlo simulation) measured with single-photon emitting nuclides:

$$K_5 = \frac{\varepsilon_{\text{ap}}(E)}{\varepsilon(E)}$$

$K_5$  depends on the nuclide decay scheme, on sample geometry and composition and on detector parameters.

For the special case when the activity concentration (of a radionuclide emitting more than one gamma line) is obtained by matrix methods the appropriate literature reference should be used [1].

### **1.2. Sample**

A sample preparation depends on type of samples. For example, liquid samples may be analysed as they are, but pre-concentration of the analyte is frequently encountered.

The solid samples usually require drying and subsequent procedures to achieve uniform distribution of radionuclides in the sample (grinding, homogenization and in some cases sieving as well). For non-destructive analysis the sub-sample is weighed, inserted into a measuring container which must be gas tight if radon decay products are to be measured.

If quantitative extraction of the analyte is carried out from the sample or sub-sample the resultant final sample is inserted into a plastic vial after extraction.

### **1.3. Analyte**

The analyte in gamma-ray spectrometry is a radionuclide, subject to the decay process in which  $\gamma$ -rays or X rays are being emitted of which the energy and emission rate is assessed in the measurement. The analyte in neutron activation analysis is an element of which stable isotope(s), via a nuclear reaction with neutrons, has been converted into radionuclide(s) subject to decay process in which  $\gamma$ -rays or X rays are being emitted of which the energy and emission rate is assessed in the measurement.

### **1.4. Measurand**

The measurand in gamma-ray spectrometry is the activity concentration of the analyte, to be derived from the registered photon emission rate.

## **2. SOURCES OF UNCERTAINTY**

Identification of the uncertainty sources in nuclear analytical techniques is an important step for reporting high quality data. The most important uncertainty sources and magnitude of their contribution in the case of gamma spectrometry are given in Table 1.

TABLE 1. Sources of Uncertainties

Uncertainty source	Symbol used	Typical uncertainty range (%)	Typical uncertainty value (%)
Counting	N	0.1 - 20	5
Emission probability	$\gamma$	0.1 - 11	< 2
Attenuation correction	$K_3$	0.1 - 5	<1
Coincidence correction	$K_5$	1 - 15	<3
Half-life	$T_{1/2}$	0.01 –1	<0.2
Detector efficiency	$\epsilon$	1 – 5	2
Radiochemical procedures		1-10	3
Sample weight	m	0.01- 1	<0.5

These values are only illustrative. For each practical situation a complete uncertainty evaluation must be done, taking into consideration all possible sources of uncertainty. In the majority of cases, radiochemical procedures are performed after gamma-spectrometric measurements, avoiding introduction of supplementary uncertainty in the results.

The uncertainty is reported as standard uncertainty, combined standard uncertainty or expanded uncertainty [3-5].

The sources of standard uncertainties can be grouped according to their origin into 4 categories:

- from preparation of test portion
- from energy and efficiency calibration
- from the measurement of test portion
- from the nuclear data

### 2.1 Preparation of test portion

The sources of uncertainties which may arise during the preparation of test portion are the following:

- uncertainty due to analyte losses and/or contamination,
- uncertainty in sample mass or volume,
- uncertainty due to sample inhomogeneity,
- uncertainty due to preconcentration procedure.

### 2.2. Energy and efficiency calibration

The sources of uncertainties which may be introduced as a consequence of energy and efficiency calibration procedures are the following:

- uncertainty due to instabilities during the counting period,
- uncertainty due to the energy calibration,
- uncertainty of the detector efficiency calibration.

### 2.3. Measurement of test portion

As a consequence of measurement of test portion the following contributions as uncertainties of sources may appear:

- uncertainty due to differences in counting geometries of samples and standards,
- uncertainty due to random coincidences,
- uncertainty due to true coincidences,
- uncertainty due to dead time effects,
- uncertainty due to decay time effects (measuring time, decay and counting time),
- uncertainty due to self-attenuation correction,
- uncertainty due to net peak area determination,
- uncertainty due to counting statistics.

### 2.4. Nuclear data

- uncertainty due to half-life,
- uncertainty due to emission probability.

## 3. CALCULATION OF UNCERTAINTY

In most cases the quantity of interest (the measurand) is not the quantity that can be directly measured. Its value has to be derived from values of several other quantities.

The activity concentration (or specific activity) of radionuclides (analytes) in environmental samples is a function of several quantities (detector efficiency, gamma ray emission probability, counting rate, corrections factors etc.) and each of these quantities have an associated uncertainty [6].

The combined standard uncertainty of the quantity of interest (the measurand,  $y$ ) could be derived by applying the “error propagation law “ of Gauss. Thus, the combined standard uncertainty of  $y$ ,  $u_c(y)$ , is calculated in terms of component uncertainties,  $u(x_i)$ , as follows:

$$u_c(y(x_1, \dots, x_n)) = \sqrt{\sum_{i=1}^n \left( \frac{\partial y}{\partial x_i} \right)^2 (u(x_i))^2},$$

where  $y(x_1, x_2, \dots, x_n)$  is a function of several quantities  $x_1, x_2, \dots, x_n$ .

Each variable's contribution is just the square of the associated uncertainty expressed as a standard deviation multiplied by the square of the associated partial derivative.

The above equation is valid only if the quantities  $x_i$  are independent (uncorrelated), and if  $u(x_i) \ll x_i$ . In most cases this equation has been used even when the above mentioned restrictions are not met.

If the variables  $x_1, x_2, \dots, x_n$  are not independent, the relationship is more complex. However the following relation is obtained supposing that the function  $y$  is differentiable:

$$u_c(y(x_1, \dots, x_n)) = \sqrt{\sum_{i=1}^n \left(\frac{\partial y}{\partial x_i}\right)^2 (u(x_i))^2 + 2 \sum_{i=1}^n \sum_{j>i}^n \left(\frac{\partial y}{\partial x_i}\right) \left(\frac{\partial y}{\partial x_j}\right) \text{cov}(x_i, x_j)}$$

where  $\text{cov}(x_i, x_j)$  is the covariance between  $x_i$  and  $x_j$ .

The expanded uncertainty  $u$  is obtained by multiplying the combined standard uncertainty by a suitable coverage factor  $k_\alpha$ . The unknown value of the measurand (the activity concentration) is believed to lie in the interval  $y \pm u$  with a confidence level of approximately  $\alpha$ .

## 4. QUANTIFICATION OF UNCERTAINTY

Not all of the above mentioned uncertainty components will contribute significantly to the combined uncertainty. The first step in the quantification of uncertainty is therefore a preliminary estimation of the contribution of each component to the combined uncertainty, in order to eliminate those which are not significant.

### 4.1. *A-priori* known quantifiable sources of uncertainty

#### 4.1.1. *Stability of the measuring system*

Stability of the measuring system must be ensured in order to obtain good results. The task is to control the stability of the measuring system rather than to correct the results of measurement.

With present day electronics it is much easier to assure the stability of the system. Results obtained using an unstable measuring system must be rejected. The sample must be measured again in proper conditions.

#### 4.1.2. *Energy calibration*

The object of energy calibration is to derive a relationship between a peak position in the spectrum and the corresponding gamma-ray energy. This is normally performed before measuring the sample. Whatever source is used it is wise to ensure that the calibration energies cover the entire range over which the spectrometer is to be used. Experience suggests that the linearity of modern ADCs is extremely good.

The energy calibration is a simple but critical step. The measured energies are only used to identify the nuclides and, thus, the uncertainty in the energy is no longer used in the following calculations.

#### 4.1.3. *Efficiency uncertainty*

Most algorithms used for efficiency calibration assume that the true efficiency function can be represented by a fitted analytical function. However, the correct allocation of uncertainties to an interpolated efficiency value is a complex problem. The uncertainty of the efficiency value calculated with the interpolation function cannot be only obtained from the uncertainties in the parameters. The possible correlations between the measured input efficiency data must be considered [11].

There are also energy regions where the true efficiency curve systematically deviates from the fitted curve. This systematic difference is only rarely included in the uncertainty computed by the algorithms.

A computational approach that yields acceptable results is the Monte Carlo method which is based on the simulation of individual photon histories [7]. The Monte Carlo simulation is an attractive means because any source-detector configuration and any sample matrix can be modelled over the energy interval of interest. Thus Monte Carlo calculation can provide the shape of the efficiency curve and the efficiency uncertainty at any energy. In order to evaluate the matrix and coincidence corrections, the GESPECOR method has been used at IAEA-MEL [8].

#### ***4.1.4. Uncertainty of gamma emission probabilities***

For gamma emission probabilities, good data sources for a limited number of radionuclides are in IAEA-TECDOC-619 [9] and in Firestone and Shirley [10]. In a few cases this kind of uncertainty could be a major contributor to the combined uncertainty.

#### ***4.1.5. Uncertainty in the half life***

The published uncertainty in the half-life should be used to calculate a contribution to the overall uncertainty of the result. In broad terms, published values for half lives are less reliable than gamma energies, but the uncertainty in the half life is still small compared with other uncertainty sources. IAEA TECDOC-619 [9] as well as Firestone and Shirley [10] are a good source for data on a limited number of nuclides of interest.

### **4.2. Uncertainties to be quantified from the measurement results**

All other parameters are to be obtained from the measurement process unless some of the sample parameters (such as matrix etc.) are provided by the customer.

#### ***4.2.1. Uncertainty due to differences in counting geometries of sample and standards***

The counting geometry of sample and standards should be the same. In order to minimise the uncertainties, the differences should be kept at a minimum. A proper mock up standard with the same physical and chemical properties as the sample should be used in non-destructive analysis.

#### ***4.2.2. Uncertainty due to random coincidences***

Even with good pile-up rejection there could be some residual random coincidences. Any full-energy photon which is summed with another pulse will not be recorded in the single photon peak and represents therefore a loss of counts or efficiency. This loss is count rate dependent, however, for low count rates this correction factor could be taken as 1 and the associated uncertainty can be neglected.

#### ***4.2.3. Uncertainty due to true coincidences***

In the case of a nuclide decaying through a cascade of successive photon emissions located close to a detector, coincidence-summing effects could be important, especially in the case of high efficiency semiconductor detectors.

Information on photons in cascade is more difficult to obtain. The main source is Nuclear Data Sheets. The best way to treat this problem is to use identical geometry for calibration and the measured sample, and also to have the same composition of radionuclides emitting photons in cascades (like  $^{60}\text{Co}$ ,  $^{152}\text{Eu}$ ,  $^{154}\text{Eu}$ ,  $^{133}\text{Ba}$ ,  $^{88}\text{Y}$ , etc.) in both samples. Usually, this will not be a realistic solution of the calibration problem. Radionuclides emitting photons in cascades are not appropriate for performing the fit necessary to obtain the efficiency curve. The solution is the use of the Monte-Carlo calculation of coincidence corrections or in the use of the same radionuclides for calibration and for measuring the sample.

#### ***4.2.4. Uncertainty due to dead time effects***

We neglect the uncertainties associated with dead time effects, because counting rates in environmental samples are usually very low.

#### ***4.2.5. Uncertainty due to decay time effects***

The decay time effects (measuring time, decay and counting time) usually can be neglected as exact timing is available.

#### ***4.2.6. Uncertainty due to self-attenuation correction***

If the composition and the density of the sample to be measured differ from the calibration sample, self-attenuation corrections to the efficiency should be applied. These corrections depend on the sample geometry, composition and density, and on detector parameters. Of course, the corrections are higher for large volume high Z and density samples and for low energy photons.

If the major elements of the sample matrix are known, then the relative uncertainty of the self-attenuation correction factor is less than 1% (for energies higher than 60 keV) and less than 5% for energies less than 40 keV.

#### ***4.2.7. Uncertainty due to counting statistics***

Generally the uncertainty due to counting statistics is one of the most important sources of uncertainty. The mathematical procedure used to derive net peak areas and standard associated uncertainties is based, in many cases, on a simple background subtraction (including the background peak subtraction in the case of existence of a such peak at the given energy, both in the sample and the background spectra).

The subtraction of instrumental background gives the corrected net peak area (N) as follows :

$$N = N_s \frac{t_s}{t_b} N_b,$$

where

$N_s$  is the net peak area in the sample spectrum,

$N_b$  is the corresponding net area of the background peak. This must be available from a separate analysis performed on the background spectrum,

$t_s$  is the live time of the sample spectrum,

$t_b$  is the live time of the background spectrum.

In the case of overlapping peaks most often a matrix solution [1] is used in order to derive the net peak area and associated counting uncertainty. In the following it is assumed that the corrected net peak area ( $N$ ) and the related uncertainty ( $u_N$ ) are obtained as values directly from the fitting procedure. These quantities are used as input parameters for uncertainty estimation.

The magnitude of counting uncertainty due to the presence of a background peak is presented in Fig.1 as a function of the corrected sample net area ( $N$ ) and the background peak net area ( $N_b$ ). If there is no corresponding peak in the background spectrum  $N_b$  is set to 0.1 counts.

#### 4.2.8. Uncertainty due to sample weighing

It is assumed that the uncertainty due to sample weighing is estimated on the basis of information available on the precision of the balance used in the measurement process or from control charts of repetitive measurements.

#### 4.2.9. Correlations in uncertainties

Propagating uncertainties needs to take into account existing correlations. In some special cases the input variables used for calculation of uncertainty of activity concentration may be correlated. One example of possible correlation which may appear in the case of efficiency calibration purposes of more than one gamma-line belonging to the same radionuclide is given in reference [11].

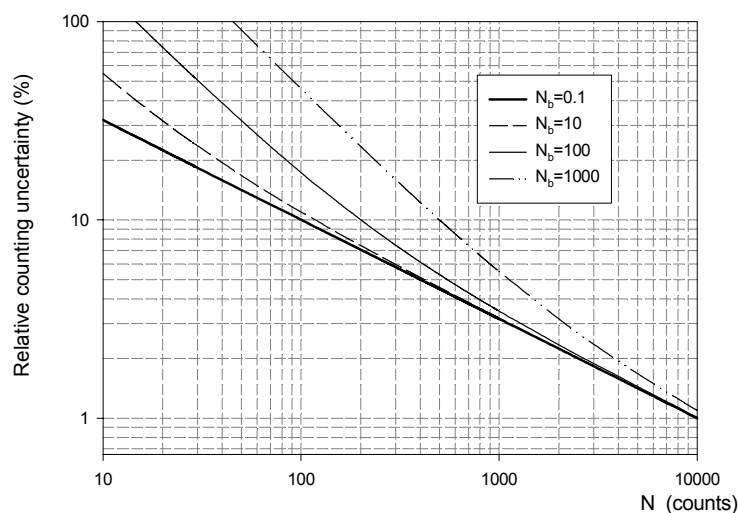


Fig. 1. Dependence of the relative counting uncertainty of the corrected net peak area ( $N$ ) for different values of the background peak net area ( $N_b$ )

## 5. CASE STUDIES

### EXAMPLE 1

#### 1. Features

##### [8] 1.1. Technique

Gamma-ray spectrometry using aHPGe coaxial detector ( 150% relative efficiency). Efficiency calculation was performed using a mixed standard containing radionuclide-emitting gamma-rays of different energies.

##### 1.2. Sample

A 70 g sediment sample was analyzed in the disk geometry ( $\varnothing$  7.9 x 1.0 cm ) The sample was freeze-dried, grounded, homogenized and sieved.

1.3. Analyte: The analyte is  $^{40}\text{K}$ .

1.4 Measurand: The measurand is activity concentration of  $^{40}\text{K}$ .

#### 2. The sources of uncertainties

The sources of uncertainties for this example are presented in Table 2.

#### 3. Results

The results are presented in Table 5.

### EXAMPLE 2

#### 1. Features

##### 1.1. Technique

Gamma-ray spectrometry using a HPGe coaxial detector (150% relative efficiency). Efficiency calculation was performed using Monte Carlo simulation. The coincidence and self-attenuation correction was performed using GESPECOR software.

##### 1.2. Sample

A 70 g sediment sample was analyzed in the disk geometry ( $\varnothing$  7.9 x 1.0 cm). The sample was freeze-dried, ground, homogenized and sieved.

1.3. Analyte: The analyte is  $^{60}\text{Co}$ .

1.4. Measurand: The measurand is the activity concentration of  $^{60}\text{Co}$ .

#### 2. The sources of uncertainties

The sources of uncertainties for this example are presented in Table 3.

#### 3. Results

The results are presented in Table 6.

## EXAMPLE 3

### 1. Features

#### 1.1. Technique

Gamma-ray spectrometry using a HPGe coaxial detector ( 150% relative efficiency). Efficiency calculation was performed using a mixed standard containing radionuclides emitting gamma-rays of different energies.

#### 1.2. Sample

A 450 g sediment sample was analyzed in the Marinelli container. The sample was freeze-dried, ground, homogenized and sieved.

1.3. Analyte: The analyte is  $^{137}\text{Cs}$ .

1.4. Measurand: The measurand is the activity concentration of  $^{137}\text{Cs}$ .

### 2. The sources of uncertainties

The sources of uncertainties for this example are presented in Table 4.

### 3. Results

The results are presented in Table 7.

## REFERENCES

- [1] DEBERTIN, K., HELMER, R.G. - Gamma and X ray Spectrometry with Semiconductor Detectors, North-Holland, Elsevier, 1988.
- [2] GILMORE, G., Practical Gamma Ray Spectrometry, J.Hemingway Ed., John Wiley and Sons, New-York, 1996.
- [3] EURACHEM, "Quantifying Uncertainty in Analytical Measurement", Editor: Laboratory of the Government Chemist Information Services, Teddington (Middlesex) & London (1995). ISBN 0-948926-08-2.
- [4] INTERNATIONAL ORGANISATION FOR STANDARDISATION, Guide to the Expression of Uncertainty in Measurement, First Edition, Geneva, 1993 (ISBN 92-67-10188-9).
- [5] CURRIE, L.A., Nomenclature in evaluation of analytical methods including detection and quantification capabilities, Pure & Appl. Chem. **67** (10) (1995) 1699-1723.
- [6] BAMBYNEK W., Uncertainty Assignment in Radionuclide Metrology, Proc.of the First International Summer School La Rabida, Huelva, Spain, M. Garcia-Leon, G. Madurga, editors World Scientific, New-Jersey (1987).
- [7] KAMBOJ, S., KAHN, B., Evaluation of Monte-Carlo simulation of photon counting efficiency for germanium detectors, Health Physics (1996) 512-519.
- [8] SIMA, O., ARNOLD, D., DOVLETE C., GESPECOR software, MATec GmbH, Gelnhausen (1996).
- [9] INTERNATIONAL ATOMIC ENERGY AGENCY, X ray and Gamma-ray Standards for Detector Calibration, IAEA-TECDOC-619, Vienna (1991).
- [10] FIRESTONE, R.B., SHIRLEY S.V., Table of isotopes, John Wiley and Sons, New-York (1996).
- [11] VENTURINI, I. VANIN, V.R., HPGe Detector Efficiency Calibration for Extended Sources in the 50-1400 keV Energy Range, Appl.Radiat. Isot. **44** (1993) 999-1002.
- [12] WINKLER, G., On the Role of Covariances for Uncertainty Estimates in Radioactivity Measurements, Appl. Radiat. Isot. **49** (1998) 1153-1157.

**TABLE 2****The sources of uncertainties and their quantification ( $^{40}\text{K}$  in sediment)**

Uncertainty component symbol	Uncertainty component identification	Method used to evaluate the standard uncertainty	Relative Standard Uncertainty %
	Sample preparation		
$u_{10}$	-sample mass -analyte losses and/or contamination -sample inhomogeneity -sample pre-concentration procedure	repeated weighing or estimated from manufacturer data. Gaussian distribution assumed. non-destructive analyses- negligible based on previous experience – negligible for this sample size not used	0.15
	Counting		
$u_{20}$	-detector efficiency calibration -stability during the counting period -differences in counting geometries of sample and standards	Estimated from fitted calibration curve using the commercial software since the equipment used is kept in stable environment - negligible contribution no differences between sample and standard geometry, no contribution to uncertainty	2.8

TABLE 2 (cont.)

Uncertainty component symbol	Uncertainty component identification	Method used to evaluate the standard uncertainty	Relative Standard Uncertainty %
u <sub>31</sub>	-correction factor for decay between sampling and measurement	Estimated from the expression. Negligible contribution	
u <sub>32</sub>	-decay during counting period	Estimated from the expression. Negligible contribution	
u <sub>33</sub>	-self attenuation correction factor	Estimated from Monte Carlo simulations when needed.	1.3
u <sub>34</sub>	-correction factor for random summing	Estimated from the expression. Negligible contribution for low count rate	
u <sub>35</sub>	-true coincidence correction factor	Estimated from Monte Carlo simulations when needed.	
u <sub>36</sub>	-background corrected net area of the sample peak	Estimated from the measurement results (background and sample). Poisson distribution is used.	8.2
	Nuclear data		
u <sub>40</sub>	-emission probability	Based on nuclear data sheets. Gaussian distribution assumed	1.0

**TABLE 3**  
**The sources of uncertainties and their quantification (<sup>60</sup>Co in sediment)**

Uncertainty component symbol	Uncertainty component identification	Method used to evaluate the standard uncertainty	Relative Standard Uncertainty %
	Sample preparation		
U <sub>10</sub>	-sample mass	repeated weighing or estimated from manufacturer data. Gaussian distribution assumed.	0.15
	-analyte losses and /or contamination	non-destructive analyses- negligible	
	-sample inhomogeneity	based on previous experience – negligible for this sample size	
	-sample pre-concentration procedure	not used	
	Counting		
U <sub>20</sub>	Detector efficiency calibration	Estimated from fitted calibration curve using the commercial software	2.0
	Stability during the counting period	since the equipment used is kept in stable environment -negligible contribution	
	Differences in counting geometries of sample and standards	no differences between sample and standard geometry, no contribution to uncertainty	

TABLE 3 (cont.)

Uncertainty component symbol	Uncertainty component identification	Method used to evaluate the standard uncertainty	Relative Standard Uncertainty %
u <sub>31</sub>	correction factor for decay between sampling and measurement	Estimated from the expression. Negligible contribution	
u <sub>32</sub>	decay during counting period	Estimated from the expression. Negligible contribution	
u <sub>33</sub>	self attenuation correction factor	Estimated from Monte Carlo simulations when needed.	1.0
u <sub>34</sub>	correction factor for random summing	Estimated from the expression. Negligible contribution for low count rate	
u <sub>35</sub>	true coincidence correction factor	Estimated from Monte Carlo simulations when needed.	1.5
u <sub>36</sub>	background corrected net area of the sample peak	Estimated from the measurement results (background and sample). Poisson distribution is used.	4.1
	Nuclear data		
u <sub>40</sub>	emission probability	Based on nuclear data sheets. Gaussian distribution assumed	0.022

**TABLE 4****The sources of uncertainties and their quantification ( $^{137}\text{Cs}$  in sediment)**

Uncertainty component Symbol	Uncertainty component identification	Method used to evaluate the standard uncertainty	Relative Standard Uncertainty %
	Sample preparation		
$u_{10}$	-sample mass	repeated weighing or estimated from manufacturer data. Gaussian distribution assumed.	0.15
	-analyte losses and /or contamination	non-destructive analyses- negligible	
	-sample inhomogeneity	based on previous experience – negligible for this sample size	
	-sample pre-concentration procedure	not used	
	Counting		
$u_{20}$	Detector efficiency calibration	Estimated from fitted calibration curve using the commercial software	6.0
	Stability during the counting period	since the equipment used is kept in stable environment -negligible contribution	
	Differences in counting geometries of sample and standards	no differences between sample and standard geometry, no contribution to uncertainty	

**TABLE 4 (cont.)**

Uncertainty component symbol	Uncertainty component identification	Method used to evaluate the standard uncertainty	Relative Standard Uncertainty %
u <sub>31</sub>	correction factor for decay between sampling and measurement	Estimated from the expression. Negligible contribution	
u <sub>32</sub>	decay during counting period	Estimated from the expression. Negligible contribution	
u <sub>33</sub>	self attenuation correction factor	Estimated from Monte Carlo simulations when needed.	2.0
u <sub>34</sub>	correction factor for random summing	Estimated from the expression. Negligible contribution for low count rate	
u <sub>35</sub>	true coincidence correction factor	Estimated from Monte Carlo simulations when needed.	
u <sub>36</sub>	background corrected net area of the sample peak	Estimated from the measurement results (background and sample). Poisson distribution is used.	3.2
	Nuclear data		
u <sub>40</sub>	emission probability	Based on nuclear data sheets. Gaussian distribution assumed	0.24

**TABLE 5****Worked example on the uncertainty components of the <sup>40</sup>K determination in sediment sample**

No.	Variable Name	Symbol of the variable	Value	Uncertainty component symbol	Uncertainty value	Conversion factor to standard uncertainty	Relative standard uncertainty (u)	Sensitivity factor	Percent to contribution to combined uncertainty (u <sub>c</sub> )
1	Mass of the sample	m (kg)	0.070	u <sub>10</sub>	0.0001	1	0.15	1	0.03
2	Detector efficiency	ε	0.036	u <sub>20</sub>	0.001	1	2.8	1	10.2
3	Correction factor for decay between sampling and meas.	K <sub>1</sub>	1.0	u <sub>31</sub>	-	1	-	1	-
4	Correction factor for decay during counting period	K <sub>2</sub>	1.0	u <sub>32</sub>	-	1	-	1	-
5	Self attenuation correction factor	K <sub>3</sub>	0.98	u <sub>33</sub>	0.0098	1	1.0	1	1.3
6	Correction factor for random summing	K <sub>4</sub>	0.999	u <sub>34</sub>	-	1	-	1	-
7	Coincidence correction factor	K <sub>5</sub>	1.0	u <sub>35</sub>	-	1	-	1	-
8	Background corrected net area of the sample peak	N	368	u <sub>36</sub>	30	1	8.2	1	87.2
9	Emission probability	γ	0.1067	u <sub>40</sub>	0.001	1	1.0	1	1.3

Value of the measurand (activity concentration) A = 7.1 Bq/kg

Relative combined standard uncertainty u<sub>c</sub> (A) = 4.9%

Relative expanded uncertainty U (A) = 9.8% (coverage factor=2)

Value of the measurand ± expanded uncertainty = 7.1 ± 1.3

**TABLE 6****Worked example on the uncertainty components of the  $^{60}\text{Co}$  determination in sediment sample**

No.	Variable Name	Symbol of the variable	Value	Uncertainty Component Symbol	Uncertainty value	Conversion factor to standard uncertainty	Relative standard uncertainty y (u)	Sensitivity factor	Percent to contribution to combined uncertainty ( $u_c$ )
1	Mass of the sample	m (kg)	0.070	$u_{10}$	0.0001	1	0.15	1	0.09
2	Detector efficiency	$\epsilon$	0.0415	$u_{20}$	0.0008	1	2.0	1	16.7
3	Correction factor for decay between sampling and meas.	$K_1$	0.954	$u_{31}$	-	1	-	1	-
4	Correction factor for decay during counting period	$K_2$	0.999	$u_{32}$	-	1	-	1	-
5	Self attenuation correction factor	$K_3$	0.959	$u_{33}$	0.009	1	1.0	1	3.3
6	Correction factor for random summing	$K_4$	0.999	$u_{34}$	-	1	-	1	-
7	Coincidence correction factor	$K_5$	0.844	$u_{35}$	0.013	1	1.5	1	9.4
8	Background corrected net area of the sample peak	N	1019	$u_{36}$	42	1	4.1	1	70.5
9	Emission probability	$\gamma$	0.9986	$u_{40}$	0.0002	1	0.022	1	0.04

Value of the measurand (activity concentration)  $A = 2.3 \text{ Bq/kg}$

Relative combined standard uncertainty  $u_c(A) = 4.9\%$

Relative expanded uncertainty  $U(A) = 9.8\%$  (coverage factor=2)

Value of the measurand  $\pm$  expanded uncertainty  $= 2.3 \pm 0.2$

**TABLE 7****Worked example on the uncertainty components of the  $^{137}\text{Cs}$  determination in sediment sample**

No.	Variable Name	Symbol of the variable	Value	Uncertainty component symbol	Uncertainty value	Conversion factor to standard uncertainty	Relative standard uncertainty (u)	Sensitivity factor	Percent to contribution to combined uncertainty ( $u_c$ )
1	Mass of the sample	m (kg)	0.070	$u_{10}$	0.0001	1	0.15	1	0.04
2	Detector efficiency	$\epsilon$	0.015	$u_{20}$	0.0009	1	6	1	71.6
3	Correction factor for decay between sampling and meas.	$K_1$	1.0	$u_{31}$	-	1	-	1	-
4	Correction factor for decay during counting period	$K_2$	1.0	$u_{32}$	-	1	-	1	-
5	Self attenuation correction factor	$K_3$	0.985	$u_{33}$	0.02	1	2.0	1	7.9
6	Correction factor for random summing	$K_4$	0.999	$u_{34}$	-	1	-	1	-
7	Coincidence correction factor	$K_5$	1.0	$u_{35}$	-	1	-	1	-
8	Background corrected net area of the sample peak	N	958	$u_{36}$	31	1	3.2	1	20.3
9	Emission probability	$\gamma$	0.851	$u_{40}$	0.002	1	0.24	1	0.1

Value of the measurand (activity concentration)  $A = 16.9$  Bq/kg

Relative combined standard uncertainty  $u_c(A) = 7.1\%$

Relative expanded uncertainty  $U(A) = 14.2\%$  (coverage factor=2)

Value of the measurand  $\pm$  expanded uncertainty  $= 16.9 \pm 2.4$

## PRACTICAL EXAMPLE

### Determination of activity concentration of $^{40}\text{K}$

Determination of activity concentration of  $^{40}\text{K}$  in a sediment sample (see Table 5) is performed on the basis of identification of a peak in the spectrum at 1460.7 keV.

The corresponding activity concentration of  $^{40}\text{K}$  in the sample, is calculated as:

$$A = \frac{N}{\varepsilon \gamma t_s m K_1 K_2 K_3 K_4 K_5}$$

with:

$$N = N_s \frac{t_s}{t_b} N_b$$

using the following experimental values:

$N_s = 399$  (the net peak area in the sample spectrum)

$N_b = 64$  ( net peak area in the background spectrum)

$t_s = 197049$  sec (sample live counting time)

$t_b = 409618$  sec (background live counting time)

$$N = 399 - \frac{197049}{409618} 64 = 368.2 \approx 368$$

$M=0.07$  kg (sample mass)

$\varepsilon=0.036$  (detection efficiency at 1460.7 keV)

$T_{1/2} = 1.277 \cdot 10^9$  years

$\gamma =0.1067$  is the emission probability of the 1460.7 keV gamma line

$K_1$  is the decay correction factor. In our case the period ( $\Delta t$ ) between sampling date and measuring date is 130 days,(  $\Delta t \ll T_{1/2} = 1.277 \cdot 10^9$  years ) then:

$$K_1 = \exp\left(-\frac{\ln(2)\Delta t}{T_{1/2}}\right) = 1.0$$

$K_2$  is the correction factor for the nuclide decay during counting. Because  $T_r = 197049$  sec  $\ll T_{1/2} = 1.277 \cdot 10^9$  years , this correction factor is:

$$K_2 = \frac{T_{1/2}}{\ln(2) T_r} \left(1 - \exp\left(-\frac{\ln(2) T_r}{T_{1/2}}\right)\right) = 1.0$$

$K_3$  is the correction factor for self-attenuation in the measured sample compared with the calibration sample. This correction factor must be taken into account when matrix of calibration sample and measured sample is not the same. For this sample, using the Monte Carlo computations we find for the energy 1460.7 keV the following correction factor:

$$K_3 = 0.964$$

$K_4$  is the correction factor for loss due to random summing. If we assume that resolution time ( $\tau$ ) of system is  $\tau \approx 6\mu s$  and the mean total count rate  $R \approx 1p/sec$  then we obtain for this correction factor:

$$K_4 = \exp(-2 R \tau) = 0.99998$$

For radionuclide K-40 the coincidence correction factor  $K_5 = 1.0$  because this radionuclide has no cascade of successive photon emission.

Finally we get for activity concentration of  $^{40}K$  in the sample:

$$A = \frac{N}{\varepsilon \gamma t_s M K_1 K_2 K_3 K_4 K_5} = \frac{368}{0.036 \cdot 0.1067 \cdot 197049 \cdot 0.07 \cdot 1.0 \cdot 1.0 \cdot 0.964 \cdot 0.9999 \cdot 1.0} =$$

$$A = 7.22 \text{ Bq kg}^{-1}$$

### Uncertainty evaluation of activity concentration

1) Uncertainty of the net area (N) of the peak as given by the gamma analysis code is  $u(N) = 30$ .

2) Uncertainty of  $K_1$  correction factor is given by:  $u(K_1) = K_1 \cdot \Delta t \cdot u(\lambda)$

Assuming a relative uncertainty of 1 % for  $\lambda$  we obtain:

$$u(\lambda) = \lambda \cdot 1 / 100 = 0.693 / 4.661 / 10^{11} / 100 = 1.487 \cdot 10^{-14}$$

$$u(K_1) = 1 \cdot 130 \cdot 1.487 \cdot 10^{-14} = 1.933 \cdot 10^{-12}$$

3) Uncertainty of  $K_2$  is given by the expression:  $u(K_2) = \frac{1 - K_2 (1 + \lambda t_r)}{\lambda} u(\lambda)$

$$u(K_2) = \frac{1 - 1(1 + 0.693 / 4.661 \cdot 10^{11} \cdot 197049)}{0.693 / 4.661 \cdot 10^{11}} \cdot 1.487 \cdot 10^{-14} = 2.93 \cdot 10^{-9}$$

4) Uncertainty of  $K_3$  as resulted after self-attenuation calculations is  $u(K_3) = 0.00964$

5) Uncertainty of  $K_4$  is given by the formula:

$$u(K_4) = \sqrt{(2R \exp(-2 R \tau))^2 \cdot u^2(\tau) + (2\tau \exp(-2 R \tau))^2 \cdot u^2(R)}$$

$$u(K_4) = \sqrt{(2 \cdot 1 \cdot \exp(-2 \cdot 1 \cdot 10^{-6}))^2 \cdot (10^{-6})^2 + (2 \cdot 6 \cdot 10^{-6} \exp(-2 \cdot 1 \cdot 10^{-6}))^2 \cdot (1)^2} = 1.2165 \cdot 10^{-5}$$

6) Uncertainty of  $K_5$  is  $u(K_5) = 0$  because no coincidence corrections are needed.

7) Uncertainty of sample mass  $u(M) = 0.000105$

8) Uncertainty of emission probability  $u(\gamma)$  for the 1460.7 keV gamma line is  $u(\gamma) = 0.001064$

9) Uncertainty of detection efficiency at 1460.7 keV is  $u(\varepsilon) = 0.001$ .

The relative combined standard uncertainty  $\frac{u_c(A)}{A}$  of the activity concentration is given by formula:

$$\frac{u_c(A)}{A} = \sqrt{\frac{u(M)^2}{M^2} + \frac{u(N)^2}{N^2} + \frac{u(\gamma)^2}{\gamma^2} + \frac{u(\varepsilon)^2}{\varepsilon^2} + \frac{u(K)^2}{K^2}}$$

with:

$$\frac{u(K)}{K} = \sqrt{\frac{u(K_1)^2}{K_1^2} + \frac{u(K_2)^2}{K_2^2} + \frac{u(K_3)^2}{K_3^2} + \frac{u(K_4)^2}{K_4^2} + \frac{u(K_5)^2}{K_5^2}}$$

and  $K = K_1 \cdot K_2 \cdot K_3 \cdot K_4 \cdot K_5$

Finally, using above expressions we obtain for the relative combined standard uncertainty  $u_c(A) = 8.73 \%$

Relative expanded uncertainty  $= 2 * 8.73 = 17.46 \%$

Expanded uncertainty of the activity concentration  $= 7.1 * 17.46 / 100 = 1.3 \text{ Bq kg}^{-1}$

Value of measurand is then:  $7.2 \pm 1.3 \text{ Bq kg}^{-1}$

# ALPHA-SPECTROMETRIC ANALYSIS OF ENVIRONMENTAL SAMPLES

G. KANISCH

Bundesforschungsanstalt für Fischerei, Institut für Fischereiökologie, Hamburg, Germany

## Abstract

The example evaluates the uncertainty sources for the determination of different actinides in environmental samples. The analytical procedure involves sample preparation steps for drying, ashing and dissolution and further radiochemical separation and electroplating of the isolated radionuclides. The radioactivity is measured by a solid state detector coupled to a multichannel spectrometer. An isotopic tracer is used to determine the overall chemical yield and to ensure traceability to a national standard. The example describes and quantifies in great detail the uncertainty sources related to the sample preparation, the use of the isotopic tracer, the measured counting rates and corrections for background radiation, the time intervals and decay corrections, and the nuclear parameters. The example investigates to some extent the effect of covariances between the different parameters.

## 1. INTRODUCTION

The alpha-spectrometric analysis refers to the determination of various actinides (Pu, Am, Cm, Np, Th and U) and Po in environmental samples such as biological material, sediment and soil. The discussion of the analysis procedure starts with drying as the first sample preparation step. It is further assumed that after drying the sample has to be ashed in order to remove the organic material. All possible losses of the analyte and associated uncertainties can be recorded by a tracer radionuclide from which an accurately known amount of activity was added to the ash of the sample at the beginning of the radiochemical procedure. However, not only the chemical yield is determined by the use of the tracer but it is in this example also required to ensure the traceability to a national standard. It has to be emphasised that the general radiochemical procedure in the following example, dealing with plutonium, is based on a) that the recovery of the analyte and the tracer radionuclide are identical, and b) that the analysis starts with leaching with 8 M nitric acid. For more details of the separation techniques, see (1).

It is assumed that Si semiconductor detectors are used for the measurement. E. Holm (2) presented a sufficient overview about many details of the alpha measurement and the different tracer radionuclides which can be used as yield monitors for the various actinides. The counting rates are obtained as the difference of the gross count rates and their corresponding blank count rates, the latter containing also possible contributions of the detector background.

## 2. SPECIFICATION

### 2.1.1. Technique

The wet weight of the sample has to be determined. The sample then has to be dried and ashed (e.g. at 80°C and between 450 and 500°C, respectively). The ash is removed into a glass beaker and a known amount of the tracer (Pu-242) is added to the ash sample. Perform the radiochemistry and prepare a thin alpha source for alpha spectrometry by the electroplating method. Use an alpha spectroscopy module with a Si semiconductor detector, vacuum chamber, electronic modules and a multichannel analyser (MCA) to measure the counting rates of the analyte (Pu-238) and the tracer (Pu-242).

### 2.1.2. The sample consists of fillets of fresh fish.

2.1.3. The analyte is Pu-238.

2.1.4 The measurand is the activity concentration of Pu-238 in fish fillets, in Bq kg<sup>-1</sup> wet weight, referred to the date of sampling.

## 2.2. Calculation of measurand

$$a_A = \frac{A_A}{m_a \cdot q} \cdot f_1 \cdot f_2 \cdot f_3 \cdot f_4 \quad \text{in Bq kg}^{-1} \text{ wet weight} \quad (2.1)$$

at the date of sampling, with:

$$A_A = c_T \cdot V_T \cdot \left[ \frac{R_{GA} - R_{BA}}{R_{GT} - R_{BT}} - q_I \right] \cdot \left( \frac{p_{\alpha T}}{p_{\alpha A}} \right) \quad \text{in Bq} \quad (2.2)$$

$a_A$  the activity concentration of the analyte referred to the date of sampling in Bq kg<sup>-1</sup> wet weight

$A_A$  the amount of activity of the analyte on the electroplated source in Bq

$m_a$  mass of ashed sample used for the alpha analysis in kg

$q$  mass ratio wet weight per ash weight

$c_T$  certified concentration of the tracer solution in Bq ml<sup>-1</sup>, referred to the date of calibration

$V_T$  volume taken from the tracer solution in ml

$R_{GA}$  gross counting rate of the analyte in s<sup>-1</sup> (with counting time  $t_G$ )

$R_{BA}$  blank counting rate of the analyte in s<sup>-1</sup> (counting time  $t_B$ )

$R_{GT}$  gross counting rate of the tracer radionuclide in s<sup>-1</sup> (counting time  $t_G$ )

$R_{BT}$  blank counting rate of the tracer radionuclide in s<sup>-1</sup> (counting time  $t_B$ )

$q_I$  isotopic impurity ratio of the analyte in the tracer solution

$p_{\alpha A}$  sum of alpha emission probabilities of those individual alpha lines of the analyte which contribute to the channel region in the alpha spectrum which is used to determine its gross count rate (usually very close to unity)

$p_{\alpha T}$  sum of alpha emission probabilities of those individual alpha lines of the tracer radionuclide which contribute to the channel region in the alpha spectrum which is used to determine its gross count rate (usually very close to unity)

$f_1$  correction for decay of the analyte in the time interval from the end of sampling to the beginning of the measurement

$f_2$  correction for decay of the analyte during the counting interval  $t_G$

$f_3$  correction for decay of the tracer radionuclide in the time interval from its calibration date to the beginning of the measurement

$f_4$  correction for decay of the tracer radionuclide during the counting interval  $t_G$

The decay correction factors are defined as follows:

$$f_1 = \exp(+\lambda_A \cdot (t_S - t_E)) \quad (2.3)$$

$$f_2 = \lambda_A t_G / (1 - \exp(-\lambda_A t_G)) \quad (2.4)$$

$$f_3 = \exp(-\lambda_T \cdot (t_S - t_C)) \quad (2.5)$$

$$f_4 = \lambda_T t_G / (1 - \exp(-\lambda_T t_G)) \quad (2.6)$$

with

- $\lambda_A$  decay constant of analyte in  $s^{-1}$ ,
- $\lambda_T$  decay constant of tracer radionuclide in  $s^{-1}$ ,
- $t_E$  end of sampling time,
- $t_S$  beginning of measurement time,
- $t_C$  time of calibration of the tracer radionuclide solution,
- $t_G$  counting time interval of the gross counting in s.

The radiochemical yield  $\eta$  of the analyte, an indicator of the performance of the procedure, can be calculated from:

$$\eta = \frac{(R_{GT} - R_{BT})}{\varepsilon \cdot c_T \cdot V_T} \quad (2.7)$$

with:

- $\varepsilon$ : detection efficiency for alpha particles.

### 2.3. Sample data and parameters known prior to the analysis

- $t_S - t_E$  :  $6.307 \cdot 10^7$  s (2 years)
- $t_S - t_C$  :  $1.892 \cdot 10^8$  s (6 years)
- $\lambda_A$  :  $2.51 \cdot 10^{-10} s^{-1}$
- $\lambda_T$  :  $5.88 \cdot 10^{-14} s^{-1}$
- $p_{\alpha A}$  : 1.0000
- $p_{\alpha T}$  : 1.0000
- $c_T$  : 0.28 Bq ml<sup>-1</sup>, referred to the date of calibration
- $V_T$  : 0.25 ml
- $R_{BA}$  :  $8.0 \cdot 10^{-6} s^{-1}$  (blank counting rate for the analyte peak, obtained from a few separate blank analyses, see 3.3.d)
- $u(R_{BA})$  :  $6.4 \cdot 10^{-6} s^{-1}$  (standard uncertainty of  $R_{BA}$ , obtained from a few separate blank analyses, see 3.3.d)
- $R_{BT}$  :  $7.0 \cdot 10^{-5} s^{-1}$  (blank counting rate for the tracer peak, obtained from a few separate blank analyses, see 3.3.e)
- $u(R_{BT})$  :  $5.6 \cdot 10^{-5} s^{-1}$  (standard uncertainty of  $R_{BT}$ , obtained from a few separate blank analyses, see 3.3.e)
- $q_I$  :  $1.1 \cdot 10^{-3}$ : ratio of net counting rate of the analyte to the net counting rate of the tracer, obtained as a mean of ratios measured on a few separately electroplated tracer sources
- $u(q_I)$  :  $2.4 \cdot 10^{-4}$  (standard uncertainty of  $q_I$ , derived from a few separately electroplated tracer sources, see 3.8)
- $\varepsilon$  : 0.295

## 2.4. Measured data and parameters from the analysis

tare weight (for mass ratio; 1 digit balance)		2.9318 kg
gross weight wet		8.5887 kg
net weight wet	$m_W$	5.6569 kg
gross weight after ashing		3.0040 kg
net weight of ash	$m_A$	0.0722 kg

$$q = \frac{m_W}{m_A} : \quad 78.35 \text{ (mass ratio)}$$

tare weight (ash for analysis; 2 digit balance)		0.25603 kg
gross weight of ash		0.32803 kg
net weight of ash	$m_a$	0.07200 kg

$t_G$ :	$1.000 \cdot 10^6$ s (gross counting time interval)
$t_B$ :	$1.000 \cdot 10^6$ s (blank counting time interval)
$R_{GA}$ :	$4.0 \cdot 10^{-4}$ s <sup>-1</sup> (gross counting rate of the analyte peak)
$R_{GT}$ :	$1.7 \cdot 10^{-2}$ s <sup>-1</sup> (gross counting rate of the tracer peak)

## 3. IDENTIFICATION OF UNCERTAINTY SOURCES

The cause and effect diagram in Figure 1 shows the contributions of different sources of uncertainty.

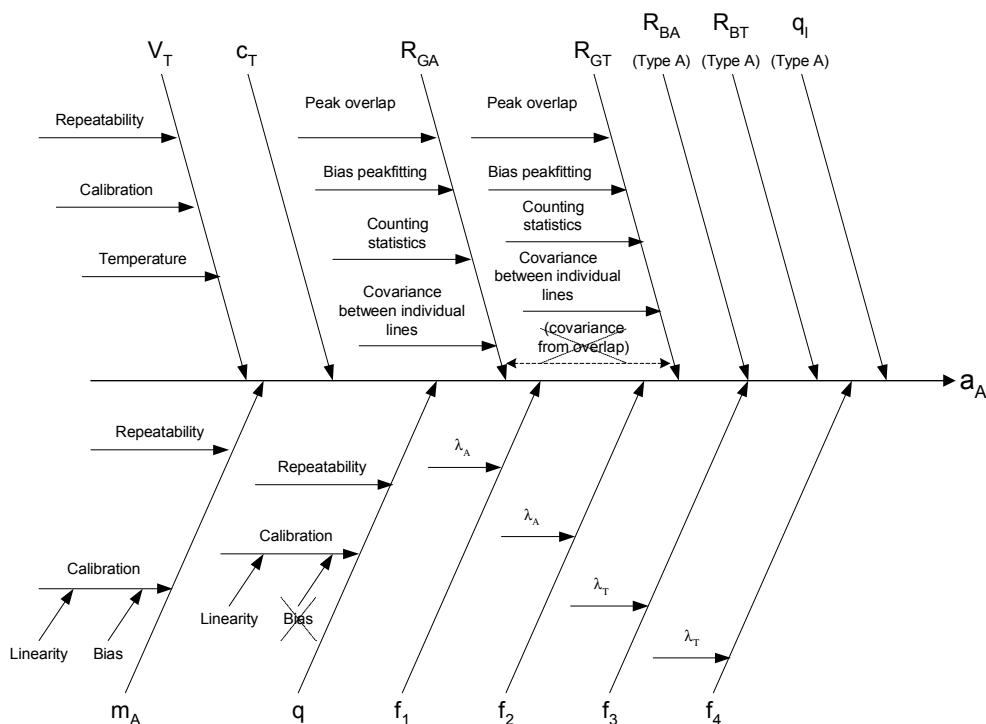


Fig. 1. Cause and Effect Diagram.

### 3.1. Sample preparation

3.1.1. Determination of the wet weight of the full sample  $m_w$

$$u(m_w) = \left( u^2(\text{gross weight wet}) + u^2(\text{tare weight}) \right)^{1/2}$$

3.1.2. Determination of the ash weight of the full sample  $m_A$

$$u(m_A) = \left( u^2(\text{gross weight ash}) + u^2(\text{tare weight}) \right)^{1/2}$$

3.1.3. Calculated value of the ratio of weights  $q = m_w / m_A$

$$\frac{u(q)}{q} = \left\{ \left( \frac{u(m_w)}{m_w} \right)^2 + \left( \frac{u(m_A)}{m_A} \right)^2 \right\}^{1/2}$$

Generally, the variables  $m_w$  and  $m_A$  are correlated, because the identical tare weight is used twice for their measurement. Using a simple formula from (3) it could be shown that, if the gross weights are not too close to the tare weight, the covariance term in the uncertainty of  $q$  can be neglected.

3.1.4. Mass of ash  $m_a$  used for the analysis:

$$u(m_a) = \left( u^2(\text{gross weight ash}) + u^2(\text{tare weight}) \right)^{1/2}$$

(the tare weight in this measurement is different from that in the step of the measurement of  $q$ )

3.1.5. A fractional loss of an actinide analyte during the step of ashing needs not to be considered: it is assumed that they are very small.

### 3.2. Amount of tracer added to the ash sample

3.2.1. Uncertainty of activity  $c_T$  of the certified tracer solution:  $u(c_T)/c_T$  is 0.0071.

3.2.2. Uncertainty components of volume  $V_T$  taken with a pipette from the tracer solution:

- The uncertainty of the internal volume (0.25 ml) of a pipette is given as 0.2% (manufacturer), which is converted to standard uncertainty by dividing by  $\sqrt{6}$  (triangular distribution, see (4)) yielding 0.1%.
- A series of fill and weigh measurements may result in a relative standard uncertainty of 0.25%.
- According to the EURACHEM Guide (4) a variation of  $\pm 3^\circ\text{C}$  of the environment temperature will result in an uncertainty component of  $V_T \cdot 3 \cdot 2.1 \cdot 10^{-4} / 1.96 \text{ ml} = V_T \cdot 3.2 \cdot 10^{-4} \text{ ml}$  (already converted to standard uncertainty).

These three uncertainty components have to be combined to the relative standard uncertainty  $u(V_T)/V_T$  of 0.26%, where the contribution of the temperature correction is insignificant.

### 3.3. Measured counting rates

The common method to determine the peak areas is to integrate the channel counts in a region of interest (ROI) (2), which has the width of about 4xFwhm (Full width at half maximum) and is centred asymmetrically around the expected peak position (about 3xFwhm to the left and 1xFwhm to the right; Fwhm about 25-50 keV). If a significant overlap between adjacent radionuclide peaks occur, the method for the determination of peak areas that became more available in recent years, even in the case of low-statistics spectra, is to de-convolute overlapping peaks, but also isolated peaks, by use of the numerical non-linear weighted least squares fitting (5-6). These authors are using the peak shape function given by Bortels and Collaers (7); one major advantage of this peak shape is that the peak area itself is a fitting parameter, which makes the calculation of its associated uncertainty very easy. It is important to use proper statistical weights in the fitting procedure to avoid the possible underestimation of the peak area (8-9). It is recommended to use the calculated function values for each channel count instead of the counts measured in each channel to determine the statistical weights (5).

The mathematical procedure of determining peak areas by the fitting-method need not to be presented here. It is assumed that if such a method (i.e. programme) is used it will give practically correct results for the peak area and its standard uncertainty. Essentially for the calculation of the peak area uncertainty is, however, that by adding up the areas of individually fitted lines of the same radionuclide peak to the total area, covariances between their individual areas must be used. If this is done, for peaks which are not severely overlapped by others and which are not too small, the uncertainty of the total peak area of size N is practically close to the expected value of  $\sqrt{N}$ .

For the following we will assume that the case of non-overlapping peaks applies, where the simple peak area integration of gross channel counts can be used.

3.3.1. The standard uncertainty of the gross counting rate  $R_{GA}$  of the analyte peak from the sample spectrum (counting time  $t_G$ ) is:

$$u(R_{GA}) = \sqrt{\frac{R_{GA}}{t_G}}$$

3.3.2. The standard uncertainty of the gross counting rate  $R_{GT}$  of the tracer radionuclide peak from the sample spectrum (counting time  $t_G$ ) is:

$$u(R_{GT}) = \sqrt{\frac{R_{GT}}{t_G}}$$

3.3.3. Uncertainties of blank counting rates  $R_{BA}$  and  $R_{BT}$  of the analyte and the tracer radionuclide, respectively:

It is assumed that measured blank counts are determined by the simple peak area integration of gross channel counts. It is strongly recommended that, for the purpose of the analysis of

environmental samples, a series of blank analyses is performed yielding different blank sources, which have to be measured with counting times much longer than that used for gross counting of the analyte samples sources. *It is often observed, that the variation (calculated as the sample standard deviation from the series) is larger than expected from counting statistics alone (which would follow Poisson or Gaussian distributions).*

Therefore, the following method is recommended to determine the uncertainties of the blank counting rates.

- 3.3.4. From a series of n prepared and measured blank sources, the blank counting rate  $R_{BA}$  and its uncertainty are obtained from:

$$R_{BA} = \frac{\sum_{i=1}^n R_{BA,i}}{n} \quad \text{and} \quad u(R_{BA}) = \sqrt{\frac{\sum_{i=1}^n (R_{BA,i} - R_{BA})^2}{n-1}}$$

- 3.3.5. From a series of n prepared and measured blank sources, the blank counting rate  $R_{BT}$  and its uncertainty are obtained from:

$$R_{BT} = \frac{\sum_{i=1}^n R_{BT,i}}{n} \quad \text{and} \quad u(R_{BT}) = \sqrt{\frac{\sum_{i=1}^n (R_{BT,i} - R_{BT})^2}{n-1}}$$

- 3.3.6. The counting rates are assumed to be live-time corrected. As these corrections are extremely low in the case of alpha spectrometry of environmental samples, their uncertainties need not to be considered.

- 3.3.7. If significant overlap of the peaks occurs, especially in the case of samples with higher activity, the simple method would produce systematic errors of the peak areas, which can not easily be corrected for. In this case, the use of the peak fitting method is recommended, which usually makes this error very small, smaller than the associated statistical counting uncertainty.

- 3.3.8. If significant overlap of the peaks of the analyte and the tracer peak occurs, then, generally, covariances between the single areas of the one with those of the other radionuclide must be considered (10), as from both total peak areas, additionally to be corrected for background (blank), a ratio is calculated (see Eq. (2.2)). However, it was tested by the author in the case of plutonium and americium spectra with larger peak areas, that with consideration of these covariances the correction of the standard uncertainty of this peak area ratio was less than the 1/25 of the value of the uncorrected uncertainty. ). *Therefore, it is concluded for alpha spectrometry of environmental samples, that these covariances need not to be considered at all.* Although only a small contribution from these covariances was estimated for the more overlapping case of Pu-239 and Pu-240, where the ratio Pu-239/Pu-240 was to be determined (10), this, however, generally holds in such a special case only in the case of ultra-high resolution alpha spectrometry.

### 3.4. Time intervals

It can be assumed that uncertainties of different time intervals need not to be considered, as they are extremely low.

### 3.5. Decay constants of radionuclides, taken from (11)

3.5.1. Relative uncertainty of the decay constant of the analyte:  $u(\lambda_A)/\lambda_A = 0.0034$

3.5.2. Relative uncertainty of the decay constant of the tracer radionuclide:  
 $u(\lambda_T)/\lambda_T = 0.0029$

### 3.6. Decay corrections

The uncertainties of the decay correction factors  $f_1, f_2, f_3, f_4$ , defined by the equations (2.3)–(2.6), are calculated as follows:

$$3.6.1. \quad u(f_1) = f_1 \cdot (t_S - t_E) \cdot u(\lambda_A)$$

$$3.6.2. \quad u(f_2) = f_2 \cdot (1 - f_2 \cdot \exp(-\lambda_A t_G)) \cdot \frac{u(\lambda_A)}{\lambda_A}$$

$$3.6.3. \quad u(f_3) = f_3 \cdot (t_S - t_C) \cdot u(\lambda_T)$$

$$3.6.4. \quad u(f_4) = f_4 \cdot (1 - f_4 \cdot \exp(-\lambda_T t_G)) \cdot \frac{u(\lambda_T)}{\lambda_T}$$

### 3.7. Sums of alpha emission probabilities, taken from (11)

3.7.1. Uncertainty of the sum of emission probabilities  $p_{\alpha T}$  of the tracer radionuclide (the full uncertainty cannot be evaluated, as the existent covariances between single emission probabilities are not published):  $u(p_{\alpha T})/p_{\alpha T} = 0.0024$ .

3.7.2. Uncertainty of the sum of emission probabilities  $p_{\alpha A}$  of the analyte (the full uncertainty cannot be evaluated, as the existent covariances between single emission probabilities are not published):  $u(p_{\alpha A})/p_{\alpha A} = 0.0064$ .

### 3.8. Isotopic impurity of the analyte in the tracer solution

This is determined as a mean of ratios of the net counting rate of the analyte to the net counting rate of the tracer, which are obtained from measurements on a few separately electroplated tracer sources. Thereby, the standard uncertainty  $u(q_I)$  is estimated by repeated measurements.

## 4. CALCULATION OF THE RESULT AND THE COMBINED STANDARD UNCERTAINTY

4.1. The calculation of the result for the activity concentration of the analyte is done with the equations (2.2) and (2.1):

$$A_A = 0.280 \cdot 0.250 \left[ \frac{(4.00 \cdot 10^{-4} - 8.00 \cdot 10^{-6})}{(1.70 \cdot 10^{-2} - 7.00 \cdot 10^{-5})} - 1.1 \cdot 10^{-3} \right] \cdot \left( \frac{1.0000}{1.0000} \right) = 1.544 \cdot 10^{-3} \text{ Bq}$$

$$a_A = \frac{1.544 \cdot 10^{-3}}{0.07200 \cdot 78.35} \cdot 1.04856 \cdot 0.99947 \cdot 0.99999 \cdot 1.00000 = 2.868 \cdot 10^{-4} \text{ Bq kg}^{-1} \text{ wet weight}$$

4.2. The radiochemical yield can be obtained by Eq. (2.7) as follows:

$$\eta = \frac{(1.70 \cdot 10^{-2} - 7.00 \cdot 10^{-5})}{0.295 \cdot 0.280 \cdot 0.250} = 0.82$$

4.3. The individual uncertainty components and their sensitivity factors and percent contributions to the square of the combined uncertainty of the measurand are given in Table 1. The sensitivity factors  $\partial f / \partial x_i$  and percent contributions  $\left( \frac{\partial f}{\partial x_i} \frac{u(x_i)}{u_C} \right)^2 \cdot 100$  (see (4), Appendix D, D.3), were obtained by using a numerical method.

4.4. The relative combined standard uncertainty  $u_C(a_A) / a_A$  of the activity concentration  $a_A$  of the analyte in the analysed sample, referred to the end of sampling date, is calculated from the uncertainties listed in Table 1 with the following formulae:

$$\frac{u_C(a_A)}{a_A} = \left\{ \left( \frac{u_C(A_A)}{A_A} \right)^2 + \left( \frac{u(m_a)}{m_a} \right)^2 + \left( \frac{u(q)}{q} \right)^2 + \left( \frac{u(f_1)}{f_1} \right)^2 + \left( \frac{u(f_2)}{f_2} \right)^2 + \left( \frac{u(f_3)}{f_3} \right)^2 + \left( \frac{u(f_4)}{f_4} \right)^2 \right\}^{1/2}$$

with:

$$\frac{u_C(A_A)}{A_A} = \left\{ \left( \frac{u(c_T)}{c_T} \right)^2 + \left( \frac{u(V_T)}{V_T} \right)^2 + \left( \frac{u(y)}{y} \right)^2 + \left( \frac{u(p_{\alpha,A})}{p_{\alpha,A}} \right)^2 + \left( \frac{u(p_{\alpha,T})}{p_{\alpha,T}} \right)^2 \right\}^{1/2},$$

and

$$y = \frac{R_{GA} - R_{BA}}{R_{GT} - R_{BT}} - q_I,$$

$$u^2(y) = u^2 \left( \frac{R_{GA} - R_{BA}}{R_{GT} - R_{BT}} \right) + u^2(q_I),$$

$$u^2 \left( \frac{R_{GA} - R_{BA}}{R_{GT} - R_{BT}} \right) = \left( \frac{R_{GA} - R_{BA}}{R_{GT} - R_{BT}} \right)^2 \cdot \left[ \left( \frac{u(R_{GA} - R_{BA})}{(R_{GA} - R_{BA})} \right)^2 + \left( \frac{u(R_{GT} - R_{BT})}{(R_{GT} - R_{BT})} \right)^2 \right],$$

$$\left( \frac{u(R_{GA} - R_{BA})}{(R_{GA} - R_{BA})} \right)^2 = \frac{u^2(R_{GA}) + u^2(R_{BA})}{(R_{GA} - R_{BA})^2},$$

$$\left( \frac{u(R_{GT} - R_{BT})}{(R_{GT} - R_{BT})} \right)^2 = \frac{u^2(R_{GT}) + u^2(R_{BT})}{(R_{GT} - R_{BT})^2} .$$

From the lengthy calculations (not shown) one obtains:

$$\frac{u_C(a_A)}{a_A} = 0.0591; \text{ or } u_C(a_A) = 1.696 \cdot 10^{-5} \text{ Bq kg}^{-1} \text{ wet weight.}$$

From Table 1 it can be estimated that in this example the contributions of the 5 parameters  $R_{GA}$ ,  $R_{BA}$ ,  $R_{GT}$ ,  $q_I$  and  $c_T$  amount to 97.1 % of the square of the combined uncertainty.

4.5. As the result one obtains:

$$a_A = 2.87 \cdot 10^{-4} \quad \text{Bq kg}^{-1} \text{ wet weight,}$$

$$u_C(a_A) = 1.70 \cdot 10^{-5} \quad \text{Bq kg}^{-1} \text{ wet weight.}$$

**Table 1:** Individual uncertainty components and their sensitivity factors and contributions to the square of the combined uncertainty

Symbol/Reference To list	Value of variable	Uncertainty	Conversion factor to standard uncertainty	Standard uncertainty (u)	Sensitivity factor	Percent contribution to (u <sub>c</sub> ) <sup>2</sup>
<i>Mass ratio q:</i>						
gross weight wet	8.5887 kg	0.0003 kg	1	0.0003 kg		
tare weight	2.9318 kg	0.0003 kg	1	0.0003 kg		
wet weight $m_w$ (3.1.a)	5.6569 kg	0.00042 kg	1	0.00042 kg		
gross weight ash	3.0040 kg	0.0003 kg	1	0.0003 kg		
ash weight $m_A$ (3.1.b)	0.0722 kg	0.00042 kg	1	0.00042 kg		
mass ratio q (3.1.c)	78.35	0.46	1	0.46	$-3.66 \cdot 10^{-6}$	0.987
<i>Ash weight for analysis:</i>						
gross weight ash	0.32803 kg	0.00003 kg	1	0.00003 kg		
tare weight	0.25603 kg	0.00003 kg	1	0.00003 kg		
$m_a$ (3.1.d)	0.07200 kg	0.000042 kg	1	0.000042 kg	$-3.98 \cdot 10^{-3}$	0.010
<i>Tracer concentration:</i>						
$c_T$ (3.2.a)	0.280 Bq ml <sup>-1</sup>	0.002 Bq ml <sup>-1</sup>	1	0.002 Bq ml <sup>-1</sup>	$1.02 \cdot 10^{-3}$	1.459
<i>Volume of tracer:(3.2.b)</i>						
i) pipetted volume:	0.250 ml	0.0005 ml	$1/\sqrt{6}$	0.0002 ml		
ii) fill and weigh:	factor=1	0.0025	1	0.0025		
iii) $\pm 3$ °C variation:	factor=1	0.00063	1/1.96	0.00032		
<i>combined uncertainty:</i>	0.250 ml x 1 x 1			0.00066 ml	$1.15 \cdot 10^{-3}$	0.200
<i>Decay corrections:</i>						
$f_1$ (3.6.a)	1.04856	0.00017	1	0.00017	$2.74 \cdot 10^{-4}$	0.001
$f_2$ (3.6.b)	0.99947	0.0000027	1	0.0000027	$2.87 \cdot 10^{-4}$	0.000
$f_1$ (3.6.c)	0.99999	$1.1 \cdot 10^{-8}$	1	$1.1 \cdot 10^{-8}$	$2.87 \cdot 10^{-4}$	0.000
$f_1$ (3.6.d)	1.00000	$1.7 \cdot 10^{-10}$	1	$1.7 \cdot 10^{-10}$	$2.87 \cdot 10^{-4}$	0.000
<i>Counting rates:</i>						
$R_{GA}$ (3.3.a)	$4.00 \cdot 10^{-4} \text{ s}^{-1}$	$2.00 \cdot 10^{-5} \text{ s}^{-1}$	1	$2.00 \cdot 10^{-5} \text{ s}^{-1}$	$7.68 \cdot 10^{-1}$	82.021
$R_{BA}$ (3.3.d)	$8.00 \cdot 10^{-6} \text{ s}^{-1}$	$6.40 \cdot 10^{-6} \text{ s}^{-1}$	1	$6.40 \cdot 10^{-6} \text{ s}^{-1}$	$-7.68 \cdot 10^{-1}$	8.399
$R_{GT}$ (3.3.b)	$1.70 \cdot 10^{-2} \text{ s}^{-1}$	$1.30 \cdot 10^{-4} \text{ s}^{-1}$	1	$1.30 \cdot 10^{-4} \text{ s}^{-1}$	$-1.78 \cdot 10^{-2}$	1.858
$R_{BT}$ (3.3.e)	$7.00 \cdot 10^{-5} \text{ s}^{-1}$	$5.60 \cdot 10^{-5} \text{ s}^{-1}$	1	$5.60 \cdot 10^{-5} \text{ s}^{-1}$	$1.78 \cdot 10^{-2}$	0.345
<i>Alpha emission probabilities:</i>						
$p_{\alpha T}$ (3.7.a)	1.0000	0.0024	1	0.0024	$2.87 \cdot 10^{-4}$	0.165
$p_{\alpha A}$ (3.7.b)	1.0000	0.0064	1	0.0064	$-2.87 \cdot 10^{-4}$	1.171
<i>Isotopic impurity:</i>						
$q_1$ (3.8)	$1.1 \cdot 10^{-3}$	$2.4 \cdot 10^{-4}$	1	$2.4 \cdot 10^{-4}$	$-1.30 \cdot 10^{-2}$	3.385

## LIST OF SYMBOLS

$a_A$	the activity concentration of the analyte referred to the date of sampling in Bq kg <sup>-1</sup> wet or dry weight
$A_A$	the amount of activity of the analyte on the electroplated source in Bq
$c_T$	certified concentration of the tracer solution in Bq ml <sup>-1</sup>
$f_1$	correction for decay of the analyte in the time interval from the end of sampling to the beginning of the measurement
$f_2$	correction for decay of the analyte in the counting interval $t_G$
$f_3$	correction for decay of the tracer radionuclide in the time interval from its calibration date to the beginning of the measurement
$f_4$	correction for decay of the tracer radionuclide in the counting interval $t_G$
$m_A$	ash weight of the full sample in kg
$m_a$	mass of ashed sample used for the alpha analysis in kg
$m_W$	wet weight of the full sample in kg
$p_{\alpha A}$	sum of alpha emission probabilities of those individual alpha lines of the analyte which contribute to the channel region in the alpha spectrum which is used to determine its gross count rate (usually very close to unity)
$p_{\alpha T}$	sum of alpha emission probabilities of those individual alpha lines of the tracer radionuclide which contribute to the channel region in the alpha spectrum which is used to determine its gross count rate (usually very close to unity)
$q$	mass ratio wet weight per ash weight, if the result is required on wet weight basis
$q_I$	isotopic impurity ratio of the analyte in the tracer solution
$R_{BA}$	blank counting rate of the analyte in s <sup>-1</sup> (counting time $t_B$ )
$R_{BT}$	blank counting rate of the tracer radionuclide in s <sup>-1</sup> (counting time $t_B$ )
$R_{GA}$	gross counting rate of the analyte in s <sup>-1</sup> (counting time $t_G$ )
$R_{GT}$	gross counting rate of the tracer radionuclide in s <sup>-1</sup> (counting time $t_G$ )
$t_B$	counting time interval of the blank counting in s
$t_S$	beginning of measurement time
$t_C$	time of calibration of the tracer radionuclide solution
$t_G$	counting time interval of the gross counting in s
$t_E$	end of sampling time
$V_T$	volume taken from the tracer solution in ml
$\varepsilon$	detection efficiency for alpha particles
$\eta$	radiochemical yield of the analyte
$\lambda_A$	decay constant of analyte in s <sup>-1</sup>
$\lambda_T$	decay constant of tracer radionuclide in s <sup>-1</sup>

## REFERENCES

- [1] DE REGGE, P., BODEN, R., Review of Chemical Separation Techniques Applicable to Alpha Spectrometric Measurements, Nucl. Instr. Meth. Phys. Res. 223 (1984) 181-187.
- [2] HOLM, E., Review of Alpha-Particle Spectrometric Measurements of Actinides. Int. J. Appl. Radiat. Isot. 35 (1984) 285-290.
- [3] WINKLER, G., On the Role of Covariances for Uncertainty Estimates in Radioactivity Measurements. Appl. Radiat. Isot. 49 (1998) 1153-1157.
- [4] EURACHEM, "Quantifying Uncertainty in Analytical Measurement", Editor: Laboratory of the Government Chemist Information Services, Teddington (Middlesex) & London (1995). ISBN 0-948926-08-2.
- [5] BORTELS, G., HURTGEM, C., SANTRY, D., Nuclide Analysis on Low-statistics Alpha-particle Spectra: An Experimental Verification for Pu Isotopes, Appl. Radiat. Isot. 46 (1995) 1135-1144.
- [6] MARTIN SANCHEZ, A., VERA TOME, F., RUBIO MONTERO, P., Fitting of Alpha Spectra. Application to Low-level Measurements, Appl. Radiat. Isot. 47 (1996) 899-903.
- [7] BORTELS, G., COLLAERS, P., Analytical function for fitting peaks in alpha-particle spectra from Si detectors, Appl. Radiat. Isot. 38 (1987) 831-837.
- [8] BAKER, S., COUSINS, R.D., Clarification of the Use of Chi-Square and Likelihood Functions in Fits to Histograms, Nucl. Instr. Meth. In Phys. Res. 221 (1984) 437-442.
- [9] BEVINGTON, P.R., Data Reduction and Error Analysis for the Physical Sciences, McGraw-Hill, New York (1969).
- [10] SIBBENS, G., Uncertainty Assessment in the Analysis of Alpha-particle Spectra. Appl. Radiat. Isot. 49 (1998) 1241-1244.
- [11] BUNDESMINISTERIUM FÜR UMWELT, NATURSCHUTZ UND REAKTORSICHERHEIT (BMU), 1992. Meßanleitungen für die Überwachung der Radioaktivität in der Umwelt und zur Erfassung radioaktiver Emissionen aus kerntechnischen Anlagen. Stand: 1.9.1992. Chapter IV.6. Gustav Fischer Verlag, Stuttgart (1992).  
(Ministry for Environment, Nature Conservation and Reactor Safety, 1992. Guide to methods for the monitoring of radioactivity in the environment and for registration of radioactive emissions from nuclear power installations. Status: 1.9.1992.)

# ALPHA-SPECTROMETRIC ANALYSIS OF ENVIRONMENTAL SAMPLES — SPREADSHEET APPROACH

L. HOLMES

Institute for Reference Materials and Measurements (IRMM), Joint Research Centre,  
European Commission, Geel, Belgium

## Abstract

The example evaluates the uncertainty sources for the determination of different actinides in environmental samples according to the spreadsheet method and refers thereby to the example prepared for this guide by G. Kanisch. The analytical procedure involves sample preparation steps for drying, ashing and dissolution and further radiochemical separation and electroplating of the isolated radionuclides. The radioactivity is measured by a solid state detector coupled to a multichannel spectrometer. An isotopic tracer is used to determine the overall chemical yield and to ensure traceability to a national standard.

## 1. INTRODUCTION

This paper is based on the work into quantifying uncertainties in alpha spectrometry by G. Kanisch [1, This guide]. Whereas, in [1], a complete mathematical approach was used to quantify the overall uncertainty, in this paper, the “spreadsheet” method for uncertainty calculation [2,3] will be described, and applied to the same example and data presented in [1].

## 2. THE SPREADSHEET APPROACH

The “spreadsheet” approach can be simply performed in any commercial spreadsheet package (such as Microsoft Excel). The method takes advantage of an approximate numerical method of differentiation. This requires only the equation used to calculate the final result, and the individual numerical values of the parameters in this equation, with their associated individual uncertainties. For a full description of the mathematical theory behind the method, see [2].

The following key steps in the method are detailed below, using a simple example with artificial data.

**Step 1.** First, we need to define the equation that is used to calculate the final result. In this example, suppose the result,  $y$ , is determined from Equation 1. We then need the values of the four parameters ( $A$ ,  $B$ ,  $C$  and  $D$ ), along with each of their standard absolute uncertainties. These parameters (and uncertainties) may have been determined experimentally (*e.g.* the weight of a sample) or obtained from an external source (*e.g.* the calibration certificate of a standard).

The parameters, with their numerical values and uncertainties are listed vertically in the spreadsheet (see Figure 1), and the result calculated using Equation 1. This is the “real” result.

$$y = \frac{A \cdot B \cdot C}{D} \quad (1)$$

	Parameter	Value	Standard Absolute Uncertainty	
	A	12	0.125	
	B	160	0.367	
	C	0.9998	0.00001	
	D	0.45	0.003	
	<b>Result, y :</b>	4265.81		

Fig. 1. Summary of parameters, values and uncertainties.

**Step 2.** In the spreadsheet, the four parameters are now listed horizontally (see Figure 2) and the values of the parameters copied to each column. Now, under the column heading of a parameter (e.g. A), add on the value of the uncertainty to the value of the parameter. So, under column A, we change the value of 12 to 12.125 (A + Uncertainty of A), leaving the values of the other parameters in that column as before. Recalculate the value of ‘y’ under each column, using the new values, to give the “varied” results.

	Parameter	Value	Standard Absolute Uncertainty						
					A	B	C	D	
	A	12	0.125		12.125	12	12	12	
	B	160	0.367		160	160.367	160	160	
	C	0.9998	0.00001		0.9998	0.9998	0.99981	0.9998	
	D	0.45	0.003		0.45	0.45	0.45	0.453	
	<b>Result, y :</b>	4265.81		<b>Varied</b>	4310.25	4275.60	4265.86	4237.56	

Fig. 2. Calculation of the result for the values augmented with their individual uncertainties.

**Step 3.** The difference (residual) between the “varied” result and the “real” result is calculated for each parameter at the foot of its column (see Figure 3). This residual is then squared, and summed up across all four parameters. The overall uncertainty can then be estimated by taking the square root of this “sum of squares”.

So, from this, we have a final value of  $4265.81 \pm 53.56$ .

Parameter	Value	Standard Absolute Uncertainty		A	B	C	D
A	12	0.125		12.125	12	12	12
B	160	0.367		160	160.367	160	160
C	0.9998	0.00001		0.9998	0.9998	0.99981	0.9998
D	0.45	0.003		0.45	0.45	0.45	0.453
Result, y :	4265.81		Varied Results	4310.25	4275.60	4265.86	4237.56
			Residuals	-44.44	-9.78	-0.04	28.25
			Residual Squared	1974.52	95.74	0.00	798.09
			Sum of Squares	2868.35		Uncertainty	53.56

Fig. 3. Calculation of the residuals, their squares and the sum of squares.

**Step 4.** It can be very useful to estimate the percent contribution each of the parameters makes to the overall uncertainty. This can be simply done with the spreadsheet method. For each parameter, divide its “residual squared” value by the total “sum of squares” value. In this example, the values are calculated in Figure 4, where it can be clearly seen that parameter A makes up the majority of the uncertainty, with parameter C making little contribution. If overall uncertainties are to be reduced, then more effort should be put into reducing the certainty of parameter A.

	A	B	C	D
Percent (%) Contributions :	68.8	3.3	0.0	27.8

Fig. 4. Relative contribution of the uncertainty of individual parameter values to the uncertainty of the result.

The uncertainty calculated by this method (53.56), can be compared to that calculated using the full mathematical approach. Equation 2 and Figure 5 show how this is calculated in the usual way, using the same values and uncertainties as listed in Figure 1.

$$\frac{u(y)}{y} = \left[ \left( \frac{u(A)}{A} \right)^2 + \left( \frac{u(B)}{B} \right)^2 + \left( \frac{u(C)}{C} \right)^2 + \left( \frac{u(D)}{D} \right)^2 \right]^{1/2} \quad (2)$$

		A	B	C	D
	$u(x_i) / x_i$	0.010416667	0.0022938	1.0002E-05	0.00666667
	$(u(x_i) / x_i)^2$	0.000108507	5.261E-06	1.0004E-10	4.4444E-05
	<b>Sum</b>	0.000158213			
	<b>Square Root</b>	0.012578266			
	If y =	4265.81			
<b>Then,</b>	<b>u(y) =</b>	53.66			

Fig. 5. Calculation of the uncertainty on the result according to the error propagation method.

As can be seen, the spreadsheet method and the full mathematical approach give very similar overall uncertainties (53.56 compared to 53.66). However, it must be noted, that the spreadsheet approach is only valid when the uncertainty of a parameter is small compared to the parameter and that the function  $y(x_1, x_2, \dots, x_n)$  is linear with respect to all parameters. Although this is not always the case (for example, the uncertainty on the count rate in alpha spectrometry is often large, which will be seen in section 3), the method still gives a good estimate of the overall uncertainty.

Although this was a simple example using either methods, the spreadsheet approach becomes particularly useful as the situation becomes more complex, as in the case of alpha spectrometry.

### 3. THE SPEADSHEET APPROACH APPLIED TO ALPHA SPECTROMETRY

The method outlined in section 2 was applied to the data and equations given in [1]. Equation 3 shows the basic function that is defined to be used in the spreadsheet approach (which is further combined with Equation 4).

$$a_A = \frac{A_A}{m_a \cdot q} \cdot f_1 \cdot f_2 \cdot f_3 \cdot f_4 \quad (3)$$

Where,

- $a_A$  Activity concentration of the analyte, referred to the date of sampling (Bq kg<sup>-1</sup> of wet weight)
- $A_A$  Activity of analyte on electroplated source (Bq)
- $m_a$  Mass of ashed sample used (kg)
- $q$  Mass ratio (wet/dry) of sample
- $f_1$  Correction for decay of analyte from sampling to measurement
- $f_2$  Correction for decay of analyte during counting period
- $f_3$  Correction for decay of tracer from calibration to use
- $f_4$  Correction for decay of tracer during counting period

And,

$$A_A = c_T \cdot V_T \cdot \left[ \frac{R_{GA} - R_{BA}}{R_{GT} - R_{BT}} - q_I \right] \cdot \left( \frac{P_{\alpha T}}{P_{\alpha A}} \right) \quad (4)$$

Where,

$c_T$	Certified concentration of tracer solution (Bq ml <sup>-1</sup> ) at date of calibration
$V_T$	Volume of tracer used (ml)
$R_{GA}$	Gross counting rate of analyte (s <sup>-1</sup> )
$R_{BA}$	Blank counting rate of the analyte (s <sup>-1</sup> )
$R_{GT}$	Gross counting rate of tracer radionuclide (s <sup>-1</sup> )
$R_{BT}$	Blank counting rate of the tracer radionuclide (s <sup>-1</sup> )
$q_I$	Isotopic impurity ratio of analyte in tracer solution
$P_{\alpha T}$	Sum of alpha emission probabilities for tracer region of interest
$P_{\alpha A}$	Sum of alpha emission probabilities for analyte region of interest

Figure 6 gives the input data for the spreadsheet, whilst Figure 7 shows the completed table for the spreadsheet approach. All of the data for each parameter has been taken from [1], along with the standard uncertainties on each parameter. The only data missing from [1] was the uncertainties on the blank count rates. For this reason, the uncertainties on the blank (of the sample and tracer) were not calculated as defined in sections 3.3.d and 3.3.e of [1], but by the method described for the sample and tracer peaks in section 3.3.a and 3.3.b of [1]. This will account for a minor discrepancy in the value of the overall uncertainty obtained here and that obtained in [1].

### 3.1 Comparison of Both Uncertainties

Using all of the data listed in [1], together with the final formulae that is given in section 4.4 of [1], the relative combined standard uncertainty,  $u_C(a_A)$  can be calculated, by the full mathematical approach. From this, an uncertainty of  $1.59 \times 10^{-5}$  was found. This is slightly different to the result given in [1] ( $1.70 \times 10^{-5}$ ) because, as already mentioned, different uncertainties were used in the blank determinations. However, when this uncertainty is compared to that calculated using the spreadsheet approach ( $1.58 \times 10^{-5}$ ), it can be seen that the spreadsheet approach actually gives a very good estimate of the overall uncertainty, despite having a very large single uncertainty from the sample counting statistics. In fact, it can be seen that the uncertainty on the count rate of the sample peak makes up 88% of the overall uncertainty.

	Parameter	Value	Standard Uncertainty
	$m_a$	0.072	4.24264E-05
	$q$	78.35041551	0.460442845
	$f_1$	1.015956537	5.47E-05
	$f_2$	1.000125505	4.26736E-07
	$f_3$	0.999988875	3.23E-08
	$f_4$	1.00E+00	8.74E-11
	$c_T$	0.28	0.002
	$V_T$	0.25	0.000658755
	$R_{GA}$	4.00E-04	0.00002
	$R_{BA}$	8.00E-06	2.82843E-06
	$R_{GT}$	1.70E-02	0.000130384
	$R_{BT}$	7.00E-05	8.37E-06
	$q_i$	1.10E-03	2.40E-04
	$P_{\alpha T}$	1	0.0024
	$P_{\alpha A}$	1	0.0064
	<b>Result, <math>a_A</math></b>	<b>2.78E-04</b>	

Fig. 6. Summary of parameters, values and uncertainties for the alpha spectrometry example.

### 3.2 Other Uses of the Spreadsheet Approach

Apart from (i) providing a quick method to determine the overall uncertainty and (ii) allowing the analyst to see which parameters contribute the most to the overall uncertainty, it can also be used as a tool to minimise uncertainties in the future. Once all data has been input into the spreadsheet, parameters can be easily changed to ascertain their effect on the overall uncertainty. For example, if the count time of the analyte peak in the sample is doubled, the effect is immediately seen on the uncertainty on the sample count rate, and hence on the overall uncertainty. This can be a useful tool to determine where effort should be placed in order to reduce uncertainties.

	$m_a$	$q$	$f_1$	$f_2$	$f_3$	$f_4$	$c_T$	$V_T$	$R_{GA}$	$R_{BA}$	$R_{GT}$	$R_{BT}$	$q_l$	$P_{\alpha T}$
	0.072042426	0.072	0.072	0.072	0.072	0.072	0.072	0.072	0.072	0.072	0.072	0.072	0.072	0.072
	78.35041551	78.81086	78.35041551	78.35042	78.35042	78.35042	78.350416	78.35042	78.35042	78.35041551	78.35042	78.35042	78.35042	78.35042
	1.015956537	1.015957	1.02E+00	1.015957	1.015957	1.015957	1.0159565	1.015957	1.015957	1.015956537	1.015957	1.015957	1.015957	1.015957
	1.000125505	1.000126	1.000125505	1.000126	1.000126	1.000126	1.0001255	1.000126	1.000126	1.000125505	1.000126	1.000126	1.000126	1.000126
	0.999988875	0.999989	0.999988875	0.999989	1.00E+00	0.999989	0.9999889	0.999989	0.999989	0.999988875	0.999989	0.999989	0.999989	0.999989
	1.00E+00	1.00E+00	1.00E+00	1.00E+00	1.00E+00	1.00E+00	1.00E+00	1.00E+00	1.00E+00	1.00E+00	1.00E+00	1.00E+00	1.00E+00	1.00E+00
	0.28	0.28	0.28	0.28	0.28	0.28	0.282	0.28	0.28	0.28	0.28	0.28	0.28	0.28
	0.25	0.25	0.25	0.25	0.25	0.25	0.25	0.250659	0.25	0.25	0.25	0.25	0.25	0.25
	4.00E-04	4.00E-04	4.00E-04	4.00E-04	4.00E-04	4.00E-04	4.00E-04	4.00E-04	4.20E-04	4.00E-04	4.00E-04	4.00E-04	4.00E-04	4.00E-04
	8.00E-06	8.00E-06	8.00E-06	8.00E-06	8.00E-06	8.00E-06	8.00E-06	8.00E-06	8.00E-06	1.08E-05	8.00E-06	8.00E-06	8.00E-06	8.00E-06
	1.70E-02	1.70E-02	1.70E-02	1.70E-02	1.70E-02	1.70E-02	1.70E-02	1.70E-02	1.70E-02	1.70E-02	1.71E-02	1.70E-02	1.70E-02	1.70E-02
	7.00E-05	7.00E-05	7.00E-05	7.00E-05	7.00E-05	7.00E-05	7.00E-05	7.00E-05	7.00E-05	7.00E-05	7.00E-05	7.84E-05	7.00E-05	7.00E-05
	1.10E-03	1.10E-03	1.10E-03	1.10E-03	1.10E-03	1.10E-03	1.10E-03	1.10E-03	1.10E-03	1.10E-03	1.10E-03	1.10E-03	1.34E-03	1.10E-03
	1	1	1	1	1	1	1	1	1	1	1	1	1	1.0024
	1	1	1	1	1	1	1	1	1	1	1	1	1	1
<b>Varied Result</b>	2.78E-04	2.76E-04	2.78E-04	2.78E-04	2.78E-04	2.78E-04	2.80E-04	2.79E-04	2.93E-04	2.76E-04	2.76E-04	2.78E-04	2.75E-04	2.79E-04
<b>Residual</b>	1.64E-07	1.62E-06	-1.50E-08	-1.19E-10	-8.97E-12	-2.43E-14	-1.99E-06	-7.33E-07	-1.49E-05	2.11E-06	2.23E-06	-1.44E-07	3.03E-06	-6.67E-07
<b>Square of Residuals</b>	2.68E-14	2.64E-12	2.24E-16	1.41E-20	8.05E-23	5.91E-28	3.94E-12	5.37E-13	2.22E-10	4.44E-12	4.98E-12	2.08E-14	9.16E-12	4.45E-13
<b>Sum of squares</b>	2.51E-10		<b>Uncertainty</b>	1.58E-05										
<b>% Contribution :</b>	$m_a$	$q$	$f_1$	$f_2$	$f_3$	$f_4$	$c_T$	$V_T$	$R_{GA}$	$R_{BA}$	$R_{GT}$	$R_{BT}$	$q_l$	$P_{\alpha T}$
	0.011	1.05	0.0001	0.0000	0.0000	0.0000	1.571	0.214	88.329	1.767	1.982	0.008	3.646	0.177
<b>Factors which make up <math>A_A</math> :</b>			98.938	%										

Fig. 7. Full uncertainty calculation for the alpha spectrometry example according to the spreadsheet method.

#### 4. SUMMARY

The spreadsheet approach is a relatively quick and easy method to estimate the overall uncertainty on a result, once the uncertainties of its individual components have been ascertained. In the example presented here for alpha spectrometry, it gave an uncertainty that was comparable to that obtained through a rigorous, lengthy and complicated mathematical treatment of the data. Furthermore, it is easy to see which of the components contribute the most to the overall uncertainty (and hence can be examined more closely) and a simple exercise in minimising future uncertainties can be performed.

#### REFERENCES

- [1] KANISCH, G., Quantifying Uncertainties in the Alpha-Spectrometric Analysis of Environmental Samples. This document.
- [2] KRAGTEN, J., Calculating Standard Deviations and Confidence Intervals with a Universally Applicable Spreadsheet Technique, *Analyst*, **119** (1994) 2161-2166.
- [3] ELLISON, S.L.R., ROSSLEIN, M., WILLIAMS, A., BERGLUND, M., HAESSELBARTH, W., HEDEGAARD, K., KARLS, R., MANSSON, M., STEPHANY, R., VAN DER VEEN, A., WEGSCHEIDER, W., VAN DE WIEL, H., WOOD, R., PAN XIU RONG, SALIT, M., SQUIRRELL, A., YUSUSDA, K., JOHNSON, R., JUNG-KEUN LEE, MOWREY, M., DE REGGE, P., FAJGELJ, A., GALSWORT, D., EURACHEM/CITAC Guide “Quantifying Uncertainty in Analytical Measurement”, Second Edition, Editors: S. L. R. Ellison, M. Rosslein, A Williams, (2000), Appendix E.2.

# DETERMINATION OF STRONTIUM-89 AND STRONTIUM-90 IN SOILS AND SEDIMENTS

H. JANSZEN

Physikalisch-Technische Bundesanstalt, Braunschweig, Germany

## Abstract

The quantification of uncertainty in the determination of Sr-90 in environmental samples using a low-level proportional counter system for the final radioactivity measurement is covered in this example. This example includes also the evaluation of the uncertainty for the determination of Sr-89.

The example is rather complex for the following reasons:

- the determination of chemical yield of the separation is done by adding a known quantity of strontium to the sample and measuring the quantity recovered; however the environmental sample might contain already some strontium, which has to be determined separately and corrected for;
- the Sr-90 is measured indirectly through its daughter product Y-90; the ratio of Y-90 to Sr-90 is affected by the chemical separation and depends on the time intervals between the separation and the measurements;
- Sr-90 interferes with the Sr-89 measurement and Y-90 interferes with both of them, but the extent of the interference is dependent on the chemical separation and its timing with respect to the measurement. The example addresses the uncertainty sources in the sample weighing and preparation, in the determination of the chemical yield, in the count rates and the background corrections for the radioactivity measurement, in the efficiency of the radiation detectors, and in the correction factors for radioactive decay and build-up.

## 1. INTRODUCTION

The example discusses sources of uncertainties related to the determination of the specific activities of Sr-89 and Sr-90 in environmental samples of soils and sediments. The analytical method is based on the radiochemical separation of strontium and yttrium and subsequent measurements of appropriate sources in a conventional low-level proportional counter system.

A radiochemical procedure commonly used is the fuming nitric acid method. It covers the conversion of the strontium contained in the sample to an extractable form, precipitation of strontium and calcium, separation of strontium from calcium, scavenging of interfering radionuclides (e.g. radium, barium, lead) and precipitation of strontium as carbonate. The total decomposition of the sample matrix is essential for the assay of radioactive strontium. Any residue obtained after sample dissolution has, therefore, to be checked for gross alpha and beta activity. The chemical yield of the procedure has to be monitored by an appropriate yield tracer. In the example described here, inactive strontium and yttrium are used for this purpose. Atomic emission or atomic absorption spectrometry, X ray fluorescence and radioactive Sr-85 tracer may be used as alternatives.

No details of the radiochemical procedure are given in this document, since the method is described in detail in the literature, e. g. [1,2]. The radiochemical process will rather be treated as an operator which requires certain input quantities and which acts on the sample so that the desired output quantities are obtained.

## 2. DESCRIPTION OF THE METHOD

### 2.1. Principles

The method of strontium analysis is outlined in Fig. 1, and the corresponding timing diagram is shown in Fig. 2. The time of sampling  $t_0$  is also used as the reference time for reporting the

measurement results. Prior to any radiochemical sample treatment, a weighed amount of inactive strontium tracer is added to allow the chemical yield of the procedure to be monitored. After the radiochemical separation at time  $t_1$ , strontium carbonate is collected on a high-density filter paper of known mass, which is then measured in the proportional counter system. The period of time between strontium separation and measurement of the strontium carbonate source, i.e.  $t_2 - t_1$ , should be at least 14 days. In this case, the Y-90 activity of the source is more than 97 percent of the Sr-90 activity. Furthermore, the correction for ingrowth of yttrium during a measurement is less than 1 percent for a counting period of up to 1 day.

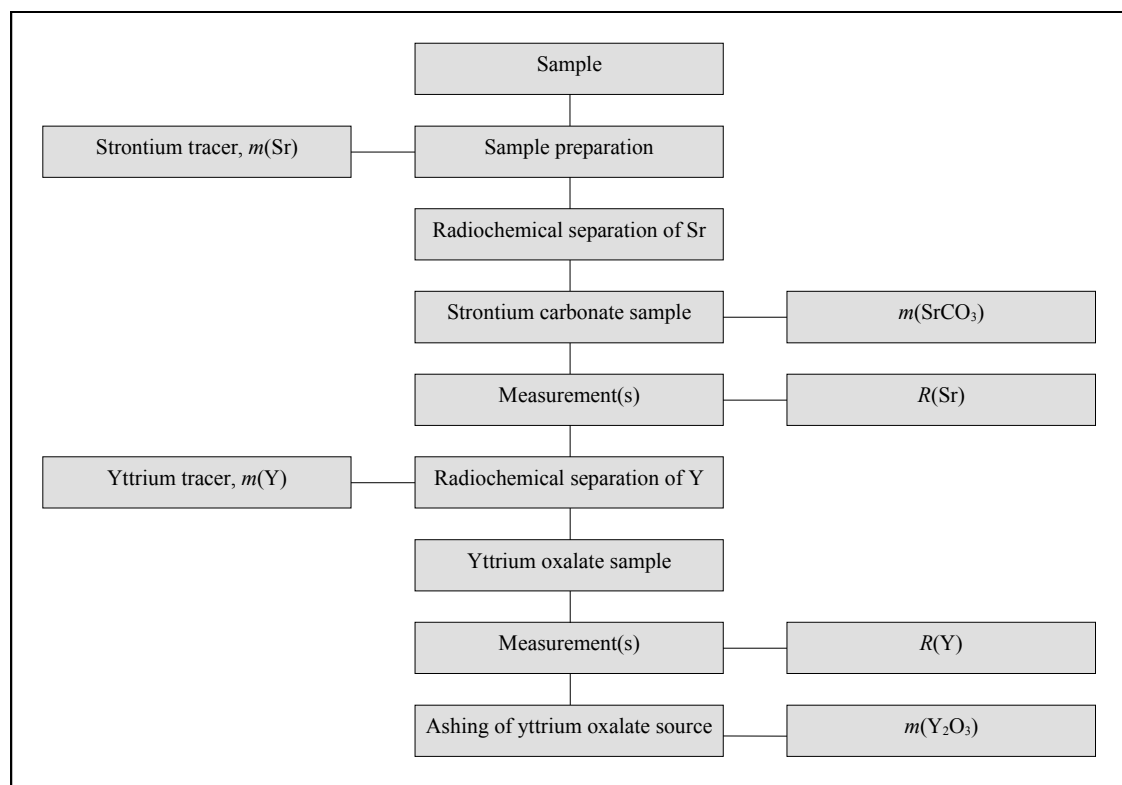


*Fig.1. Outline of the radiochemical procedure of strontium separation and source preparation.*

A series of measurements on the strontium carbonate source should be performed during a period of time long enough to check whether radionuclides other than Sr-89, Sr-90 and Y-90 are contained in the source, e.g. Ba-140 and Ra-226. If contamination can be quantified from the series of measurements, appropriate corrections should be applied. The results of the measurements are later used to determine the Sr-89 activity in the sample.

The strontium carbonate is then washed off the filter, inactive yttrium tracer is added to the solution, yttrium is separated at time  $t_4$  and collected on a filter paper in the form of yttrium oxalate. The yttrium oxalate source is measured in the proportional counter system. The decay of Y-90 in the source should be observed for at least five days. The residual count rate of the source should be determined after the Y-90 has decayed to less than 1% of the initial count rate, i.e. after 18 days, to check the radiochemical purity of the source. If long-lived radionuclides can be identified from the residual count rate, appropriate corrections should be applied to the measurement results. After completion of the measurements, the yttrium oxalate source is ashed in order to convert yttrium oxalate to yttrium oxide.

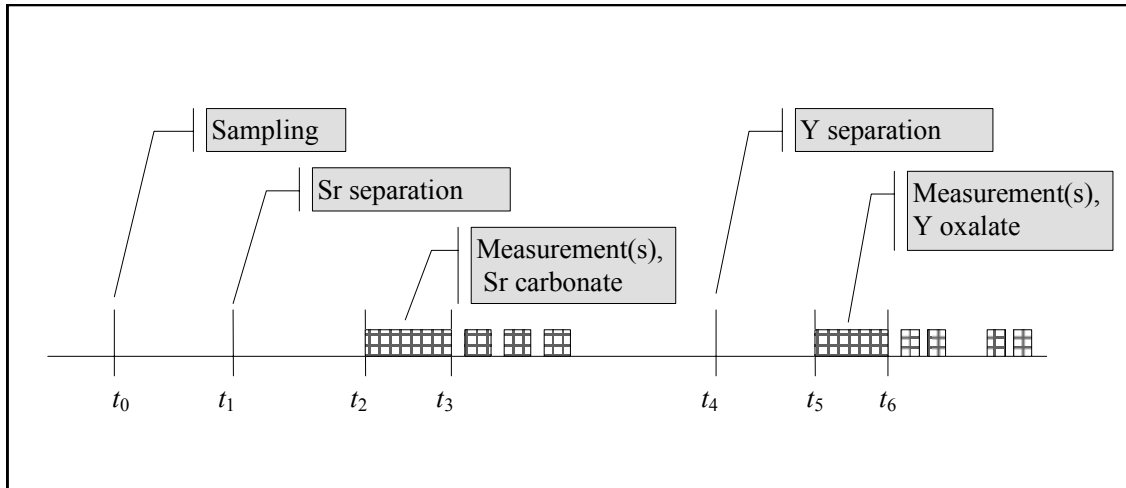


Fig. 2. Timing of sample preparation and measurements.

The mass of yttrium oxide is used to determine the chemical yield of the yttrium separation. In addition to the radiochemical procedures and the associated measurements on the strontium carbonate and the yttrium oxalate samples, the counting system has to be calibrated in terms of efficiencies for the radionuclides of interest, i.e. Sr-89, Sr-90, Y-90, in the respective matrices. To this end, standard solutions of Sr-89 and Sr-90 must be available in the laboratory. The sources are often covered with thin mylar foils to protect them from mechanical damage during the measurements. Aluminium absorbers may be used to reduce the contribution of Sr-90 to the count rates in the measurements of the strontium carbonate source. It should be noted that the same procedures must be applied in the calibration measurements.

Appropriate corrections have to be applied to the calculations of the final Sr-89 and Sr-90 activities, to take the blank effects into account, which are introduced by radioactive contaminants of the chemicals and by the laboratory equipment.

## 2.2. Chemical yields

The chemical yield  $\eta_{\text{Sr}}$  of the strontium separation and purification procedure is determined from the masses of strontium contained in the sample and in the strontium carbonate source. It should be noted that the sample may already contain a measurable amount of inactive strontium which interferes with the strontium tracer added and which has to be quantified prior to the chemical treatments.

$$\eta_{\text{Sr}} = \frac{m(\text{Sr}, \text{SrCO}_3 \text{ source})}{m(\text{Sr}, \text{Tracer}) + m(\text{Sr}, \text{Sample})} \quad (2.1)$$

$$m(\text{Sr}, \text{SrCO}_3 \text{ source}) = \frac{M(\text{Sr})}{M(\text{SrCO}_3)} \cdot m(\text{SrCO}_3 \text{ source}) \quad (2.2)$$

$$m(\text{Sr}, \text{Tracer}) = C_{\text{Sr}} \cdot m(\text{Sr tracer solution}) \quad (2.3)$$

where

$m(\text{Sr}, \text{SrCO}_3 \text{ source})$	mass of strontium in the strontium carbonate source,
$m(\text{Sr}, \text{Tracer})$	mass of strontium added to the sample as yield tracer,
$m(\text{Sr}, \text{Sample})$	mass of strontium already present in the sample,
$m(\text{SrCO}_3 \text{ source})$	mass of strontium carbonate in the strontium carbonate source,
$m(\text{Sr tracer solution})$	mass of the strontium tracer solution added to the sample,
$M(\text{Sr})$	relative atomic mass of strontium,
$M(\text{SrCO}_3)$	relative molecular mass of strontium carbonate,
$C_{\text{Sr}}$	concentration of strontium in the strontium tracer solution.

[4]

The chemical yield  $\eta_Y$  of the yttrium separation is determined from the mass of yttrium tracer added to the dissolved strontium carbonate source and the mass of yttrium oxide after ashing of the yttrium oxalate source. It is assumed that yttrium potentially present in the sample is removed quantitatively during strontium separation.

$$\eta_Y = \frac{m(\text{Y}, \text{Y}_2\text{O}_3 \text{ ash})}{m(\text{Y}, \text{Tracer})} \quad (2.4)$$

$$m(\text{Y}, \text{Y}_2\text{O}_3 \text{ ash}) = \frac{2 \cdot M(\text{Y})}{M(\text{Y}_2\text{O}_3)} \cdot m(\text{Y}_2\text{O}_3 \text{ ash}) \quad (2.5)$$

$$m(\text{Y}, \text{Tracer}) = C_Y \cdot m(\text{Y tracer solution}) \quad (2.6)$$

where

$m(\text{Y}, \text{Y}_2\text{O}_3 \text{ ash})$	mass of yttrium in the ashed yttrium oxalate source,
$m(\text{Y}, \text{Tracer})$	mass of yttrium added to the dissolved strontium carbonate source as yield tracer,
$m(\text{Y}_2\text{O}_3 \text{ ash})$	mass of the ashed yttrium oxalate source,
$m(\text{Y tracer solution})$	mass of the yttrium tracer solution added to the dissolved strontium carbonate source,
$M(\text{Y})$	relative atomic mass of yttrium,
$M(\text{Y}_2\text{O}_3)$	relative molecular mass of yttrium oxide,
$C_Y$	concentration of yttrium in the yttrium tracer solution.

As to (2.1) and (2.4), it is essential that the precipitates contain only strontium carbonate and yttrium oxalate, respectively. This assumption must be verified experimentally by independent analytical measurements.

### 2.3. Counting of the strontium carbonate source and Sr-89 activity

In the following it is assumed that no radionuclides other than Sr-89, Sr-90 and Y-90 are present in the strontium carbonate source. In this case

$$\boxed{a(\text{Sr} - 89, t_0) = \frac{A(\text{Sr} - 89, t_0)}{m(\text{Sample})}} \quad (2.7)$$

$$A(\text{Sr} - 89, t_0) = \frac{(R_{\text{Sr}}(t_2, t_3) - w \cdot R_Y(Y - 90, t_5, t_6)) \cdot f_7}{\eta_{\text{Sr}} \cdot \varepsilon_{\text{Sr}}(\text{Sr} - 89) \cdot f_1} - A(\text{Sr blank}) \quad (2.8)$$

$$w = \frac{\varepsilon_{Sr}(Sr-90) \cdot f_3 / f_8 + \varepsilon_{Sr}(Y-90) \cdot f_5 / f_9}{\eta_Y \cdot \varepsilon_Y(Y-90) \cdot f_4 \cdot f_6} \cdot f_{10} \quad (2.9)$$

where

$a(Sr-89, t_0)$	specific activity of Sr-89 in the sample at reference time $t_0$ ,
$A(Sr-89, t_0)$	activity of Sr-89 in the sample at reference time $t_0$ ,
$A(Sr \text{ blank})$	blank activity of measurements of the strontium carbonate source,
$m(\text{Sample})$	mass of sample,
$R_{Sr}(t_2, t_3)$	total count rate of the strontium carbonate source observed in the time interval $t_3 - t_2$ , corrected for dead-time loss and background,
$R_Y(Y-90, t_5, t_6)$	Y-90 count rate of the yttrium oxalate source observed in the time interval $t_6 - t_5$ , corrected for dead-time loss and background,
$t_0$	date of sampling, reference time for results,
$t_2$	beginning of measurement of the strontium carbonate source,
$t_3$	end of measurement of the strontium carbonate source,
$t_5$	beginning of measurement of the yttrium oxalate source,
$t_6$	end of measurement of the yttrium oxalate source,
$\eta_{Sr}$	chemical yield for strontium carbonate source preparation,
$\eta_Y$	chemical yield for yttrium oxalate source preparation,
$\varepsilon_{Sr}(Sr-89)$	detection efficiency for Sr-89 in the strontium carbonate source,
$\varepsilon_{Sr}(Sr-90)$	detection efficiency for Sr-90 in the strontium carbonate source,
$\varepsilon_{Sr}(Y-90)$	detection efficiency for Y-90 in the strontium carbonate source,
$\varepsilon_Y(Y-90)$	detection efficiency for Y-90 in the yttrium oxalate source.

#### 2.4. Counting of the yttrium oxalate source and Sr-90 activity

The specific activity of Sr-90 is determined from the measurements of the yttrium oxalate source by the following equations. Again, it is assumed that no interfering long-lived radionuclides are present in the yttrium oxalate source.

$$\boxed{a(Sr-90, t_0) = \frac{A(Sr-90, t_0)}{m(\text{Sample})}} \quad (2.10)$$

$$A(Sr-90, t_0) = \frac{R_Y(Y-90, t_5, t_6) \cdot f_{10}}{\eta_{Sr} \cdot \eta_Y \cdot \varepsilon_Y(Y-90) \cdot f_2 \cdot f_4 \cdot f_6} - A(Y\text{blank}) \quad (2.11)$$

where

$a(Sr-90, t_0)$	specific activity of Sr-90 in the sample at reference time $t_0$ ,
$A(Sr-90, t_0)$	activity of Sr-90 in the sample at reference time $t_0$ ,
$A(Y \text{ blank})$	blank activity of measurements of the yttrium oxalate source,
$m(\text{Sample})$	mass of sample,
$R_Y(Y-90, t_5, t_6)$	Y-90 count rate of the yttrium oxalate source observed in the time interval $t_6 - t_5$ , corrected for dead-time loss and background,
$t_0$	date of sampling, reference time for results,
$t_2$	beginning of measurement of the strontium carbonate source,
$t_3$	end of measurement of the strontium carbonate source,
$t_4$	time of yttrium separation,
$t_5$	beginning of measurement of the yttrium oxalate source,

$t_6$	end of measurement of the yttrium oxalate source,
$\eta_{Sr}$	chemical yield for strontium carbonate source preparation,
$\eta_Y$	chemical yield for yttrium oxalate source preparation,
$\varepsilon_Y(Y-90)$	detection efficiency for Y-90 in the yttrium oxalate source.

## 2.5. Build-up and decay correction factors

The count rates observed in the measurements have to be corrected for different timing effects which are due to the radioactive build-up and decay of the investigated nuclides during the time of the analysis. Although some of the correction factors are very close to unity in all practical cases, a complete list of formulae is given in this chapter.

$f_1$  Correction for decay of Sr-89 in the period from the reference time to beginning of measurement of the strontium carbonate source.

$$f_1 = \exp(-\lambda_{Sr-89} \cdot (t_2 - t_0)) \quad (2.12)$$

$f_2$  Correction for decay of Sr-90 in the period from the reference time to strontium separation.

$$f_2 = \exp(-\lambda_{Sr-90} \cdot (t_1 - t_0)) \quad (2.13)$$

$f_3$  Correction for decay of Sr-90 in the period from strontium separation to beginning of measurement of the strontium carbonate source.

$$f_3 = \exp(-\lambda_{Sr-90} \cdot (t_2 - t_1)) \quad (2.14)$$

$f_4$  Correction for decay of Y-90 in the period from yttrium separation to beginning of measurement of the yttrium oxalate source.

$$f_4 = \exp(-\lambda_{Y-90} \cdot (t_5 - t_4)) \quad (2.15)$$

$f_5$  Correction for build-up of Y-90 from Sr-90 in the period from strontium separation to beginning of measurement of the strontium carbonate source.

$$f_5 = 1 - \exp(-\lambda_{Y-90} \cdot (t_2 - t_1)) \quad (2.16)$$

$f_6$  Correction for build-up of Y-90 from Sr-90 in the period from strontium separation to yttrium separation.

$$f_6 = 1 - \exp(-\lambda_{Y-90} \cdot (t_4 - t_1)) \quad (2.17)$$

$f_7$  Correction for decay of Sr-89 during the measurement of the strontium carbonate source.

$$f_7 = \lambda_{Sr-89} \cdot (t_3 - t_2) / (1 - \exp(-\lambda_{Sr-89} \cdot (t_3 - t_2))) \quad (2.18)$$

$f_8$  Correction for decay of Sr-90 during the measurement of the strontium carbonate source.

$$f_8 = \lambda_{Sr-90} \cdot (t_3 - t_2) / (1 - \exp(-\lambda_{Sr-90} \cdot (t_3 - t_2))) = 1,0000... \quad (2.19)$$

$f_9$  Correction for build-up and decay of Y-90 during the measurement of the strontium carbonate source.

$$f_9 = \frac{\lambda_{Y-90} \cdot (t_3 - t_2) \cdot (1 - \exp(-\lambda_{Y-90} \cdot (t_2 - t_1)))}{\lambda_{Y-90} \cdot (t_3 - t_2) + \exp(-\lambda_{Y-90} \cdot (t_3 - t_1)) - \exp(-\lambda_{Y-90} \cdot (t_2 - t_1))} \quad (2.20)$$

$f_{10}$  Correction for decay of Y-90 during the measurement of the yttrium oxalate source.

$$f_{10} = \lambda_{Y-90} \cdot (t_6 - t_5) / (1 - \exp(-\lambda_{Y-90} \cdot (t_6 - t_5))) \quad (2.21)$$

### 3. EVALUATION OF UNCERTAINTY COMPONENTS

#### 3.1. Uncertainty in weighing

As regards the evaluation of uncertainty components in weighing procedures reference should be made to the EURACHEM document [3]. The uncertainties assigned to the calibration of the balance, to the buoyancy correction and to short-term fluctuations of the environmental conditions are the most prominent components of the uncertainty associated to mass. For the example dealt with in this paper it is assumed that the standard uncertainty in mass determination is  $u(m) = 2 \cdot 10^{-4}$  g, regardless of the balance load. It is furthermore assumed that correlation between the results of weighing can be neglected.

As an example, the uncertainty quantification for the determination of the mass of the strontium carbonate source is given in Tab. 1.

$$m(\text{SrCO}_3 \text{ source}) = m(\text{SrCO}_3 \text{ filter}) - m(\text{filter}) \quad (3.1)$$

$$u_c^2(m(\text{SrCO}_3 \text{ source})) = u^2(m(\text{SrCO}_3 \text{ filter})) + u^2(m(\text{filter})) \quad (3.2)$$

Table 1: Uncertainty quantification for the evaluation of the strontium carbonate source mass  $m(\text{SrCO}_3 \text{ source})$ .

Symbol	Value of variable	Standard uncertainty $u_i$	Sensitivity factor $c_i$	Contribution to standard uncertainty $u_c$
$m(\text{SrCO}_3 \text{ filter})$	0.5182 g	0.0002 g	1.000	0.0002 g
$m(\text{filter})$	0.1753 g	0.0002 g	-1.000	0.0002 g
<b><math>m(\text{SrCO}_3 \text{ source})</math></b>	<b>0.3429 g</b>			<b>0.0003 g</b>

#### 3.2. Uncertainty of chemical yield

The relative standard uncertainties assigned to the relative atomic and molecular masses are far below 0,1% and hence their contributions to the uncertainties assigned to the chemical yields can, therefore, be neglected. The uncertainty quantification for the evaluation of  $\eta_{\text{Sr}}$  is shown in Tab. 2, using the sensitivity factors  $c_i$  derived from (2.1). It is assumed that no covariances exist between the measurands. The amount of strontium in the sample has been determined prior to chemical treatment by an X ray fluorescence analysis.

The uncertainty associated to  $\eta_{\text{Sr}}$  is completely governed by the uncertainty of the amount of strontium contained in the sample. The situation becomes even more puzzling if the strontium content in the sample cannot be analysed in the laboratory due to lack of equipment. In this case an estimate of this figure may be introduced into the evaluation, which must be taken from the literature or other sources of experience. Furthermore, the application of an inactive strontium tracer requires that all strontium contained in the sample matrix and determined prior to the radiochemical procedure is quantitatively processed in the analysis.

$$\begin{aligned} c_1 &= \partial \eta_{\text{Sr}} / \partial m(\text{SrCO}_3 \text{ source}) \\ &= 0,5935 \cdot (C_{\text{Sr}} \cdot m(\text{Sr tracer solution}) + m(\text{Sr, Sample}))^{-1} \end{aligned} \quad (3.3)$$

$$c_2 = \frac{\partial \eta_{Sr}}{\partial m(\text{Sr, Sample})} = -0,5935 \cdot m(\text{SrCO}_3 \text{ source}) \cdot (C_{Sr} \cdot m(\text{Sr tracer solution}) + m(\text{Sr, Sample}))^{-2} \quad (3.4)$$

$$c_3 = \frac{\partial \eta_{Sr}}{\partial m(\text{Sr tracer solution})} = -0,5935 \cdot C_{Sr} \cdot m(\text{SrCO}_3 \text{ source}) \cdot (C_{Sr} \cdot m(\text{Sr tracer solution}) + m(\text{Sr, Sample}))^{-2} \quad (3.5)$$

$$c_4 = \frac{\partial \eta_{Sr}}{\partial C_{Sr}} = -0,5935 \cdot m(\text{Sr tracer solution}) \cdot m(\text{SrCO}_3 \text{ source}) \cdot (C_{Sr} \cdot m(\text{Sr tracer solution}) + m(\text{Sr, Sample}))^{-2} \quad (3.6)$$

$$u_c^2(\eta_{Sr}) = c_1^2 \cdot u^2(m(\text{SrCO}_3 \text{ source})) + c_2^2 \cdot u^2(m(\text{Sr, Sample})) + c_3^2 \cdot u^2(m(\text{Sr tracer solution})) + c_4^2 \cdot u^2(C_{Sr}) \quad (3.7)$$

Table 2: Uncertainty quantification for the evaluation of the chemical yield  $\eta_{Sr}$  of the strontium source preparation.

Symbol	Value of variable	Standard uncertainty $u_i$	Sensitivity factor $c_i$	Contribution to standard uncertainty $u_c$
$m(\text{SrCO}_3 \text{ source})$	0.3429 g	0.0003 g	$2.276 \text{ g}^{-1}$	0.00069
$m(\text{Sr, Sample})$	0.057 g	0.018 g	$-2.99 \text{ g}^{-1}$	0.054
$m(\text{Sr tracer solution})$	10.1201 g	0.0003 g	$-0.0603 \text{ g}^{-1}$	0.000018
$C_{Sr}$	0.02014	0.00017	-30.28	0.0052
<b><math>\eta_{Sr}</math></b>	<b>0.780</b>			<b>0.055</b>

For the chemical yield  $\eta_Y$  of the yttrium source preparation the sensitivity factors  $c_i$  are obtained from (2.4). The uncertainty quantification is shown in Tab. 3.

$$c_1 = \frac{\partial \eta_Y}{\partial m(\text{Y}_2\text{O}_3 \text{ ash})} = 0,7874 \cdot C_Y^{-1} \cdot m(\text{Y tracer solution})^{-1} \quad (3.8)$$

$$c_2 = \frac{\partial \eta_Y}{\partial m(\text{Y tracer solution})} = -0,7874 \cdot m(\text{Y}_2\text{O}_3 \text{ ash}) \cdot C_Y^{-1} \cdot m(\text{Y tracer solution})^{-2} \quad (3.9)$$

$$c_3 = \frac{\partial \eta_Y}{\partial C_Y} = -0,7874 \cdot m(\text{Y}_2\text{O}_3 \text{ ash}) \cdot C_Y^{-2} \cdot m(\text{Y tracer solution})^{-1} \quad (3.10)$$

$$u_c^2(\eta_Y) = c_1^2 \cdot u^2(m(\text{Y}_2\text{O}_3 \text{ ash})) + c_2^2 \cdot u^2(m(\text{Y tracer solution})) + c_3^2 \cdot u^2(C_Y) \quad (3.11)$$

Table 3: Uncertainty quantification for the evaluation of the chemical yield  $\eta_Y$  of the yttrium source preparation.

Symbol	Value of variable	Standard uncertainty $u_i$	Sensitivity factor $c_i$	Contribution to standard uncertainty $u_c$
$m(\text{Y}_2\text{O}_3 \text{ ash})$	0.0522 g	0.0004 g	$17.93 \text{ g}^{-1}$	0.0072
$m(\text{Y tracer solution})$	4.2307 g	0.0003 g	$-0.221 \text{ g}^{-1}$	0.000067
$C_Y$	0.01038	0.00011	-90.2	0.010
<b><math>\eta_Y</math></b>	<b>0.936</b>			<b>0.013</b>

### 3.3. Uncertainty of count rate

Count rates are corrected for dead-time loss and background in the counting system. For a dead-time of the non-extendable type of  $10 \mu\text{s}$  and count rates of up to  $100 \text{ s}^{-1}$  the dead-time correction is less than 0,1% and the contribution to the uncertainty assigned to the count rate is at least one order of magnitude lower. The uncertainty introduced by the dead-time correction is, therefore, neglected here.

The timer used to set the counting intervals  $\Delta t$  is calibrated against a pulse generator of known frequency  $\nu$ . A maximum relative frequency shift of  $2 \cdot 10^{-4}$  is stated for the pulse generator in the calibration certificate. A symmetric, rectangular a priori probability distribution of half-width  $1 \cdot 10^{-4}$  is assumed, for which a relative standard uncertainty of  $u(\nu)/\nu = u(\Delta t)/\Delta t = 1 \cdot 10^{-4}/\sqrt{3} = 5.8 \cdot 10^{-5}$  is evaluated according to [4].

The uncertainty quantifications for the counting of the strontium carbonate source and the yttrium oxalate source are shown in Tab. 4 and Tab. 5, respectively. In both cases it is assumed that either no radionuclides other than Sr-89, Sr-90 and Y-90 could be detected in the sources, or that the respective count rate has been corrected for contributions from interfering contaminants.

$$R = R_G - R_B = \frac{N_G}{\Delta t} f_{\tau G} - \frac{N_B}{\Delta t_B} f_{\tau B} \quad (3.12)$$

where

$R$	count rate,	
$N$	number of counts observed in time interval $\Delta t$ ,	
$\Delta t$	time interval of counting,	
$f_{\tau}$	correction factor for dead-time loss.	
	$f_{\tau} = (1 - \tau N/\Delta t)^{-1/2}$	(3.13)

The indices G and B in (3.12) refer to gross counts and background counts, respectively.

$$c_1 = \partial R / \partial N_G = f_{\tau G} / \Delta t \quad (3.14)$$

$$c_2 = \partial R / \partial N_B = -f_{\tau B} / \Delta t_B \quad (3.15)$$

$$c_3 = \partial R / \partial f_{\tau G} = N_G / \Delta t \quad (3.16)$$

$$c_4 = \partial R / \partial f_{\tau B} = -N_B / \Delta t_B \quad (3.17)$$

$$c_5 = \partial R / \partial \Delta t = -N_G \cdot f_{\tau G} / \Delta t^2 \quad (3.18)$$

$$c_6 = \partial R / \partial \Delta t_B = N_B \cdot f_{\tau B} / \Delta t_B^2 \quad (3.19)$$

$$u_c^2(R) = c_1^2 \cdot u^2(N_G) + c_2^2 \cdot u^2(N_B) + c_3^2 \cdot u^2(f_{\tau G}) + c_4^2 \cdot u^2(f_{\tau B}) + c_5^2 \cdot u^2(\Delta t) + c_6^2 \cdot u^2(\Delta t_B) \quad (3.20)$$

Table 4: Uncertainty quantification for the evaluation of the count rate  $R_{Sr}(t_2, t_3)$  of the strontium carbonate source.

Symbol	Value of variable	Standard uncertainty $u_i$	Sensitivity factor $c_i$	Contribution to standard uncertainty $u_c$
$N_G = N_{Sr}(t_2, t_3)$	13652	117	$2.00 \cdot 10^{-5} \text{ s}^{-1}$	$0.0024 \text{ s}^{-1}$
$N_B$	1360	37	$-1.25 \cdot 10^{-5} \text{ s}^{-1}$	$0.0005 \text{ s}^{-1}$
$f_{\tau G}$	1.0000	$\approx 0$	$0.273 \text{ s}^{-1}$	$\approx 0 \text{ s}^{-1}$
$f_{\tau B}$	1.0000	$\approx 0$	$-0.017 \text{ s}^{-1}$	$\approx 0 \text{ s}^{-1}$
$\Delta t = t_3 - t_2$	50000 s	3 s	$-5.5 \cdot 10^{-6} \text{ s}^{-2}$	$0.00002 \text{ s}^{-1}$
$\Delta t_B$	80000 s	5 s	$2.1 \cdot 10^{-7} \text{ s}^{-2}$	$\approx 0 \text{ s}^{-1}$
<b><math>R_{Sr}(t_2, t_3)</math></b>	<b><math>0.2560 \text{ s}^{-1}</math></b>			<b><math>0.0024 \text{ s}^{-1}</math></b>

Table 5: Uncertainty quantification for the evaluation of the count rate  $R_Y(Y-90, t_5, t_6)$  of the yttrium oxalate source.

Symbol	Value of variable	Standard uncertainty $u_i$	Sensitivity factor $c_i$	Contribution to standard uncertainty $u_c$
$N_G = N_Y(Y-90, t_5, t_6)$	8304	92	$1.67 \cdot 10^{-5} \text{ s}^{-1}$	$0.0016 \text{ s}^{-1}$
$N_B$	1392	38	$-1.25 \cdot 10^{-5} \text{ s}^{-1}$	$0.0005 \text{ s}^{-1}$
$f_{\tau G}$	1.0000	$\approx 0$	$0.138 \text{ s}^{-1}$	$\approx 0 \text{ s}^{-1}$
$f_{\tau B}$	1.0000	$\approx 0$	$-0.017 \text{ s}^{-1}$	$\approx 0 \text{ s}^{-1}$
$\Delta t = t_6 - t_5$	60000 s	4 s	$-2.3 \cdot 10^{-6} \text{ s}^{-2}$	$0.00001 \text{ s}^{-1}$
$\Delta t_B$	80000 s	5 s	$2.2 \cdot 10^{-7} \text{ s}^{-2}$	$\approx 0 \text{ s}^{-1}$
<b><math>R_Y(Y-90, t_5, t_6)</math></b>	<b><math>0.1210 \text{ s}^{-1}</math></b>			<b><math>0.0016 \text{ s}^{-1}</math></b>

### 3.5. Uncertainty of detection efficiency

The detection efficiencies of the proportional counter system are determined by measuring reference sources of the respective radionuclide under experimental conditions identical to those of sample analysis. The reference sources are prepared from radioactive standard solutions of Sr-89 and Sr-90 issued by a national metrology institute. The preparation of Sr-89 and Sr-90 reference sources comprises the mixing of weighed amounts of standard solution and strontium carrier, precipitation as strontium carbonate, evaluation of the chemical yield and of the thickness of the source matrix. An additional yttrium carrier and radiochemical separation of yttrium from Sr-90 sources are required when Y-90 reference sources are prepared. In this case, Y-90 and Sr-90 must be in radioactive equilibrium. A batch of reference sources is usually prepared, with the thickness of the source matrix differing to allow for interpolation of detection efficiencies applied in sample analysis.

The evaluation of the uncertainty components of the detection efficiency is virtually the same as described in chapters 3.1 for weighing, 3.2 for chemical yields and 3.3 for count rates. In addition, the uncertainty in the specific activity of the respective standard solution must be taken into account.

In general, the detection efficiency is calculated according to

$$\varepsilon = \frac{R}{a \cdot m \cdot \eta} \quad (3.21)$$

where

- $\varepsilon$  detection efficiency of the proportional counter,
- $R$  count rate of the reference source in the proportional counter, corrected for dead-time loss and background,
- $a$  specific activity of the standard solution,
- $m$  mass of standard solution used to prepare the reference source,
- $\eta$  chemical yield.

The corresponding sensitivity factors are

$$c_1 = \partial\varepsilon/\partial R = (a \cdot m \cdot \eta)^{-1} \quad (3.22)$$

$$c_2 = \partial\varepsilon/\partial a = -R \cdot (m \cdot \eta)^{-1} \cdot a^{-2} \quad (3.23)$$

$$c_3 = \partial\varepsilon/\partial m = -R \cdot (a \cdot \eta)^{-1} \cdot m^{-2} \quad (3.24)$$

$$c_4 = \partial\varepsilon/\partial \eta = -R \cdot (a \cdot m)^{-1} \cdot \eta^{-2} \quad (3.25)$$

and the combined uncertainty is

$$u_c^2(\varepsilon) = c_1^2 \cdot u^2(R) + c_2^2 \cdot u^2(a) + c_3^2 \cdot u^2(m) + c_4^2 \cdot u^2(\eta). \quad (3.26)$$

As an example, the uncertainty quantification for the evaluation of the detection efficiency  $\varepsilon_{\text{Sr}}(\text{Sr-89})$  for strontium carbonate sources is shown in Tab. 6.

Table 6: Uncertainty quantification for the evaluation of the detection efficiency  $\varepsilon_{\text{Sr}}(\text{Sr-89})$  for strontium carbonate sources.

Symbol	Value of variable	Standard uncertainty $u_i$	Sensitivity factor $c_i$	Contribution to standard uncertainty $u_c$
$R_{\text{Sr}}(\text{Sr-89})$	239.4 s <sup>-1</sup>	0.5 s <sup>-1</sup>	0.00146 s	0.00073
$A(\text{Sr-89})$	1160 Bq/g	17 Bq/g	-0.0003 g/Bq	0.0051
$M(\text{Sr-89})$	0.6014 g	0.0003 g	-0.579 g <sup>-1</sup>	0.00018
$\eta_{\text{Sr}}$	0.985	0.024	-0.354	0.0085
<b><math>\varepsilon_{\text{Sr}}(\text{Sr-89})</math></b>	<b>0.348</b>			<b>0.010</b>

The results obtained for the detection efficiencies of this example are summarised as follows:

$$\varepsilon_{\text{Sr}}(\text{Sr-89}) = 0.348 \pm 0.010$$

$$\varepsilon_{\text{Sr}}(\text{Sr-90}) = 0.214 \pm 0.011$$

$$\varepsilon_{\text{Sr}}(\text{Y-90}) = 0.409 \pm 0.015$$

$$\varepsilon_{\text{Y}}(\text{Y-90}) = 0.437 \pm 0.016.$$

The detection efficiencies  $\varepsilon_{\text{Sr}}(\text{Sr-90})$ ,  $\varepsilon_{\text{Sr}}(\text{Y-90})$  and  $\varepsilon_{\text{Y}}(\text{Y-90})$  are correlated since the same values of the specific activity of the Sr-90 standard solution and the chemical yield of the strontium separation are used in the calculations.

### 3.6. Uncertainty of correction factors

The standard uncertainties assigned to the correction factors  $f_1$  to  $f_{10}$  are virtually determined by the standard uncertainties reported for the half-lives of the radionuclides. The uncertainties obtained for the time intervals can be neglected. In the following most of the uncertainties are estimated numerically from the variation in the value of the respective function. For the sake of simplicity, formulae for relative standard uncertainties are presented here.

The time interval between sampling and radiochemical treatment of the sample may be long compared with the half-life of Sr-89 so that the correction factor  $f_1$  for the decay of Sr-89 may be far from unity. In this case, the standard uncertainty associated with  $f_1$  has to be considered. The relative standard uncertainties evaluated for correction factors  $f_2$  to  $f_9$  are below 0.1 percent for all relevant time intervals. The uncertainty quantification for the evaluation of the weighting factor  $w$  defined in (2.9) for the evaluation of the Sr-89 activity is shown in Tab. 7. The calculations are performed numerically and are not presented here.

$$\frac{u(f_1)}{f_1} = \lambda_{\text{Sr-89}} \cdot (t_2 - t_0) \cdot \frac{u(\lambda_{\text{Sr-89}})}{\lambda_{\text{Sr-89}}} \quad (3.27)$$

$$\frac{u(f_2)}{f_2} = \lambda_{\text{Sr-90}} \cdot (t_1 - t_0) \cdot \frac{u(\lambda_{\text{Sr-90}})}{\lambda_{\text{Sr-90}}} \quad (3.28)$$

$$\frac{u(f_3)}{f_3} = \lambda_{\text{Sr-90}} \cdot (t_2 - t_1) \cdot \frac{u(\lambda_{\text{Sr-90}})}{\lambda_{\text{Sr-90}}} \quad (3.29)$$

$$\frac{u(f_4)}{f_4} = \lambda_{\text{Y-90}} \cdot (t_5 - t_4) \cdot \frac{u(\lambda_{\text{Y-90}})}{\lambda_{\text{Y-90}}} \quad (3.30)$$

$$\frac{u(f_5)}{f_5} = \lambda_{\text{Y-90}} \cdot (t_2 - t_1) \cdot \frac{\exp(-\lambda_{\text{Y-90}} \cdot (t_2 - t_1))}{1 - \exp(-\lambda_{\text{Y-90}} \cdot (t_2 - t_1))} \cdot \frac{u(\lambda_{\text{Y-90}})}{\lambda_{\text{Y-90}}} \quad (3.31)$$

$$\frac{u(f_6)}{f_6} = \lambda_{\text{Y-90}} \cdot (t_4 - t_1) \cdot \frac{\exp(-\lambda_{\text{Y-90}} \cdot (t_4 - t_1))}{1 - \exp(-\lambda_{\text{Y-90}} \cdot (t_4 - t_1))} \cdot \frac{u(\lambda_{\text{Y-90}})}{\lambda_{\text{Y-90}}} \quad (3.32)$$

$$\frac{u(f_7)}{f_7} = \left\{ 1 - \lambda_{\text{Sr-89}} \cdot (t_3 - t_2) \cdot \frac{\exp(-\lambda_{\text{Sr-89}} \cdot (t_3 - t_2))}{1 - \exp(-\lambda_{\text{Sr-89}} \cdot (t_3 - t_2))} \right\} \cdot \frac{u(\lambda_{\text{Sr-89}})}{\lambda_{\text{Sr-89}}} \quad (3.33)$$

$$\frac{u(f_8)}{f_8} = \left\{ 1 - \lambda_{\text{Sr-90}} \cdot (t_3 - t_2) \cdot \frac{\exp(-\lambda_{\text{Sr-90}} \cdot (t_3 - t_2))}{1 - \exp(-\lambda_{\text{Sr-90}} \cdot (t_3 - t_2))} \right\} \cdot \frac{u(\lambda_{\text{Sr-90}})}{\lambda_{\text{Sr-90}}} \quad (3.34)$$

$$u(f_9) = \frac{\partial f_9}{\partial \lambda_{\text{Y-90}}} \cdot u(\lambda_{\text{Y-90}}), \text{ calculated numerically} \quad (3.35)$$

$$\frac{u(f_{10})}{f_{10}} = \left\{ 1 - \lambda_{\text{Y-90}} \cdot (t_6 - t_5) \cdot \frac{\exp(-\lambda_{\text{Y-90}} \cdot (t_6 - t_5))}{1 - \exp(-\lambda_{\text{Y-90}} \cdot (t_6 - t_5))} \right\} \cdot \frac{u(\lambda_{\text{Y-90}})}{\lambda_{\text{Y-90}}} \quad (3.36)$$

Table 7: Uncertainty quantification for the evaluation of the weighting factor  $w$ .

Symbol	Value of variable	Standard uncertainty $u_i$	Sensitivity factor $c_i$	Contribution to standard uncertainty $u_c$
$\varepsilon_{Sr}(Sr-90)$	0.214	0.011	2.85	0.032
$\varepsilon_{Sr}(Y-90)$	0.409	0.015	2.77	0.042
$\varepsilon_Y(Y-90)$	0.437	0.016	-3.99	0.064
$\eta_Y$	0.936	0.013	-1.86	0.025
$f_3$	0.9991	$\approx 0$	0.610	$\approx 0$
$f_4$	0.9384	$\approx 0$	-1.86	$\approx 0$
$f_5$	0.9716	$\approx 0$	1.17	$\approx 0$
$f_6$	0.9996	$\approx 0$	-1.74	$\approx 0$
$f_8$	1.0000	$\approx 0$	-0.609	$\approx 0$
$f_9$	0.9979	$\approx 0$	-1.14	$\approx 0$
$f_{10}$	1.0928	$\approx 0$	1.60	$\approx 0$
<b><math>w</math></b>	<b>1.743</b>			<b>0.086</b>

### 3.7. Uncertainty of blank effect

The procedure of evaluating the uncertainty associated with the laboratories' blank effect is virtually the same as described in the previous chapters. The results and the assigned standard uncertainties for the example are as follows:

$$A(\text{Sr blank}) = (0.002 \pm 0.005) \text{ Bq}$$

$$A(\text{Y blank}) = (0.003 \pm 0.007) \text{ Bq}.$$

## 4. COMBINED STANDARD UNCERTAINTY

The combined standard uncertainties associated with the specific activities are evaluated according to (2.7) and (2.10). It is assumed that the correlation between detection efficiency values is weak so that it can be ignored here. A summary of the uncertainty components for the evaluation of the specific activities of Sr-89 and Sr-90 in the sample is shown in Tab. 8. The input quantities to the uncertainty quantifications discussed in the previous chapters are not listed again in this table.

### 4.1. Strontium-89 analysis

$$c_1 = \frac{\partial a(\text{Sr-89}, t_0)}{\partial A(\text{Sr blank})} = -\frac{1}{m(\text{Sample})} \quad (4.1)$$

$$c_2 = \frac{\partial a(\text{Sr-89}, t_0)}{\partial R_{Sr}(t_2, t_3)} = \frac{f_7}{\eta_{Sr} \cdot \varepsilon_{Sr}(\text{Sr-89}) \cdot f_1 \cdot m(\text{Sample})} \quad (4.2)$$

$$c_3 = \frac{\partial a(\text{Sr}-89, t_0)}{\partial R_Y(Y-90, t_5, t_6)} = -\frac{w \cdot f_7}{\eta_{\text{Sr}} \cdot \varepsilon_{\text{Sr}}(\text{Sr}-89) \cdot f_1 \cdot m(\text{Sample})} \quad (4.3)$$

$$c_4 = \frac{\partial a(\text{Sr}-89, t_0)}{\partial w} = -\frac{R_Y(Y-90, t_5, t_6) \cdot f_7}{\eta_{\text{Sr}} \cdot \varepsilon_{\text{Sr}}(\text{Sr}-89) \cdot f_1 \cdot m(\text{Sample})} \quad (4.4)$$

$$c_5 = \frac{\partial a(\text{Sr}-89, t_0)}{\partial f_7} = \frac{R_{\text{Sr}}(t_2, t_3) - w \cdot R_Y(Y-90, t_5, t_6)}{\eta_{\text{Sr}} \cdot \varepsilon_{\text{Sr}}(\text{Sr}-89) \cdot f_1 \cdot m(\text{Sample})} \quad (4.5)$$

$$c_6 = \frac{\partial a(\text{Sr}-89, t_0)}{\partial \eta_{\text{Sr}}} = -\frac{R_{\text{Sr}}(t_2, t_3) - w \cdot R_Y(Y-90, t_5, t_6)}{\eta_{\text{Sr}}^2 \cdot \varepsilon_{\text{Sr}}(\text{Sr}-89) \cdot f_1 \cdot m(\text{Sample})} \cdot f_7 \quad (4.6)$$

$$c_7 = \frac{\partial a(\text{Sr}-89, t_0)}{\partial \varepsilon_{\text{Sr}}(\text{Sr}-89)} = -\frac{R_{\text{Sr}}(t_2, t_3) - w \cdot R_Y(Y-90, t_5, t_6)}{\eta_{\text{Sr}} \cdot \varepsilon_{\text{Sr}}^2(\text{Sr}-89) \cdot f_1 \cdot m(\text{Sample})} \cdot f_7 \quad (4.7)$$

$$c_8 = \frac{\partial a(\text{Sr}-89, t_0)}{\partial f_1} = -\frac{R_{\text{Sr}}(t_2, t_3) - w \cdot R_Y(Y-90, t_5, t_6)}{\eta_{\text{Sr}} \cdot \varepsilon_{\text{Sr}}(\text{Sr}-89) \cdot f_1^2 \cdot m(\text{Sample})} \cdot f_7 \quad (4.8)$$

$$c_9 = \frac{\partial a(\text{Sr}-89, t_0)}{\partial m(\text{Sample})} = -\frac{A(\text{Sr}-89, t_0)}{m^2(\text{Sample})} \quad (4.9)$$

$$u_c^2(a(\text{Sr}-89, t_0)) = c_1^2 \cdot u^2(A(\text{Sr blank})) + c_2^2 \cdot u^2(R_{\text{Sr}}(t_2, t_3)) + c_3^2 \cdot u^2(R_Y(Y-90, t_5, t_6)) + c_4^2 \cdot u^2(w) + c_5^2 \cdot u^2(f_7) + c_6^2 \cdot u^2(\eta_{\text{Sr}}) + c_7^2 \cdot u^2(\varepsilon_{\text{Sr}}(\text{Sr}-89)) + c_8^2 \cdot u^2(f_1) + c_9^2 \cdot u^2(m(\text{Sample})) \quad (4.10)$$

## 4.2. Strontium-90 analysis

$$c_1 = \frac{\partial a(\text{Sr}-90, t_0)}{\partial A(\text{Y blank})} = -\frac{1}{m(\text{Sample})} \quad (4.11)$$

$$c_2 = \frac{\partial a(\text{Sr}-90, t_0)}{\partial R_Y(Y-90, t_5, t_6)} = \frac{f_{10}}{\eta_{\text{Sr}} \cdot \eta_Y \cdot \varepsilon_Y(Y-90) \cdot f_2 \cdot f_4 \cdot f_6 \cdot m(\text{Sample})} \quad (4.12)$$

$$c_3 = \frac{\partial a(\text{Sr}-90, t_0)}{\partial f_{10}} = \frac{R_Y(Y-90, t_5, t_6)}{\eta_{\text{Sr}} \cdot \eta_Y \cdot \varepsilon_Y(Y-90) \cdot f_2 \cdot f_4 \cdot f_6 \cdot m(\text{Sample})} \quad (4.13)$$

$$c_4 = \frac{\partial a(\text{Sr}-90, t_0)}{\partial \eta_{\text{Sr}}} = -\frac{R_Y(Y-90, t_5, t_6) \cdot f_{10}}{\eta_{\text{Sr}}^2 \cdot \eta_Y \cdot \varepsilon_Y(Y-90) \cdot f_2 \cdot f_4 \cdot f_6 \cdot m(\text{Sample})} \quad (4.14)$$

$$c_5 = \frac{\partial a(\text{Sr}-90, t_0)}{\partial \eta_Y} = -\frac{R_Y(Y-90, t_5, t_6) \cdot f_{10}}{\eta_{\text{Sr}} \cdot \eta_Y^2 \cdot \varepsilon_Y(Y-90) \cdot f_2 \cdot f_4 \cdot f_6 \cdot m(\text{Sample})} \quad (4.15)$$

$$c_6 = \frac{\partial a(\text{Sr-90}, t_0)}{\partial \varepsilon_Y(\text{Y-90})} = - \frac{R_Y(\text{Y-90}, t_5, t_6) \cdot f_{10}}{\eta_{\text{Sr}} \cdot \eta_Y \cdot \varepsilon_Y^2(\text{Y-90}) \cdot f_2 \cdot f_4 \cdot f_6 \cdot m(\text{Sample})} \quad (4.16)$$

$$c_7 = \frac{\partial a(\text{Sr-90}, t_0)}{\partial f_2} = - \frac{R_Y(\text{Y-90}, t_5, t_6) \cdot f_{10}}{\eta_{\text{Sr}} \cdot \eta_Y \cdot \varepsilon_Y(\text{Y-90}) \cdot f_2^2 \cdot f_4 \cdot f_6 \cdot m(\text{Sample})} \quad (4.17)$$

$$c_8 = \frac{\partial a(\text{Sr-90}, t_0)}{\partial f_4} = - \frac{R_Y(\text{Y-90}, t_5, t_6) \cdot f_{10}}{\eta_{\text{Sr}} \cdot \eta_Y \cdot \varepsilon_Y(\text{Y-90}) \cdot f_2 \cdot f_4^2 \cdot f_6 \cdot m(\text{Sample})} \quad (4.18)$$

$$c_9 = \frac{\partial a(\text{Sr-90}, t_0)}{\partial f_6} = - \frac{R_Y(\text{Y-90}, t_5, t_6) \cdot f_{10}}{\eta_{\text{Sr}} \cdot \eta_Y \cdot \varepsilon_Y(\text{Y-90}) \cdot f_2 \cdot f_4 \cdot f_6^2 \cdot m(\text{Sample})} \quad (4.19)$$

$$c_{10} = \frac{\partial a(\text{Sr-90}, t_0)}{\partial m(\text{Sample})} = - \frac{A(\text{Sr-90}, t_0)}{m^2(\text{Sample})} \quad (4.20)$$

$$u_c^2(a(\text{Sr-90}, t_0)) = c_1^2 \cdot u^2(A(\text{Y blank})) + c_2^2 \cdot u^2(R_Y(\text{Y-90}, t_5, t_6)) + c_3^2 \cdot u^2(f_{10}) + c_4^2 \cdot u^2(\eta_{\text{Sr}}) + c_5^2 \cdot u^2(\eta_Y) + c_6^2 \cdot u^2(\varepsilon_Y(\text{Y-90})) + c_7^2 \cdot u^2(f_2) + c_8^2 \cdot u^2(f_4) + c_9^2 \cdot u^2(f_6) + c_{10}^2 \cdot u^2(m(\text{Sample})) \quad (4.21)$$

## 5. REPORTING OF RESULTS

The results for the specific activities of Sr-89 and Sr-90 are calculated according to the formulae given in chapters 2.3 and 2.4. The associated uncertainties result from the formulae given in chapter 4.

$$a(\text{Sr-89}, t_0) = (16 \pm 9) \text{ Bq/kg} \quad \text{at reference time } t_0 \quad (5.1)$$

$$a(\text{Sr-90}, t_0) = (4.8 \pm 0.8) \text{ Bq/kg} \quad \text{at reference time } t_0 \quad (5.2)$$

The reported uncertainty of measurement is stated as the expanded uncertainty  $U = k \cdot u_c$ , which is the combined standard uncertainty  $u_c$  multiplied by the coverage factor  $k = 2$ . For a normal distribution it corresponds to a coverage probability of approximately 95% [5].

Table 8: Summary of the uncertainty components for the evaluation of the specific activities of Sr-89 and Sr-90.

Symbol/Reference	Value of variable	Uncertainty	Conversion factor to standard uncertainty	Standard uncertainty $u_i$	Sr-89 assay		Sr-90 assay	
					Sensitivity factor $c_i$	Percent contribution to $u_c^2(a(\text{Sr-89}))$	Sensitivity factor $c_i$	Percent contribution to $u_c^2(a(\text{Sr-90}))$
$R_{\text{Sr}}(t_2, t_3)$ (2.8)	$0.2560 \text{ s}^{-1}$	$0.0024 \text{ s}^{-1}$	1	$0.0024 \text{ s}^{-1}$	$0.321 \text{ g}^{-1}$	4.3		
$R_{\text{Y}}(\text{Y-90}, t_5, t_6)$ (2.11)	$0.1210 \text{ s}^{-1}$	$0.0016 \text{ s}^{-1}$	1	$0.0016 \text{ s}^{-1}$	$-0.629 \text{ g}^{-1}$	5.8	$0.0400 \text{ g}^{-1}$	2.5
$\eta_{\text{Sr}}$ (2.1)	0.780	0.055	1	0.055	$-0.0209 \text{ Bq/g}$	7.6	$-0.00621 \text{ Bq/g}$	71.7
$\eta_{\text{Y}}$ (2.4)	0.936	0.013	1	0.013			$-0.00517 \text{ Bq/g}$	2.8
$\varepsilon_{\text{Sr}}(\text{Sr-89})$ (3.21)	0.348	0.010	1	0.010	$-0.0467 \text{ Bq/g}$	1.3		
$\varepsilon_{\text{Y}}(\text{Y-90})$ (3.21)	0.437	0.016	1	0.016			$-0.0111 \text{ Bq/g}$	19.4
$w$ (2.9)	1.743	0.086	1	0.086	$-0.0436 \text{ Bq/g}$	81.0		
$A(\text{Sr blank})$ (2.8)	0.002 Bq	0.005 Bq	1	0.005 Bq	$-0.0109 \text{ g}^{-1}$	$\approx 0$		
$A(\text{Y blank})$ (2.11)	0.003 Bq	0.007 Bq	1	0.007 Bq			$-0.0109 \text{ g}^{-1}$	3.6
$f_1$ (2.12)	0.1113	0.0004	1	0.0004	$-0.146 \text{ Bq/g}$	$\approx 0$		
$f_2$ (2.13)	0.99040	0.00010	1	0.00010			$-0.00489 \text{ Bq/g}$	$\approx 0$
$f_4$ (2.15)	0.93837	0.00009	1	0.00009			$-0.00516 \text{ Bq/g}$	$\approx 0$
$f_6$ (2.17)	0.999557	0.000006	1	0.000006			$-0.00485 \text{ Bq/g}$	$\approx 0$
$f_7$ (2.18)	1.00397	$\approx 0$	1	$\approx 0$	$0.0162 \text{ Bq/g}$	$\approx 0$		
$f_{10}$ (2.20)	1.09281	0.00015	1	0.00015			$0.00443 \text{ Bq/g}$	$\approx 0$
$m(\text{Sample})$ (2.7)	92.1240 g	0.0003 g	1	0.0003 g	$-0.00018 \text{ Bq/g}^2$	$\approx 0$	$-0.00005 \text{ Bq/g}^2$	$\approx 0$

## LIST OF SYMBOLS

$a(\text{Sr-89}, t_0)$	Specific activity of Sr-89 in the sample at reference time $t_0$ .
$a(\text{Sr-90}, t_0)$	Specific activity of Sr-90 in the sample at reference time $t_0$ .
$A(\text{Sr-89}, t_0)$	Activity of Sr-89 in the sample at reference time $t_0$ .
$A(\text{Sr-90}, t_0)$	Activity of Sr-90 in the sample at reference time $t_0$ .
$A(\text{Sr blank})$	Blank activity of measurements of the strontium carbonate source.
$A(\text{Y blank})$	Blank activity of measurements of the yttrium oxalate source.
$C_{\text{Sr}}$	Concentration of strontium in the strontium tracer solution.
$C_{\text{Y}}$	Concentration of yttrium in the yttrium tracer solution.
$f_1$	Correction for decay of Sr-89 in the period from the reference time to beginning of measurement of the strontium carbonate source.
$f_2$	Correction for decay of Sr-90 in the period from the reference time to strontium separation.
$f_3$	Correction for decay of Sr-90 in the period from strontium separation to beginning of measurement of the strontium carbonate source.
$f_4$	Correction for decay of Y-90 in the period from yttrium separation to beginning of measurement of the yttrium oxalate source.
$f_5$	Correction for build-up of Y-90 from Sr-90 in the period from strontium separation to beginning of measurement of the strontium carbonate source.
$f_6$	Correction for build-up of Y-90 from Sr-90 in the period from strontium separation to yttrium separation.
$f_7$	Correction for decay of Sr-89 during the measurement of the strontium carbonate source.
$f_8$	Correction for decay of Sr-90 during the measurement of the strontium carbonate source.
$f_9$	Correction for build-up and decay of Y-90 during the measurement of the strontium carbonate source.
$f_{10}$	Correction for decay of Y-90 during the measurement of the yttrium oxalate source.
$m(\text{Sample})$	Mass of sample.
$m(\text{Sr, Sample})$	Mass of strontium already present in the sample.
$m(\text{Sr tracer solution})$	Mass of the strontium tracer solution added to the sample.
$m(\text{Y tracer solution})$	Mass of the yttrium tracer solution added to the strontium carbonate source.
$m(\text{Sr, Tracer})$	Mass of strontium in the strontium tracer solution added.
$m(\text{Y, Tracer})$	Mass of yttrium in the yttrium tracer solution added.
$m(\text{SrCO}_3 \text{ source})$	Mass of strontium carbonate in the strontium carbonate source.
$m(\text{Sr, SrCO}_3 \text{ source})$	Mass of strontium in the strontium carbonate source.
$m(\text{Y}_2\text{O}_3 \text{ ash})$	Mass of the ashed yttrium oxalate source.
$m(\text{Y, Y}_2\text{O}_3 \text{ ash})$	Mass of yttrium in the ashed yttrium oxalate source.
$M(\text{Sr})$	Relative atomic mass of strontium.
$M(\text{Y})$	Relative atomic mass of yttrium.
$M(\text{SrCO}_3)$	Relative molecular mass of strontium carbonate.
$M(\text{Y}_2\text{O}_3)$	Relative molecular mass of yttrium oxide.
$R_{\text{Sr}}(t_2, t_3)$	Total count rate of the strontium carbonate source observed in the time interval $t_3-t_2$ , corrected for dead-time loss and background.
$R_{\text{Sr}}(\text{Sr-89}, t_2, t_3)$	Sr-89 count rate of the strontium carbonate source observed in the time interval $t_3-t_2$ , corrected for dead-time loss and background.

$R_Y(Y-90, t_5, t_6)$	Y-90 count rate of the yttrium oxalate source observed in the time interval $t_6-t_5$ , corrected for dead-time loss and background.
$t_0$	Date of sampling, reference time for results, 27-Jan-1998, 09.00 CET.
$t_1$	Time of strontium separation, 22-Jun-1998, 16.15 CEST.
$t_2$	Beginning of measurement of the strontium carbonate source, 06-Jul-1998, 09.30 CEST.
$t_3$	End of measurement of the strontium carbonate source.
$t_4$	Time of yttrium separation, 22-Jul-1998, 10.26 CEST.
$t_5$	Beginning of measurement of the yttrium oxalate source, 22-Jul-1998, 16.19 CEST.
$t_6$	End of measurement of the yttrium oxalate source.
$\varepsilon_{Sr}(Sr-89)$	Detection efficiency for Sr-89 in the strontium carbonate source.
$\varepsilon_{Sr}(Sr-90)$	Detection efficiency for Sr-90 in the strontium carbonate source.
$\varepsilon_{Sr}(Y-90)$	Detection efficiency for Y-90 in the strontium carbonate source.
$\varepsilon_Y(Y-90)$	Detection efficiency for Y-90 in the yttrium oxalate source.
$\eta_{Sr}$	Chemical yield for strontium carbonate source preparation.
$\eta_Y$	Chemical yield for yttrium oxalate source preparation.
$\lambda_{Sr-89}$	Sr-89 decay constant, $\lambda_{Sr-89} = 1.5877(22) \cdot 10^{-7} \text{ s}^{-1}$ .
$\lambda_{Sr-90}$	Sr-90 decay constant, $\lambda_{Sr-90} = 7.63(8) \cdot 10^{-10} \text{ s}^{-1}$ .
$\lambda_{Y-90}$	Y-90 decay constant, $\lambda_{Y-90} = 3.004(5) \cdot 10^{-6} \text{ s}^{-1}$ .

## REFERENCES

- [1] INTERNATIONAL ATOMIC ENERGY AGENCY, Measurement of Radionuclides in Food and the Environment, A Guidebook, IAEA Technical Reports Series No. 295, IAEA, Vienna (1989).
- [2] BUNDESMINISTERIUM FÜR UMWELT, NATURSCHUTZ UND REAKTORSICHERHEIT (BMU), Meßanleitungen für die Überwachung der Radioaktivität in der Umwelt und zur Erfassung radioaktiver Emissionen aus kerntechnischen Anlagen, Gustav Fischer Verlag, Stuttgart (1992).  
(FEDERAL MINISTRY FOR THE ENVIRONMENT, NATURE CONSERVATION AND REACTOR SAFETY, Guide to monitoring radioactivity in the environment and to registering radioactive emissions from nuclear power installations, Gustav Fischer Publishers, Stuttgart (1992).)
- [3] EURACHEM, "Quantifying Uncertainty in Analytical Measurement", Editor: Laboratory of the Government Chemist Information Services, Teddington (Middlesex) & London (1995). ISBN 0-948926-08-2.
- [4] INTERNATIONAL ORGANISATION FOR STANDARDISATION, Guide to the Expression of Uncertainty in Measurement, First Edition, Geneva (1993).
- [5] EUROPEAN COOPERATION FOR ACCREDITATION OF LABORATORIES, Expression of the Uncertainty of Measurement in Calibration, Publication Reference EAL-R2, Edition 1 (1997).

# RADIOCHEMICAL DETERMINATION OF STRONTIUM-90 IN ENVIRONMENTAL SAMPLES BY LIQUID SCINTILLATION COUNTING

J. MORENO, N. VAJDA\*, K. BURNS, P.R. DANESI, P. DE REGGE, A. FAJGELJ

Agency's Laboratories, International Atomic Energy Agency, Seibersdorf

\*Technical University of Budapest, Budapest, Hungary

## Abstract

The quantification of uncertainty in the determination of Sr-90 in environmental samples using liquid scintillation counting for the final radioactivity measurement is covered in this example. The determination of the chemical yield is done by adding a known quantity of strontium to the sample; corrections have to be made for the presence of the stable strontium in the original sample which contribute to the overall uncertainty. From measurements made in different energy windows, the Sr-90 activity is obtained and corrected for the interference caused by the Y-90 daughter isotope. The uncertainty introduced by this approach is discussed in detail. The procedure is applied to the determination of Sr-90 in three IAEA environmental reference materials. Comprehensive sets of tables, including all raw data, intermediate calculations and end results, provide guidance through the radioanalytical procedures. The quantification of uncertainty is extensively documented according to the error propagation method and according to the spreadsheet method.

## 1. INTRODUCTION

The radiochemical procedure described here for the determination of  $^{90}\text{Sr}$  is part of a sequential determination of low-level activity concentrations of  $^{90}\text{Sr}$ ,  $^{241}\text{Am}$  and Pu radionuclides in environmental samples. The detailed description of the procedure can be found in the literature [1, 2, 3].

In this work only those main aspects related to the determination of  $^{90}\text{Sr}$  and their related uncertainties will be presented. A short description of the procedure is presented emphasising the possible sources of uncertainties. Figure 1 shows the "Cause-effect diagram" for the determination of  $^{90}\text{Sr}$  activity concentration. This diagram illustrates all components and subcomponents that contribute to the combined uncertainty in the activity concentration.

### 1.1. Summary of the Radiochemical Procedure

Two dissolution methods are applied: 1) the classical decomposition with a mixture of mineral acids and 2) the high-pressure microwave digestion method. The radiochemical procedure involves the separation of Pu and Np from Am and Sr by anion exchange followed by the preconcentration of Am and Sr by coprecipitation with calcium oxalate. Am is separated from Sr by extraction chromatography using TRU resin. For further purification of the Am fraction (separation from REE) anion exchange chromatography is used. The final Sr separation and purification is performed by extraction chromatography using Sr resin [1].

The measurement of the  $^{90}\text{Sr}$  activity is performed by Liquid-Scintillation Counting (LSC) employing a low energy window which includes the entire  $^{90}\text{Sr}$  spectrum plus some tailing from any in-grown  $^{90}\text{Y}$  and, a high energy window chosen above the  $^{90}\text{Sr}$  maximum  $\beta$ -energy which is used to measure  $^{90}\text{Y}$  in order to correct the  $^{90}\text{Y}$  tailing in the  $^{90}\text{Sr}$  window (see session 2). The calibration of the LSC (see details in session 2.3.3) is carried out using a certified standard solution of  $^{90}\text{Sr}$  which assures the traceability to a national radioactive standard. The recovery factor for  $^{90}\text{Sr}$  (assuming a total isotopic exchange between the stable strontium isotopes and the measurand  $^{90}\text{Sr}$ ) is determined by gravimetry and the calculation is based on a standardised strontium carrier solution.

## 1.2. Sample Preparation and Dissolution

It is assumed that a representative sample is taken for the analysis. Ten grams of ashed material are usually taken for the analysis. If no stable strontium is present in the sample, ten milligrams of strontium carrier and spikes of  $^{243}\text{Am}$  and either  $^{236}\text{Pu}$  or  $^{242}\text{Pu}$  tracers are added. The selection of the amount of the strontium carrier depends on the amount of natural strontium already present in the sample. The Sr concentration in the sample and the associated uncertainty must be known prior to the analysis. Several techniques can be used to measure strontium in the sample: Atomic Absorption Spectrophotometry, XRF analysis, etc.

The use of HF is recommended for sample dissolution in order to facilitate the total decomposition of the matrix. Strontium-90 might be contained in the lattice of the silicate material or in refractory oxides. Therefore any residue obtained after the sample dissolution has to be checked for gross alpha/beta activity. The sequential treatment with mineral acids used in this procedure usually results in the dissolution of greater than 99 % of the sample, and the resulting solution is filtered through a 0.2  $\mu\text{m}$  polypropylene membrane filter. The filter containing any insoluble residue is dried and measured for gross alpha/beta activity in a gas proportional counter to ensure the residue does not contain any significant levels of radioactivity. If the gross alpha/beta activity measured in the digestion residue is much higher than the typical background, then the residue has to be either dissolved using a fusion technique or the dissolution procedure for this particular sample has to be changed. The leachate solution is used for the radiochemical separation.

## 1.3. Radiochemical Separation of Pu, Am and Sr

Once the sample is in solution, the recovery factor of  $^{90}\text{Sr}$  can be determined from the recovery of stable strontium carrier. Strontium has only one stable oxidation state in solution and therefore isotopic exchange between carrier and  $^{90}\text{Sr}$  occurs once the sample is dissolved.

## 2. EQUATIONS

### 2.1. Equations Used to Calculate the Activity Concentration of $^{90}\text{Sr}$ “a”

The determination of the activity concentration of  $^{90}\text{Sr}$  is performed using the double energetic windows method. This method permits the  $^{90}\text{Sr}$  determination without waiting until radiochemical equilibrium  $^{90}\text{Sr}/^{90}\text{Y}$  has been reached. The first energetic window A includes all the  $^{90}\text{Sr}$  spectrum and the low energy region of  $^{90}\text{Y}$  spectrum. The window B includes the high energy region of  $^{90}\text{Y}$  spectrum. The  $^{90}\text{Sr}$  activity is determined by subtracting the contribution of  $^{90}\text{Y}$  in region A using the amount of  $^{90}\text{Y}$  recorded in region B and the measured ratio of  $^{90}\text{Y}$  in region A to region B (see details in session 2.3.3). The activity concentration of  $^{90}\text{Sr}$  (a) can be calculated according to equation (1) or to the modified equation (2):

$$a = [K \cdot f_1 \cdot f_2 \cdot f_{ad}] / (m_{ash} \cdot r_{Sr} \cdot \epsilon_{Sr} \cdot 60) \quad (1)$$

$$a = \{ [I_A - I_{A,Bkg} - f_y \cdot (I_B - I_{B,Bkg})] \cdot \exp(\lambda_{Sr} \cdot t_1) \cdot f_2 \cdot f_{ad} \} / (m_{ash} \cdot r_{Sr} \cdot \epsilon_{Sr} \cdot 60) \quad (2)$$

$$K = I_A - I_{A,Bkg} - f_y \cdot (I_B - I_{B,Bkg}) \quad (3)$$

$$f_1 = \exp(\lambda_{Sr} \cdot t_1) \quad (4)$$

$$f_2 = (\lambda_{Sr} \cdot t_s) / (1 - \exp(-\lambda_{Sr} \cdot t_s)) \quad (5)$$

Where,

$I_A$	gross count rate in the region A (channels 25 to 250), (cpm)
$I_B$	gross count rate in the region B (channels 250 to 1000), (cpm)
$I_{A,Bkg}$	background count rate in the region A (channels 25 to 250), (cpm)
$I_{B,Bkg}$	background count rate in the region B (channels 250 to 1000), (cpm)
$m_{ash}$	sample mass of ash, (kg) (see session 2.3.1)
$r_{Sr}$	recovery factor (see session 2.3.2)
$f_y$	factor taking into account the Y contribution to the $^{90}Sr$ window (see session 2.3.3)
$\epsilon_{Sr}$	efficiency of LSC for measuring $^{90}Sr$ (see session 2.3.3)
$K$	net count rate of the $^{90}Sr$ in region A corrected for the $^{90}Y$ in-growth, (cpm)
$f_1$	correction for decay of $^{90}Sr$ in the time interval “ $t_1$ ” from the reference date of the sample until the beginning of the measurement
$f_2$	correction for decay of $^{90}Sr$ in the counting interval $t_s$
$t_1$	time elapsed from the reference date until the beginning of the measurements, (s)
$t_s$	counting time of the sample, (min)
$f_{ad}$	ratio of ashed weight to dry weight

Since the counting time of the sample  $t_s$  (normally less than 400 minutes) is much smaller than the half life of  $^{90}Sr$  (28.7 years), the correction for decay of  $^{90}Sr$  in this counting interval  $t_s$  is negligible ( $f_2$  is essentially 1). Therefore this factor will be not further considered in this report.

The chemical recovery factor of strontium in the sample experiment and also in the calibration experiment (see explanation in session 2.2.2) is determined by gravimetry using the formula below:

$$r_{Sr} = f_g \cdot (m_{oxal.+pap} - m_{pap}) / (C_{Sr,sol} \cdot m_{sol} + C_{Sr,nat} \cdot m_{ash}) \quad (6)$$

Where,

$f_g$	gravimetric factor of Sr in monohydrate strontium oxalate ( $SrC_2O_4 \cdot H_2O$ )
$m_{oxal.+pap}$	mass of strontium oxalate and the filter paper, (mg)
$m_{pap}$	mass of filter paper, (mg)
$C_{Sr,sol}$	concentration of the Sr standardized carrier solution, (mg Sr/g solution)
$m_{sol}$	mass of the carrier solution added to the sample, (g)
$C_{Sr,nat}$	concentration of natural strontium in the sample, (mg Sr/g ash sample)
$m_{ash}$	mass of ashed sample, (g)

Both the efficiency ( $\epsilon_{Sr}$ ) and the shape tailing parameter ( $f_y$ ) are obtained from an independent calibration experiment where strontium is separated from yttrium (see explanation in session 2.3.2). The following equations are used:

$$f_y = (I_{y,A} - I_{A,Bkg}) / (I_{y,B} - I_{B,Bkg}) \quad (7)$$

$$\varepsilon_{\text{Sr}} = \{[I_{\text{A,CAL}} - I_{\text{A,Bkg}} - f_y \cdot (I_{\text{B,CAL}} - I_{\text{B,Bkg}})] \cdot \exp(+\lambda_{\text{Sr}} \cdot t_{1,\text{CAL}})\} / (r_{\text{Sr,CAL}} \cdot a_{0,\text{Sr}} \cdot 60) \quad (8)$$

$$\varepsilon_{\text{Sr}} = [K_{\text{CAL}} \cdot f_{1,\text{CAL}}] / [r_{\text{Sr,CAL}} \cdot a_{0,\text{Sr}} \cdot 60] \quad (9)$$

$$K_{\text{CAL}} = I_{\text{A,CAL}} - I_{\text{A,Bkg}} - f_y \cdot (I_{\text{B,CAL}} - I_{\text{B,Bkg}}) \quad (10)$$

Where,

$K_{\text{CAL}}$	net count rate of the $^{90}\text{Sr}$ in region A corrected for the $^{90}\text{Y}$ in-growth in the calibration experiment, (cpm)
$I_{\text{A,CAL}}$	gross count rate in A, (cpm)
$I_{\text{B,CAL}}$	gross counts of $^{90}\text{Y}$ in window B, (cpm)
$\varepsilon_{\text{Sr}}$	efficiency of Sr in window A
$r_{\text{Sr,CAL}}$	recovery factor of Sr in the calibration experiment
$f_y$	ratio of the counting rate from $^{90}\text{Y}$ in A to B in the $^{90}\text{Y}$ spectrum
$a_{0,\text{Sr}}$	known added activity of $^{90}\text{Sr}$ at the reference date of the certified standard solution (Bq)
$f_{1,\text{CAL}}$	correction for decay of $^{90}\text{Sr}$ in the time interval from the calibration date to the beginning of the measurements ( $t_{1,\text{CAL}}$ ), see for example equation (4)
$\lambda_{\text{Sr}}$	decay constant of $^{90}\text{Sr}$ ( $7.63 \times 10^{-10} \text{ s}^{-1}$ )
$t_{1,\text{CAL}}$	time interval from the reference date of the $^{90}\text{Sr}/^{90}\text{Y}$ certified standard solution to the beginning of the measurements, (s)
$I_{\text{Y,A}}$	gross count rate of $^{90}\text{Y}$ in window A
$I_{\text{Y,B}}$	gross count rate of $^{90}\text{Y}$ in window B

Without considering covariance terms, the uncertainty of the activity (equation 2) is calculated using the general formula given elsewhere [4], in particular:

$$\begin{aligned} u_a^2 &= (\partial a / \partial I_A)^2 \cdot u_{I_A}^2 + (\partial a / \partial I_{\text{A,Bkg}})^2 \cdot u_{I_{\text{A,Bkg}}}^2 + (\partial a / \partial I_B)^2 \cdot u_{I_B}^2 + (\partial a / \partial I_{\text{B,Bkg}})^2 \cdot u_{I_{\text{B,Bkg}}}^2 \\ &+ (\partial a / \partial f_y)^2 \cdot u_{f_y}^2 + (\partial a / \partial \varepsilon_{\text{Sr}})^2 \cdot u_{\varepsilon_{\text{Sr}}}^2 + (\partial a / \partial r_{\text{Sr}})^2 \cdot u_{r_{\text{Sr}}}^2 + (\partial a / \partial m_{\text{ash}})^2 \cdot u_{m_{\text{ash}}}^2 \\ &+ (\partial a / \partial f_{\text{ad}})^2 \cdot u_{f_{\text{ad}}}^2 + (\partial a / \partial \lambda_{\text{Sr}})^2 \cdot u_{\lambda_{\text{Sr}}}^2 + (\partial a / \partial t_1)^2 \cdot u_{t_1}^2 + (\partial a / \partial f_2)^2 \cdot u_{f_2}^2 \end{aligned} \quad (11)$$

Where,

$u_a$	combined standard uncertainty in the activity concentration of $^{90}\text{Sr}$ , (Bq/kg)
$u_{I_A}$	standard uncertainty of the gross count rate in region A, (cpm)
$u_{I_{\text{A,Bkg}}}$	standard uncertainty of the background count rate in region A, (cpm)
$u_{I_B}$	standard uncertainty of the gross count rate in region B, (cpm)
$u_{I_{\text{B,Bkg}}}$	standard uncertainty of the background count rate in region B, (cpm)
$u_{f_y}$	standard uncertainty of the determination of factor $f_y$
$u_{\varepsilon_{\text{Sr}}}$	combined standard uncertainty in the determination of the efficiency
$u_{r_{\text{Sr}}}$	combined standard uncertainty in the determination of the recovery factor
$u_{m_{\text{ash}}}$	standard uncertainty in weighing the sample, (kg, ash basis)
$u_{f_{\text{ad}}}$	combined standard uncertainty in the determination of the ash/dry ratio
$u_{t_1}$	standard uncertainty in the determination of $t_1$ , (s)
$u_{f_2}$	standard uncertainty in the determination of factor $f_2$
$u_{\lambda_{\text{Sr}}}$	uncertainty in the decay constant of $^{90}\text{Sr}$ ( $0.08 \times 10^{-10} \text{ s}^{-1}$ )

$\partial a / \partial x_i$  partial derivative of the activity with respect to all the parameters  $x_i$   
(see session 2.2)

## 2.2. Calculation of the Partial Derivatives or Sensitivity Factors “ $\partial a / \partial x_i$ ”

Differentiating equation (1) and assuming that the values for the result “a” and “K” have been already calculated, we may have:

$$\partial a / \partial I_A = +a / K \quad (12)$$

$$\partial a / \partial I_B = -f_y \cdot a / K \quad (13)$$

Since in the calibration experiment the count rates of separated  $^{90}\text{Sr}$  and  $^{90}\text{Y}$  are much higher than the background count rates in windows A and B ( $I_{A,\text{Bkg}}$ ,  $I_{B,\text{Bkg}}$ ), a small variation in  $I_{A,\text{Bkg}}$  and  $I_{B,\text{Bkg}}$  (see equations 7 and 8) will not produce any significant change in either the efficiency  $\epsilon_{\text{Sr}}$  or in the tailing parameter  $f_y$ . This assumption which will be proved later (see session 3, Table 6) significantly simplifies the differentiation of a in respect to  $I_{A,\text{Bkg}}$  and  $I_{B,\text{Bkg}}$ :

$$\partial a / \partial I_{A,\text{Bkg}} = -a / K \quad (14)$$

$$\partial a / \partial I_{B,\text{Bkg}} = +f_y \cdot a / K \quad (15)$$

$$\partial a / \partial f_y = -[(I_B - I_{B,\text{Bkg}})] \cdot a / K \quad (16)$$

$$\partial a / \partial \epsilon_{\text{Sr}} = -a / \epsilon_{\text{Sr}} \quad (17)$$

$$\partial a / \partial r_{\text{Sr}} = -a / r_{\text{Sr}} \quad (18)$$

$$\partial a / \partial m_{\text{ash}} = -a / m_{\text{ash}} \quad (19)$$

$$\partial a / \partial f_{\text{ad}} = +a / f_{\text{ad}} \quad (20)$$

$$\partial a / \partial \lambda_{\text{Sr}} = +a t_1 \quad (21)$$

$$\partial a / \partial t_1 = +a \lambda_{\text{Sr}} \quad (22)$$

$$\partial a / \partial f_2 = +a / f_2 \quad (23)$$

Therefore the final expression for the calculation of uncertainty in the activity is as follows:

$$\begin{aligned} u_a^2 &= (a / K)^2 \cdot u_{I_A}^2 + (-a / K)^2 \cdot u_{I_{A,\text{Bkg}}}^2 + (-f_y \cdot a / K)^2 \cdot u_{I_B}^2 \\ &+ (f_y \cdot a / K)^2 \cdot u_{I_{B,\text{Bkg}}}^2 + \{ -[(I_B - I_{B,\text{Bkg}})] \cdot a / (K \cdot f_1 \cdot f_{\text{ad}} \cdot f_2) \}^2 \cdot u_{f_y}^2 \\ &+ (-a / \epsilon_{\text{Sr}})^2 \cdot u_{\epsilon_{\text{Sr}}}^2 + (-a / r_{\text{Sr}})^2 \cdot u_{r_{\text{Sr}}}^2 + (-a / m_{\text{ash}})^2 \cdot u_{m_{\text{ash}}}^2 + (a / f_{\text{ad}})^2 \cdot u_{f_{\text{ad}}}^2 \\ &+ (-a \cdot t_1)^2 \cdot u_{\lambda_{\text{Sr}}}^2 + (-a \cdot \lambda_{\text{Sr}})^2 \cdot u_{t_1}^2 + (a / f_2)^2 \cdot u_{f_2}^2 \end{aligned} \quad (24)$$

## 2.3. Calculation of the uncertainties of the individual components and derived parameters

### 2.3.1. Uncertainty in weighing the sample $u_{m,ash}$ and in the determination of the ash/dry ratio $u_{f,ad}$

We recommend the EURACHEM document [4] to calculate uncertainties associated with the determination of mass by difference in weighing. For example:

$$m_{ash} = m_{crucible+ash} - m_{crucible} \quad (25)$$

$$u_{m,ash}^2 = u_1^2 + u_2^2 \quad (26)$$

Where,

$m_{ash}$	mass of the sample on ash basis, (g)
$m_{crucible+ash}$	mass of the tare crucible and ash, (g)
$m_{crucible}$	mass of the tare crucible, (g)
$u_1$	uncertainties associated with the variability of weights by difference in the corresponding region
$u_2$	uncertainties associated with the calibration of the balance

Since the activity concentration should be reported on dry basis for geological materials and on wet basis for biological materials, the dry/wet ( $f_{dw}$ ) and ash/dry ( $f_{ad}$ ) ratios should be determined prior to analysis. Usually the  $f_{dw}$  is determined on small subsamples and the ash/wet ratio ( $f_{aw}$ ) is determined on bigger subsamples. Then, the ( $f_{ad}$ ) is calculated through as follows:

$$f_{dw} = (m_{dry,sub1+t1} - m_{t1}) / (m_{wet,sub1+t1} - m_{t1}) \quad (27)$$

$$f_{aw} = (m_{ash,sub2+t2} - m_{t2}) / (m_{wet,sub2+t2} - m_{t2})$$

$$f_{ad} = f_{aw} / f_{dw} \quad (28)$$

Where,

$f_{dw}$	dry/wet ratio
$f_{aw}$	ash/wet ratio
$f_{ad}$	ash/dry ratio
$m_{wet,sub1+t1}$	total weight of the wet subsample and the tare container used for the dry/wet ratio determination, (g)
$m_{dry,sub1+t1}$	total weight of the dry subsample and the tare container for the dry/wet ratio determination, (g)
$m_{t1}$	mass of the tare container used for the dry/wet ratio determination, (g)
$m_{ash,sub2+t2}$	total weight of the ash subsample and the tare container used for the ash/wet ratio determination, (g)
$m_{wet,sub2+t2}$	total weight of the wet subsample and the tare container used for the ash/wet ratio determination, (g)
$m_{t2}$	mass of the tare container used for the ash/wet ratio determination, (g)

In the experiment for the determination of the dry/wet ratio (also in the ash/wet ratio determination) two different masses are weighed on the same balance using the same tare container. Therefore, the covariance term should be considered when calculating the uncertainty in the ratios of net weights. For cases similar to these, Winkler [5] proposed the following formula to calculate the combined uncertainty considering the covariance term:

$$\begin{aligned}
 u_{f,dw}^2 &= (u_{m_{dry,sub1+t1}}^2 + u_{m_{t1}}^2) / (m_{dry,sub1+t1} - m_{t1})^2 + \\
 &\quad (u_{m_{wet,sub1+t1}}^2 + u_{m_{t1}}^2) / (m_{wet,sub1+t1} - m_{t1})^2 - \\
 &\quad 2 \cdot u_{m_{t1}} \cdot u_{m_{t1}} / [(m_{dry,sub1+t1} - m_{t1}) \cdot (m_{wet,sub1+t1} - m_{t1})]
 \end{aligned} \tag{29}$$

Where,

$u_{f,dw}$	combined uncertainty in the determination of the dry/wet ratio
$u_{m_{wet,sub1+t1}}$	uncertainty in weighing the wet subsample and the tare container (dry/wet determination), (g)
$u_{m_{dry,sub1+t1}}$	uncertainty in weighing the dry subsample and the tare container (dry/wet determination), (g)
$u_{m_{t1}}$	uncertainty in weighing the tare container used for the dry/wet ratio determination, (g)

The same approach is applied for calculating the combined uncertainty in the determination of the ash/wet ratio:

$$\begin{aligned}
 u_{f,aw}^2 &= (u_{m_{ash,sub2+t2}}^2 + u_{m_{t2}}^2) / (m_{ash,sub2+t2} - m_{t2})^2 + \\
 &\quad (u_{m_{wet,sub2+t2}}^2 + u_{m_{t2}}^2) / (m_{wet,sub2+t2} - m_{t2})^2 - \\
 &\quad 2 \cdot u_{m_{t2}} \cdot u_{m_{t2}} / [(m_{ash,sub2+t2} - m_{t2}) \cdot (m_{wet,sub2+t2} - m_{t2})]
 \end{aligned} \tag{30}$$

Where,

$u_{f,aw}$	combined uncertainty in the determination of the ash/wet ratio
$u_{m_{wet,sub2+t2}}$	uncertainty in weighing the wet subsample and the tare container (ash/wet ratio determination), (g)
$u_{m_{dry,sub2+t2}}$	uncertainty in weighing the dry subsample and the tare container (ash/wet ratio determination), (g)
$u_{m_{t2}}$	uncertainty in weighing the tare container used for the ash/wet ratio determination, (g)

Once  $u_{f,dw}$  and  $u_{f,aw}$  are calculated according to equations 29 and 30 respectively, the combined standard uncertainty in the ash/dry ratio  $f_{ad}$  is calculated according to the formula given below:

$$u_{f,ad}^2 / f_{ad}^2 = u_{f_{aw}}^2 / f_{aw}^2 + u_{f_{dw}}^2 / f_{dw}^2 \tag{31}$$

Where,

$u_{f,ad}$	combined uncertainty in the determination of the ash/dry ratio
------------	--

### 2.3.2. Uncertainty in the determination of the chemical recovery factor ( $u_r$ )

Equation 6 is used to calculate the recovery factor:

$$r_{Sr} = f_g \cdot (m_{\text{oxal+pap}} - m_{\text{pap}}) / (C_{Sr,\text{sol}} \cdot m_{\text{sol}} + C_{Sr,\text{nat}} \cdot m_{\text{ash}}) \quad (6)$$

Where,

$f_g$	gravimetric factor of Sr in $\text{SrC}_2\text{O}_4 \cdot \text{H}_2\text{O}$
$m_{\text{oxal+pap}}$	mass of strontium oxalate and filter paper, (mg)
$m_{\text{pap}}$	mass of filter paper, (mg)
$C_{Sr,\text{sol}}$	concentration of the Sr standardized carrier solution, (mg Sr/g solution)
$m_{\text{sol}}$	mass of the carrier solution added to the sample, (g)
$C_{Sr,\text{nat}}$	concentration of natural strontium in the sample, (mg Sr/g ash sample)
$m_{\text{ash}}$	sample mass on ash basis, (g)

Differentiating equation (6) and assuming that the value for the result “ $r_{Sr}$ ” has been already calculated, we may have:

$$\partial r_{Sr} / \partial f_g = + r_{Sr} / f_g \quad (31)$$

$$\partial r_{Sr} / \partial m_{\text{oxal+pap}} = + r_{Sr} / (m_{\text{oxal+pap}} - m_{\text{pap}}) \quad (32)$$

$$\partial r_{Sr} / \partial m_{\text{pap}} = - r_{Sr} / (m_{\text{oxal+pap}} - m_{\text{pap}}) \quad (33)$$

$$\partial r_{Sr} / \partial C_{Sr,\text{sol}} = - r_{Sr} \cdot m_{\text{sol}} / (C_{Sr,\text{sol}} \cdot m_{\text{sol}} + C_{Sr,\text{nat}} \cdot m_{\text{ash}}) \quad (34)$$

$$\partial r_{Sr} / \partial m_{\text{sol}} = - r_{Sr} \cdot C_{Sr,\text{sol}} / (C_{Sr,\text{sol}} \cdot m_{\text{sol}} + C_{Sr,\text{nat}} \cdot m_{\text{ash}}) \quad (35)$$

$$\partial r_{Sr} / \partial C_{Sr,\text{nat}} = - r_{Sr} \cdot m_{\text{ash}} / (C_{Sr,\text{sol}} \cdot m_{\text{sol}} + C_{Sr,\text{nat}} \cdot m_{\text{ash}}) \quad (36)$$

$$\partial r_{Sr} / \partial m_{\text{ash}} = - r_{Sr} \cdot C_{Sr,\text{nat}} / (C_{Sr,\text{sol}} \cdot m_{\text{sol}} + C_{Sr,\text{nat}} \cdot m_{\text{ash}}) \quad (37)$$

Where,

$\partial r / \partial x_i$  = partial derivative of the recovery factor with respect with all the parameters  $x_i$

Therefore the combined uncertainty in the determination of the recovery factor is calculated according to the following equation:

$$\begin{aligned} u_{r,Sr}^2 &= (+r_{Sr} / f_g)^2 \cdot u_{f_g}^2 + (+r_{Sr} / (m_{\text{oxal+pap}} - m_{\text{pap}}))^2 \cdot u_{m_{\text{oxal+pap}}}^2 \\ &+ (-r_{Sr} / (m_{\text{oxal+pap}} - m_{\text{pap}}))^2 \cdot u_{m_{\text{pap}}}^2 \\ &+ (-r_{Sr} \cdot m_{\text{sol}} / (C_{Sr,\text{sol}} \cdot m_{\text{sol}} + C_{Sr,\text{nat}} \cdot m_{\text{ash}}))^2 \cdot u_{m_{\text{pap}}}^2 \\ &+ (-r_{Sr} \cdot C_{Sr,\text{sol}} / (C_{Sr,\text{sol}} \cdot m_{\text{sol}} + C_{Sr,\text{nat}} \cdot m_{\text{ash}}))^2 \cdot u_{m_{\text{sol}}}^2 \\ &+ (-r_{Sr} \cdot m_{\text{ash}} / (C_{Sr,\text{sol}} \cdot m_{\text{sol}} + C_{Sr,\text{nat}} \cdot m_{\text{ash}}))^2 \cdot u_{C_{Sr,\text{sol}}}^2 \\ &+ (-r_{Sr} \cdot m_{\text{ash}} / (C_{Sr,\text{sol}} \cdot m_{\text{sol}} + C_{Sr,\text{nat}} \cdot m_{\text{ash}}))^2 \cdot u_{C_{Sr,\text{nat}}}^2 \\ &+ (-r_{Sr} \cdot C_{Sr,\text{nat}} / (C_{Sr,\text{sol}} \cdot m_{\text{sol}} + C_{Sr,\text{nat}} \cdot m_{\text{ash}}))^2 \cdot u_{m_{\text{ash}}}^2 \end{aligned} \quad (38)$$

Where,

$u_{fg}$	uncertainty in the calculation of the gravimetric factor
$u_{moxal}$	uncertainty in weighing the strontium oxalate and the filter paper
$u_{m,pap}$	uncertainty in weighing the filter paper
$u_{C_{Sr,sol}}$	uncertainty in the concentration of Sr in the carrier solution, (mg Sr/g sol.)
$u_{m,sol}$	uncertainty in weighing the carrier solution, (g)
$u_{C_{Sr,nat}}$	uncertainty in the concentration of Sr in the sample, (mg Sr/g ash)
$u_{m,ash}$	uncertainty in weighing the sample by difference, (g)

### 2.3.2.1. Uncertainty of the gravimetric factor $u_{fg}$

The gravimetric factor ( $f_g$ ) and its associated uncertainties are calculated using the equation below:

$$f_g = A_{Sr} / M_{SrC_2O_4 \cdot H_2O} \quad (39)$$

$$u_{fg}^2 / f_g^2 = u_{A,Sr}^2 / A_{Sr}^2 + u_{M, SrC_2O_4 \cdot H_2O}^2 / M_{SrC_2O_4 \cdot H_2O}^2 \quad (40)$$

Where,

$A_{Sr}$	atomic mass of Sr, (in unified atomic mass units, u)
$M_{SrC_2O_4 \cdot H_2O}$	molecular weight of strontium oxalate, (in unified atomic mass units, u)

The uncertainty in the formula weight of strontium oxalate can be derived by combining the uncertainties in the atomic weights of its constituents:

Table 1. Calculation of the atomic weight standard uncertainties

Element	Atomic Weight, A	Quoted Uncertainty	Standard Uncertainty
C	12.011	0.001	0.00058
H	1.00794	0.00007	0.00004
O	15.99944	0.0003	0.00017
Sr	87.62	0.01	0.00577

The values of atomic weights and their uncertainties are taken from [Journal of Pure and Applied Chemistry].

Table 2. Calculation of the uncertainty in the calculation of the gravimetric factor  $f_g$

Number of atoms in one molecule of $\text{SrC}_2\text{O}_4\cdot\text{H}_2\text{O}$	Calculation $\text{g}\cdot\text{mol}^{-1}$	Result $\text{g}\cdot\text{mol}^{-1}$	Uncertainty $\text{g}\cdot\text{mol}^{-1}$	Uncertainty of the gravimetric factor of Strontium in strontium oxalate, $u_{f,g}$ $\text{g}\cdot\text{mol}^{-1}$
2xC	2x12.011	24.022	0.00116	<b>3.287575E-5</b>
2xH	2x1.00794	2.01588	0.00008	
5xO	5x15.99944	79.997	0.00085	
1xSr	1x87.62	87.62	0.00577	
<b>molecular weight, M</b>	$\Sigma$	<b>193.65488</b>	<b>0.005947</b>	
			$u_{F(\text{SrC}_2\text{O}_4\cdot\text{H}_2\text{O})}$	

### 2.3.3. Uncertainty associated with the determination of the efficiency of $^{90}\text{Sr}$ “ $\epsilon_{\text{Sr}}$ ” and the contribution of $^{90}\text{Y}$ in region A “ $f_y$ ”

Both the efficiency “ $\epsilon_{\text{Sr}}$ ” and the shape tailing parameter “ $f_y$ ” are obtained from an independent experiment where strontium is separated from yttrium. A sample aliquot is taken from a certified standard solution of  $^{90}\text{Sr}$  -  $^{90}\text{Y}$ . The recovery factor of strontium is controlled gravimetrically by weighing the strontium oxalate precipitated from the strontium fraction. The calculation of both parameters and associated uncertainties are described using the formula below:

From the  $^{90}\text{Y}$  spectrum (yttrium fraction) the ratio of the net counting rates “ $f_y$ ” from  $^{90}\text{Y}$  in A to B is calculated. The factor should be independent of the activity of Y in the sample and is dependent on the composition of the sample-scintillation cocktail solution. The quenching indicator parameter such as the  $t_{\text{SIE}}$  has to be controlled permanently. Since  $f_y$  and therefore the efficiency “ $\epsilon_{\text{Sr}}$ ” is dependent on  $t_{\text{SIE}}$ , a basic assumption in the evaluation is that  $t_{\text{SIE}}$  has been kept constant in both the calibration and the sample measurement experiments. The measurement procedure described in the present report has been designed to assure this assumption.

The tailing parameter is calculated using the equation (7):

$$f_y = (I_{y,A} - I_{A,\text{Bkg}}) / (I_{y,B} - I_{B,\text{Bkg}}) \quad (7)$$

By applying the uncertainty propagation law, the uncertainty in  $f_y$  can be calculated according to the formula below:

$$u_{f_y}^2 / f_y^2 = (u_{I_{y,A}}^2 + u_{I_{A,\text{Bkg}}}^2) / (I_{y,A} - I_{A,\text{Bkg}})^2 + (u_{I_{y,B}}^2 + u_{I_{B,\text{Bkg}}}^2) / (I_{y,B} - I_{B,\text{Bkg}})^2 \quad (41)$$

In counting statistics (Poisson statistics) when the number of counts “N” is higher than 10, the standard deviation of the counting rate “I” is approximately the square root of the counting rate divided by the time. Although this approach is valid for the radioactive decay, it is often observed when using liquid scintillation analysers that this theory does not describe properly the dispersion of the results around the background. Obviously, this can be explained by the different nature of the components influencing the stability of low level scintillation analyzers. For this reason it is recommended when estimating the dispersion around the background or reagent blank count rates to prepare several sources and measure the variation as standard deviation from the series:

$$I_{Bkg} = \Sigma (I_{Bkg,i}) / n \quad (42)$$

$$uI_{Bkg} = [\Sigma (I_{Bkg,i} - I_{Bkg}) / n-1]^{1/2} \quad (43)$$

Where,

$I_{Bkg}$  mean value of the background (or reagent blank) count rate, (cpm)  
 $n$  number of experiments  
 $I_{Bkg,i}$  background (or reagent blank) count rate in each measurement, (cpm)

From the **<sup>90</sup>Sr spectrum** the net count rate of the <sup>90</sup>Sr in region A corrected for the <sup>90</sup>Y in-growth is calculated:

$$K_{CAL} = I_{A,CAL} - I_{A,Bkg} - f_y \cdot (I_{B,CAL} - I_{B,Bkg}) \quad (44)$$

and then the counting efficiency of <sup>90</sup>Sr is calculated according to equation (8):

$$\epsilon_{Sr} = \{[I_{A,CAL} - I_{A,Bkg} - f_y \cdot (I_{B,CAL} - I_{B,Bkg})] \cdot \exp(-\lambda_{Sr} \cdot t_{1,CAL})\} / (r_{Sr,CAL} \cdot a_{o,Sr} \cdot 60) \quad (8)$$

Where,

$K_{CAL}$  net count rate of the <sup>90</sup>Sr in region A corrected for the <sup>90</sup>Y in-growth in the calibration experiment, (cpm)  
 $I_{A,CAL}$  gross count rate in A, (cpm)  
 $I_{B,CAL}$  gross counts of <sup>90</sup>Y in window B, (cpm)  
 $r_{Sr,CAL}$  recovery factor of Sr in the calibration experiment  
 $a_{o,Sr}$  known added activity (from a certified standard solution) of <sup>90</sup>Sr at the time of measurement, (Bq)  
 $\lambda_{Sr}$  decay constant of <sup>90</sup>Sr ( $7.63 \times 10^{-10} \text{ s}^{-1}$ )  
 $t_{1,CAL}$  time interval from the reference date of the <sup>90</sup>Sr/<sup>90</sup>Y certified standard solution to the beginning of the measurements, (s)  
 $I_{Y,A}$  gross count rate of <sup>90</sup>Y in window A  
 $I_{Y,B}$  gross count rate of <sup>90</sup>Y in window B

The recovery factor in the calibration experiment is calculated according to equation (6) and considering that in this case  $C_{Sr,nat}$  is zero:

$$R_{Sr,CAL} = f_g \cdot (m_{oxal+pap,CAL} - m_{pap,CAL}) / (C_{Sr,sol} \cdot m_{sol,CAL}) \quad (45)$$

Where,

$f_g$	gravimetric factor of Sr in monohydrate strontium oxalate ( $\text{SrC}_2\text{O}_4 \cdot \text{H}_2\text{O}$ )
$m_{\text{oxal} + \text{pap,CAL}}$	mass of strontium oxalate and the filter paper in the calibration experiment, (mg)
$m_{\text{pap,CAL}}$	mass of filter paper in the calibration experiment, (mg)
$C_{\text{Sr,sol}}$	concentration of the Sr standardized carrier solution, (mg Sr/g solution)
$m_{\text{sol,CAL}}$	mass of the carrier solution added to the sample in the calibration experiment, (g)

When combining equation 8 and 45 we obtain the final expression to calculate the efficiency  $\epsilon_{\text{Sr}}$  :

$$\epsilon_{\text{Sr}} = \{ [I_{\text{A,CAL}} - I_{\text{A,Bkg}} - f_y \cdot (I_{\text{B,CAL}} - I_{\text{B,Bkg}})] \cdot \exp(-\lambda_{\text{Sr}} \cdot t_{1,\text{CAL}}) \cdot C_{\text{Sr,sol}} \cdot m_{\text{sol,CAL}} \} / [f_g \cdot (m_{\text{oxal} + \text{pap,CAL}} - m_{\text{pap,CAL}}) \cdot a_{\text{o,Sr}} \cdot 60] \quad (46)$$

Differentiating equation (46) and assuming that the values for the result “ $\epsilon_{\text{Sr}}$ ” and “ $K_{\text{CAL}}$ ” have been already calculated, we may have:

$$\partial \epsilon_{\text{Sr}} / \partial I_{\text{A,CAL}} = +\epsilon_{\text{Sr}} / K_{\text{CAL}} \quad (47)$$

$$\partial \epsilon_{\text{Sr}} / \partial I_{\text{A,Bkg}} = -(I_{\text{y,B}} - I_{\text{B,CAL}}) \cdot \epsilon_{\text{Sr}} / [(I_{\text{y,B}} - I_{\text{B,Bkg}}) \cdot K_{\text{CAL}}] \quad (48)$$

$$\partial \epsilon_{\text{Sr}} / \partial I_{\text{B,CAL}} = -(I_{\text{y,A}} - I_{\text{A,Bkg}}) \cdot \epsilon_{\text{Sr}} / [(I_{\text{y,B}} - I_{\text{B,Bkg}}) \cdot K_{\text{CAL}}] \quad (49)$$

$$\partial \epsilon_{\text{Sr}} / \partial I_{\text{B,Bkg}} = +(I_{\text{y,A}} - I_{\text{A,CAL}}) \cdot \epsilon_{\text{Sr}} / [(I_{\text{y,B}} - I_{\text{B,Bkg}}) \cdot K_{\text{CAL}}] + \epsilon_{\text{Sr}} / (I_{\text{y,B}} - I_{\text{B,Bkg}}) \quad (50)$$

$$\partial \epsilon_{\text{Sr}} / \partial I_{\text{y,A}} = -(I_{\text{B,CAL}} - I_{\text{B,Bkg}}) \cdot \epsilon_{\text{Sr}} / [K_{\text{CAL}} \cdot (I_{\text{y,B}} - I_{\text{B,Bkg}})] \quad (51)$$

$$\partial \epsilon_{\text{Sr}} / \partial I_{\text{y,B}} = +(I_{\text{A,CAL}} - I_{\text{A,Bkg}}) \cdot \epsilon_{\text{Sr}} / [(I_{\text{y,B}} - I_{\text{B,Bkg}}) \cdot K_{\text{CAL}}] - \epsilon_{\text{Sr}} / (I_{\text{y,B}} - I_{\text{B,Bkg}}) \quad (52)$$

$$\partial \epsilon_{\text{Sr}} / \partial \lambda_{\text{Sr}} = +\epsilon_{\text{Sr}} \cdot t_{1,\text{CAL}} \quad (53)$$

$$\partial \epsilon_{\text{Sr}} / \partial t_{1,\text{CAL}} = +\epsilon_{\text{Sr}} \cdot \lambda_{\text{Sr}} \quad (54)$$

$$\partial \epsilon_{\text{Sr}} / \partial a_{\text{o,Sr}} = -\epsilon_{\text{Sr}} / a_{\text{o,Sr}} \quad (55)$$

$$\partial \epsilon_{\text{Sr}} / \partial f_g = -\epsilon_{\text{Sr}} / f_g \quad (56)$$

$$\partial \epsilon_{\text{Sr}} / \partial C_{\text{Sr,sol}} = +\epsilon_{\text{Sr}} / C_{\text{Sr,sol}} \quad (57)$$

$$\partial \epsilon_{\text{Sr}} / \partial m_{\text{sol,CAL}} = +\epsilon_{\text{Sr}} / m_{\text{sol,CAL}} \quad (58)$$

$$\epsilon_{\text{Sr}} / \partial m_{\text{oxal} + \text{pap,CAL}} = -\epsilon_{\text{Sr}} / (m_{\text{oxal} + \text{pap,CAL}} - m_{\text{pap,CAL}}) \quad (59)$$

$$\epsilon_{\text{Sr}} / \partial m_{\text{pap,CAL}} = +\epsilon_{\text{Sr}} / (m_{\text{oxal} + \text{pap,CAL}} - m_{\text{pap,CAL}}) \quad (60)$$

Where,

$\partial \epsilon_{\text{Sr}} / \partial x_i$  partial derivative of the efficiency with respect to all the input parameters  $x_i$

The combined uncertainty in the efficiency is therefore calculated by using the following formula:

$$\begin{aligned}
u_{\epsilon, Sr}^2 = & \epsilon_{Sr}^2 / K_{CAL}^2 \cdot \{ u_{IA, CAL}^2 + [(I_{y, B} - I_{B, CAL}) / (I_{y, B} - I_{B, Bkg})]^2 \cdot u_{IA, Bkg}^2 \\
& + [(I_{y, A} - I_{A, Bkg}) / (I_{y, B} - I_{B, Bkg})]^2 \cdot u_{IB, CAL}^2 + [(I_{B, CAL} - I_{B, Bkg}) / (I_{y, B} - I_{B, Bkg})]^2 \cdot u_{IY, A}^2 \} \\
& + \{ (I_{y, A} - I_{A, CAL}) \cdot \epsilon_{Sr} / [(I_{y, B} - I_{B, Bkg}) \cdot K_{CAL}] + \epsilon_{Sr} / (I_{y, B} - I_{B, Bkg}) \}^2 \cdot u_{IB, Bkg}^2 \\
& + \{ \epsilon_{Sr} \cdot (I_{A, CAL} - I_{A, Bkg}) / [(I_{y, B} - I_{B, Bkg}) \cdot K_{CAL}] - \epsilon_{Sr} / (I_{y, B} - I_{B, Bkg}) \}^2 \cdot u_{IY, B}^2 \\
& + (-\epsilon_{Sr} / a_{o, Sr})^2 \cdot u_{ao, Sr}^2 + (\epsilon_{Sr} \cdot t_{1, CAL})^2 \cdot u_{\lambda, Sr}^2 + (\epsilon_{Sr} \cdot \lambda_{Sr})^2 \cdot u_{t_{1, CAL}}^2 + (-\epsilon_{Sr} / f_g)^2 \cdot u_{fg}^2 \\
& + (\epsilon_{Sr} / C_{Sr, sol})^2 \cdot u_{C_{Sr, sol}}^2 + (\epsilon_{Sr} / m_{sol, CAL})^2 \cdot u_{m_{sol, CAL}}^2 \\
& + [-\epsilon_{Sr} / (m_{oxal + pap, CAL} - m_{pap, CAL})]^2 \cdot u_{m_{oxal + pap, CAL}}^2 \\
& + [\epsilon_{Sr} / (m_{oxal + pap, CAL} - m_{pap, CAL})]^2 \cdot u_{m_{pap, CAL}}^2
\end{aligned} \tag{61}$$

Where,

$t_{s, CAL}$	counting time in the calibration experiment, (min)
$u_{t_{1, CAL}}$	standard uncertainty in the determination of $t_{1, CAL}$ , (s)
$u_{\lambda, Sr}$	uncertainty in the decay constant of $^{90}Sr$ ( $0.08 \times 10^{-10} s^{-1}$ )
$u_{fg}$	uncertainty in the calculation of the gravimetric factor
$u_{m_{oxal + pap, CAL}}$	uncertainty in weighing the strontium oxalate and the filter paper in the calibration experiment, (mg)
$u_{m_{pap, CAL}}$	uncertainty in weighing the filter paper in the calibration experiment, (mg)
$u_{C_{Sr, sol}}$	uncertainty in the concentration of Sr in the carrier solution, (mg Sr/g sol.)
$u_{m_{sol, CAL}}$	uncertainty in weighing the carrier solution, (g)

### 3. EXAMPLES

The examples concern the determination of  $^{90}Sr$  in Soil-6, IAEA-135 and IAEA-367. To calculate the combined uncertainties in the recovery factors, efficiency and activity concentrations of  $^{90}Sr$ , in addition to the classical method based on differentiation, a spreadsheet method proposed by Kragten [6] has been applied.

#### 3.1. Recovery Factor

Tables 3-5 show the spreadsheets for calculating the uncertainties in the determination of the recovery factors in Soil-6, IAEA-135 and IAEA-367, respectively. It can be noticed that the sensitivity factors obtained by both methods give essentially the same results. The contribution of the input parameters to the combined uncertainty varies from sample to sample. In Soil-6 and IAEA-135 the major contributors are the uncertainty in the concentration of the Sr standardised carrier solution " $C_{Sr, sol}$ " and uncertainties associated with weighing the final source of Sr oxalate. Since the reference material IAEA-367 has a coral matrix, the amount of the natural Sr already present in the sample is unusually high. The latter

explains why in this case the major contribution to the combined uncertainty in the recovery factor is actually associated with the concentration of natural Sr in the sample “ $C_{Sr,nat}$ ”.

### 3.2. Efficiency

The results are presented in Table 6. The sensitivity factors obtained by both the numerical and the differential methods give no significant differences. The major contributors to the combined uncertainty in the efficiency are the following parameters: activity of the certified standard solution,  $a_{o,Sr}$  (63%); the concentration of the Sr standardised carrier solution,  $C_{Sr,sol}$  (8.6 %) , and parameters associated with weighing the final source of Sr oxalate (7.6 % each). The most sensible parameters (see the relative sensitivity factors) are those related with weighing the final Sr source and the gross count rate in window A,  $I_{A,CAL}$ . The less sensible parameters are the background count rates in windows A and B “ $I_{A,Bkg}$  and  $I_{B,Bkg}$ ”.

### 3.3. Activity Concentrations

Tables 7-9 show the results obtained when calculating the combined uncertainties in the activity concentrations of  $^{90}Sr$  in Soil-6, IAEA-135 and IAEA-367; respectively. In all cases, the values of the sensitivity factors obtained by both methods are essentially the same. The contribution of each component to the combined uncertainty depends on the sample. In general, the major contributors are mainly those associated with the counting statistics especially  $I_{A,Bkg}$ ,  $I_A$ ,  $I_{B,Bkg}$  and  $I_B$  and in a minor extend with the efficiency “ $\epsilon_{Sr}$ ”. Nevertheless, in IAEA-367 the contribution of the recovery factor becomes important. In Soil-6 and IAEA-135, the most sensible parameters are the count rate in window A “ $I_A$ ” and the background count rate  $I_{A,Bkg}$ . For the sample IAEA-367, which contains higher activity level of  $^{90}Sr$ , the most sensible parameter is the count rate in window A “ $I_A$ ”. In all cases, the less sensible parameter is the tailing parameter  $f_y$ .

Tables 10, 11 and 12 show a summary of all input parameters, their uncertainties, sensitivity factors and contributions to the combined uncertainty in the activity concentrations of  $^{90}Sr$  for Soil-6, IAEA-135 and IAEA-367, respectively.

## LIST OF PARAMETERS, THEIR DEFINITIONS AND UNITS

$I_A$	gross count rate in the region A (channels 25 to 250), (cpm)
$I_B$	gross count rate in the region B (channels 250 to 1000), (cpm)
$I_{A,Bkg}$	background count rate in the region A (channels 25 to 250), (cpm)
$I_{B,Bkg}$	background count rate in the region B (channels 250 to 1000), (cpm)
$m_{ash}$	mass of ashed sample, (kg)
$r_{Sr}$	recovery factor strontium
$f_y$	factor taking into account the Y contribution to the $^{90}Sr$ window
$\epsilon_{Sr}$	efficiency of LSC for measuring $^{90}Sr$
$K$	net count rate of the $^{90}Sr$ in region A corrected for the $^{90}Y$ in-growth, (cpm)
$f_1$	correction for decay of $^{90}Sr$ in the time interval " $t_1$ " from the reference date of the certified reference solution until the beginning of the measurement
$f_2$	correction for decay of $^{90}Sr$ in the counting interval $t_s$
$t_1$	time elapsed from the reference date until the beginning of the measurements, (s)
$t_s$	counting time of the sample, (min)
$t_{s,CAL}$	counting time in the calibration experiment, (min)
$f_g$	gravimetric factor of Sr in monohydrate strontium oxalate ( $SrC_2O_4 \cdot xH_2O$ )
$m_{oxal+pap}$	mass of strontium oxalate and the filter paper, (mg)
$m_{pap}$	mass of filter paper, (mg)
$m_{oxal+pap,CAL}$	mass of strontium oxalate and the filter paper in the calibration experiment, (mg)
$m_{pap,CAL}$	mass of filter paper in the calibration experiment, (mg)
$C_{Sr,sol}$	concentration of the Sr standardized carrier solution, (mg Sr/g solution)
$m_{sol}$	mass of the carrier solution added to the sample, (g)
$m_{sol}$	mass of the carrier solution added to the sample in the calibration experiment, (g)
$C_{Sr,nat}$	concentration of natural strontium in the sample, (mg Sr/g ash sample)
$K_{CAL}$	net count rate of the $^{90}Sr$ in region A corrected for the $^{90}Y$ in-growth in the calibration experiment, (cpm)
$I_{A,CAL}$	gross count rate in A, (cpm)
$I_{B,CAL}$	gross count rate in B, (cpm)
$I_{Y,A}$	gross count rate of $^{90}Y$ in window A
$I_{Y,B}$	gross count rate of $^{90}Y$ in window B
$r_{Sr,CAL}$	recovery factor of Sr in the calibration experiment
$a_{o,Sr}$	known added activity (from a certified standard solution) of $^{90}Sr$ at the time of measurement, (Bq)
$\lambda_{Sr}$	decay constant of $^{90}Sr$ ( $7.63 \times 10^{-10} s^{-1}$ )
$t_{1,CAL}$	time interval from the reference date of the $^{90}Sr/^{90}Y$ certified standard, (s) solution to the beginning of the measurements, (s)
$f_{1,CAL}$	correction for decay of $^{90}Sr$ in the time elapsed from the reference date of the certified reference solution until the beginning of the measurement for the calibration experiment ( $t_{1,CAL}$ )
$f_{dw}$	ratio of dry weight dry to wet ratio
$f_{ad}$	ratio of ashed weight to dry weight
$m_{t1}$	mass of the tare container used for the dry/wet ratio determination, (g)
$m_{t2}$	mass of the tare container used for the ash/wet ratio determination, (g)
$m_{wet,sub1+t1}$	total weight of the wet subsample and the tare container used for the dry/wet ratio determination, (g)
$m_{dry,sub1+t1}$	total weight of the dry subsample and the tare container for the dry/wet ratio determination, (g)
$m_{wet,sub2+t2}$	total weight of the wet subsample and the tare container used for the ash/wet

	ratio determination, (g)
$m_{\text{ash,sub2+t2}}$	total weight of the ash subsample and the tare container used for the ash/wet ratio determination, (g)
$m_{\text{crucible+ash}}$	mass of the crucible and ash, (g)
$m_{\text{crucible}}$	mass of the tare crucible, (g)
$A_{\text{Sr}}$	atomic mass of strontium, (in unified atomic mass units)
$A_{\text{C}}$	atomic mass of carbon, (in unified atomic mass units)
$A_{\text{O}}$	atomic mass of oxygen, (in unified atomic mass units)
$A_{\text{H}}$	atomic mass of hydrogen, (in unified atomic mass units)
$M_{\text{SrC}_2\text{O}_4\cdot\text{H}_2\text{O}}$	molecular weight of strontium oxalate, (in unified atomic mass units)
$u_a$	combined standard uncertainty in the activity concentration of $^{90}\text{Sr}$ , (Bq/kg)
$u_{\text{IA}}$	standard uncertainty of the gross count rate in region A, (cpm)
$u_{\text{IA,Bkg}}$	standard uncertainty of the background count rate in region A, (cpm)
$u_{\text{IB}}$	standard uncertainty of the gross count rate in region B, (cpm)
$u_{\text{IB,Bkg}}$	standard uncertainty of the background count rate in region B, (cpm)
$u_{f_y}$	standard uncertainty of the determination of factor $f_y$
$u_e$	combined standard uncertainty in the determination of the efficiency
$u_{r,\text{Sr}}$	combined standard uncertainty in the determination of the recovery factor
$u_{m,\text{ash}}$	standard uncertainty in weighing the sample, (kg, ash basis)
$u_{f,\text{ad}}$	combined standard uncertainty in the determination of the ash/dry ratio
$u_{t_1}$	standard uncertainty in the determination of $t_1$ , (s)
$u_{f_2}$	standard uncertainty in the determination of factor $f_2$
$u_{\lambda,\text{Sr}}$	uncertainty in the decay constant of $^{90}\text{Sr}$ ( $0.08 \times 10^{-10} \text{ s}^{-1}$ )
$u_{f_g}$	uncertainty in the calculation of the gravimetric factor
$u_{\text{moxal}}$	uncertainty in weighing the strontium oxalate and the filter paper, (mg)
$u_{m,\text{pap}}$	uncertainty in weighing the filter paper, (mg)
$u_{\text{CSr,sol}}$	uncertainty in the concentration of Sr in the carrier solution, (mg Sr/g sol.)
$u_{m,\text{sol}}$	uncertainty in weighing the carrier solution, (g)
$u_{\text{CSr,nat}}$	uncertainty in the concentration of Sr in the sample, (mg Sr/g ash)
$u_{m,\text{ash}}$	uncertainty in weighing the sample by difference, (g)
$u_{t_1,\text{CAL}}$	standard uncertainty in the determination of $t_{1,\text{CAL}}$ (s)
$u_{\text{moxal+pap,CAL}}$	uncertainty in weighing the strontium oxalate and the filter paper in the calibration experiment, (mg)
$u_{\text{mpap,CAL}}$	uncertainty in weighing the filter paper in the calibration experiment, (mg)
$u_{\text{CSr,sol}}$	uncertainty in the concentration of Sr in the carrier solution, (mg Sr/g sol.)
$u_{\text{msol,CAL}}$	uncertainty in weighing the carrier solution, (g)
$u_{f,\text{dw}}$	uncertainty in the determination of the dry/wet ratio
$u_{f,\text{ad}}$	uncertainty in the determination of the ash/dry ratio
$u_{m,\text{wet,sub}}$	uncertainty in weighing the wet subsample, (g)
$u_{m,\text{dry,sub}}$	uncertainty in weighing the dry subsample, (g)
$u_{f,\text{dw}}$	combined uncertainty in the determination of the dry/wet ratio
$u_{f,\text{aw}}$	combined uncertainty in the determination of the ash/wet ratio
$u_{m,\text{wet,sub1+t1}}$	uncertainty in weighing the wet subsample and the tare container (dry/wet determination), (g)
$u_{m,\text{dry,sub1+t1}}$	uncertainty in weighing the dry subsample and the tare container (dry/wet determination), (g)
$u_{\text{mt1}}$	uncertainty in weighing the tare container used for the dry/wet ratio determination, (g)
$u_{\text{mt1}}$	uncertainty in weighing the tare container used for the dry/wet ratio determination, (g)

$u_{f,dw}$	combined uncertainty in the determination of the dry/wet ratio combined uncertainty in the determination of the ash/wet ratio
$u_{mwet,sub2+t2}$	uncertainty in weighing the wet subsample and the tare container (ash/wet determination), (g)
$u_{mash,sub2+t2}$	uncertainty in weighing the ash subsample and the tare container (ash/wet determination), (g)
$u_{mt2}$	uncertainty in weighing the tare container used for the ash/wet ratio determination, (g)
$u_{f,aw}$	combined uncertainty in the determination of the ash/wet ratio combined uncertainty in the determination of the ash/wet ratio
$u_1$	uncertainties associated with the variability of weights by difference in the corresponding region, (kg)
$u_2$	uncertainties associated with the calibration of the balance, (kg)
$u_{t1,CAL}$	standard uncertainty in the determination of $t_{1,CAL}$ , (s)
$u_{\lambda,Sr}$	uncertainty in the decay constant of $^{90}\text{Sr}$ ( $0.08 \times 10^{-10} \text{ s}^{-1}$ )
$\partial y / \partial x_i$	partial derivatives or sensitivity factors of the output parameters (recovery factor, efficiency, activity concentration) with respect to all the input parameters $x_i$
RSF	relative sensitivity factor defined as the relative change in the output quantity $y$ divided by the relative change in the input quantity $x_i$

Table 3. Spreadsheet method for uncertainty calculation in the recovery factor (Soil-6)

	Parameter $x_i$	$m_{sol}$	$C_{Sr,sol}$	$C_{Sr,nat}$	$m_{ash}$	$f_g$	$m_{pap}$	$m_{pap+oxal}$
Sample	Unit	g	mg/g	mg/g	g		mg	mg
Soil-6	Value $x_i$	10.509	0.9660	0.108	5.128	0.4525	35.85	54.02
	$u_{x_i}$	9.E-05	0.0050	0.004	9.E-05	3.29E-05	0.09	0.09
Parameter $x_i$								
$m_{sol}$	10.509	<b>10.509</b>	10.509	10.509	10.509	10.509	10.509	10.509
$C_{Sr,sol}$	0.966	0.966	<b>0.9710</b>	0.966	0.966	0.966	0.966	0.966
$C_{Sr,nat}$	0.108	0.108	0.1080	<b>0.112</b>	0.108	0.108	0.108	0.108
$m_{ash}$	5.128	5.128	5.128	5.128	<b>5.128</b>	5.128	5.128	5.128
$f_g$	0.4525	0.4525	0.4525	0.4525	0.4525	<b>0.4525</b>	0.4525	0.4525
$m_{pap}$	35.85	35.850	35.8500	35.85	35.85	35.85	<b>35.94</b>	35.85
$m_{pap+oxal}$	54.02	54.020	54.0200	54.02	54.02	54.02	54.02	<b>54.11</b>
$r_{Sr}$	<b>0.768</b>	<b>0.768</b>	<b>0.764</b>	<b>0.766</b>	<b>0.768</b>	<b>0.768</b>	<b>0.764</b>	<b>0.772</b>
$m_{Sr,carrier} + m_{Sr,nat}$	10.7							
$r_{i,Sr} - r_{Sr}$		-6.24E-06	-3.75E-03	-1.47E-03	-6.97E-07	5.58E-05	-3.80E-03	3.80E-03
$S(r_{i,Sr} - r_{Sr})^2$		4.52E-05	3.89E-11	1.41E-05	2.16E-06	4.86E-13	3.11E-09	1.45E-05
$u_{r,Sr}$	<b>0.007</b>							
$u_{r,Sr}/r_{Sr}$ , %	0.88							
SF by Kragten	$\delta r_{Sr}/\delta x_i$	-0.069	-0.750	-0.367	-0.008	1.697	-0.042	0.042
SF by Differentiation	$\delta r_{Sr}/\delta x_i$	-0.069	-0.754	-0.368	-0.008	1.697	-0.042	0.042
Contribution, %	$[(\delta r_{Sr}/\delta x_i)^2 \cdot u_{x_i}^2] \cdot 100/u_{r,Sr}^2$	0.000	31.15	4.78	0.000	0.007	32.03	32.03
RSF, %	$(\delta r_{Sr}/\delta x_i) \cdot y/x_i$	-0.95	-0.95	-0.05	-0.05	1.00	-1.98	2.96
	$[(\delta r_{Sr}/\delta x_i)^2 \cdot u_{x_i}^2]$	3.89E-11	1.42E-05	2.17E-06	4.86E-13	3.11E-09	1.45E-05	1.45E-05
$U_{r,Sr}$ Algebraic M.	<b>0.007</b>							

See explanation of symbols in section 4.

Table 4: Spreadsheet method for uncertainty calculation in the recovery factor (IAEA-135)

	Parameter $x_i$	$m_{sol}$	$C_{Sr,sol}$	$C_{Sr,nat}$	$m_{ash}$	$f_g$	$m_{pap}$	$m_{pap+oxal}$
Sample	Unit	g	mg/g	mg/g	g		mg	mg
IAEA-135	Value $x_i$	10.37	0.9660	0.187	1.09	0.4525	34.86	53.80
	$u_{x_i}$	9.E-05	0.0050	0.0044	9.E-05	3.29E-05	0.09	0.09
Parameter $x_i$								
$m_{sol}$	10.37	<b>10.37</b>	10.37	10.37	10.37	10.37	10.37	10.37
$C_{Sr,sol}$	0.966	0.966	<b>0.9710</b>	0.966	0.966	0.966	0.966	0.966
$C_{Sr,nat}$	0.187	0.187	0.1870	<b>0.1914</b>	0.187	0.187	0.187	0.187
$m_{ash}$	1.09	1.093	1.0929	1.09	<b>1.09296</b>	1.09	1.09	1.09
$f_g$	0.4525	0.4525	0.4525	0.4525	0.4525	<b>0.4525</b>	0.4525	0.4525
$m_{pap}$	34.862	34.862	34.8620	34.862	34.862	34.862	<b>34.949</b>	34.862
$m_{pap+oxal}$	53.804	53.804	53.8040	53.804	53.804	53.804	53.804	<b>53.891</b>
$r_{Sr}$	<b>0.838</b>	<b>0.838</b>	<b>0.834</b>	<b>0.838</b>	<b>0.838</b>	<b>0.838</b>	<b>0.835</b>	<b>0.842</b>
$m_{Sr,carrier} + m_{Sr,nat}$	10.2							
$r_{i,Sr} - r_{Sr}$		-7.13E-06	-4.23E-03	-3.94E-04	-1.38E-06	6.09E-05	-3.85E-03	3.85E-03
$\Sigma(r_{i,Sr} - r_{Sr})^2$		4.77E-05	5.08E-11	1.79E-05	1.55E-07	1.91E-12	3.71E-09	1.48E-05
$u_{r,Sr}$	<b>0.007</b>							
$u_{r,Sr}/r_{Sr}$ , %	0.82							
<b>SF by Kragten</b>	$\delta r_{Sr}/\delta x_i$	-0.079	-0.846	-0.090	-0.015	1.853	-0.044	0.044
<b>SF by Differentiation</b>	$\delta r_{Sr}/\delta x_i$	-0.079	-0.851	-0.090	-0.015	1.853	-0.044	0.044
<b>Contribution, %</b>	$[(\delta r_{Sr}/\delta x_i)^2 \cdot u_{x_i}^2] \cdot 100 / u_{r,Sr}^2$	0.000	37.52	0.33	0.000	0.008	31.07	31.07
<b>RSF, %</b>	$(\delta r_{Sr}/\delta x_i) \cdot y / x_i$	-0.98	-0.98	-0.02	-0.02	1.00	-1.85	2.83
	$[(\delta r_{Sr}/\delta x_i)^2 \cdot u_{x_i}^2]$	5.08E-11	1.81E-05	156E-07	1.91E-12	3.71E-09	1.48E-05	1.48E-05
<b><math>u_{r,Sr}</math> Algebraic M.</b>	<b>0.007</b>							

See explanation of symbols in section 4.

Table 5 Spreadsheet method for uncertainty calculation in the recovery factor (IAEA-367)

	Parameter $x_i$	$m_{sol}$	$C_{Sr,sol}$	$C_{Sr,nat}$	$m_{ash}$	$f_g$	$m_{pap}$	$m_{pap+oxal}$
Sample	Unit	g	mg/g	mg/g	g		mg	mg
IAEA-367	Value $x_i$	10.421	0.9660	4.48	5.029	0.4525	33.96	76.2
	$u_{x_i}$	9.E-05	0.0050	0.14	9.E-05	3.29E-05	0.09	0.09
Parameter $x_i$								
$m_{sol}$	10.42	<b>10.42</b>	10.42	10.42	10.42	10.42	10.42	10.42
$C_{Sr,sol}$	0.966	0.966	<b>0.971</b>	0.966	0.966	0.966	0.966	0.966
$C_{Sr,nat}$	4.48	4.48	4.48	<b>4.615</b>	4.48	4.48	4.48	4.48
$m_{ash}$	5.029	5.029	5.0290	5.029	<b>5.029</b>	5.029	5.029	5.029
$f_g$	0.4525	0.4525	0.4525	0.4525	0.4525	<b>0.452</b>	0.4525	0.4525
$m_{pap}$	33.96	33.960	33.9600	33.96	33.96	33.96	<b>34.050</b>	33.960
$m_{pap+oxal}$	76.2	76.200	76.2000	76.2	76.2	76.2	76.2	<b>76.290</b>
$r_{i,Sr} - r_{Sr}$								
$r_{Sr}$	<b>0.586</b>	<b>0.586</b>	<b>0.585</b>	<b>0.574</b>	<b>0.586</b>	<b>0.586</b>	<b>0.585</b>	<b>0.588</b>
$m_{Sr,carrier} + m_{Sr,nat}$	32.6							
$r_{i,Sr} - r_{Sr}$		-1.56E-06	-9.36E-04	-1.20E-02	-7.25E-06	4.26E-05	-1.25E-03	1.25E-03
$\Sigma(r_{i,Sr} - r_{Sr})^2$	1.47E-04	2.45E-12	8.76E-07	1.43E-04	5.26E-11	1.81E-09	1.56E-06	1.56E-06
$u_{r,Sr}$	<b>0.012</b>							
$u_{r,Sr}/r_{Sr}$ , %	2.07							
<b>SF by Kragten</b>	$\delta r_{Sr}/\delta x_i$	-0.017	-0.187	-0.089	-0.081	1.296	-0.014	0.014
<b>SF by Differentiation</b>	$\delta r_{Sr}/\delta x_i$	-0.017	-0.187	-0.090	-0.081	1.296	-0.014	0.014
<b>Contribution, %</b>	$[(\delta r_{Sr}/\delta x_i)^2 \cdot u_{x_i}^2] \cdot 100/u_{r,Sr}^2$	0.000	0.60	97.28	0.000	0.001	1.06	1.06
<b>RSF, %</b>	$(\delta r_{Sr}/\delta x_i) \cdot y/x_i$	-0.31	-0.31	-0.69	-0.69	1.00	-0.81	1.80
	$[(\delta r_{Sr}/\delta x_i)^2 \cdot u_{x_i}^2]$	2.45E-12	8.78E-07	1/49E-04	5.26E-11	1.81E-09	1.56E-06	1.56E-06
<b><math>U_{r,Sr}</math> Algebraic M.</b>	<b>0.012</b>							

See explanation of symbols in section 4.

Table 6 Spreadsheet method for uncertainty calculation in the efficiency of the liquid-scintillation counter for the detection of <sup>90</sup>Sr

Parameter x <sub>i</sub>	t <sub>s,CALSr</sub>	m <sub>sol,CAL</sub>	C <sub>Sr,sol</sub>	f <sub>g</sub>	m <sub>pap,CAL</sub>	m <sub>paper+oxal,CAL</sub>	a <sub>o,Sr</sub>	I <sub>Y,A</sub>	I <sub>Y,B</sub>	I <sub>B,CAL</sub>	I <sub>B,Bkg</sub>	I <sub>A,CAL</sub>	I <sub>A,Bkg</sub>	λ <sub>Sr</sub>	t <sub>1,CALSr</sub>	
Unit	min	g	mg/g		mg	mg	dpm	cpm	cpm	cpm	cpm	cpm	cpm	s <sup>-1</sup>	s	
Value x <sub>i</sub>	100	10.30	0.966	0.45245	34.96	53.56	634.59	82.5	159.1	79.10	5.05	349.7	7.1	7.63E-10	2.26E+08	
u <sub>xi</sub>	0	9E-05	0.005	0.00003	0.09	0.09	8.884	0.9	1.3	0.89	0.30	1.9	0.3	8.00E-12	3.00E+02	
<b>Parameter x<sub>i</sub></b>																
m <sub>sol,CAL</sub>	10.30	<b>10.30</b>	10.30	10.30	10.30	10.30	10.30	10.30	10.30	10.30	10.30	10.30	10.30	10.30	10.30	
C <sub>Sr,sol</sub>	0.966	0.966	<b>0.97</b>	0.966	0.966	0.966	0.966	0.966	0.966	0.966	0.966	0.966	0.966	0.966	0.966	
f <sub>g</sub>	0.4525	0.4525	0.4525	<b>0.4525</b>	0.4525	0.4525	0.4525	0.4525	0.4525	0.4525	0.4525	0.4525	0.4525	0.4525	0.4525	
m <sub>pap,CAL</sub>	34.96	34.96	34.96	34.96	<b>35.05</b>	34.96	34.96	34.96	34.96	34.96	34.96	34.96	34.96	34.96	34.96	
m <sub>pap+oxal,CAL</sub>	53.56	53.56	53.56	53.56	53.56	<b>53.65</b>	53.56	53.56	53.56	53.56	53.56	53.56	53.56	53.56	53.56	
a <sub>o,Sr</sub>	634.59	634.59	634.59	634.59	634.59	634.59	<b>643.48</b>	634.59	634.59	634.59	634.59	634.59	634.59	634.59	634.59	
I <sub>Y,A</sub>	82.53	82.53	82.53	82.53	82.53	82.53	82.53	<b>83.44</b>	82.53	82.53	82.53	82.53	82.53	82.53	82.53	
I <sub>Y,B</sub>	159.12	159.12	159.12	159.12	159.12	159.12	159.12	159.12	<b>160.38</b>	159.12	159.12	159.12	159.12	159.12	159.12	
I <sub>B,CAL</sub>	79.10	79.10	79.10	79.10	79.10	79.10	79.10	79.10	79.10	<b>79.99</b>	79.10	79.10	79.10	79.10	79.10	
I <sub>B,Bkg</sub>	5.05	5.05	5.05	5.05	5.05	5.05	5.05	5.05	5.05	5.05	<b>5.35</b>	5.05	5.05	5.05	5.05	
I <sub>A,CAL</sub>	349.73	349.73	349.73	349.73	349.73	349.73	349.73	349.73	349.73	349.73	349.73	<b>351.60</b>	349.73	349.73	349.73	
I <sub>A,Bkg</sub>	7.09	7.09	7.09	7.09	7.09	7.09	7.09	7.09	7.09	7.09	7.09	7.09	<b>7.39</b>	7.09	7.09	
λ <sub>Sr</sub>	7.63E-10	7.63E-10	7.63E-10	7.63E-10	7.63E-10	7.63E-10	7.63E-10	7.63E-10	7.63E-10	7.63E-10	7.63E-10	7.63E-10	7.63E-10	<b>7.71E-10</b>	7.63E-10	
t <sub>1,CALSr</sub>	2.26E+08	2.26E+08	2.26E+08	2.26E+08	2.26E+08	2.26E+08	2.26E+08	2.26E+08	2.26E+08	2.26E+08	2.26E+08	2.26E+08	2.26E+08	2.26E+08	<b>2.26E+08</b>	
ε <sub>Sr</sub>	<b>0.678</b>	<b>0.678</b>	<b>0.682</b>	<b>0.678</b>	<b>0.681</b>	<b>0.675</b>	<b>0.669</b>	<b>0.677</b>	<b>0.679</b>	<b>0.677</b>	<b>0.678</b>	<b>0.682</b>	<b>0.678</b>	<b>0.679</b>	<b>0.678</b>	
<b>K<sub>CAL, cpm</sub></b>	<b>306.382</b>															
ε <sub>Sr</sub>	<b>0.678</b>	ε <sub>i,Sr</sub> - ε <sub>Sr</sub>	5.93E-06	3.51E-03	-4.93E-05	3.30E-03	-3.27E-03	-9.36E-03	-9.66E-04	6.52E-04	-9.64E-04	1.69E-04	4.14E-03	-3.45E-04	1.23E-03	1.55E-07
Σ(ε <sub>i,Sr</sub> - ε <sub>Sr</sub> ) <sup>2</sup>	<b>1.43E-04</b>	(ε <sub>i,Sr</sub> - ε <sub>Sr</sub> ) <sup>2</sup>	3.51E-11	1.23E-05	2.43E-09	1.09E-05	1.07E-05	8.77E-05	9.34E-07	4.25E-07	9.29E-07	2.86E-08	1.71E-05	1.19E-07	1.50E-06	2.41E-14
u <sub>e</sub> Num. M.	<b>0.012</b>															
u <sub>e</sub> /ε <sub>Sr</sub> , %	<b>1.8</b>															
SF by Kragten	δe/δx <sub>i</sub>	0.066	0.702	-1.499	0.037	-0.036	-0.0011	-0.0011	0.00052	-0.0011	0.00056	0.0022	-0.0011	1.53E+08	5.17E-10	
SF by Differenti.	δe/δx <sub>i</sub>	0.066	0.702	<b>-1.499</b>	0.036	-0.036	-0.0011	-0.0011	0.00052	-0.0011	0.00056	0.0022	-0.0011	1.53E+08	5.17E-10	
Contribution, %	$\frac{[(\delta e/\delta x_i)^2 \cdot u_{xi}^2]}{100/u_e^2}$	0.00	8.64	0.00	7.55	7.55	63.21	0.65	0.30	0.65	0.02	12.02	0.08	1.05	0.00	
RSF, %	(δy/δx <sub>i</sub> ).y/x <sub>i</sub>	1.00	0.99	-1.00	1.88	-2.88	-1.00	-0.13	0.12	-0.13	0.00	1.13	-0.01	0.17	0.17	
u <sub>e</sub> Algebr. M.	<b>0.012</b>	$[(\delta e/\delta x_i)^2 \cdot u_{xi}^2]$	3.51E-11	1.23E-05	2.43E-09	1.08E-05	1.08E-05	9.34E-07	9.34E-07	4.32E-07	9.29E-07	2.85E-08	1.71E-05	1.19E-071	1.50E-06	2.41E-14
SF – Sens. Fact.		<b>RSF - Relative Sensitivity Factor ( relative change in the output quantity y divided by the relative change in the input quantity x<sub>i</sub>)</b>														

See explanation of symbols in section 4.

Table 7 Spreadsheet method for uncertainty calculation in the activity concentration (Soil-6)

	Parameter $x_i$	$m_{ash}$	$f_{ad}$	$r_{Sr}$	$\epsilon_{Sr}$	$f_y$	$I_B$	$I_{B,Bkg}$	$I_A$	$I_{A,Bkg}$	$\lambda_{Sr}$	$t_{1,Sr}$
	Unit	kg					cpm	cpm	cpm	cpm	$s^{-1}$	s
<b>Sample</b>	<b>Value <math>x_i</math></b>	5.13E-03	0.97140	0.768	0.675	0.49	6.89	5.05	11.12	7.09	7.63E-10	4.84E+08
<b>SOIL-6</b>	<b><math>u_{xi}</math></b>	9.00E-08	0.00060	0.007	0.012	0.01	0.13	0.27	0.17	0.27	8.00E-12	3.60E+03
<b><math>t_{Sr}</math>, min</b>	400											
<b><math>m_{ash}</math></b>	5.13E-03	<b>0.005</b>	0.00513	0.0051	0.0051	0.0051	0.0051	0.0051	0.0051	0.0051	0.0051	0.0051
<b><math>f_{ad}</math></b>	9.71E-01	0.9714	<b>0.972</b>	0.9714	0.9714	0.9714	0.9714	0.9714	0.9714	0.9714	0.9714	0.9714
<b><math>r_{Sr}</math></b>	0.768	0.768	0.768	<b>0.775</b>	0.768	0.768	0.768	0.768	0.768	0.768	0.768	0.768
<b><math>\epsilon_{Sr}</math></b>	0.675	0.675	0.675	0.675	<b>0.687</b>	0.675	0.675	0.675	0.675	0.675	0.675	0.675
<b><math>f_y</math></b>	<b>0.49</b>	0.49	0.49	0.49	0.49	<b>0.498</b>	0.49	0.49	0.49	0.49	0.49	0.49
<b><math>I_B</math></b>	6.89	6.89	6.89	6.89	6.89	6.89	<b>7.021</b>	6.89	6.89	6.89	6.89	6.89
<b><math>I_{B,Bkg}</math></b>	5.05	5.05	5.05	5.05	5.05	5.05	5.05	<b>5.320</b>	5.05	5.05	5.05	5.05
<b><math>I_A</math></b>	11.12	11.12	11.12	11.12	11.12	11.12	11.12	11.12	<b>11.287</b>	11.12	11.12	11.12
<b><math>I_{A,Bkg}</math></b>	7.09	7.09	7.09	7.09	7.09	7.09	7.09	7.09	7.09	<b>7.360</b>	7.09	7.09
<b><math>\lambda_{Sr}</math></b>	7.63E-10	7.63E-10	7.63E-10	7.63E-10	7.63E-10	7.63E-10	7.63E-10	7.63E-10	7.63E-10	7.63E-10	<b>7.71E-10</b>	7.63E-10
<b><math>t_{1,Sr}</math></b>	4.84E+08	4.84E+08	4.84E+08	4.84E+08	4.84E+08	4.84E+08	4.84E+08	4.84E+08	4.84E+08	4.84E+08	4.84E+08	<b>4.84E+08</b>
<b>A</b>	<b>27.6</b>	<b>27.56</b>	<b>27.58</b>	<b>27.31</b>	<b>27.09</b>	<b>27.44</b>	<b>26.99</b>	<b>28.73</b>	<b>29.03</b>	<b>25.18</b>	<b>27.67</b>	<b>27.56</b>
<b><math>a_i - a</math></b>		-4.84E-04	1.70E-02	-2.49E-01	-4.73E-01	-1.24E-01	-5.67E-01	1.17E+00	1.47E+00	-2.38E+00	1.07E-01	7.57E-05
<b><math>K_i</math>, cpm</b>	<b>3.1284</b>	2.34E-07	2.90E-04	6.20E-02	2.24E-01	1.53E-02	3.21E-01	1.36E+00	2.16E+00	5.66E+00	1.15E-02	5.73E-09
<b><math>\Sigma(a_i - a)^2</math></b>	<b>9.807</b>	<b><math>(a_i - a)^2</math></b>										
<b><math>u_a</math> Bq/kg</b>	<b>3.1</b>											
<b><math>u_a/\alpha_i</math>, %</b>	<b>11.36</b>											
<b>SF by Kragten</b>	$\delta a/\delta x_i$	-5373.47	28.37	-35.56	-39.41	-16.21	-4.32	4.32	8.81	-8.81	1.34E+10	0.00
<b>SF by Differentiation</b>	$\delta a/\delta x_i$	-5373.57	28.37	-35.89	-40.82	-16.21	-4.32	4.32	8.81	-8.81	1.34E+10	0.00
<b>Contribution, %</b>	$[(\delta a/\delta x_i)^2 \cdot u_{xi}^2] \cdot 100/u_a^2$	0.00	0.00	0.64	2.44	0.16	3.27	13.83	21.96	57.59	0.12	0.00
	$(\delta a/\delta x_i)^2 \cdot u_{xi}^2$	0.00	0.00	0.06	0.24	0.02	0.32	1.36	2.16	5.66	1.1E-02	5.7E-09
<b>RSF</b>	$(\delta a/\delta x_i) \cdot (a/x_i)$	-1.00	1.00	-1.00	-1.00	-0.29	-1.08	0.79	3.55	-2.27	0.37	0.37
<b><math>S(a_i - a)^2</math></b>	<b>9.825</b>											
<b><math>u_a</math> Bq/kg</b>	<b>3.1</b>											
<b><math>u_a/a</math>, %</b>	<b>11.37</b>											
<b>SF-Sensitivity Factor</b>		RSF – Relative Sensitivity Factor (relative change in the output quantity y divided by the relative change in the input quantity xi) Reference Date 30/1/83										

See explanation of symbols in section 4.

Table 8 Spreadsheet method for uncertainty calculation of the activity concentration of Sr-90 in IAEA-135

	Parameter $x_i$	$m_{ash}$	$f_{ad}$	$r_{Sr}$	$\epsilon_{Sr}$	$f_y$	$I_B$	$I_{B,Bkg}$	$I_A$	$I_{A,Bkg}$	$\lambda_{Sr}$	$T_{1,Sr}$
	Unit	kg					cpm	cpm	cpm	cpm	$s^{-1}$	s
<b>Sample</b>	<b>Value <math>x_i</math></b>	1.09E-03	0.9075	0.838	0.675	0.49	5.65	5.05	9.58	7.09	7.63E-10	2.03E+08
<b>IAEA-135</b>	<b><math>u_{xi}</math></b>	9.00E-08	0.001	0.007	0.012	0.01	0.12	0.27	0.15	0.13	8.00E-12	3.60E+03
<b><math>t_{Sr}</math>, min</b>	400											
<b><math>m_{ash}</math></b>	0.00109	<b>0.0011</b>	0.0011	0.0011	0.0011	0.0011	0.0011	0.0011	0.0011	0.0011	0.0011	0.0011
<b><math>f_{ad}</math></b>	0.9075	0.9075	<b>0.9085</b>	0.9075	0.9075	0.9075	0.9075	0.9075	0.9075	0.9075	0.9075	0.9075
<b><math>r_{Sr}</math></b>	0.838	0.838	0.838	<b>0.8450</b>	0.838	0.838	0.838	0.838	0.838	0.838	0.838	0.838
<b><math>\epsilon_{Sr}</math></b>	0.675	0.675	0.675	0.675	<b>0.687</b>	0.675	0.675	0.675	0.675	0.675	0.675	0.675
<b><math>f_y</math></b>	0.49	0.49	0.49	0.49	0.49	<b>0.4976</b>	0.49	0.49	0.49	0.49	0.49	0.49
<b><math>I_B</math></b>	5.65	5.65	5.65	5.65	5.65	5.65	<b>5.77</b>	5.65	5.65	5.65	5.65	5.65
<b><math>I_{B,Bkg}</math></b>	5.05	5.05	5.05	5.05	5.05	5.05	5.05	<b>5.32</b>	5.05	5.05	5.05	5.05
<b><math>I_A</math></b>	9.58	9.58	9.58	9.58	9.58	9.58	9.58	9.58	<b>9.73</b>	9.58	9.58	9.58
<b><math>I_{A,Bkg}</math></b>	7.09	7.09	7.09	7.09	7.09	7.09	7.09	7.09	7.09	<b>7.22</b>	7.09	7.09
<b><math>\lambda_{Sr}</math></b>	7.63E-10	7.63E-10	7.63E-10	7.63E-10	7.63E-10	7.63E-10	7.63E-10	7.63E-10	7.63E-10	7.63E-10	<b>7.71E-10</b>	7.63E-10
<b><math>t_{1,Sr}</math></b>	2.03E+08	2.03E+08	2.03E+08	2.03E+08	2.03E+08	2.03E+08	2.03E+08	2.03E+08	2.03E+08	2.03E+08	2.03E+08	<b>2.03E+08</b>
<b>A</b>	<b>62.7</b>	<b>62.69</b>	<b>62.77</b>	<b>62.18</b>	<b>61.62</b>	<b>62.57</b>	<b>61.03</b>	<b>66.47</b>	<b>67.12</b>	<b>58.90</b>	<b>62.80</b>	<b>62.70</b>
<b><math>a_i - a</math></b>		-5.16E-03	6.91E-02	-5.19E-01	-1.08E+00	-1.31E-01	-1.66E+00	3.78E+00	4.42E+00	-3.80E+00	1.02E-01	1.72E-04
<b>K, cpm</b>	<b>2.196</b>	2.67E-05	4.77E-03	2.70E-01	1.16E+00	1.71E-02	2.76E+00	1.43E+01	1.95E+01	1.44E+01	1.04E-02	2.97E-08
<b><math>S(a_i - a)^2</math></b>	<b>52.462</b>	<b><math>(a_i - a)^2</math></b>										
<b><math>u_a</math> Bq/kg</b>	<b>7.2</b>											
<b><math>u_a/a</math>, %</b>	<b>11.6</b>											
<b>SF by Kragten</b>	$\delta a/\delta x_i$	-57362.92	69.09	-74.20	-89.65	-17.13	-13.99	13.99	28.55	-28.55	1.27E+10	0.00
<b>SF by Differentiation</b>	$\delta a/\delta x_i$	-57367.64	69.09	-74.82	-92.86	-17.13	-13.99	13.99	28.55	-28.55	1.27E+10	0.00
<b>Contribution, %</b>	$[(\delta a/\delta x_i)^2 \cdot u_{xi}^2] \cdot 100/u_a^2$	0.00	0.01	0.52	2.36	0.03	5.26	27.15	37.15	27.49	0.02	0.00
	$(\delta a/\delta x_i)^2 \cdot u_{xi}^2$	0.00	0.00	0.27	1.24	0.02	2.76	14.27	19.52	14.45	1.0E-02	3.0E-08
<b>RSF</b>	$(\delta a/\delta x_i) \cdot (a/x_i)$	-1.00	1.00	-1.00	-1.00	-0.13	-1.26	1.13	4.36	-3.23	0.15	0.15
<b><math>S(a_i - a)^2</math></b>	<b>52.551</b>											
<b><math>u_a</math> Bq/kg</b>	<b>7.2</b>											
<b><math>u_a/a</math>, %</b>	<b>11.6</b>											
<b>SF – Sensitivity Factor</b>		RSF – Relative Sensitivity Factor (relative change in the output quantity y divided by the relative change in the input quantity xi) Ref.Date 1/1/92										

See explanation of symbols in section 4.

Table 9 Spreadsheet method for uncertainty calculation of the activity concentration of Sr-90 in IAEA-367

	Parameter $x_i$	$m_{ash}$	$f_{ad}$	$r_{Sr}$	$\epsilon_{Sr}$	$f_y$	$I_B$	$I_{B,Bkg}$	$I_A$	$I_{A,Bkg}$	$\lambda_{Sr}$	$t_{1,Sr}$
	Unit	kg					cpm	cpm	cpm	cpm	$s^{-1}$	s
Sample	Value $x_i$	5.03E-03	0.9287	0.586	0.675	0.49	7.97	5.05	19.82	7.09	7.63E-10	2.66E+08
IAEA-367	$u_{x_i}$	9.00E-08	0.0004	0.012	0.012	0.01	0.14	0.27	0.22	0.27	8.00E-12	3.60E+03
$t_{Sr, min}$	400											
$m_{ash}$	0.0050	0.0050	0.0050	0.0050	0.0050	0.0050	0.0050	0.0050	0.0050	0.0050	0.0050	0.0050
$f_{ad}$	0.9287	0.9287	0.9291	0.9287	0.9287	0.9287	0.9287	0.9287	0.9287	0.9287	0.9287	0.9287
$r_{Sr}$	0.586	0.586	0.586	0.5980	0.586	0.586	0.586	0.586	0.586	0.586	0.586	0.586
$\epsilon_{Sr}$	0.675	0.675	0.675	0.675	0.6872	0.675	0.675	0.675	0.675	0.675	0.675	0.675
$f_y$	0.49	0.49	0.49	0.49	0.49	0.4976	0.49	0.49	0.49	0.49	0.49	0.49
$I_B$	7.97	7.97	7.97	7.97	7.97	7.97	8.1112	7.97	7.97	7.97	7.97	7.97
$I_{B,Bkg}$	5.05	5.05	5.05	5.05	5.05	5.05	5.05	5.3200	5.05	5.05	5.05	5.05
$I_A$	19.82	19.82	19.82	19.82	19.82	19.82	19.82	19.82	20.0426	19.82	19.82	19.82
$I_{A,Bkg}$	7.09	7.09	7.09	7.09	7.09	7.09	7.09	7.09	7.09	7.3600	7.09	7.09
$\lambda_{Sr}$	7.63E-10	7.63E-10	7.63E-10	7.63E-10	7.63E-10	7.63E-10	7.63E-10	7.63E-10	7.63E-10	7.63E-10	7.71E-10	7.63E-10
$t_{1,Sr}$	2.6587E+08	2.6587E+08	2.6587E+08	2.6587E+08	2.6587E+08	2.6587E+08	2.6587E+08	2.6587E+08	2.6587E+08	2.6587E+08	2.6587E+08	2.6587E+08
A	107.7	107.66	107.71	105.50	105.78	107.45	107.00	108.92	109.78	105.09	107.89	107.66
$a_i - a$		0.00	0.05	-2.16	-1.88	-0.21	-0.66	1.26	2.12	-2.57	0.23	2.96E-04
$K, cpm$	11.30	3.71E-06	2.15E-03	4.67E+00	3.53E+00	4.51E-02	4.34E-01	1.59E+00	4.50E+00	6.62E+00	0.052546822	8.74521E-08
$S(a_i - a)^2$	21.442	$(a_i - a)^2$										
$u_a$ Bq/kg	4.6											
$u_a/a, \%$	4.3											
SF by Kragten	$\delta a/\delta x_i$	-2.141E+04	115.92	-180.03	-156.66	-27.82	-4.67	4.67	9.53	-9.53	2.87E+10	8.21E-08
SF by Different.	$\delta a/\delta x_i$	-2.141E+04	115.92	-183.72	-159.45	-27.82	-4.67	4.67	9.53	-9.53	2.86E+10	8.21E-08
Contribution, %	$[(\delta a/\delta x_i)^2 \cdot u_{x_i}^2] \cdot 100/u_a^2$	0.00	0.01	22.34	16.82	0.21	2.00	7.30	20.67	30.41	0.24	0.00
	$(\delta a/\delta x_i)^2 \cdot u_{x_i}^2$	0.00	0.00	4.86	3.66	0.05	0.43	1.59	4.50	6.62	0.05	0.00
RSF	$(\delta a/\delta x_i) \cdot (a/x_i)$	-1.00	1.00	-1.00	-1.00	-0.13	-0.35	0.22	1.75	-0.63	0.20	0.20
$S(a_i - a)^2$	21.76	1.71E-05	0.01	22.34	16.82	0.21	2.00	7.30	20.67	30.41	0.24	0.00
$u_a$ Bq/kg	4.7											
$u_a/a, \%$	4.33											
SF – Sens. Fact.		RSF – Relative Sensitivity Factor (relative change in the output quantity y divided by the relative change in the input quantity xi)										Ref.Date 1/1/90

See explanation of symbols in section 4.

Table 10. Quantifying Uncertainties in Soil-6 (Reference Date 30/January/1983) [7]

Symbol/ Reference to list	Value of variable	Uncertainty	Conversion factor to standard uncertainty	Standard uncertainty (u)	Sensitivity factor	Percent contribution to (u <sub>c</sub> ) <sup>2</sup>
m <sub>ash</sub> ; kg	5.13E-03	9E-08	1.0	9E-08	-5374	0.00
f <sub>ad</sub>	9.7914E-01	6.0E-03	1.0	6.0E-03	28.37	0.00
r <sub>Sr</sub>	0.768	0.007	1.0	0.007	-35.89	0.64
ε <sub>Sr</sub>	0.675	0.012	1.0	0.012	-40.82	2.44
f <sub>y</sub>	0.490	0.008	1.0	0.008	-16.21	0.16
I <sub>B</sub> ; cpm	6.89	0.13	1.0	0.13	-4.32	3.27
I <sub>B,Bkg</sub> ; cpm	5.05	0.27	1.0	0.27	+4.32	13.83
I <sub>A</sub> ; cpm	11.12	0.17	1.0	0.17	+8.81	21.96
I <sub>A,Bkg</sub> ; cpm	7.09	0.27	1.0	0.27	-8.81	57.59
λ <sub>Sr</sub> ; s <sup>-1</sup>	7.63E-10	8.00E-12	1.0	8.00E-12	+1.3E10	0.012
t <sub>1/2</sub> ; s	4.84E+8	3.60E+3	1.0	3.60E+3	+2.1E-8	0.00
a ± u <sub>a</sub> , Bq/kg	27.6 ± 3.1					

Table 11. Quantifying Uncertainties in IAEA-135 (Reference Date 1/January/1992)

Symbol/ Reference to list	Value of variable	Uncertainty	Conver sion factor to standard uncertainty	Standard uncertainty (u)	Sensitivity factor	Percent contribution to (u <sub>c</sub> ) <sup>2</sup>
m <sub>ash</sub> ; kg	1.093E-3	9E-08	1.0	9E-08	-57368	0.00
f <sub>ad</sub>	0.9075	0.0010	1.0	0.0010	69.09	0.01
r <sub>Sr</sub>	0.838	0.007	1.0	0.007	-74.82	0.52
ε <sub>Sr</sub>	0.675	0.012	1.0	0.012	-92.86	2.36
f <sub>y</sub>	0.490	0.008	1.0	0.008	-17.13	0.03
I <sub>B</sub> ; cpm	5.65	0.12	1.0	0.12	-13.99	5.26
I <sub>B,Bkg</sub> ; cpm	5.05	0.27	1.0	0.27	+13.99	27.15
I <sub>A</sub> ; cpm	9.58	0.15	1.0	0.15	+28.55	37.15
I <sub>A,Bkg</sub> ; cpm	7.09	0.27	1.0	0.13	-28.55	27.49
λ <sub>Sr</sub> ; s <sup>-1</sup>	7.63E-10	8.00E-12	1.0	8.00E-12	1.27E+10	0.02
t <sub>1/2</sub> ; s	2.03E+8	3.60E+3	1.0	3.60E+3	4.78E-8	0.00
a ± u <sub>a</sub> , Bq/kg	62.7 ± 7.2					

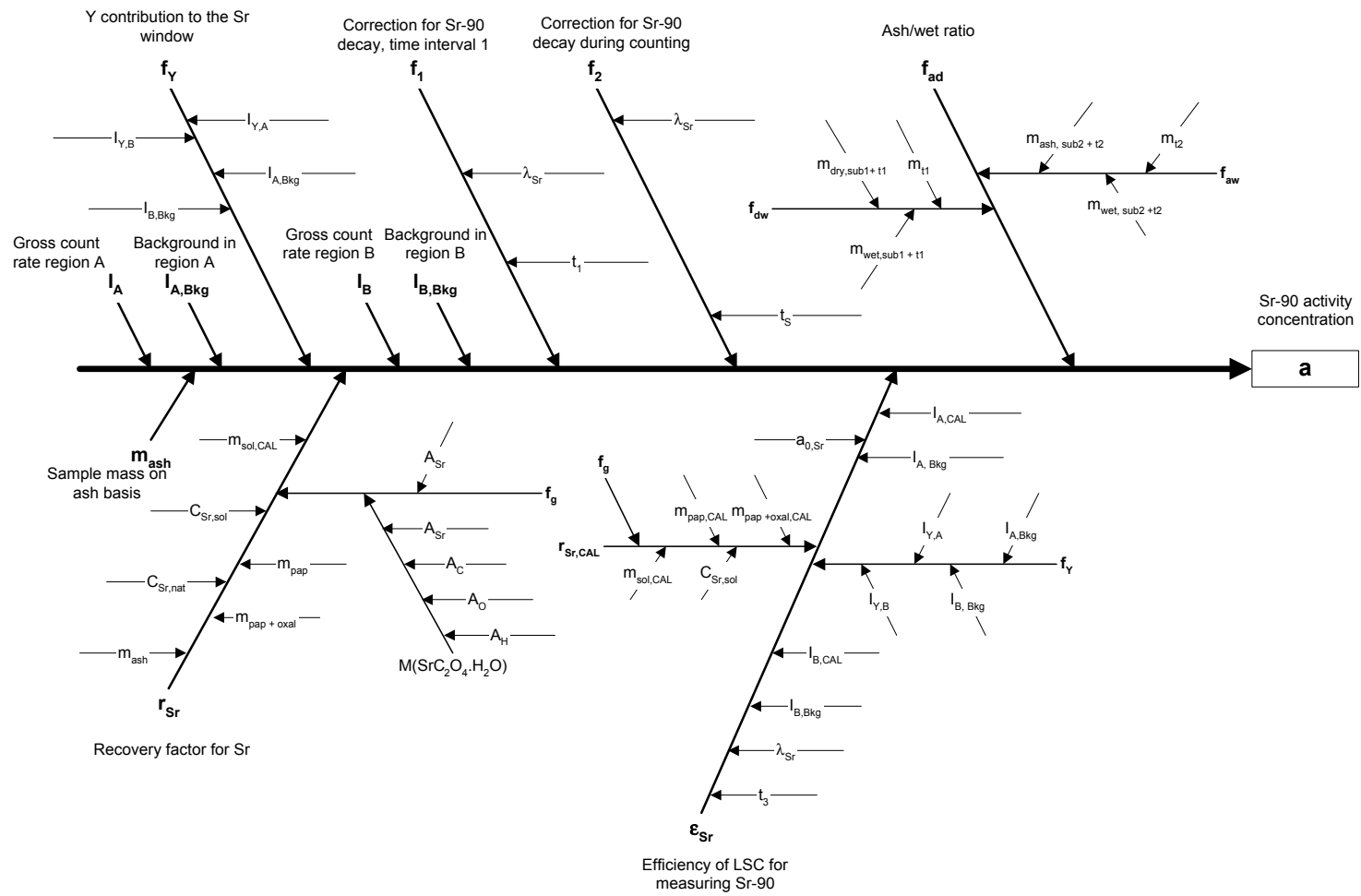
Table 12. Quantifying Uncertainties in IAEA-367 (Reference Date 1/January/1990)

Symbol/ Reference to list	Value of variable	Uncer- tainty	Conversion factor to standard uncertainty	Standard uncertainty (u)	Sensitivity factor	Percent contribution to $(u_c)^2$
$m_{ash}; \text{kg}$	5.029E-03	9E-08	1.0	9E-08	-21408	0.00
$f_{ad}$	0.9287	0.0004	1.0	0.0004	115.92	0.01
$r_{Sr}$	0.586	0.012	1.0	0.012	-183.72	22.34
$\epsilon_{Sr}$	0.675	0.012	1.0	0.012	-159.45	16.82
$f_y$	0.490	0.008	1.0	0.008	-27.82	0.21
$I_{B}; \text{cpm}$	7.97	0.14	1.0	0.14	-4.67	2.00
$I_{B,Bkg}; \text{cpm}$	5.05	0.27	1.0	0.27	+4.67	7.30
$I_{A}; \text{cpm}$	19.82	0.22	1.0	0.22	+9.53	20.67
$I_{A,Bkg}; \text{cpm}$	7.09	0.27	1.0	0.27	-9.53	30.41
$\lambda_{Sr}; \text{s}^{-1}$	7.63E-10	8.00E-12	1.0	8.00E-12	+2.86E+10	0.24
$t_1; \text{s}$	2.66E+8	3.60E+3	1.0	3.60E+3	+8.21E+8	0.00
$a \pm u_a,$ $\text{Bq/kg}$	$107.7 \pm 4.6$					

## REFERENCES

- [1] VAJDA, N., GHODS-ESPHANANI, A., COOPER, E., DANESI, P.R., Determination of Radiostrontium in Soil Samples Using a Crown Ether, J.Radioanal. Nuc.Chem. 162 (2) (1992) 307-323.
- [5] MORENO, J., VAJDA, N., LAROSA, J.J., DANESI, P.R., ZEILLER, E., SINOJMERI, M., Combined Procedure for Determination of  $^{90}\text{Sr}$ ,  $^{241}\text{Am}$  and Pu in soil samples, J. Radioanal. Nucl. Chem. 226 (1-2) (1997) 279-284.
- [6] MORENO, J., LAROSA, J.J., DANESI, P.R., VAJDA, N., BURNS, K., DE REGGE, P., SINOJMERI, M., Determination of  $^{241}\text{Pu}$  by Liquid Scintillation counting in the Combined Procedure for Pu Radionuclides,  $^{241}\text{Am}$  and  $^{90}\text{Sr}$  Analysis in Environmental Samples, Journal of Radioactivity and Radiochemistry 9 (2) (1998) 35-44.
- [7] EURACHEM, "Quantifying Uncertainty in Analytical Measurement", Editor: Laboratory of the Government Chemist Information Services, Teddington (Middlesex) & London (1995). ISBN 0-948926-08-2.
- [8] WINKLER, G., On the Role of Covariances for Uncertainty Estimates in Radioactivity Measurements, Appl. Radiat. Isot. 49 (1998)1153-1157
- [9] KRAGTEN, J., Calculating standard Deviations and Confidence Intervals with a Universally Applicable Spreadsheet Technique, Analyst, Vol. 119 (1994) 2161-2165
- [10] INTERNATIONAL ATOMIC ENERGY AGENCY, AQCS Catalogue edition 2002/2003, page 20.

Figure 1



# TRITIUM ASSAY IN WATER SAMPLES USING ELECTROLYTIC ENRICHMENT AND LIQUID SCINTILLATION SPECTROMETRY

K. ROZANSKI<sup>a</sup>, M. GRÖNING<sup>b</sup>

<sup>a</sup> Faculty of Physics and Nuclear Techniques, University of Mining and Metallurgy, Krakow, Poland

<sup>b</sup> Isotope Hydrology Laboratory, International Atomic Energy Agency, Vienna

## Abstract

Tritium, produced during atmospheric thermonuclear tests, is used as a global transient tracer for studying dynamics in the hydrological cycle. Because of the very low level of radioactivity involved in those studies, the water samples have to be purified from interfering radionuclides and the tritium is enriched by electrolysis before the measurement can be made. In the given example the uncertainty sources related to the distillation and the electrolytic enrichment are identified and quantified, in addition to the usual uncertainty sources for low level radioactivity measurements, such as counting rate, background radiation and decay correction factors. The example elaborates on two case studies involving different levels of tritium in order to illustrate the relative importance of the different sources of uncertainty as a function of the measured radioactivity. It is shown that for low tritium levels the uncertainty on the count rate is dominating, whereas for higher tritium levels the major contribution to the total uncertainty is due to the enrichment parameter.

## 1. INTRODUCTION

In this contribution the most important sources of uncertainty are discussed associated with the determination of the tritium (<sup>3</sup>H) activity concentration in natural water samples using electrolytic enrichment and liquid scintillation spectrometry. This quantity is of interest mainly for hydrological and oceanographic applications of tritium. Tritium has been released into the atmosphere during thermonuclear tests and is being used as a global transient tracer for studying dynamics of the hydrological cycle [1]. Tritium is a  $\beta$ -decaying radionuclide ( $E_{\max}=18.6$  keV), with the recently re-evaluated half-life value equal  $4500 \pm 8$  days [2] corresponding to 12.32 tropical years<sup>1</sup>. This half-life value is in good agreement with that given in the Evaluated Nuclear Structure Data File (mirror site at IAEA: <http://www-nds.iaea.or.at/ensdf/>). The formerly recommended half-life value of 12.43 years [3] should not be used anymore in light of new half-life determinations [4] and the comprehensive re-evaluation of all published experimental tritium half-life determinations [2].

The example is concerned with the specific type of electrolytic enrichment cells developed and being used at the IAEA Isotope Hydrology Laboratory (anodes: stainless steel; cathodes: mild steel; volume 250 ml and 500 ml). The enrichment procedure and the uncertainties involved in this process may vary with the type of the cells used, e.g. higher initial volume of the samples, higher enrichment factor, different design of the cells, different material used for fabrication of the cells, etc. [5,6]. The characteristic feature of the enrichment process is that the samples are processed in batches, usually around 20 samples at time. Technical details of the enrichment system being used at IAEA can be found elsewhere [7-10].

Throughout this contribution the tritium concentration in the analysed sample is reported as tritium activity concentration (Bq/kg). In brackets tritium units (TU) are reported since this quantity is still widely used. One Tritium Unit is defined as:

---

<sup>1</sup> A tropical year is defined as the time between two successive passages of the sun through the vernal equinox: 365.242191 days.

$$1 \text{ TU} \equiv \frac{[{}^3\text{H}]}{[{}^1\text{H}]} = 10^{-18}$$

One TU corresponds to  $0.11919 \pm 0.00021$  Bq/kg. The following numerical constants and parameters were used to convert TU to Bq/kg:

Avogadro constant  $N_A = 6.02214199 (\pm 0.00000047) \cdot 10^{23} \text{ mol}^{-1}$  [11]

molar mass of water  $m_{\text{H}_2\text{O}} = 0.01801528 \text{ kg} \cdot \text{mol}^{-1}$

tritium half-life  $T_{1/2} = 4500 \pm 8$  days [2]

tritium decay constant  $\lambda = (1.5403 \pm 0.0027) \times 10^{-4} \text{ d}^{-1}$

The contribution will not explicitly discuss the uncertainty introduced by changes of the used tritium standard in a laboratory. Effects like a necessary recalculation of reported tritium values due to changes in the applied tritium half-life will be discussed in a separate publication.

## 2. METHOD

The method consist of two major parts: (i) pre-concentration of tritium in the analysed water sample using electrolytic enrichment, and (ii) detection of tritium activity in the concentrated sample using liquid scintillation spectrometry. Each part can be broken down into individual steps (see Table 1). The following formula is used to calculate the tritium activity concentration in the analysed sample:

$$A_T = \frac{N_{SA} \cdot A_{ST}}{N_{ST} \cdot Z_I} \cdot D \quad (1)$$

where:

$N_{SA}$  - net count rate of the sample (cpm)

$N_{ST}$  - net count rate of the standard (cpm)

$A_{ST}$  - activity concentration of the standard (Bq/kg)

$Z_I$  - tritium enrichment factor for the given sample

$D$  - factor taking into account decay of tritium in the sample from the date of measurement to the date of sampling.

Equation (1) is valid under the assumption that the mass of the sample and the standard used for radioactivity measurement are the same, and both are measured in identical conditions (cf. sections 3.6 and 3.7)

Gross and net count rates are defined as:

$$N_{SA} = N_{GSA} - N_B \quad (2)$$

$$N_{ST} = N_{GST} - N_B \quad (3)$$

$$N_{GSA} = \sum_{i=1}^n \frac{N_{GSA,i}}{n} \quad (4)$$

$$N_{GST} = \sum_{i=1}^m \frac{N_{GST,i}}{m} \quad (5)$$

$$N_B = \sum_{i=1}^k \frac{N_{B,i}}{k} \quad (6)$$

where:

$n, m, k$  - number of individual measurements of the sample, standard and background in the given run, respectively;

$N_{GSA,i}, N_{GST,i}, N_{B,i}$  - individual (gross) count rates for the sample, standard and background, respectively, in the given measurement run.

The tritium enrichment factor is given by the formula [8]:

$$Z_I = \exp \left\{ \frac{P \cdot Q}{(W_I - W_F) F} \ln \frac{W_I}{W_F} \right\} \quad (7)$$

where:

$Q$  - number of ampere-hours for the given enrichment run (Ah)

$W_I$  - initial mass of water (including  $\text{OH}^-$  ions) in the given electrolytic cell (g)

$W_F$  - final mass of water (including  $\text{OH}^-$  ions) in the given electrolytic cell (g)

$F$  - Faraday constant  $F = 2.975$  (Ah/g)

$P$  - average enrichment parameter for the given electrolytic cell

$$P = \frac{1}{n} \sum_{i=1}^n P_i \quad (8)$$

where:

$P_i$  - enrichment parameter obtained during spike run  $i$  for the given electrolytic cell

$n$  - number of spike runs for the given cell for which the average enrichment parameter is calculated.

The enrichment parameter is defined by the formula:

$$P_i = \frac{F \cdot (W_{IS} - W_{FS})}{Q} \cdot \frac{\ln(Z_{IS})}{\ln\left(\frac{W_{IS}}{W_{FS}}\right)} \quad (9)$$

where:

$W_{IS}$  - initial mass of water in the given cell during spike run  $i$  (g)

$W_{FS}$  - final mass of water in the given cell during spike run  $i$  (g)

$Z_{IS}$  - enrichment factor for the given cell during spike run  $i$ , derived from the following formula:

$$Z_{IS} = \frac{N_{SPF}}{N_{SPI}} \quad (10)$$

where:

$N_{SPF}$  - net count rate of the spike water from the given cell, enriched during spike run  $i$   
 $N_{SPI}$  - net count rate of the spike water (before enrichment).

Net count rates of the spike water are calculated in an analogous way as regular samples (equations 2,4,6).

The decay correction factor  $D$  is calculated as:

$$D = \exp(-\lambda \cdot t) \quad (11)$$

where:

$\lambda$  - decay constant for tritium equal to  $(1.5403 \pm 0.0027) \times 10^{-4} \text{ d}^{-1}$   
 $t$  - time elapsed between the sampling and the measurement [d].

During routine operation of the electrolytic enrichment system, full spike runs are carried out every 3-4 months. In addition, for each run three cells (different in each consecutive run) are filled up with spike water. Each electrolytic run (24 cells connected in row) consists usually of 19 samples, three spike waters and two tritium-free waters (background samples to control the contamination level – see Appendix 1).

Each measurement run in liquid scintillation spectrometer consists usually of 19 enriched samples, three enriched spike samples, two enriched background samples (tritium-free water), three background samples and three standard samples.

The different steps for the determination of the tritium activity concentration in a sample are shown in Table 1. The influence of the different sources of uncertainty on the combined uncertainty of the result can be seen from a cause and effect diagram (Figure 1).

Table 1. Break down of the method into steps.

Step	Description	Symbol	Sources of uncertainty
1	Distillation of water samples (initial distillation)		Possibility of contamination for samples with low tritium content
2	Weighing of cells before electrolysis	$W_{CE}, W_{CL}, W_I$	Uncertainty of electronic balance, buoyancy forces, mass loss due to gas production in chemical reaction
3	Electrolysis of water samples	$Q$	Uncertainty of amperehour-meter, current leaks
4	Weighing of cells after electrolysis	$W_{CE}, W_{CF}, W_F$	Uncertainty of electronic balance, buoyancy forces
5	Neutralisation and distillation of water samples after enrichment (final distillation)		Possibility of contamination for samples with low tritium content, too high pH of the distilled sample
6	Preparation of the scintillation mixture	$V_W$	Uncertainty of pipettes used, temperature of the preparation process, excessive exposure of the scintillation mixture to sunlight
7	Radioactivity measurement	$N_{SA}, N_{ST}, N_B, N_{SPL}, N_{SPF}$	Random variations of count rates, long-term stability of the spectrometer, static charges, fluorescence
8	Calculating the actual enrichment parameter for sample cell	$P$	Long-term stability of the enrichment system, temperature of the enrichment process, losses of water due to evaporation from the cells, propagation of uncertainties associated with steps 2-7
9	Calculating the enrichment factor for each sample	$Z_I$	Long-term stability of the enrichment system, temperature of the enrichment process, losses of water due to evaporation from the cells, propagation of uncertainties associated with steps 2-8
10	Calculating the decay correction factor	$D$	Uncertainty of the decay constant for tritium
11	Assessing the uncertainty of the used tritium standard and dilution	$A_{ST}$	Uncertainty of the certified high-level standard, dilution procedure
12	Calculating tritium activity concentration in the analysed sample	$A_T$	Propagation of uncertainties associated with steps 2-11

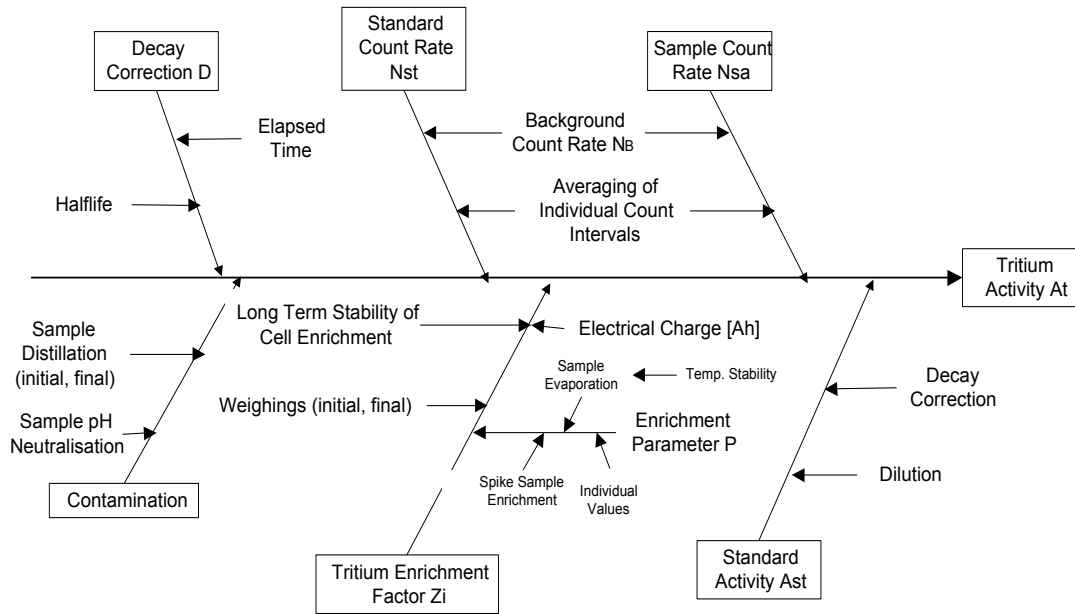


Fig. 1. Fishbone Diagram (Cause and Effect Diagram) showing the influence of the different parameters in Formula (1) on the final result  $A_T$ .

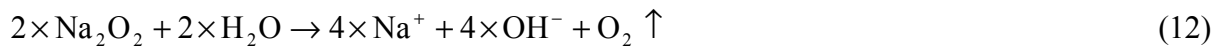
### 3. EVALUATING UNCERTAINTY COMPONENTS

#### 3.1. Distillation of water samples

This step does not contribute directly to the combined standard uncertainty of the measured quantity  $A_T$ . However, it may contribute to the overall contamination level of the measured samples (see Appendix 1).

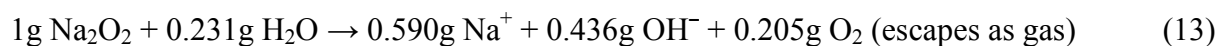
#### 3.2. Weighing of cells and distilled water samples before electrolysis

This step starts with weighing of the empty electrolytic cell ( $W_{CE}$ ). Then, the prescribed amount of solid  $\text{Na}_2\text{O}_2$  ( $W_{\text{Na}_2\text{O}_2}$ ), here 1g, is completely dissolved in about 100g of distilled sample water by shaking in a glass bulb. During the dissolution the  $\text{Na}_2\text{O}_2$  reacts with water according to the following equation:



After complete dissolution of the  $\text{Na}_2\text{O}_2$  additional sample water is filled into the bulb up to a volumetric calibration mark (250ml). The solution is transferred into the cell and the exact weight determined by a further weighing of the filled cell ( $W_{CI}$ ).

According to the above  $\text{Na}_2\text{O}_2$  reaction equation the produced oxygen gas escapes into the air and therefore slightly reduces the weight of the remaining solution. For the dissolution of 1g  $\text{Na}_2\text{O}_2$  in water, the following masses react stoichiometrically:



Therefore the initial mass of the solution is reduced by the loss of oxygen in the reaction (0.205g) or more general by  $0.205 \times W_{\text{Na}_2\text{O}_2}$ . However, at room temperature of 20°C this chemical reaction is quite slow; even 5 minutes after complete dissolution of the  $\text{Na}_2\text{O}_2$  the weight loss due to oxygen generation is only 0.03g, after 30 minutes it is about 0.08g and after 4 hours it amounts to 0.1g. As in the case of the IAEA laboratory, where the cell weighing ( $W_{CI}$ ) takes place 30 minutes after preparation of the solution, this mass loss has to be taken into account as added constant (here 0.08g). Then the initial water weight can be determined by subtracting the weights of the empty cell and of the added  $\text{Na}_2\text{O}_2$ , modified by the mass of lost oxygen. The slow reaction may be caused by intermediate reactions involved, e.g. producing  $\text{H}_2\text{O}_2$ , which later on could dissociate to produce the oxygen gas with some delay.

In addition a buoyancy correction term has to be applied for  $W_{CI}$  to correct for the decrease of specific density of the complete system of cells and water (steel and water) compared to the empty cells and the calibration weight (steel), which results in a slight underestimation of the actual determined mass. In Appendix 3 an example is given for the determination of the actual value of the buoyancy correction term as used below (0.27grams in our example).

The initial mass of water including  $\text{OH}^-$  ( $W_I$ ) is determined as a difference of weights by subtracting the mass of added  $\text{Na}^+$  and that of escaping  $\text{O}_2$ :

$$W_I = (W_{CI} + 0.27) - W_{CE} - (0.59 + 0.205 - 0.08) \times W_{\text{Na}_2\text{O}_2} \quad (14)$$

Typical readings are:

Empty cell ( $W_{CE}$ ): 1457.30g

Cell filled with water and dissolved  $\text{Na}_2\text{O}_2$  ( $W_{CI}$ ): 1707.26g

Net weight of solid  $\text{Na}_2\text{O}_2$  in small container ( $W_{\text{Na}_2\text{O}_2}$ ): 1.00g

Initial mass of water including  $\text{OH}^-$  ( $W_I$ ): 249.52g

The first uncertainty components are due to the variability of weighing by difference in the appropriate region, and the uncertainty associated with the calibration of the balance. The quality control log shows a standard deviation of 0.09g for check weighings of weights up to 2000g, to be taken twice for the two necessary cell weighings. A similar check for the weighing of the  $\text{Na}_2\text{O}_2$  gives a standard uncertainty of 0.01g. The calibration certificate establishes that a weight obtained by difference within the range of 2000g is within 0.1g of the displayed value with 95% confidence. This quantity therefore needs to be divided by 1.96 to give the component of uncertainty as a standard deviation at  $0.1/1.96=0.052\text{g}$ . The numerical factor 0.205 due to the chemical stoichiometric reaction of  $\text{Na}_2\text{O}_2$  with water is assumed having no significant uncertainty. The uncertainty of the time dependent weight loss due to produced oxygen gas out of the solution is estimated to be 0.02g at the time of 30 minutes. The contribution to  $u(W_I)$  resulting from buoyancy forces is estimated to 0.01g, mainly from the uncertainty of the specific density of the cell. The five components are then combined by taking the square root of the sum of their squares to give an uncertainty  $u(W_I)$ :

$$u(W_I) = \sqrt{2 \cdot 0.09^2 + 0.01^2 + 0.052^2 + 0.02^2 + 0.01^2} = 0.14 \text{ g} \quad (15)$$

### 3.3. Electrolysis of water samples

The measured quantity during the electrolysis is the electrical charge flowing through the cells. The used charge is 697 Ah. The instrument used is an electronic amperehour-meter. The certified accuracy of the instrument is 0.5% of the measured charge. Thus:

$$\frac{u(Q)}{Q} = 0.005 \quad (16)$$

### 3.4. Weighing of cells after electrolysis

After completion of the enrichment process a weighing of the cells is performed. The final equivalent mass of the water including  $\text{OH}^-$  ( $W_F$ ) is derived as a difference:

$$W_F = (W_{CF} + 0.02\text{g}) - W_{CE} - 0.59 \times W_{\text{Na}_2\text{O}_2} \quad (17)$$

with 0.02 being the respective buoyancy correction term and 0.59 being the mass fraction of  $\text{Na}^+$  in the initially added  $\text{Na}_2\text{O}_2$ .

Typical readings are:

Cell with water after enrichment, including NaOH ( $W_{CF}$ ): 1470.66g

Final equivalent mass of water including  $\text{OH}^-$  ( $W_F$ ): 12.79g

The standard uncertainty  $u(W_F)$  is calculated in an analogous way as in section 3.2 except that the uncertainty contribution of the oxygen loss is not applicable here. The contribution to  $u(W_F)$  resulting from buoyancy forces is negligible. The standard uncertainty  $u(W_F)$  is equal 0.14g.

The final equivalent mass of water  $W_F$  takes also into account the hydrogen fixed in the  $\text{OH}^-$  and is therefore a hydrogen balance expressed as water equivalent. The mass of total extractable water ( $W_E$ ) is smaller since the total mass of NaOH has to be subtracted from the solution mass as remaining solid residue (1.026 times the mass of initially added  $\text{Na}_2\text{O}_2$ ). It is:

$$W_E = (W_{CF} + 0.02\text{g}) - W_{CE} - 1.026 \times W_{\text{Na}_2\text{O}_2} = 12.35\text{g} \quad (18)$$

### 3.5. Final distillation of the samples

This step does not contribute directly to the combined standard uncertainty of the measured quantity  $A_T$ . However, it may contribute to the overall contamination level in the measured samples (see Appendix 1).

In case of applying a high temperature of more than 150°C to the residual solid NaOH, it will be converted to  $\text{Na}_2\text{O}$  ( $2 \times \text{NaOH} \rightarrow \text{Na}_2\text{O} + \text{H}_2\text{O}$ ), which can potentially increase the extractable water amount  $W_E$  by up to 0.25g.

### 3.6. Preparation of the scintillation mixture

For the measurement of the tritium activity in a liquid scintillation spectrometer a mixture consisting of 10 ml water plus 12 ml scintillation cocktail is prepared in a special polyethylene counting vial for each enriched sample, background and standard. To transfer water to the counting vials a set of calibrated pipettes is used. The quoted accuracy is equal

$\pm 0.015$  ml. Thus, the corresponding standard uncertainty will be equal  $0.015/\sqrt{3}=0.0087$  ml [12]. The standard uncertainty associated with temperature variations during the preparation of the scintillation mixture (within  $3^{\circ}\text{C}$  of the stated operating temperature) is equal to around 0.003 ml. The standard uncertainty associated with repeated deliveries of the same volume of water sample was determined experimentally and is equal 0.0091 ml. Thus, the total standard uncertainty associated with transfer of water (measured samples, standard, background) to the counting vials is equal:

$$u(V_w) = \sqrt{0,0087^2 + 0.003^2 + 0.0091^2} = 0.013 \text{ ml} \quad (19)$$

This component is included in the uncertainty of the net count rates for standard and samples (see next section).

### 3.7. Radioactivity measurement

Typical measurement run consists of 19 enriched samples, three enriched spikes, two enriched tritium-free waters, three tritium-free waters and three standards. All samples are measured sequentially. The spectrometer accumulates usually 45 readings per sample (10-minutes intervals) within a week; 450 minutes being the typical duration for a single measurement run to achieve an acceptable uncertainty of the final result for hydrological purposes. At the IAEA no spike samples are included in the normal measurement run, since the tritium activity of the spike is initially carefully determined in relation to the used tritium standard (see section 3.11) with much higher precision than possible during a normal measurement run.

Non-statistical effects can contribute to the observed count rates. These include fluorescence which might be induced by excessive exposure to UV radiation (e.g. direct sunlight) during preparation of the scintillation mixture, static charges (during transport of counting vials into the counting chamber) and/or pulse surges in the power supply network.

The distribution of individual readings for each sample around the mean value is therefore investigated statistically through calculation of the sample standard deviation:

$$u_x = \sqrt{\frac{\sum_{i=1}^n (N_i - N)^2}{(n-1)}} \quad (20)$$

$N_i$  – individual gross count rates recorded for the given type of sample ( $N_{GSA,i}$ ;  $N_{GST,i}$ ;  $N_{B,i}$ ).

$N$  – average count rate for a sample.

$n$  – number of individual readings.

The outlier rejection procedure is then applied: all individual readings of the given sample for which  $N_i$  differs from  $N$  by more than  $2.8 \times u_x$  are rejected. The final  $N$  and  $u_x$  for each measured sample are then calculated from the remaining accepted readings using eqs.(2-6) and eq. (20), respectively.

The calculated uncertainties of the average (gross) count rates for the samples, standard and the background resulting from counting statistics (obeying Poisson distribution) and stability of the spectrometer are then calculated as a standard deviation of the mean for the population of individual readings after outlier rejection:

$$u_{\bar{x}} = \sqrt{\frac{\sum_{i=1}^n (N_i - \bar{N})^2}{n(n-1)}} \quad (21)$$

The uncertainty values for those count rates at the IAEA Isotope Hydrology Laboratory are derived from routine measurements with Packard ultra-low level counters in its specially designed and concrete shielded underground laboratory. At locations with less shielding the background count rates and the resulting uncertainties may be higher. The uncertainties for the three different types of instruments at the IAEA laboratory vary considerably; this will certainly be also the case for instruments from other manufacturers. The typical uncertainties for the used counter type<sup>2</sup> Packard 2770TR are:

$u(N_{GSA}) = 0.15$  cpm (sample with a gross count rate of 10.06 cpm and a tritium activity concentration equal 3.58 Bq/kg (30 TU)) enriched by a factor of 17;

$u(N_{GST}) = 1.18$  cpm (standard with a gross count rate of 313.6 cpm and a tritium activity concentration equal 2145 Bq/kg ( $1.8 \times 10^4$  TU));

$u(N_B) = 0.045$  cpm (for typical background level of 0.94 cpm for the Packard 2770TR).

The standard uncertainties of the net count rates of the sample and standard are then calculated according to the law of uncertainty propagation. As additional component the uncertainty of the scintillation mixture preparation is included ( $V_W$ ). For  $N_{SA}$  and  $N_{ST}$  the standard uncertainty reads:

$$u(N_{SA}) = N_{SA} \times \sqrt{\left( \frac{\sqrt{u(N_{GSA})^2 + u(N_B)^2}}{N_{SA}} \right)^2 + \left( \frac{u(V_W)}{V_W} \right)^2} = 9.12 \times \sqrt{(0.019)^2 + (0.0013)^2} = 0.157 \text{cpm} \quad (22)$$

$$u(N_{ST}) = N_{ST} \times \sqrt{\left( \frac{\sqrt{u(N_{GST})^2 + u(N_B)^2}}{N_{ST}} \right)^2 + \left( \frac{u(V_W)}{V_W} \right)^2} = 312.7 \times \sqrt{(0.0142)^2 + (0.0013)^2} = 1.25 \text{cpm} \quad (23)$$

It should be noted that the above uncertainties are related only to the counting statistics and to the long-term stability of the spectrometer during the given counting run.

The variability of the background count rate over all runs in a three years' period is in the same range ( $\pm 0.050$  cpm).

### 3.8. Evaluating uncertainty of the average enrichment parameter P

The actual average enrichment parameter for the given cell is calculated as the arithmetic mean of the values of enrichment parameter obtained during the electrolytic runs in which the

---

<sup>2</sup> The use of product names is for identification purposes only and does not constitute endorsement by the International Atomic Energy Agency

cell contained spike water. This value is modified each time when spike water is loaded again to the given cell (the new average is calculated).

The standard uncertainty of the actual value of enrichment parameter is calculated as sample standard deviation of the population of individual enrichment parameters available for the given cell:

$$u(P) = \sqrt{\frac{\sum_{i=1}^n (P_i - P)^2}{n-1}} \quad (24)$$

where  $n$  stands for number of spike runs available for the given cell. The typical standard uncertainty of  $P$  for the cell type discussed in this example (250 ml) is equal:

$$u(P) = 0.006$$

An alternative method can be used to derive the average enrichment parameter  $P$  in cases in which all electrolytic cells show only small differences in the individual enrichment parameters. The average  $P$  value for the cells at the IAEA laboratory is  $0.964 \pm 0.006$ . The average enrichment parameter for a given run can then be calculated from individual values derived from three or more different spike cells. Under this condition the enrichment performance is re-determined for each run individually. Then obviously equation (8) does not apply anymore and has to be modified accordingly. This method is mandatory to be applied in the initial period of the operation of an enrichment system, when yet not enough information is available from only few performed spike runs.

### 3.9. Evaluating uncertainty of the tritium enrichment factor $Z_I$

The standard uncertainty of the enrichment factor  $Z_I$  for the given cell is calculated from eq. (7) using the law of uncertainty propagation:

$$u(Z_I) = \sqrt{\left(\frac{\partial Z_I}{\partial Q}\right)^2 (u(Q))^2 + \left(\frac{\partial Z_I}{\partial P}\right)^2 (u(P))^2 + \left(\frac{\partial Z_I}{\partial W_I}\right)^2 (u(W_I))^2 + \left(\frac{\partial Z_I}{\partial W_F}\right)^2 (u(W_F))^2} \quad (25)$$

By calculating partial derivatives of  $Z_I$  (see Appendix 2) and inserting the appropriate values of the parameters and their estimated standard uncertainties we obtain:

$$u(Z_I) = 0.41$$

The largest contribution to the standard uncertainty  $u(Z_I)$  stems from the uncertainty of the enrichment parameter (around 75%).

### 3.10. Evaluating uncertainty of the decay correction factor $D$

The standard uncertainty of the decay correction factor is calculated using the law of uncertainty propagation applied to eq. (11) (see Appendix 2). For typical delay times between the sampling and the measurement equal six months and a maximum uncertainty of one day, the calculated standard uncertainty is equal:

$$u(D) = 1.6 \times 10^{-4}$$

### 3.11. Uncertainty of the tritium activity concentration of used standard $A_{ST}$

Most laboratories will prepare their tritium laboratory standards from calibrated standards, which are available from several national institutions. As an example here a tritium standard is described as available from the US National Institute of Standards and Technology (NIST), which is used in the IAEA Isotope Hydrology Laboratory. Three NIST tritiated water standards are available with total tritium activities in the range of 3.2 MBq, 105 kBq and 1.1 kBq. According to the certificate the material SRM 4927F (approx. 5ml water) had a tritium activity concentration of  $634.7 \text{ kBq}\cdot\text{g}^{-1} \pm 0.72\%$  (as relative expanded uncertainty with  $k=2$ ) at 3 September 1998.

The dilution of the SRM 4927F hot tritium standard is done gravimetrically by careful weighing of the tritium standard and of tritium free water from a deep artesian well and transfer into one litre glass bottles with greased glass stopcocks. The transfer of the small amounts of tritium standard is done by weighing it in 5ml and 20ml syringes on high precision balances with a resolution of a tenth of a milligram. An intermediate dilution of about 5g standard in 1000g tritium free water is prepared (dilution 1). In a second step this intermediate solution is further diluted by mixing 20g of this dilution into 1000g of tritium free water (dilution 2). Later similar dilution steps are carried out using dilution 2 to produce larger amounts of the actual used laboratory tritium standard (roughly 2145 Bq/kg or 18000 TU) in quantities of about 10 litres and of the laboratory tritium spike (roughly 119 Bq/kg or 1000 TU) in quantities of about 150 litres.

A careful assessment of all uncertainty sources of the weighing procedures and dilutions is carried out according to the procedures outlined in section 3.2 with emphasis of small drift effects of the used balances to reduce the overall uncertainties as much as possible. The uncertainty contribution of the dilution process to prepare low activity laboratory standards can be reduced to a negligible fraction. The procedure is therefore not described in detail here. The combination of those uncertainty components with the stated uncertainty of the SRM 4927F tritium activity (at the one sigma level) results in a uncertainty statement for the used laboratory tritium standard  $A_{ST}$ :

$$\frac{u(A_{ST})}{A_{ST}} = 0.004 \quad (26)$$

A similar uncertainty statement can be derived for the laboratory tritium spike. At the IAEA laboratory the ratio of laboratory standard / laboratory spike is calculated from the dilution procedure and verified by careful measurements. This has the major advantage that further measurements of the spike count rate can be avoided which otherwise would be necessary in each liquid scintillation run.

## 4. EVALUATION OF COMBINED STANDARD UNCERTAINTY

After the discussion of individual uncertainty components in chapter 3 now a last parameter has to be discussed before the combined standard uncertainty of the measured quantity  $A_T$  can be expressed. This is the influence of the tritium activity concentration  $A_T$  of a given sample on the combined standard uncertainty of  $A_T$ . The sample tritium activity concentration combined with the electrolytic tritium enrichment factor is determining the sample net count rate  $N_{SA}$  and its uncertainty. In order to illustrate the influence of the sample activity concentration on the final uncertainty result, two cases will be considered, bracketing the range of natural concentrations of tritium in meteoric waters:

- Case A: The sample tritium activity concentration  $A_T = 0.119$  Bq/kg is near to the detection limit of even highly sensitive analytical procedures, providing a sample net count rate  $N_{SA}=0.304$  cpm with  $u(N_{SA})=0.070$  cpm (at a tritium enrichment of 17);
- Case B: The sample tritium activity concentration  $A_T = 3.58$  Bq/kg is at the higher side of environmental tritium levels, providing a sample net count rate  $N_{SA}=9.12$  cpm with  $u(N_{SA})=0.16$  cpm (with tritium enrichment).

The set of all values for the parameters in eq. (1) is given in Table 2. From these values the combined standard uncertainty of the tritium activity concentration  $A_T$  of a sample can be calculated. In the following, two equivalent methods for that evaluation will be discussed.

In section 4.1 the combined standard uncertainty is expressed using the law of uncertainty propagation by calculating the squares of the partial derivatives of  $A_T$  for the individual parameters, called sensitivity factors, and multiplying them with the squares of the individual parameter uncertainties. The square-root of the sum of these products provides the exact derivation of the combined standard uncertainty. This approach is valid for any functional relationship (also for non-linear equations as in eq. (7) for  $Z_I$ ), but is limited to uncertainties being reasonably small compared to the measured values [13]<sup>3</sup>.

In section 4.2 the combined standard uncertainty is evaluated using the square-root of the sum of squares of relative standard uncertainties for the individual parameters. This is equivalent to the former approach for linear equations of a purely multiplicative form, and provides an easy insight into the overall contribution of each uncertainty component.

The results of both approaches are then discussed in section 4.3 and in the last section some measures are discussed to optimise the measurement precision.

#### 4.1 Derivation of the combined standard uncertainty using partial derivatives

The combined standard uncertainty of the measured quantity  $A_T$  can be expressed by standard uncertainties of the parameters listed in eq. (1) using the law of uncertainty propagation by calculating the partial derivatives of  $A_T$  and inserting the appropriate values of the different parameters:

$$u(A_T) = \sqrt{\left(\frac{\partial A_T}{\partial N_{SA}}\right)^2 (u(N_{SA}))^2 + \left(\frac{\partial A_T}{\partial N_{ST}}\right)^2 (u(N_{ST}))^2 + \left(\frac{\partial A_T}{\partial A_{ST}}\right)^2 (u(A_{ST}))^2 + \left(\frac{\partial A_T}{\partial Z_I}\right)^2 (u(Z_I))^2 + \left(\frac{\partial A_T}{\partial D}\right)^2 (u(D))^2} \quad (27)$$

The partial derivative of  $A_T$  for a particular parameter is also called sensitivity factor for this parameter (see its definition in [12], page 17). The formulas for the partial derivatives are given in Appendix 2. In Table 2 the different parameter values and sensitivity factors are listed for the tritium activity concentrations of cases A and B. The combined standard uncertainty for  $A_T$  is then calculated according to eq. (27).

---

<sup>3</sup> In practice, the law of uncertainty can be safely applied for uncertainties below 10% of the measured values.

Table 2. The summary of uncertainty components for the analysed quantity  $A_T$ , derived from equation (1).

Two cases are reported:  $A_T = 0.119$  Bq/kg (Case A) and  $A_T = 3.58$  Bq/kg (Case B). The fourth column contains calculated combined standard uncertainties for the variables appearing in eq. (1). Evaluation of these uncertainties is discussed in detail in the sections listed in the first column of the table. Sensitivity factors being the partial derivatives of eq. (1) for the given variable are stated in the fourth column. The square of the sensitivity factor multiplied with the square of the combined standard uncertainties of each variable in eq. (27) is used to calculate in the last column the percent contribution to  $u^2(A_T)$  of the uncertainty associated with the given variable.

Reference List	Variable	Value	Combined standard uncertainty	Sensitivity factor	Percent contribution to $u^2(A_T)$
Section 3.6; 3.7	$N_{SA}$	A: 0.304 cpm B: 9.12 cpm	A: 0.070 cpm B: 0.157 cpm	0.392 0.392	A: 99 B: 19
Section 3.6; 3.7	$N_{ST}$	A: 312.7 cpm B: 312.7 cpm	A: 1.2 cpm B: 1.2 cpm	$3.8 \times 10^{-4}$ 0.011	A: negligible B: 0.5
Section 4	$A_{ST}$	A: 2145 Bq/kg B: 2145 Bq/kg	A: 8.6 Bq/kg B: 8.6 Bq/kg	$5.6 \times 10^{-5}$ 0.0017	A: negligible B: 0.5
Section 3.8; 3.9	$Z_I$	A: 17.02 B: 17.02	A: 0.41 B: 0.41	0.007 0.21	A: 1 B: 80
Section 3.10	$D$	A: 0.972 B: 0.972	A: $1.6 \times 10^{-4}$ B: $1.6 \times 10^{-4}$	1.12 3.68	A: negligible B: negligible

**Derivation of the combined standard uncertainty of  $A_T$  using eq. (27):**

**Case A: Sample with tritium activity concentration  $A_T = 0.119$  Bq/kg (1 TU)**

$$u(A_T) = \sqrt{7.4 \times 10^{-4} + 2.3 \times 10^{-7} + 2.3 \times 10^{-7} + 8.4 \times 10^{-6} + 3.7 \times 10^{-10}}$$

$$u(A_T) = 0.0274 \text{ Bq/kg}$$

**Case B: Sample with tritium activity concentration  $A_T = 3.58$  Bq/kg (30 TU)**

$$u(A_T) = \sqrt{3.8 \times 10^{-3} + 2.0 \times 10^{-4} + 2.1 \times 10^{-4} + 7.5 \times 10^{-3} + 3.4 \times 10^{-7}}$$

$$u(A_T) = 0.108 \text{ Bq/kg}$$

#### 4.2 Derivation of the combined standard uncertainty for linear multiplicative equations

In cases of linear equations of a purely multiplicative form, the law of uncertainty propagation can be expressed in a simple form. For  $u(A_T)$  it takes the form of eq. (28).

$$u(A_T) = A_T \cdot \sqrt{\left(\frac{u(N_{SA})}{N_{SA}}\right)^2 + \left(\frac{u(N_{ST})}{N_{ST}}\right)^2 + \left(\frac{u(A_{ST})}{A_{ST}}\right)^2 + \left(\frac{u(Z_I)}{Z_I}\right)^2 + \left(\frac{u(D)}{D}\right)^2} \quad (28)$$

The uncertainty  $u(A_T)$  of the tritium activity is calculated from the relative standard uncertainties of the five parameters in eq. (1). This special form provides an easy insight in the relative importance of the different sources of uncertainty:

The calculated standard uncertainty of the net count rate of the tritium standard is equal  $u(N_{ST}) = 1.25\text{cpm}$ . For the typical count rate of the standard  $N_{ST} = 312.7\text{ cpm}$  we have:

$$\left(\frac{u(N_{ST})}{N_{ST}}\right)^2 = 1.6 \times 10^{-5} \quad (29)$$

The certified relative standard uncertainty of the tritium activity concentration of the standard used is equal  $u(A_{ST})=0.4\%$ . The uncertainty contribution of the dilution process to prepare low activity laboratory standards is generally negligible. Thus, for the current activity concentration of the tritium standard equal  $2145\text{ Bq/kg}$ , we have:

$$\left(\frac{u(A_{ST})}{A_{ST}}\right)^2 = 1.6 \times 10^{-5} \quad (30)$$

For typical values of the enrichment factor  $Z_I = 17$  and  $u(Z_I) = 0.41$  we have:

$$\left(\frac{u(Z_I)}{Z_I}\right)^2 = 5.9 \times 10^{-4} \quad (31)$$

For a delay time between the sampling and the measurement of six months (182 days) the calculated contribution of the standard uncertainty of the decay factor  $D$  is equal:

$$\left(\frac{u(D)}{D}\right)^2 = 2.6 \times 10^{-8} \quad (32)$$

The first term in eq. (27) depends on the tritium activity concentration in the measured sample. Thus, in the following two cases will be considered, bracketing the range of natural concentrations of tritium in meteoric waters:

*Derivation of the combined standard uncertainty of  $A_T$  using eq. (28):*

Case A: Sample with tritium activity concentration  $A_T = 0.119\text{ Bq/kg}$  (1 TU)

For the sample with tritium activity concentration of  $A_T = 0.119\text{ Bq/kg}$ , the net count rate is equal  $N_{SA} = 0.304\text{ cpm}$  and the calculated standard uncertainty  $u(N_{SA}) = 0.0695\text{ cpm}$ . Therefore, the combined relative standard uncertainty of  $N_{SA}$  will be equal:

$$\left(\frac{u(N_{SA})}{N_{SA}}\right)^2 = 5.23 \times 10^{-2} \quad (33)$$

Finally, the approximated combined standard uncertainty of the measured quantity  $A_T$  using eq. (28) is equal:

$$u(A_T) = 0.119 \times \sqrt{5.23 \times 10^{-2} + 1.6 \times 10^{-5} + 1.6 \times 10^{-5} + 5.9 \times 10^{-4} + 2.6 \times 10^{-8}} \quad (34)$$

$$u(A_T) = 0.119 \times 0.230 = 0.027\text{ Bq/kg}$$

*Derivation of the combined standard uncertainty of  $A_T$  using eq. (28):*

Case B: *Sample with tritium activity concentration  $A_T = 3.58$  Bq/kg (30 TU)*

For this sample the net count rate is equal  $N_{SA} = 9.12$  cpm and the calculated standard uncertainty  $u(N_{SA}) = 0.157$  cpm. Thus, the combined relative standard uncertainty of  $N_{SA}$  is equal:

$$\left( \frac{u(N_{SA})}{N_{SA}} \right)^2 = 2.97 \times 10^{-4} \quad (35)$$

Again the combined standard uncertainty of  $A_T$  using eq. (28) is:

$$u(A_T) = 3.58 \times \sqrt{2.97 \times 10^{-4} + 1.6 \times 10^{-5} + 1.6 \times 10^{-5} + 5.9 \times 10^{-4} + 2.6 \times 10^{-8}} \quad (36)$$

$$u(A_T) = 3.58 \times 0.030 = 0.109 \text{ Bq/kg}$$

### 4.3. Comparison of the two uncertainty evaluation methods

As expected the two forms of the law of uncertainty propagation used to calculate the uncertainty budget (section 4.1 and 4.2) provide identical values for the combined standard uncertainty (within the rounding precision of input parameters used). The method using the sum of squared relative uncertainties (section 4.2) is easier to apply, but the method using partial derivatives is the far more universal method independent of the functional relationship of parameters. In particular, it has to be applied to derive the standard uncertainty of the enrichment factor  $Z_I$ , defined by equation (7).

### 4.4. Measures to improve the precision of measurements

The two cases A and B discussed above clearly show that for samples with low tritium concentrations the uncertainty of net count rate of the sample is the dominating component (>99%) of the overall combined uncertainty of  $A_T$  (see table 2). For samples with relatively high tritium concentration the most important component is the uncertainty of the enrichment parameter  $Z_I$  (80%), followed by the net count rate uncertainty (19%).

For samples near to the detection limit therefore the strategy has to be an improvement of the precision of sample and background measurements. For example the increase of the sample and background counting time will reduce the statistical uncertainty from counting statistics. Introduction of an efficient outlier identification routine (by splitting the total measurement time into intervals) may reduce the influence of static charge effects.

For higher tritium activities the careful check and optimisation of the enrichment parameters for the electrolytic cells should be performed. At the IAEA Isotope Hydrology Laboratory such an analysis and corresponding optimisation few years ago resulted in a reduction of that uncertainty component  $u(Z_I)$  by about 40% of its former value.

A check and optimisation of the counting parameters for the used liquid scintillation analyser by a series of test measurements for two background and standard samples should be considered, to find the optimal working point for minimal background count rate and highest tritium detection efficiency, adapted for each laboratory according to their special requirements.

## 5. REPORTING THE RESULTS

According to recommendations of CITAC and EURACHEM [14], the expanded uncertainty should be reported along with the analytical result. The expanded uncertainty is obtained by multiplying the combined standard uncertainty by a numerical factor, called coverage factor, which in most cases will be equal two. This corresponds to confidence limit equal ca. 95%, provided that the results of analysis have normal distribution (for details see [12]).

For the cases discussed above the expanded uncertainty is equal 0.056 Bq/kg and 0.172 Bq/kg, for sample A and B, respectively, using the simple approximation method of section 4.1. The final result of the analysis is then reported as:

Sample A: Tritium activity concentration:  $0.119 \pm 0.055$  Bq/kg  
( $1.00 \pm 0.46$  TU)

Sample B: Tritium activity concentration:  $3.57 \pm 0.22$  Bq/kg  
( $30.0 \pm 1.8$  TU)

It should be noted, however, that in nearly all cases of tritium data reporting for environmental applications only the combined standard uncertainty is reported instead of the expanded uncertainty with a coverage factor.

It is hoped that the given example will encourage more laboratories to undertake the effort to estimate the combined standard uncertainty for their laboratory operation and discontinue the unsatisfactory approach to report just the statistical standard deviation of the counting procedure.

## 6. ADDITIONAL INFORMATION

### 6.1 Evaluation of contamination level in tritium assay of water samples using electrolytic enrichment and liquid scintillation spectrometry.

Specific characteristics of tritium (gas, relatively easily oxidised to HTO), combined with omnipotent presence of water vapour, make problems of contamination during the assay of low-levels of tritium particularly critical. Tritium may originate from various sources: (i) some types of watches with fluorescent dials, (ii) tritium sources used in gas chromatography, (iii) targets used in neutron generators, (iv) medical experiments where tritium is used as a tracer [1].

Measurements of tritium require consideration of various types of contamination (“blanks”), e.g. sampling, storage and analytical blank [15]. The magnitude of the blank will depend strongly on specific procedures of sample handling, on the ambient tritium concentrations during sampling, storage and analysis and on the type of containers used to store the samples before the analysis. Here, only the problems related to analytical blank will be addressed.

The analytical blank is defined as the amount of tritium picked up by the sample during the analytical process in the laboratory (cf. Table 1). The magnitude of this blank should be determined and regularly controlled in each laboratory. The determination of blank is straightforward if concentration of tritium in the laboratory “tritium-free” water is much below the detection limit of the given analytical set-up: the samples of “tritium-free” water are treated as normal samples during all steps of the analytical procedure. If the enriched

“tritium-free” samples are then used as background samples in the radioactivity measurement, the analytical blank is corrected for even without knowing its absolute value. Alternatively, the radioactivity of enriched “tritium-free” water can be measured versus normal (not enriched) background sample and the amount of tritium picked up during the measurement process can be determined. In the analytical system described above two samples of “tritium-free” water are added to each electrolytic run.

In cases when the tritium content in the laboratory “tritium-free” water is comparable with the detection limit, the analytical blank can be estimated by linear extrapolation of the measured tritium concentrations in this water, corresponding to different degree of enrichment, to the value representing zero enrichment [15].

In addition to samples of “tritium-free” water processed in parallel to normal samples, each laboratory should introduce a system of monitoring the tritium levels in the laboratory atmosphere. The simplest way of doing this involves exposing to the laboratory atmosphere ca. 100 ml of tap water in a beaker for a prolonged time period (ca. two weeks needed to reach isotopic equilibrium with the ambient moisture). After this time period, the remaining water in the beaker will have the tritium content close to that of the laboratory atmosphere [16]. Any unexpected increase of tritium level in these samples points to possible contamination problems in the laboratory.

## 6.2 Calculation of individual uncertainty components by the method of partial derivatives and sensitivity factors

The partial derivatives of parameters for equations 7, 11 and 1 are presented here to give illustrative examples how to calculate sensitivity factors and the uncertainty of the parameters  $Z_I$ ,  $D$  and  $A_T$  as defined in the three equations.

### 6.2.1 Tritium enrichment parameter $Z_I$

The equation 7 is defining the tritium enrichment parameter  $Z_I$  with  $Z_I = \text{func}(P, Q, W_I, W_F)$

$$\left\{ \frac{P \cdot Q}{(W_I - W_F) \cdot F} \ln \frac{W_I}{W_F} \right\} \quad (7)$$

With its uncertainty being defined through equation 25 (section 3.9):

$$u(Z_I) = \sqrt{\left(\frac{\partial Z_I}{\partial Q}\right)^2 (u(Q))^2 + \left(\frac{\partial Z_I}{\partial P}\right)^2 (u(P))^2 + \left(\frac{\partial Z_I}{\partial W_I}\right)^2 (u(W_I))^2 + \left(\frac{\partial Z_I}{\partial W_F}\right)^2 (u(W_F))^2} \quad (25)$$

The four partial derivatives can be expressed as follows:

$$\frac{\partial Z_I}{\partial Q} = Z_I \cdot \frac{P}{(W_I - W_F) \cdot F} \cdot \ln\left(\frac{W_I}{W_F}\right)$$

$$\frac{\partial Z_I}{\partial P} = Z_I \cdot \frac{Q}{(W_I - W_F) \cdot F} \cdot \ln\left(\frac{W_I}{W_F}\right)$$

$$\begin{aligned}
\frac{\partial Z_I}{\partial W_I} &= Z_I \cdot \frac{\partial \left( \frac{P \cdot Q}{F} \cdot \left( \frac{\ln(W_I/W_F)}{(W_I - W_F)} \right) \right)}{\partial W_I} \\
&= Z_I \cdot \frac{P \cdot Q}{F} \cdot \left( \frac{\left( \frac{W_I - W_F}{W_I} \right) - \ln \left( \frac{W_I}{W_F} \right)}{(W_I - W_F)^2} \right) \\
\frac{\partial Z_I}{\partial W_F} &= Z_I \cdot \frac{\partial \left( \frac{P \cdot Q}{F} \cdot \left( \frac{\ln(W_I/W_F)}{(W_I - W_F)} \right) \right)}{\partial W_F} \\
&= Z_I \cdot \frac{P \cdot Q}{F} \cdot \left( \frac{\ln \left( \frac{W_I}{W_F} \right) - \frac{(W_I - W_F)}{W_F}}{(W_I - W_F)^2} \right)
\end{aligned}$$

### 6.2.2 Tritium decay correction factor $D$

The equation 11 is defining the tritium decay correction factor  $D$  with  $D = \text{func}(t, T_{1/2})$ :

$$D = \exp(-\lambda \cdot t) \quad (11)$$

with  $\lambda = \frac{\ln 2}{T_{1/2}}$  and with its uncertainty  $u(D)$  defined through the following equation:

$$u(D) = \sqrt{\left( \frac{\partial D}{\partial T_{1/2}} \right)^2 \left( u(T_{1/2}) \right)^2 + \left( \frac{\partial D}{\partial t} \right)^2 \left( u(t) \right)^2}$$

The two partial derivatives can be expressed as:

$$\frac{\partial D}{\partial T_{1/2}} = -\frac{t \cdot \ln 2}{\left( T_{1/2} \right)^2} \cdot \exp \left( -\frac{t \cdot \ln 2}{T_{1/2}} \right)$$

and

$$\frac{\partial D}{\partial t} = -\frac{\ln 2}{T_{1/2}} \cdot \exp \left( -\frac{t \cdot \ln 2}{T_{1/2}} \right)$$

### 6.2.3 Tritium activity concentration $A_T$

Eq. (1) is defining the tritium activity concentration  $A_T$  with  $A_T = \text{func}(N_{SA}, N_{ST}, A_{ST}, Z_I, D)$ :

$$A_T = \frac{N_{SA} \cdot A_{ST}}{N_{ST} \cdot Z_I} \cdot D \quad (1)$$

with its uncertainty being defined through equation 27 (section 4.1):

$$u(A_T) = \sqrt{\left(\frac{\partial A_T}{\partial N_{SA}}\right)^2 (u(N_{SA}))^2 + \left(\frac{\partial A_T}{\partial N_{ST}}\right)^2 (u(N_{ST}))^2 + \left(\frac{\partial A_T}{\partial A_{ST}}\right)^2 (u(A_{ST}))^2 + \left(\frac{\partial A_T}{\partial Z_I}\right)^2 (u(Z_I))^2 + \left(\frac{\partial A_T}{\partial D}\right)^2 (u(D))^2} \quad (27)$$

The five partial derivatives can be expressed as follows:

$$\frac{\partial A_T}{\partial N_{SA}} = \frac{A_{ST} \cdot D}{N_{ST} \cdot Z_I}$$

$$\frac{\partial A_T}{\partial N_{ST}} = -\frac{N_{SA} \cdot A_{ST} \cdot D}{(N_{ST})^2 \cdot Z_I}$$

$$\frac{\partial A_T}{\partial A_{ST}} = \frac{N_{SA} \cdot D}{N_{ST} \cdot Z_I}$$

$$\frac{\partial A_T}{\partial Z_I} = -\frac{N_{SA} \cdot A_{ST} \cdot D}{N_{ST} \cdot (Z_I)^2}$$

$$\frac{\partial A_T}{\partial D} = \frac{N_{SA} \cdot A_{ST}}{N_{ST} \cdot Z_I}$$

### 6.3 Buoyancy Correction Term

The following expression is meant as an example for buoyancy correction and is applicable to correct weights for buoyancy forces when using precision electronic balances. The formulas are based on information provided in the Mettler Toledo Weighing Guide (04/93), p.13 and in the Sartorius Master<sup>PRO</sup> Series Manual, p.22:

$$m = W \frac{1 - \rho_A / 8000 \text{ kg m}^{-3}}{1 - \rho_A / \rho_S} \quad (37)$$

where  $m$  stands for the mass of the sample and  $W$  stands for the weight readout,  $\rho_A$  and  $\rho_S$  are the densities of air and of the sample, with the former being calculated by:

$$\rho_A \cong \frac{0.348444 \cdot p - (0.00252 \cdot t - 0.020582) \cdot h}{273.15 + t} \quad (38)$$

with  $p$  is the air pressure [hPa],  $h$  is the relative air humidity [%] and  $t$  is the temperature [°C].

This formula for the sample mass  $m$  is strictly applicable only to this specific type of balances (8000kg/m<sup>3</sup> is the described density of the weights used during the calibration procedure). Other manufacturers may have used slightly different materials for the weights and, consequently, slightly different numbers may appear in the formula. The manufacturers (Mettler and Sartorius) strongly recommend to use this formula when using verified balances

of accuracy I – see Manual. It is apparent that the correction levels off when the density of the sample is equal  $8000 \text{ kg/m}^3$ . The correction may be positive or negative, depending on the density of the sample. The correction will also depend on the air density (elevation above the sea level).

A specific aspect of weighing the electrolytic cells is that they change significantly their effective density at various stages of the weighing process.

Cells are made of stainless steel (anodes), carbon steel (cathodes) and the top closing part is made of brass and insulating material. The typical density of steel is in the order of  $7.8 - 7.9 \text{ g/cm}^3$ . Brass has a density of  $8.5 - 8.9 \text{ g/cm}^3$ , depending on the specific type. The plastic part has considerably lower density (several  $\text{g/cm}^3$ ). Judging from the proportions of steel, brass and plastic material in the cell, one can safely assume that the overall average material density of the empty cell ( $\rho_m$ ) will be just around  $8.0 \text{ g/cm}^3$ . Consequently, weighing the empty cells on Sartorius Master type balances will not require any buoyancy correction.

The volume of an empty cell of the type discussed in the paper (the material volume!) can be calculated as:

$$V_E = m/\rho_m = 1457.30/8.00 = 182.16 \text{ cm}^3$$

The new, effective (material) volume of the cell after filling up with water will be:

$$V_F = V_E + V_{\text{H}_2\text{O}} = 182.16 + 250 = 432.16 \text{ cm}^3$$

Thus, the effective density of the cell filled up with water sample is:

$$\rho_F = 1707.26/432.16 = 3.95 \text{ g/cm}^3$$

Standard US Atmosphere was assumed with the density of  $\rho_A = 1.2250 \text{ kg/m}^3$  at  $p = 1013.25 \text{ mb}$  (altitude  $H = 0 \text{ m a.s.l}$ ) and a temperature of  $288.15 \text{ K}$  (Handbook of Physics and Chemistry 74<sup>th</sup> Edition, CRC, 1994). For  $H = 1000 \text{ m}$ , the air density drops to  $\rho_A = 1.1117 \text{ kg/m}^3$ .

The mass of the full cell, corrected for buoyancy forces, can be then calculated from eq. 1:

$$m = 1707.26 \times [(1 - 1.2250/8000)/(1 - 1.2250/3950)] = 1707.26 \times 1.00016 = 1707.53$$

Therefore the mass correction term amounts to:

$$\Delta m = 1707.53 - 1707.26 = 0.27 \text{ g}$$

After electrolysis, in the cell remains only ca.  $12.5 \text{ cm}^3$  of the solution. Consequently the final effective (material) volume of the cell will be:

$$V_F = 182.16 + 12.5 = 194.75 \text{ cm}^3$$

at a final effective density of:

$$\rho_F = 1470.26/194.75 = 7.55 \text{ g/cm}^3$$

Since the effective density differs only slightly from 8.00 g/cm<sup>3</sup>, the correction term will be small:

$$\Delta m = 0.02 \text{ g}$$

The table below summarizes the calculated buoyancy correction terms for two types of cells (250ml and 500 ml) and two elevations (0 m and 1000 m a.s.l.).

Type of cells	Elevation H = 0 meters a.s.l		Elevation H = 1000 meters a.s.l.	
	$\Delta m (W_{CI})$ [ g ]	$\Delta m (W_{CF})$ [ g ]	$\Delta m (W_{CI})$ [ g ]	$\Delta m (W_{CF})$ [ g ]
250 ml	0.27	0.02	0.24	0.01
500 ml	0.55	0.03	0.49	0.02

### ACKNOWLEDGEMENT

We would like to thank our colleague Randolph Auer from the IAEA Isotope Hydrology Laboratory for various fruitful discussions and improvements related to the part on sample weighing and electrolysis, as well as Claude Taylor and Walter Krause for suggestions to improve the manuscript.

### REFERENCES

- [1] ROZANSKI, K., GONFIANTINI, R., ARAGUAS-ARAGUAS, L., Tritium in the global atmosphere: distribution patterns and recent trends. *J. Phys. G: Nucl. Part. Phys.* **17** (1991) S523-S536.
- [2] LUCAS, L.L., UNTERWEGER, M.P., Comprehensive review and critical evaluation of the half-life of tritium. *J. Res. Natl. Inst. Stand. Technol.* **105**(4) (2000) 541-549.
- [3] UNTERWEGER, M.P., COURSEY, B.M., SCHIMA, F.J., MANN, W.B., Preparation and calibration of the 1978 National Bureau of Standards tritiated-water standards. *Int. J. Appl. Radiat. Isot.*, **31** (1980) 611.
- [4] UNTERWEGER, M.P., LUCAS, L.L., Calibration of the National Institute of Standards and Technology tritiated-water standards. *Appl. Radiat. Isot.*, **52** (2000) 527-531.
- [5] TAYLOR, C.B., Present status and trends in electrolytic enrichment of low-level tritium in water. In: *Methods of Low-level Counting and Spectrometry*, Proceeding series STI/PUB/592, International Atomic Energy Agency, Vienna, (1981) 303-325.
- [6] HUT, G., Low-level tritium counting facilities: A survey. *Nucl. Instr. and Meth. Phys. Res.*, **B17** (1986) 490-492.
- [7] TAYLOR, C.B., Tritium enrichment of environmental waters by electrolysis: development of cathodes exhibiting high isotopic separation and precise measurement of tritium enrichment factors. *Proc. Int. Conf. Low Radioactivities: Measurements and Applications*. High Tatras, Czechoslovakia, October 1975, Bratislava, (1977) 131-140.
- [8] TAYLOR, C.B., IAEA Isotope Hydrology Laboratory – Technical Procedure Note No.19, International Atomic Energy Agency, Vienna, (1976).
- [9] FLORKOWSKI, T., Low-level tritium assay in water samples by electrolytic enrichment and liquid scintillation counting in the IAEA laboratory, in: *Methods of Low-level Counting and Spectrometry*, International Atomic Energy Agency, Vienna, (1981) 335-353.

- [10] MORGENSTERN, U., Improvement of Reproducibility and Amount of Electrolytic Enrichment at the IAEA Tritium Laboratory. Internal Report of IAEA Isotope Hydrology, IAEA, Vienna, (1998).
- [11] MOHR, P., TAYLOR, B.N., CODATA recommended values of the fundamental physical constants: 1998, Review of Modern Physics 72(2) (2000) 351-495.
- [12] INTERNATIONAL ORGANISATION FOR STANDARDISATION, "Guide to the Expression of Uncertainty in Measurement", First Edition, Geneva (1993)., corrected and reprinted 1995.
- [13] MANDEL, J., The statistical analysis of experimental data, Dover Publications Inc., New York (1984). Corrected republication of the originally work published by Interscience Publishers, New York, 1964.
- [14] EURACHEM, "Quantifying Uncertainty in Analytical Measurement", Editor: Laboratory of the Government Chemist Information Services, Teddington (Middlesex) & London (1995). ISBN 0-948926-08-2.
- [15] WEISS, W., ROETHER, W., BADER, G., Determination of blanks on low-level tritium measurement, Int. J. Appl. Rad. Isot., **27** (1976) 217-225.
- [16] FLORKOWSKI, T., NAWALANY, M., Methods for routine control of tritium in air moisture in the laboratory, Nukleonika, **19** (1974) 331.

# CARBON-14 ASSAY IN WATER SAMPLES USING BENZENE SYNTHESIS AND LIQUID SCINTILLATION SPECTROMETRY

K. ROZANSKI, M. GRÖNING\*

Faculty of Physics and Nuclear Techniques, University of Mining and Metallurgy, Krakow, Poland

\*Isotope Hydrology Section, International Atomic Energy Agency, Vienna

## Abstract

C-14 measurements in water samples are used as a dating tool in old groundwater and oceanic water bodies in hydrology and oceanography studies. A typical sample is strontium carbonate precipitated in the field from the water sample. The chemical preparation involves the release of the carbon dioxide, its reduction to lithium carbide, the hydrolysis to acetylene and finally the conversion to benzene. C-14 is then measured in the benzene by low-level liquid scintillation counting and the radioactivity converted to percent of modern carbon (PMC), the quantity of interest in radiocarbon dating. In addition to the usual uncertainty sources associated with low level radioactivity measurements, the example quantifies the uncertainty related to the chemical conversion steps, the optional dilution with C-14 free benzene and the normalisation (using  $\delta$  C-13 in the sample) of the C-14 content to the PMC primary reference standard. The example illustrates the varying contributions of the different sources of uncertainty as a function of the PMC in the sample by elaborating on two case studies. In all cases the uncertainty on the net count rates is dominating all other sources. For samples with low PMC the uncertainty on the sample count rate is dominating, for samples with higher PMC the uncertainty is shared between the calibration standard and the sample.

## 1. INTRODUCTION

The example discusses uncertainties associated with the determination of the carbon-14 ( $^{14}\text{C}$ ) activity concentration in total dissolved inorganic carbon (TDIC) in natural water samples using benzene synthesis and liquid scintillation spectrometry. This quantity is of interest mainly for hydrology and oceanography where  $^{14}\text{C}$  is being used as a dating tool for old groundwaters and oceanic water masses [1]. Carbon-14 is a  $\beta$ -decaying radioisotope ( $E_{\text{MAX}}=155$  keV) produced by interactions of secondary cosmic radiation with atmospheric nitrogen [2]. The half-life of radiocarbon is equal  $T_{1/2}=5730 \pm 40$  years<sup>2</sup>.

The quantity of primary interest for hydrological applications of radiocarbon is the ratio of the  $^{14}\text{C}$  activity concentration in the analyzed sample (in Bq per gram of carbon) to that of a standard, expressed in per cent. This quantity is called Percent of Modern Carbon (PMC). The uncertainties involved in converting this quantity to groundwater ages depend on specific assumptions with regard to hydrodynamic and geochemical properties of the given aquifer system [3] and will not be discussed here.

## 2. METHOD

The sample, as received in the laboratory, has a form of strontium carbonate precipitated in the field from the water to be analyzed. The analysis of the  $^{14}\text{C}$  activity concentration consists of two major parts: (i) synthesis of benzene from  $\text{CO}_2$  derived from  $\text{SrCO}_3$  precipitate, and (ii) measurement of the  $^{14}\text{C}$  activity in the synthesized benzene. Each part of the analytical procedure can be broken down into individual steps (see Table 1). The following formula is used to calculate the relative  $^{14}\text{C}$  activity concentration in the analysed sample [4]:

---

<sup>2</sup> To maintain continuity in reporting radiocarbon ages it has been agreed that the old value of the  $^{14}\text{C}$  half-life  $T_{1/2} = 5569$  years is used. The ages derived using this value are referred to as conventional radiocarbon ages, BP (Before Present).

$$PMC = \left( \frac{N_{SA}}{F \cdot N_{STN}} \right) \cdot 100 \quad (1)$$

where:

$N_{SA}$  - net count rate of the sample  $C_6H_6$ , corrected for the difference between the actual mass of the sample and that of the standard, normalized for isotope fractionation to a  $\delta^{13}C$  value equal  $-25 \text{ ‰}$  versus VPBD standard,

$N_{STN}$  - net count rate of the standard  $C_6H_6$ , normalized to  $\delta^{13}C = -25 \text{ ‰}$  and corrected for radioactive decay,

$F$  - numerical factor which depends on the type of primary reference material used.

The Primary Modern Reference Standard for  $^{14}C$  dating (100% Modern) has been defined as 95% of the  $^{14}C$  activity concentration of NBS Oxalic Acid I reference material measured in 1950, normalized to  $\delta^{13}C = -19 \text{ ‰}$  versus the VPDB standard. The ratio of the  $^{14}C$  activity concentration of Oxalic Acid II (available) to Oxalic Acid I (exhausted) was established to be equal  $1.2736 \pm 0.0004$  [5]. Thus, if Oxalic Acid II is used, the F factor in eq. (1) is equal  $0.7459 \pm 0.0004$ . For Oxalic Acid I the F factor is equal 0.950. Oxalic Acid II is normalized to  $\delta^{13}C = -25 \text{ ‰}$ .

The average (gross) count rates of the sample, standard and the background for the given measurement run are calculated as:

$$N_{GSA} = \sum_{i=1}^n \frac{N_{GSA,i}}{n} \quad (2)$$

$$N_{GST} = \sum_{i=1}^m \frac{N_{GST,i}}{m} \quad (3)$$

$$N_B = \sum_{i=1}^k \frac{N_{B,i}}{k} \quad (4)$$

where:

$n, m, k$  - number of individual measurements of the sample, standard and background, respectively,

$N_{GSA}, N_{GST}, N_B$  - average count rates of the sample, standard and background, respectively,

$N_{GSA,i}, N_{GST,i}, N_{B,i}$  - individual count rates of the sample, standard and background, respectively.

The average count rate of the sample needs to be corrected for eventual differences between the actual mass of  $C_6H_6$  in the counting vial and the adopted mass of the standard and background sample:

$$N_{KSA} = N_{GSA} \cdot g \quad (5)$$

where  $g$  is defined as:

$$g = \frac{m_s}{m_i} \quad (6)$$

where:

$m_i$  – actual mass of the sample  $C_6H_6$  in the counting vial (g),

$m_s$  – adopted mass of  $C_6H_6$  in the counting vial (g),

$N_{KSA}$  – mass corrected count rate.

The corrected net count rate of the sample is calculated as:

$$N_{NSA} = N_{KSA} - N_B \quad (7)$$

If the sample is diluted with  $^{14}C$ -free benzene (cf. section 3.5), the corrected net count rate of the sample is equal:

$$N_{NSA} = (N_{GSA} - N_B) \cdot d \quad (8)$$

where  $d$  is the dilution factor defined as:

$$d = 1 + \frac{m_d}{m_i} \quad (9)$$

where  $m_d$  is the mass of  $^{14}C$ -free benzene added to the sample.

The net count rate of the standard is calculated as:

$$N_{NST} = N_{GST} - N_B \quad (10)$$

The normalized net count rate of the standard is calculated from the formula:

$$N_{ST} = N_{NST} \cdot \left[ 1 - 2 \cdot 10^{-3} \cdot (25 - \delta^{13}C_{ST}) \right] \quad (11)$$

where  $\delta^{13}C_{ST}$  is the measured  $\delta^{13}C$  value of the  $CO_2$  derived from the standard (Oxalic Acid II). The normalized net count rate of the sample ( $N_{SA}$ ) is calculated in analogous way:

$$N_{SA} = N_{NSA} \cdot \left[ 1 - 2 \cdot 10^{-3} \cdot (25 - \delta^{13}C_{SA}) \right] \quad (12)$$

The normalized net count rate for the standard needs to be corrected for radioactive decay since 1950:

$$N_{STN} = N_{ST} \cdot \exp\{\lambda \cdot (y - 1950)\} \quad (13)$$

where:

$\lambda$  - decay constant for  $^{14}C$  ( $\lambda = 1.24 \times 10^{-4} \text{ y}^{-1}$ )

$y$  - calendar year in which the standard and the sample were measured.

The synthesized samples of  $C_6H_6$  are stored in refrigerator. The storage time should be at least three weeks, to allow for decay of  $^{222}Rn$ , which may be present in the sample. Aliquots of standard and background  $C_6H_6$  are prepared in an analogous way as the analyzed sample. Measurement of  $\beta$ -activity of the samples using liquid scintillation spectrometry is carried out in batches containing usually several samples, one standard and one background sample.

In Table 1 the individual steps of the sample preparation and measurement are stated, whereas in Figure 1 the contribution of individual uncertainty components to the combined standard uncertainty can be seen.

Table 1. Brake-down of the method into steps.

Step	Description	Symbol	Sources of uncertainty
1	Production of $CO_2$ from $SrCO_3$ precipitate		Possibility of contamination for samples with low $^{14}C$ content
2	Synthesis of $C_6H_6$		Possibility of contamination for samples with low $^{14}C$ content, memory effects, impurities in the synthesized $C_6H_6$
3	Weighing of the $C_6H_6$ sample	$m_i$ , ( $m_s$ , $m_d$ )	Uncertainty of electronic balance, evaporation of $C_6H_6$
4	Calculating the correction factor	$g$	Uncertainty of electronic balance, diffusion of $C_6H_6$ in case of leaky counting vials
5	Calculating the dilution factor (required in case of low $C_6H_6$ yield)	$d$	Uncertainty of electronic balance, diffusion of $C_6H_6$ in case of leaky counting vials
6	Radioactivity measurement	$N_{GSA}, N_{GST}$ , $N_B$	Random variations of count rates, long-term stability of the spectrometer, static charges, fluorescence and/or chemiluminescence, presence of $^{222}Rn$
7	Correcting $N_{GSA}$ count rates for the differences in mass of $C_6H_6$	$N_{KSA}$	Uncertainty of the correction factor $g$
8	Calculating the net count rates for the sample and the standard	$N_{NSA}$ , $N_{NST}$	Propagation of uncertainties From steps 6 and 7
9	Correcting $N_{KSA}$ count rates for diluting with $^{14}C$ -free benzene (if required)	$N_{SA}$	Uncertainty of the dilution Factor $d$
10	Normalization of the net count rates for sample and standard to $\delta^{13}C = -25 \text{ ‰}$	$N_{SA}$ , $N_{ST}$	Uncertainty of $\delta^{13}C$ analysis
11	Correcting $N_{ST}$ count rates for the decay of the standard	$N_{STN}$	Uncertainty of the decay correction factor
12	Calculating the Percent of Modern Carbon in the analyzed sample	$PMC$	Propagation of uncertainties from steps 3-11, uncertainty of the F factor

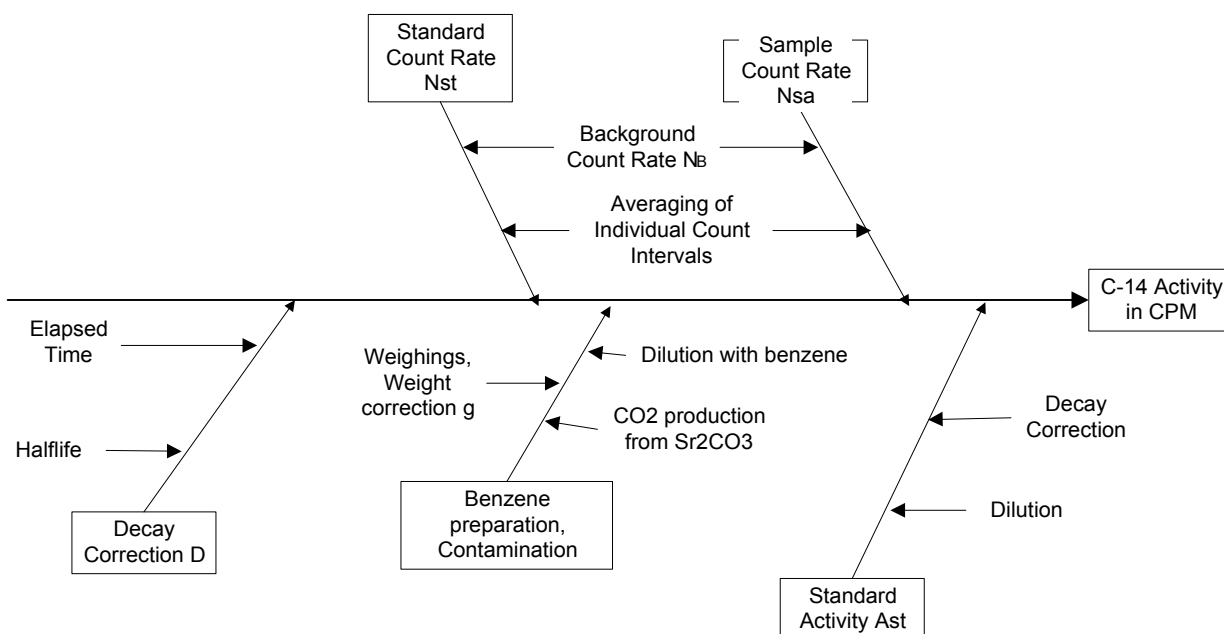


Fig. 1. Fishbone Diagram (Cause and Effect Diagram) showing the influence of the different parameters in Formula (1) and further minor components on the final result CPM.

### 3. EVALUATING UNCERTAINTY COMPONENTS

#### 3.1. Production of CO<sub>2</sub> from SrCO<sub>3</sub> precipitate

This step does not contribute directly to the combined uncertainty of the measured quantity PMC. However, it may increase this uncertainty in case of accidental partial loss of CO<sub>2</sub> and any required additional dilution step, and/or in case of leaks in the preparation line leading to contamination of the produced CO<sub>2</sub> with atmospheric carbon dioxide.

#### 3.2. Synthesis of benzene

The process consists of three major steps: (i) production of lithium carbide from the sample CO<sub>2</sub> and metallic lithium, (ii) hydrolysis of lithium carbide to acetylene, and (iii) catalytic synthesis of C<sub>6</sub>H<sub>6</sub> from C<sub>2</sub>H<sub>2</sub>. The process does not contribute directly to the combined uncertainty of the measured quantity PMC. However, if the operational instructions are not strictly observed, several effects may contribute to the combined uncertainty of the PMC value (e.g. low yield of C<sub>6</sub>H<sub>6</sub> leading to an additional dilution step, memory effects, impurities in the synthesized benzene leading to changes of the counting efficiency, and others).

#### 3.3. Weighing of the C<sub>6</sub>H<sub>6</sub> sample

This step involves weighing of the benzene sample in the counting vial. The analyzed sample of C<sub>6</sub>H<sub>6</sub> is transferred from the storage vial to the counting vial, placed directly on the electronic balance. The uncertainty associated with this step is due to the variability of weighing in the appropriate range and the uncertainty associated with the calibration of the balance. The quality control log shows a standard deviation of 1 mg for check weightings of weights matching the range of the actual masses of the samples (between 1g and 3 g). The calibration certificate establishes that a weight obtained is within 1 mg of the displayed value, with 95% confidence. This quantity therefore needs to be divided by 1.96 to give the

component of uncertainty as a standard deviation at  $1/1.96 = 0.52$  mg. These two components are then combined by taking the square root of the sum of their squares to give the standard uncertainty  $m_i$ :

$$u(m_i) = \sqrt{(1^2 + 0.52^2)} = 1.1 \text{ mg}$$

After weighing the  $C_6H_6$  sample in the counting vial, a prescribed amount of an appropriate scintillator is added and the vial is tightly closed. The standard and the background sample are prepared using analogous procedures. Thus:

$$u(m_s) = 1.1 \text{ mg}$$

### 3.4. Calculating the correction factor $g$

The standard uncertainty of the correction factor  $g$  is derived using the law of uncertainty propagation:

$$u(g) = \sqrt{\left(\frac{\partial g}{\partial m_s}\right)^2 \cdot (u(m_s))^2 + \left(\frac{\partial g}{\partial m_i}\right)^2 \cdot (u(m_i))^2} \quad (14)$$

For  $m_i = 2.956$ g and  $m_s = 3.000$ g we have:

$$u(g) = 0.53 \times 10^{-3}$$

### 3.5. Diluting the sample $C_6H_6$ with $^{14}C$ -free benzene (optional)

In cases when the amount of synthesized benzene turns out to be significantly lower than the adopted mass (e.g. 3.000g),  $^{14}C$ -free benzene is added to the sample until the prescribed mass is reached. In this case, the net count rate of the sample needs to be corrected, to account for the dilution.

The mass of the added benzene is calculated as a difference of weights of the sample before and after addition of  $^{14}C$ -free  $C_6H_6$ . The standard uncertainty of the dilution factor is derived from eq. (9) using the law of uncertainty propagation. Assuming that  $m_d = 1.550$ g and  $m_i = 1.450$ g, the dilution factor is equal  $d = 2.069$  and the corresponding standard uncertainty is given by:

$$u(d) = 1.3 \times 10^{-3}$$

### 3.6. Radioactivity measurement

A typical measurement run consists of several analyzed samples, one standard and one background sample. All samples are measured sequentially and the liquid scintillation spectrometer accumulates around 50 readings per sample (total counting time per sample around 2000 minutes).

The standard uncertainty of the measured count rates is calculated as a standard deviation of the mean for the population of individual readings:

$$u_x = \sqrt{\frac{\sum_{i=1}^n (N_i - N)^2}{n(n-1)}} \quad (15)$$

where:

$N_i$  – individual count rates recorded for the given type of sample (i.e.  $N_{GSA,i}$ ;  $N_{GST,i}$ ;  $N_{B,i}$ ).

Typical gross count rates and associated standard uncertainties (in counts per minute) for  $C_6H_6$  samples weighing 3.000g and measured in 7-ml low-potassium glass vials are equal to:

$N_{GSA} = 1.845$  cpm,  $u(N_{GSA}) = 0.031$  cpm (for sample A with PMC = 3.0%)

$N_{GSA} = 24.33$  cpm,  $u(N_{GSA}) = 0.11$  cpm (for sample B with PMC = 100%)

For standard and background samples of the same mass (3.000g), measured in identical conditions as the analyzed sample, the corresponding gross count rates and the standard uncertainties are equal to:

$N_{GST} = 32.23$  cpm,  $u(N_{GST}) = 0.12$  cpm

$N_B = 1.150$  cpm,  $u(N_B) = 0.024$  cpm

Thus, the standard uncertainty of the net count rate of the sample and the standard will be equal to:

$$u(N_{NSA}) = \sqrt{u(N_{GSA})^2 + u(N_B)^2} = \sqrt{(0.031)^2 + (0.024)^2} = 0.039 \text{ cpm (sample A)}$$

$$u(N_{NSA}) = 0.11 \text{ cpm (sample B)}$$

$$u(N_{NST}) = \sqrt{u(N_{GST})^2 + u(N_B)^2} = \sqrt{(0.12)^2 + (0.024)^2} = 0.12 \text{ cpm}$$

If the correction of the gross count rates is required due to a different mass of the sample, the corresponding standard uncertainty can be calculated from eq. (5) using the law of uncertainty propagation. Assuming the correction factor  $g=1.015$  and  $u(g) = 0.53 \times 10^{-3}$ , we obtain:

$$u(N_{KSA}) = \sqrt{(1.015)^2 \times (0.031)^2 + (1.845)^2 \times (0.53 \times 10^{-3})^2} = 0.032 \text{ cpm (sample A)}$$

$$u(N_{KSA}) = 0.11 \text{ cpm (sample B)}$$

If the sample has to be diluted, the standard uncertainty of the corrected net count rate will be calculated from eq. (8) using the law of uncertainty propagation. Assuming the dilution factor  $d=2.069$  and  $u(d)=1.3 \times 10^{-3}$  (cf. section 3.5) we obtain:

$$u(N_{NSA}) = \sqrt{(2.069)^2 \times (0.039)^2 + (0.695)^2 \times (1.3 \times 10^{-3})^2} = 0.081 \text{ cpm (sample A)}$$

$$u(N_{NSA}) = \sqrt{(2.069)^2 \times (0.11)^2 + (23.18)^2 \times (1.3 \times 10^{-3})^2} = 0.22 \text{ cpm (sample B)}$$

Note that the dilution step substantially increases the combined standard uncertainty of the corrected net count rates of the sample.

### 3.7. Normalization of the net count rate of sample and standard

The standard uncertainty associated with the calculation of the normalized net count rate of the sample and the standard can be derived from the law of uncertainty propagation, applied to eq. (13). A typical standard uncertainty of a  $\delta^{13}\text{C}$  determination is equal to  $u(\delta^{13}\text{C}) = 0.1\text{‰}$ . It turns out that for typical values of  $\delta^{13}\text{C}$  the contribution to the standard uncertainty of the net count rates associated with the normalization step is negligible.

### 3.8. Correction for the decay of the standard

Since the standard uncertainty of the decay constant is relatively small ( $\sim 7 \times 10^{-3}$ ), the contribution to the standard uncertainty of the corrected count rate of the standard is negligible. Thus:

$$u(N_{STN}) = u(N_{ST}) = 0.12 \text{ cpm}$$

## 4. EVALUATION OF COMBINED UNCERTAINTY

The combined uncertainty of the derived quantity (PMC) can be expressed by the standard uncertainties of the variables appearing in eq. (1), using the law of uncertainty propagation:

$$u(PMC) = PMC \cdot \sqrt{\left(\frac{u(N_{SA})}{N_{SA}}\right)^2 + \left(\frac{u(N_{STN})}{N_{STN}}\right)^2 + \left(\frac{u(F)}{F}\right)^2} \quad (16)$$

The reported standard deviation of the F factor is 0.0004. Thus we have:

$$\left(\frac{u(F)}{F}\right)^2 = 0.29 \times 10^{-6}$$

The calculated standard uncertainty of the net count rate of the standard, normalized and corrected for decay is equal  $u(N_{STN}) = 0.12 \text{ cpm}$ . For the net count rate of the standard equal 31.08 cpm we have:

$$\left(\frac{u(N_{STN})}{N_{STN}}\right)^2 = 0.15 \times 10^{-4}$$

The first term in eq. (16) depends on the  $^{14}\text{C}$  activity concentration in the measured sample. In the following, two cases bracketing the range of natural concentrations of  $^{14}\text{C}$  in groundwater samples will be calculated:

#### **Case A: Sample with the relative $^{14}\text{C}$ activity concentration PMC = 3 %**

For this sample the net count rate is equal  $N_{NSA} = 0.695 \text{ cpm}$  and the calculated standard uncertainty  $u(N_{SA}) = 0.039 \text{ cpm}$ . Therefore:

$$\left(\frac{u(N_{SA})}{N_{SA}}\right)^2 = 0.32 \times 10^{-2}$$

Finally, the combined standard uncertainty of the measured quantity PMC for sample A is equal:

$$u(PMC) = PMC \cdot \sqrt{0.32 \times 10^{-2} + 0.15 \times 10^{-4} + 0.29 \times 10^{-6}}$$

$$u(PMC) = 0.18 \%$$

**Case B: Sample with relative <sup>14</sup>C activity concentration PMC = 100%**

For this sample the net count rate is equal  $N_{NSA} = 23.18$  cpm and the calculated standard uncertainty  $u(N_{NSA}) = 0.11$  cpm. Therefore:

$$\left( \frac{u(N_{NSA})}{N_{NSA}} \right)^2 = 2.3 \times 10^{-5}$$

The combined standard uncertainty for sample B will be equal:

$$u(PMC) = PMC \cdot \sqrt{0.23 \times 10^{-4} + 0.15 \times 10^{-4} + 0.29 \times 10^{-6}}$$

$$u(PMC) = 0.62 \%$$

Table 2. Summary of uncertainty components for the analyzed quantity *PMC* derived from equation (1).

Two cases are reported: PMC = 3 % (Case A) and PMC = 100 % (Case B). The fourth column in the table contains derived standard uncertainties of the variables appearing in eq. (1). The evaluation of these uncertainties is discussed in detail in the sections listed in the first column of the table. Percent contribution to  $u^2(PMC)$  of the uncertainty associated with the given variable is listed in the last column.

Variable	Value	Standard Uncertainty	Sensitivity Factor	Percent contribution to $u^2(PMC)$
$N_{NSA}$	<b>A: 0.695 cpm</b> <b>B: 23.18 cpm</b>	<b>A: 0.039 cpm</b> <b>B: 0.11 cpm</b>	----	<b>A: 99.5</b> <b>B: 55.4</b>
$N_{STN}$	<b>A: 31.08 cpm</b> <b>B: 31.08 cpm</b>	<b>A: 0.12 cpm</b> <b>B: 0.12 cpm</b>	----	<b>A: 0.5</b> <b>B: 43.7</b>
$F$	<b>A: 0.7459</b> <b>B: 0.7459</b>	<b>A: 0.0004</b> <b>B: 0.0004</b>	----	<b>A: negligible</b> <b>B: 0.9</b>

The two cases discussed above clearly show that for samples with low <sup>14</sup>C concentrations, the uncertainty of the net count rate is the major component contributing to the combined uncertainty of the measured quantity PMC. For samples with a <sup>14</sup>C concentration close to 100 PMC the major contributions to the combined uncertainty are associated with the uncertainty of the net count rates for the sample and the standard.

## 5. REPORTING THE RESULTS

According to recommendations of CITAC and EURACHEM [6], the expanded uncertainty should be reported along with the analytical result. The expanded uncertainty is obtained by multiplying the combined standard uncertainty by a numerical factor, called coverage factor, which in most cases will be equal two. This corresponds to the confidence limit of ca. 95%, provided that the results of analysis are normal distributed.

For the cases discussed above the expanded uncertainty is equal 0.4% and 1.2% for sample A and B, respectively. The final result of the analysis is then reported as:

Sample A: Relative  $^{14}\text{C}$  activity concentration (Percent of Modern Carbon): 3.0 %  
Expanded uncertainty: 0.4%

Sample B: Relative  $^{14}\text{C}$  activity concentration (Percent of Modern Carbon): 100 %  
Standard uncertainty: 1.2%

## REFERENCES

- [1] TAYLOR, R.E., LONG, A., KRA, R. (Eds.) Radiocarbon After Four Decades: An Interdisciplinary Perspective, Springer Verlag, (1992).
- [2] LAL, D., Expected secular variation in the global terrestrial production rate of radiocarbon. In: E. Bard, W.S. Broecker (Eds.) The Last Deglaciation: Absolute and Radiocarbon Chronologies, Springer Verlag (1992) 113-123.
- [3] FONTES, J.Ch., Chemical and isotopic constraints on  $^{14}\text{C}$  dating of groundwater. In: Taylor, R.E., Long, A., Kra, R. (Eds.) Radiocarbon After Four Decades: An Interdisciplinary Perspective, Springer Verlag, (1992) 242-261
- [4] STUIVER, M., POLACH, H.A., Discussion: reporting of  $^{14}\text{C}$  data, Radiocarbon, 19 (1977) 353-363.
- [5] MANN, W.B., An international reference material for radiocarbon dating, Radiocarbon, 25 (1983) 519-527.
- [6] EURACHEM, "Quantifying Uncertainty in Analytical Measurement", Editor: Laboratory of the Government Chemist Information Services, Teddington (Middlesex) & London (1995). ISBN 0-948926-08-2.

# DETERMINATION OF ISOTOPIC CONTENT AND CONCENTRATION OF URANIUM BY MASS SPECTROMETRY

A. VIAN

COGEMA Etablissement de La Hague Laboratory, Beaumont, Hague Cedex, France

## Abstract

The example evaluates the uncertainty sources in the determination of uranium in aqueous solutions by spiking with an isotopic tracer, chemical separation and mass spectrometric analysis of the resulting blend. The example evaluates and quantifies the uncertainties related to consecutive volumetric dilution steps of the sample, the spiking with the isotopic tracer and its characteristics, the mass percentages in the sample and the tracer, the mass spectrometric measurements of the isotopic ratios in the blend, and the physical data. The example provides detailed measurement results, underpinning the quantification of the different sources of uncertainty, and proceeds in a very systematic way through the different steps in the analytical procedure. The partial “combined uncertainty” for the individual steps is documented by intermediary values for the parameters, their individual uncertainties and sensitivity factors, until they are finally propagated into the combined uncertainty. A particular feature of this example is the experimental verification of the combined uncertainty and several of its components by an analysis of variance.

## 1. INTRODUCTION

This example is taken from nuclear fuel reprocessing activities for which accountancy measurements of nuclear materials (uranium and plutonium) are of major importance. A schematic of the flow sheet of a reprocessing plant is given by figure 1 below.

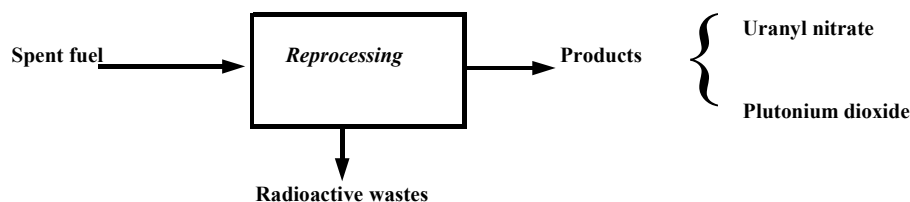


Fig. 1 Simplified reprocessing flow sheet.

Input analyses are performed to supply accountancy calculations with data on mass concentrations and isotopic contents. The analytical method is Isotope Dilution Mass Spectrometry (IDMS); the technique in use is Thermal Ionisation Mass Spectrometry (TIMS). The best precision on isotope ratios is achieved with multicollector detection (figure 2).

## 2. METHOD

### 2.1. Sample

Sample is a dissolution of spent nuclear fuel in nitric acid. The main components of this solution are listed below :

- nitric acid :  $\approx 3 \text{ mol}\cdot\text{l}^{-1}$ ,
- uranium :  $\approx 200 \text{ g}\cdot\text{l}^{-1}$ ,

- plutonium :  $\approx 2 \text{ g}\cdot\text{l}^{-1}$ ,
- fission products :  $10\text{-}20 \text{ g}\cdot\text{l}^{-1}$  of elements,
- minor actinides : Am, Np, Cm.

Isotopic characteristics of uranium and plutonium are listed in tables 1 and 2:

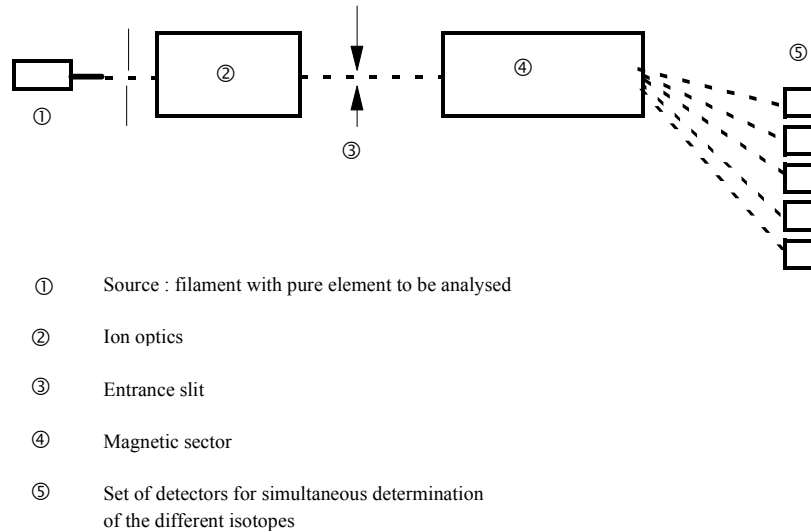


Fig. 2 Schematic view of a multicollector mass spectrometer.

Table 1.  
Isotopic characteristics of uranium

Isotope	Atom %
$^{233}\text{U}$	0
$^{234}\text{U}$	$\approx 0.01 \%$
$^{235}\text{U}$	0,5 - 2.5 %
$^{236}\text{U}$	$\approx 0.3 \%$
$^{238}\text{U}$	98 - 99 %

Table 2.  
Isotopic characteristics of plutonium

Isotope	Sample
$^{238}\text{Pu}$	1 - 3%
$^{239}\text{Pu}$	55 - 60%
$^{240}\text{Pu}$	15 - 25%
$^{241}\text{Pu}$	$\approx 10\%$

## 2.2. Principle of IDMS

IDMS is based on isotope ratio measurements. In this example, for the sake of simplicity, we make two basic assumptions :

- only uranium is to be determined, so that the relevant isotope ratio is

$$R_{3/8} = (\text{U-233})/(\text{U-238}) \quad (1)$$

- the concentration of the spike solution is determined independently from the analyses; it is the case when the spike is purchased from an external supplier, NIST for instance).

The original sample is diluted by a factor of 1000 to 2000 in nitric acid ( $\approx 1 \text{ mol}\cdot\text{l}^{-1}$ ). Uranium is purified from an aliquot of the dilution and the isotopic content is measured by TIMS.

Further, a weighed aliquot of the dilute sample is mixed to a weighed portion of a spike solution. The spike is a solution of uranium with high U-233 content, for which two parameters are certified:

- percent of U-233 relative to total uranium,
- mass concentration of total uranium.

After spiking, uranium is purified by ion exchange separation. The uranium fraction is analysed by TIMS. Uranium concentration in the sample is derived from the variation of the ratio R3/8 between the original and the spiked samples, taking into account the dilution factor. A complete description of the analysis is given in [1].

### 2.3. Steps of the procedure

The steps of the procedure are described in the diagram of figure 3.

### 2.4. Quantities

The uranium concentration  $C(\text{U})_X$  in the sample is given by the following formula (reference [1], § 8.4) :

$$C(\text{U})_X = F \cdot C(\text{U-233})_{\text{sp}} \cdot 100 / G(\text{U-238})_X \cdot (M_8/M_3) \cdot (m_{\text{sp}}/m_X) Q$$

with  $Q = [1 - b \cdot (R_{3/8})_M / (R_{3/8})_{\text{sp}}] \cdot [b \cdot (R_{3/8})_M - b \cdot (R_{3/8})_X ]^{-1}$  (2)

The quantities that are associated to the different steps of the procedure are explained in table 3.

Table 3. Key to symbols and parameters

Step	Description	Symbols
1	Dilution of the sample: dilution factor	F
	* density of nitric acid $\approx 1 \text{ mol}\cdot\text{l}^{-1}$ used as diluent	$\rho$
	* volume of the aliquot of sample for step A of dilution	$v_A$
	* volume of the volumetric flask used for step A of dilution	$V_A$
	* volume of the aliquot dilution A for step B of dilution	$v_B$
	* volume of the volumetric flask used for step B of dilution	$V_B$
2	Concentration of U-233 in the spike solution	$C(\text{U-233})_{\text{sp}}$
	* concentration of total uranium in the spike solution	$C(\text{U})_{\text{sp}}$
	* mass percentage of U-233 in the spike solution	$G(\text{U-233})_{\text{sp}}$
3	Mass percentage of U-238 in the sample	$G(\text{U-238})_x$
4	Spiking	
	* mass of spike solution	$m_{\text{sp}}$
	* mass of sample solution	$m_x$
5	Isotope ratio measurement	
	* atom ratio (U-233)/(U-238) in the spiked sample	$(R3/8)_M$
	* atom ratio(U-233)/(U-238) in the spike material	$(R3/8)_{\text{sp}}$
	* bias correction factor	b
6	Physical data	
	* atomic mass of U-238	$M_8$
	* atomic mass of U-233	$M_3$

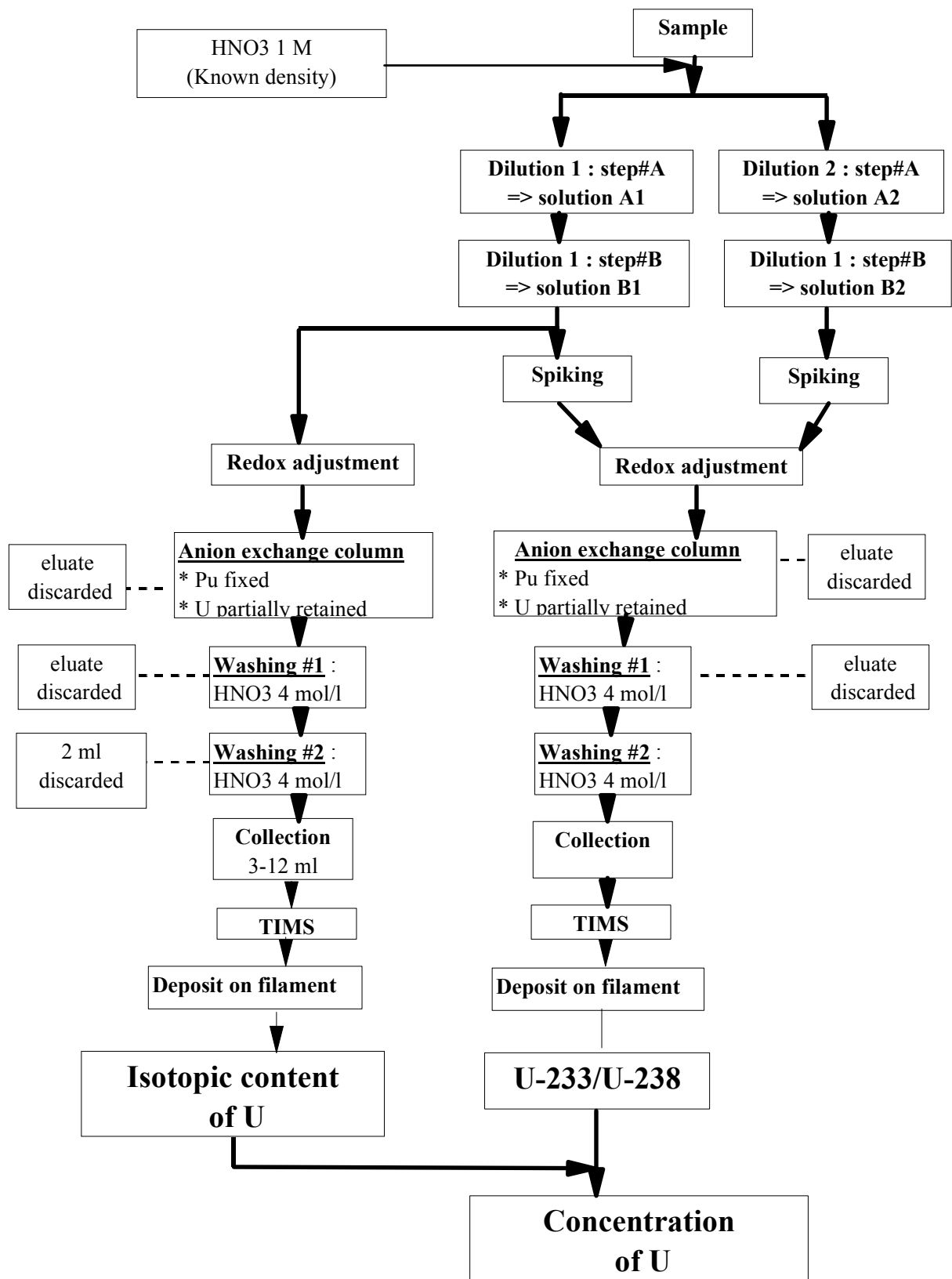


Fig. 3. Flow sheet of uranium concentration and isotopic composition measurement by Isotope Dilution Mass Spectrometry.

The sample does not contain U-233, thus

$$(R_{3/8})_X = 0$$

$$C(U)_X = F \cdot C(U-233)_{sp} \cdot 100 / G(U-238)_X \cdot (M_8/M_3) \cdot (m_{sp}/m_X) \cdot Q_1$$

$$\text{with } Q_1 = [1 - b \cdot (R_{3/8})_M / (R_{3/8})_{sp}] / [b \cdot (R_{3/8})_M] \quad (3)$$

$$C(U)_X = F \cdot C(U-233)_{sp} \cdot 100 / G(U-238)_X \cdot (M_8/M_3) \cdot (m_{sp}/m_X) \cdot \{1/[b \cdot (R_{3/8})_M] - 1/(R_{3/8})_{sp}\} \quad (4)$$

### 3. UNCERTAINTY COMPONENTS

#### 3.1. Step 1: Dilution of the sample

$$F = \rho [(V_A + v_A)/v_A] (V_B/v_B) \quad (5)$$

The density of the diluent (nitric acid  $\approx 1 \text{ mol}\cdot\text{l}^{-1}$ ), is measured with a vibrating tube density-meter. The standard uncertainty is

$$u(\rho) = 0.0001 \text{ g}\cdot\text{cm}^{-3} \quad (6)$$

The aliquot of sample for step A of dilution is taken using a pipette with a nominal delivered volume of 2 ml for deionised water. Calibration data with water cannot be used for sample uptakes of a uranium solution in nitric acid; a calibration is thus performed by replicate uptakes and weighed deliveries of a test solution :

$$* U \approx 250 \text{ g}\cdot\text{l}^{-1}$$

$$* \text{HNO}_3 \approx 3 \text{ mol}\cdot\text{l}^{-1}$$

Table 4 gives the experimental results of the calibration for the 2 ml pipette :

Table 4. 2ml Pipette calibration results

#	V (ml)	#	V (ml)
1	2.0055	11	2.0076
2	2.0064	12	2.0121
3	2.0076	13	2.0108
4	2.0089	14	2.0085
5	2.0118	15	2.0076
6	2.0055	16	2.0114
7	2.0072	17	2.0107
8	2.0080	18	2.0086
9	2.0062	19	2.0105
10	2.0060		
		<b>Mean</b>	<b>2.0085</b>
		<b>S</b>	<b>0.00217</b>

The uncertainty of the sample uptake and delivery has two components :

- uncertainty on volume adjustment and release of solution

$$u_1(v_A) = s = 0.00217 \text{ ml} \quad (7)$$

- uncertainty on certified volume

$$u_2(v_A) = s/\sqrt{19} = 0.00050 \text{ ml} \quad (8)$$

Thus, the standard uncertainty of  $v_A$  is

$$u(v_A) = \sqrt{u^2_1(v_A) + u^2_2(v_A)} = 0.00223 \text{ ml} \quad (9)$$

The 100 ml volumetric flask used for step A of dilution has a certified volume with a tolerance of  $\Delta(V_A) = \pm 0.03$  ml. Volume adjustment is assumed to be triangularly distributed around the nominal value with the range of  $\Delta(V_A) = \pm 0,03$  ml, thus the standard uncertainty is

$$u_1(V_A) = \Delta(V_A) / \sqrt{6} = 0.012 \text{ ml} \quad (10)$$

Assuming a rectangular distribution for the certified volume, the standard uncertainty is

$$u_2(V_A) = \Delta(V_A) / \sqrt{3} = 0.017 \text{ ml} \quad (11)$$

Finally, the standard uncertainty of  $V_A$  is

$$u(V_A) = \sqrt{u^2_1(V_A) + u^2_2(V_A)} = 0.021 \text{ ml} \quad (12)$$

The aliquot of dilution A for step B of dilution is taken using a pipette with a nominal delivered volume of 5 ml for deionised water. As for the 2 ml pipette, a calibration is thus performed by replicate uptakes and weighed deliveries of a test solution :

$$- U \approx 5 \text{ g}\cdot\text{l}^{-1}$$

$$- \text{HNO}_3 \approx 1 \text{ mol}\cdot\text{l}^{-1}$$

Table 5 gives the experimental results of the calibration for the 5 ml pipette.

The uncertainty of the sample uptake and delivery has two components :

- uncertainty on volume adjustment and release of solution

$$u_1(v_B) = s = 0.00285 \text{ ml} \quad (13)$$

- uncertainty on certified volume

$$u_2(v_B) = s/\sqrt{23} = 0.00059 \text{ ml} \quad (14)$$

Finally, the standard uncertainty of  $v_B$  is

$$u(v_B) = \sqrt{u^2_1(v_B) + u^2_2(v_B)} = 0.00291 \text{ ml}$$

Table 5. 5ml Pipette calibration results

#	v (ml)	#	v (ml)
1	5.0016	13	4.9995
2	5.0048	14	4.9986
3	5.0025	15	5.0010
4	4.9999	16	5.0013
5	4.9970	17	5.0065
6	4.9989	18	5.0028
7	5.0004	19	5.0009
8	5.0013	20	5.0046
9	5.0012	21	5.0026
10	5.0016	22	5.0091
11	5.0031	23	4.9988
12	5.0061		
		<b>Mean</b>	<b>5.0019</b>
		<b>s</b>	<b>0.00285</b>

The 100 ml volumetric flask used for step B of dilution has a certified volume with a tolerance of  $\Delta(V_B) = \pm 0,03$  ml. Volume adjustment is assumed to be triangularly distributed around the nominal value with the range of  $\Delta(V_B) = \pm 0,03$  ml, thus the standard uncertainty is

$$u_1(V_B) = \Delta(V_B) / \sqrt{6} = 0.012 \text{ ml} \quad (10)$$

Assuming a rectangular distribution for the certified volume, the standard uncertainty is

$$u_2(V_B) = \Delta(V_B) / \sqrt{3} = 0.017 \text{ ml} \quad (11)$$

Finally, the standard uncertainty of  $V_B$  is

$$u(V_B) = \sqrt{u_1^2(V_B) + u_2^2(V_B)} = 0.021 \text{ ml} \quad (12)$$

The standard uncertainty of F is given by the following formula

$$[u(F)/F] = \sqrt{[u(\rho)/\rho]^2 + [u(V_A)/(V_A + v_A)]^2 + [u(V_B)/(V_B)]^2 + \{u(v_A) \cdot V_A / [v_A \cdot (V_A + v_A)]\}^2 + (u(v_B)/v_B)^2} \quad (17)$$

This relationship is of the form

$$(u_F / F) = \sqrt{\sum [f_{xi} \cdot u(x_i)]^2} \quad (18)$$

It can be calculated using table 6.

Table 6. Calculation of the uncertainty on the sample dilution factor

Parameter	Value x	u	Sensitivity factor f	(f.u) <sup>2</sup>
VA	100	0.021	0.0098	
VB	100	0.021	0.0100	
VA	2.0085	0.00223	0.4881	
VB	5.0019	0.00291	0.1999	
ρ	1.03	0.0001	0.9709	
F	<b>1046</b>	<b>1.33</b>		
<b>u(F)/F</b>		<b>1.27·10<sup>-3</sup></b>		

### 3.2. Step 2: Concentration of U-233 in the spike solution

The supplier certifies the mass concentration of uranium and the mass percentages of U-233 and U-238 relative to total uranium :

- [U] = 197.058 ± 0.149 µg/g (95% confidence level),
- % U-233 = 99.612 ± 0.006
- % U-238 = 0.106 ± 0.002

The mass concentration of U-233 in the spike solution is

$$C(U-233)_{sp} = C(U)_{sp} \cdot G(U-233)_{sp} / 100 = 196.293 \text{ µg/g} \quad (19)$$

The uncertainty on the concentration is

$$u[C(U-233)_{sp}] / C(U-233)_{sp} = \sqrt{(u[C(U)_{sp}] / C(U)_{sp})^2 + (u[G(U)_{sp}] / G(U)_{sp})^2} \quad (20)$$

Table 7. Calculation of the uncertainty of the U-233 concentration in the uranium spike

Parameter	Value x	u	Sensitivity factor f	(f.u) <sup>2</sup>
C(U) <sub>sp</sub>	197.058	0.0745	0.005074648	1.4293E-07
G(U-233) <sub>sp</sub>	99.612	0.003	0.010038951	9.07025E-10
C(U-233) <sub>sp</sub>	<b>196.293</b>	<b>0.0744</b>		1.43837E-07
u[C(U-233) <sub>sp</sub> ] / C(U-233) <sub>sp</sub>		<b>3.79·10<sup>-4</sup></b>		

### 3.3. Step 3: Mass percentage of U-238 in the sample

The mass percentage of U-238 in the sample is experimentally determined.

The standard uncertainty on the mass percentage of U-238 in the sample is estimated by the standard deviation estimator s for the series of 8 replicate measurements which were performed on an input solution.

Table 8. Measurement of the U-238 mass percentage

#	G(U-238) <sub>x</sub>
1	99.172%
2	99.167%
3	99.169%
4	99.169%
5	99.169%
6	99.168%
7	99.172%
8	99.171%
<b>Mean</b>	99.170%
<b>S</b>	0.002%

$$u[G(U238)_x] = s = 0.002 \%$$

$$u[G(U238)_x] / G(U238)_x = 2.02 \cdot 10^{-5}$$

### 3.4. Step 4: Spiking

Spiking is based on weighings:

Table 9. Parameters of the spiking ratio

Step 4.i	Weighing Operation	Mass (g)	
4.0	Empty beaker	m <sub>0</sub>	50
4.1	Beaker +spike	m <sub>1</sub>	51
4.2	Beaker + spike + sample	m <sub>2</sub>	53

$$m_{sp} = m_1 - m_0 \quad (21)$$

$$m_x = m_2 - m_1 \quad (22)$$

The spiking ratio is

$$w = m_{sp} / m_x = (m_1 - m_0) / (m_2 - m_1) \quad (23)$$

The components of the uncertainty on the masses are :

- the precision  $u_1(m_0) = u_1(m_1) = u_1(m_2) = u_1 = 0.1 \text{ mg}$
- the deviation from linearity  $u_2(m_i) = u_2(m_1) = u_2(m_2) = u_2 = 0.3 \text{ mg}$
- the calibration error  $u_3(m_i) = 0.0015 \cdot m_i$

All the weighing operations are performed on the same analytical balance, thus, the errors related to the deviation from linearity, with the uncertainties  $u_2(m_i)$ , are correlated with a correlation coefficient of 1. The calibration errors, with the uncertainties  $u_3(m_i)$ , are correlated in the same way. The *residual errors* due to measurement precision, with the uncertainties  $u_1(m_i)$ , are not correlated.

The uncertainty of w is :

$$u(w)/w = \sqrt{\sum (\partial w / \partial m_i)^2 \cdot u_1^2(m_i) / w^2 + [\sum (\partial w / \partial m_i) \cdot u_2(m_i) / w]^2 + [\sum (\partial w / \partial m_i) \cdot u_3(m_i) / w]^2} \quad (24)$$

with

$$\partial w / \partial m_0 = -1 / (m_2 - m_1) = -w / (m_1 - m_0) = -w / m_{sp} \quad (25)$$

$$\partial w / \partial m_1 = (m_2 - m_0) / (m_2 - m_1)^2 = w \cdot (m_2 - m_0) / [(m_2 - m_1) \cdot (m_1 - m_0)]$$

$$\partial w / \partial m_1 = w \cdot (m_x + m_{sp}) / (m_x \cdot m_{sp}) \quad (26)$$

$$\partial w / \partial m_2 = - (m_1 - m_0) / (m_2 - m_1)^2 = -w / (m_2 - m_1) = -w / m_x \quad (27)$$

thus

$$\Sigma (\partial w / \partial m_i)^2 \cdot u_1^2(m_i) / w^2 = [(1 / m_{sp})^2 + (m_x + m_{sp})^2 / (m_x \cdot m_{sp})^2 + (1 / m_x)^2] \cdot u_1^2 \quad (28)$$

$$\Sigma (\partial w / \partial m_i) \cdot u_2(m_i) / w = [-1 / m_{sp} + (m_x + m_{sp}) / (m_x \cdot m_{sp}) - 1 / m_x] \cdot u_2 = 0 \quad (29)$$

$$\Sigma (\partial w / \partial m_i) \cdot u_3(m_i) / w = \Sigma (\partial w / \partial m_i) \cdot 0,0015 \cdot m_i / w$$

$$\Sigma (\partial w / \partial m_i) \cdot u_3(m_i) / w = 0,0015 \cdot [-m_0 / m_{sp} + m_1 \cdot (m_x + m_{sp}) / (m_x \cdot m_{sp}) - m_2 / m_x] = 0 \quad (30)$$

finally

$$u(w)/w = \sqrt{[(1 / m_{sp})^2 + (m_x + m_{sp})^2 / (m_x \cdot m_{sp})^2 + (1 / m_x)^2] \cdot u_1^2} \quad (31)$$

Table 10. Calculation of the uncertainty of the spiking ratio

Parameter	Value x (g)	u1 (g)	Sensitivity factor f	f·u1	(f·u1) <sup>2</sup>
<b>m0</b>	50	1.00·10 <sup>-4</sup>	-0.5	-0.00005	2.50E-09
<b>m1</b>	52	1.00·10 <sup>-4</sup>	1.5	0.00015	2.25E-08
<b>m2</b>	53	1.00·10 <sup>-4</sup>	-1.0	-0.00010	1.00E-08
<b>m<sub>x</sub></b>	2				
<b>m<sub>sp</sub></b>	1				
<b>w</b>	<b>0.5000</b>	<b>0.0001</b>			3.50E-08
u(w)/w		<b>2.00·10<sup>-4</sup></b>			

### 3.5. Step 5: Isotope ratio measurements

Isotope ratios are combined following the formula :

$$R = 1 / [b \cdot (R_3/8)_M] - 1 / (R_3/8)_{sp} \quad (32)$$

The supplier certifies  $(R_3/8)_{sp} = 937.5 \pm 17.0$  (95% confidence level)

$$u((R_3/8)_{sp}) = 8.50$$

The components of the uncertainty on the measured ratio  $(R_{3/8})_M$  are :

- precision  $u((R_{3/8})_M)$
- mass discrimination and calibration errors  $u(b)$

Precision on the ratio is determined by duplicate measurements for p different samples and evaluation of the within-sample variance ( $s^2$ )

Table 11. Calculation of the “within-sample” variance for isotopic ratio measurements

Sample	(TIMS1)	(TIMS2)
1	0.4815	0.4818
2	0.5934	0.5934
3	0.2814	0.2814
4	0.3928	0.3931
5	0.7627	0.7636
6	0.5956	0.5957
7	0.6187	0.6176
8	0.7207	0.7221
9	0.4582	0.4586
10	0.6384	0.6400
<b>Mean</b>	<b>0.5545</b>	
<b>p</b>	<b>10</b>	
<b>v<sub>1</sub></b>	<b>3.39E-07</b>	
<b>u<sub>1</sub></b>	<b>0.0006</b>	
<b>s%</b>	<b>0.10%</b>	

$$v_1 = \Sigma((\text{TIMS1})_i - (\text{TIMS2})_i)^2 / 2p \tag{34}$$

$$u(R_{3/8})_M = \sqrt{v_1} = 0.10\% \tag{35}$$

Measurements on U-NBS 010 are performed to check that that there is no bias

Table 12. Measurement results for reference material NBS-010

<b>Measurements</b>	<b>R5/8</b>
1	0.010134
2	0.010127
3	0.010140
4	0.010140
5	0.010140
6	0.010157
7	0.010138
8	0.010141
9	0.010150
10	0.010161
11	0.010144
12	0.010126
13	0.010138
14	0.010133
15	0.010124
16	0.010132
17	0.010140
18	0.010143
19	0.010145
20	0.010154
21	0.010143
22	0.010162
23	0.010147
24	0.010144
25	0.010132
26	0.010144
27	0.010139
28	0.010171
29	0.010151
30	0.010141
31	0.010155
32	0.010157
33	0.010140
<b>Mean (R5/8)<sub>meas</sub></b>	<b>0.010143</b>
<b>s</b>	<b>0.000011</b>

The mean value of  $N = 33$  measurements is  $(R5/8)_{\text{meas}} = 0.010143$  ; the estimate of the relative standard deviation of the mean is

$$s'\% = (s/\sqrt{N})/(R5/8)_{\text{meas}} = 0.02\% \quad (36)$$

The reference value is  $(R5/8)_{\text{NBS}} = 0.010140$ . The relative deviation of the experimental mean from the reference value is

$$\Delta\% = [(R5/8)_{\text{meas}} - (R5/8)_{\text{NBS}}] / (R5/8)_{\text{NBS}} = 0.03\% \quad (37)$$

The t parameter of Student's test is

$$t = \Delta\% / s'\% = 1.83 \quad (38)$$

No significant deviation is detected. So, we can assume that there is no bias ( $b = 1$ ):

$$u(b)/b = s'\% = 0.02\% \quad (39)$$

The uncertainty of R is :

$$u(R) = \sqrt{(\partial R/\partial b)^2 \cdot u^2(b) + [\partial R/\partial (R_3/8)_M]^2 \cdot u^2[(R_3/8)_M] + [\partial R/\partial (R_3/8)_{\text{sp}}]^2 \cdot u^2[(R_3/8)_{\text{sp}}]} \quad (40)$$

with

$$\partial R/\partial b = - (R_3/8)_M / [b(R_3/8)_M]^2 = - 1 / [b^2 \cdot (R_3/8)_M] \quad (41)$$

$$\partial R/\partial (R_3/8)_M = - b / [b \cdot (R_3/8)_M]^2 \quad (42)$$

$$\partial R/\partial (R_3/8)_{\text{sp}} = 1 / [(R_3/8)_{\text{sp}}]^2 \quad (43)$$

$$u(R) = \sqrt{1/[b \cdot (R_3/8)_M]^2 \cdot [u(b)/b]^2 + 1/[b \cdot (R_3/8)_M]^2 \cdot [u(R_3/8)_M / (R_3/8)_M]^2 + 1/[(R_3/8)_{\text{sp}}]^2 \cdot [u(R_3/8)_{\text{sp}} / (R_3/8)_{\text{sp}}]^2} \quad (44)$$

Table 13. Calculation of the uncertainty on the parameter R (combined isotopic ratio date)

Parameter	Value x	u/x	Sensitivity factor f	f.u	(f.u) <sup>2</sup>
<b>b</b>	1	2.00E-04	-1.80342651	-3.61E-04	1.30094E-07
$(R_3/8)_M$	0.5545	1.00E-03	-1.80342651	-1.80E-03	3.25235E-06
$(R_3/8)_{\text{sp}}$	937.5	9.07E-03	0.00106667	9.67E-06	9.35304E-11
<b>R</b>	<b>1.8024</b>	<b>0.0018</b>			3.38253E-06
<b>u(R)/R</b>		<b>1.83·10<sup>-3</sup></b>			

### 3.6. .Step 6: Physical data

Atomic masses of U-238 and U-233 are physical constants (table 14)

Table 14. Selected uranium atomic masses

Element	Isotope	Mass
U	233	233.0396
U	238	238.0508

Uncertainties on these data are negligible.

#### 4. COMBINED UNCERTAINTY

Formula (4) is rewritten with the symbols of section 3:

$$C(U)_X = F \cdot C(U-233)_{sp} \cdot 100 / G(U-238)_X \cdot (M_8/M_3) \cdot (m_{sp}/m_X) \cdot [1/[b \cdot (R_3/8)_M - 1/ (R_3/8)_{sp}]]$$

$$C(U)_X = F \cdot C(U-233)_{sp} \cdot 100 / G(U-238)_X \cdot (M_8/M_3) \cdot w \cdot R \quad (4)'$$

With this formulation as a product of variables, the relative combined uncertainty can be expressed simply:

$$u[C(U)_X] / C(U)_X =$$

$$\sqrt{[u(F)/F]^2 + \{u[C(U-233)_{sp}] / C(U-233)_{sp}\}^2 + \{u[G(U-238)_X] / G(U-238)_X\}^2 + [u(w)/w]^2 + [u(R)/R]^2} \quad (45)$$

Table 15. Calculation of the combined uncertainty on the uranium concentration in the sample

Parameter	Unit	Value x	u	u/x	(u/x) <sup>2</sup>
<b>F</b>	<b>g/l</b>	1046	1.33	1.27E-03	1.62E-06
<b>C(U-233)<sub>sp</sub></b>	<b>µg/g</b>	196.293	0.0744	3.79E-04	1.44E-07
<b>G(U-238)<sub>x</sub></b>	<b>percent</b>	99.170	0.002	2.02E-05	4.07E-10
<b>w</b>		0.5000	0.0001	2.00E-04	4.00E-08
<b>R</b>		1.8024	0.0033	1.83E-03	3.35E-06
<b>C(U)<sub>x</sub></b>	<b>g/l</b>	<b>190.60</b>	<b>0.43</b>	<b>2.27E-03</b>	<b>5.15E-06</b>

The expanded uncertainty of the final result is 0.86 g/l (coverage factor k =2).

#### 5. EXPERIMENTAL VERIFICATION

Replicate determinations of uranium concentration are performed according to the described procedure. A t-test shows that the mean difference between the first and second determination is not significantly different from zero. The within sample variance ( $v_{within}$ ) estimates the precision of the analysis.

Table 16. Experimental verification of the uncertainty on the uranium concentration by duplicate analyses.

	[U] <sub>1</sub> g/l	[U] <sub>2</sub> g/l	$\Delta = [U]_1 - [U]_2$	$\Delta^2/2$
	128.58	128.42	0.16	0.0128
	165.31	165.69	-0.38	0.0722
	169.07	169.60	-0.53	0.1405
	188.57	188.04	0.53	0.1405
	189.45	189.40	0.05	0.0012
	186.62	186.09	0.53	0.1405
	186.33	185.72	0.61	0.1861
	184.02	184.88	-0.86	0.3698
	203.25	202.79	0.46	0.1058
	204.86	204.35	0.51	0.1301
	209.26	208.24	1.02	0.5202
	206.21	206.20	0.01	0.0001
	197.93	197.25	0.68	0.2312
	210.38	210.83	-0.45	0.1013
	207.08	206.58	0.5	0.1250
	198.27	198.48	-0.21	0.0220
	191.74	191.72	0.02	0.0002
	202.45	202.54	-0.09	0.0041
	197.39	197.17	0.22	0.0242
	189.18	189.07	0.11	0.0061
$\Delta m$ <sup>(a)</sup>			<b>0.1445</b>	
$s(\Delta)$ <sup>(b)</sup>			<b>0.4729</b>	
N <sup>(c)</sup>			<b>20</b>	
$s(\Delta m)$ <sup>(d)</sup>			<b>0.1057</b>	
t <sup>(e)</sup>			<b>1.37</b>	
$v_{\text{within}}$ <sup>(f)</sup>				<b>0.1167</b>
$s_{\text{within}}$ <sup>(g)</sup>				<b>0.34</b>
[U] <sup>(h)</sup>				<b>190.73</b>
$s\%$ <sup>(i)</sup>				<b>0.18%</b>

(a)  $\Delta m$  = mean of the differences  $\Delta$

(b)  $s(\Delta)$  = estimate of the standard deviation of the differences

(c) N = number of paired comparisons

(d)  $s(\Delta m) = s(\Delta)/\sqrt{N}$  = estimate of the standard deviation of mean of the differences

(e)  $t = \Delta m / s(\Delta m)$

(f)  $v_{\text{within}} = \sum [\Delta^2/2] / N$

(g)  $s_{\text{within}} = \sqrt{v_{\text{within}}}$

(h)  $[U] = ([U]_1 + [U]_2) / 2$  = reported value of U concentration

(i)  $s\% = s_{\text{within}} / [U]$  = relative standard deviation.

We find an experimental relative uncertainty of 0.18%; the estimate of the combined uncertainty is 0.23%. The agreement is satisfactory.

## 6. SUMMARY

Table 17 shows the contribution of the different parameters to the total variance. Rather than listing all individual variables, it appears more interesting to gather those of common origin, as done in equation (4)'

$$C(U)_X = F \cdot C(U-233)_{sp} \cdot 100 / G(U-238)_X \cdot (M_8/M_3) \cdot w \cdot R \quad (4)'$$

The following symbolic representation as a product of modules allows the user to identify clearly the origins of uncertainties and to look for ways of improvements, at need.

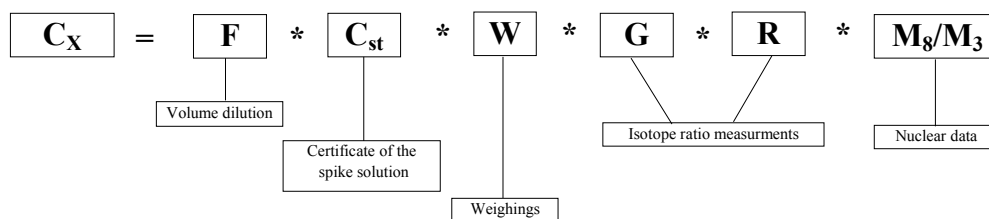


Table 17. Relative contribution of different uncertainty components to the combined uncertainty

Symbols	Value of variable	Uncertainty	Conversion factor	Standard uncertainty	Sensitivity factor	% of variance
<b>R</b>	1.8024	0.0033	1		1.12E+04	65.1%
<b>F</b>	1046	1.33	1	1.33	3.32E-02	31.4%
<b>C(U-233)<sub>sp</sub></b>	196.293	0.0744	1	0.0744	9.43E-01	2.8%
<b>w</b>	0.5000	0.0001	1	0.0001	1.45E+05	0.8%
<b>G(U-238)<sub>x</sub></b>	99.170	0.002	1	0.002	3.69E+00	0.008%
<b>C(U)<sub>x</sub></b>	<b>190.60</b>			<b>0.43</b>		

A fishbone diagram is another summary representation of the links between the sources of uncertainty and their effects (figure 4).

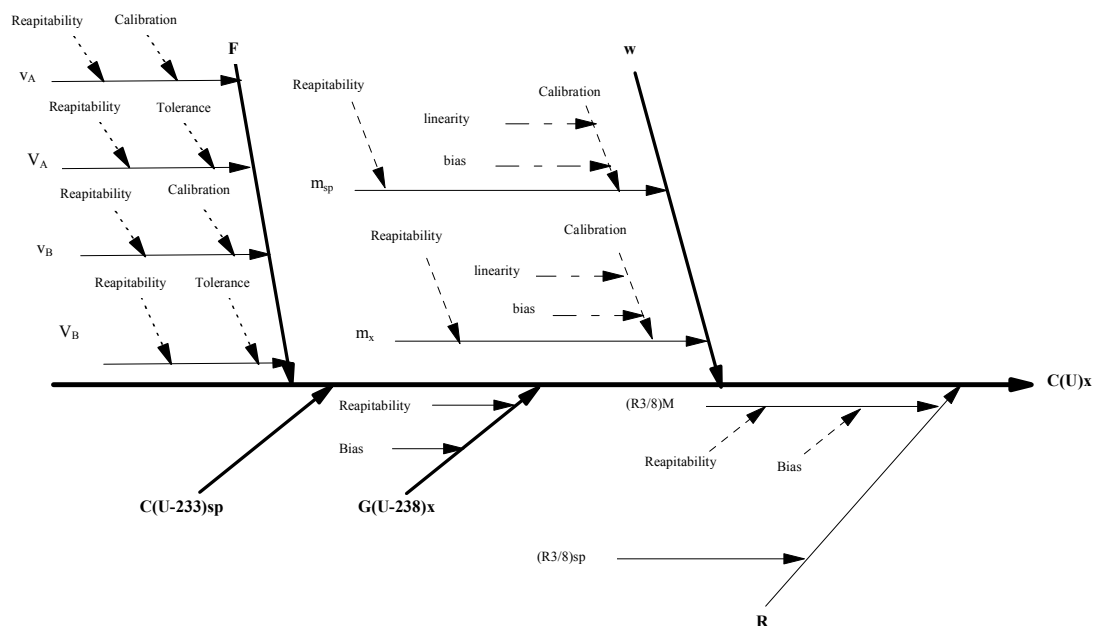


Fig. 4. Fishbone diagram.

#### ACKNOWLEDGEMENT

This IAEA Guide on Quantifying Uncertainty in Nuclear Analytical Measurements is the result of a collaborative effort between a group of experts in nuclear and related analytical techniques and IAEA staff members. The IAEA greatly appreciates the extremely valuable contributions of H. Janszen, G. Kanisch, L. Holmes, J. Kucera, P. Bode, V. Stepanek, W. Maenhaut, K. Rozanski and A. Vian, who started with the elaboration of the draft examples and the quantification of the uncertainty sources, initiating in many cases additional experimental work and careful scientific investigations, followed by several revisions after discussions and exchange of suggestions and recommendations. The essay on the quantification of uncertainty close to the limits of detection by L. Currie is gratefully acknowledged and provides essential background principles and illustrated guidance for low level radioactivity measurements. The continuing support, suggestions and encouragement received from EURACHEM and in particular from A. Williams undoubtedly contributed significantly to the realisation of this work.

#### REFERENCE

- [1] INTERNATIONAL STANDARD ORGANISATION, Determination of isotopic content and concentration of uranium and plutonium in nitric acid solution - Mass spectrometric method, ISO 8299, first edition (1993-06-01).

## LIST OF PARTICIPANTS

- Aigner, H. International Atomic Energy Agency,  
Safeguards Analytical Laboratory, Agency's Laboratories, Seibersdorf,  
A-2444 Seibersdorf, Austria  
Tel.: +43 1 2600 28525  
Fax: +43 1 2600 28577  
E-mail address: H.Aigner@iaea.org
- Bleise, R.A. International Atomic Energy Agency,  
Nutrition & Health Environment Section, Division of Human Health,  
Wagramer Strasse 5, A-1400 Vienna, Austria  
Tel.: +43 1 2600 21659  
Fax: +43 1 2600 7  
E-mail address: A.Bleise@iaea.org
- Burns, K. International Atomic Energy Agency,  
Chemistry Unit, Agency's Laboratories, Seibersdorf,  
A-2444 Seibersdorf, Austria  
Tel.: +43 1 2600 28234  
Fax: +43 1 2600 28222  
E-mail address: K.Burns@iaea.org
- Campbell, M. International Atomic Energy Agency,  
Chemistry Unit, Agency's Laboratories, Seibersdorf,  
A-2444 Seibersdorf, Austria  
Tel.: +43 1 2600 28206  
Fax: +43 1 2600 28222  
E-mail address: M.J.Campbell@iaea.org
- Currie, L.A. Atmospheric Chemistry Group,  
National Institute of Standards and Technology (NIST),  
B364 Chemistry Building,  
MD 20899 Gaithersburg, United States of America  
Tel.: +1 301 216 1134  
Fax: +1 301 975 3919  
E-mail address: lloyd.currie@nist.gov
- Danesi, P.R. International Atomic Energy Agency,  
Agency's Laboratories, Seibersdorf,  
A-2444 Seibersdorf, Austria  
Tel.: +43 1 2600 28200  
Fax: +43 1 2600 28222  
E-mail address: P.R.Danesi@iaea.org
- De Regge, P. International Atomic Energy Agency,  
Chemistry, Physics and Instrumentation Laboratory,  
Agency's Laboratories, Seibersdorf,  
A-2444 Seibersdorf  
Tel.: +43-1-2060-28207  
Fax: +43-1-2060-28222  
E-mail address: P.De\_Regge@iaea.org

- Deron, S. International Atomic Energy Agency,  
Safeguards Analytical Laboratory, Agency's Laboratories, Seibersdorf,  
A-2444 Seibersdorf, Austria  
Tel.: +43 1 2600 28503  
Fax: +43 1 2600 28577  
E-mail address: S.Deron@iaea.org
- Dovlete, C. IAEA Marine Environment Laboratory, Monaco,  
B.P. 800, MC 98012 Monaco Cedex  
Tel.: +377 9797 7272  
Fax: +377 9797 7273  
E-mail address: C.Dovlete@iaea.org
- Fajgelj, A. International Atomic Energy Agency,  
DIR-NAAL's Office, Agency's Laboratories, Seibersdorf,  
A-2444 Seibersdorf, Austria  
Tel.: +43-1-2060-28233  
Fax: +43-1-2060-28222  
E-mail address: A.Fajgelj@iaea.org
- Groening, M. International Atomic Energy Agency,  
Isotope Hydrology Laboratory, Wagrammer Strasse 5,  
A-1400 Vienna, Austria  
Tel.: +43 1 2600 21740  
Fax: +43 1 2600 7  
E-mail address: M.Groening@iaea.org
- Janszen, H. Radioactivity Department, Physikalisch-Technische Bundesanstalt – PTB,  
Bundesallee 100, D-38116 Braunschweig, Germany  
Tel.: +49 531 592 6100  
Fax: +49 531 592 6305  
E-mail address: herbert.janszen@ptb.de
- Kanisch, G. Bundesforschungsanstalt für Fischerei, Institut für Fischereiökologie,  
Wustland 2, D-22589 Hamburg, Germany  
Tel.: +49 40 3190 8640  
Fax : +49 40 3190 8603  
E-mail address: bfa-fisch.ifo@hamburg.bsh.d400.de
- Kucera, J. Nuclear Physics Institute, Academy of Sciences of the Czech Republic,  
CZ-250 68 Rez near Prague, Czech Republic  
Tel.: +420 2 6617 2268  
Fax: +420 2 685 7003  
E-mail address: kucera@ujf.cas.cz
- Maenhaut, W. Institute for Nuclear Sciences, Laboratory of Analytical Chemistry,  
University of Gent, Proeftuinstraat 86, B-9000 Gent, Belgium  
Tel.: +32 9 264 65 96  
Fax: +32 9 264 66 99  
E-mail address: maenhaut@inwchem.rug.ac.be

- Makarewicz, M. International Atomic Energy Agency,  
Chemistry Unit, Agency's Laboratories, Seibersdorf,  
A-2444 Seibersdorf, Austria  
Tel.: +43 1 2600 28347  
Fax: +43 1 2600 28222  
E-mail address: M.Makarewicz@iaea.org
- Markowicz, A. International Atomic Energy Agency,  
Instrumentation Unit, Agency's Laboratories, Seibersdorf,  
A-2444 Seibersdorf, Austria  
Tel.: +43 1 2600 28236  
Fax: +43 1 2600 28222  
E-mail address: M.Markowicz@iaea.org
- Moreno Bermudez, J. International Atomic Energy Agency,  
Chemistry Unit, Agency's Laboratories, Seibersdorf,  
A-2444 Seibersdorf, Austria  
Tel.: +43 1 2600 28269  
Fax: +43 1 2600 28222  
E-mail address: J.Moreno-Bermudez@iaea.org
- Parr, R.M. International Atomic Energy Agency,  
Nutr. & Health Env. Section,  
Wagramer Strasse 5, A-1400 Vienna, Austria  
Tel.: +43-1-2060-21657  
Fax: +43-1-2060-20607  
E-mail address: R.Parr@iaea.org
- Povinec, P. IAEA Marine Environment Laboratory, Monaco,  
Radiometrics Section, NAML, B.P. 800, MC 98012 Monaco Cedex  
Tel.: +377 9797 7272  
Fax: +377 9797 7273  
E-mail address: P.Povinec@iaea.org
- Radecki, Z. International Atomic Energy Agency,  
Chemistry Unit, Agency's Laboratories, Seibersdorf,  
A-2444 Seibersdorf, Austria  
Tel.: +43 1 2600 28226  
Fax: +43 1 2600 28222  
E-mail address: Z.Radecki@iaea.org
- Rozanski, K. Department of Environmental Physics, Faculty of Physics and Nuclear  
Technology, University of Mining and Metallurgy, al. Mickiewicza 30,  
30-059 Krakow, Poland  
Tel.: +48 12 634 1996  
Fax: +48 12 634 0010  
E-mail address: rozanski@novell.ftj.agh.edu.pl
- Smodis, B. International Atomic Energy Agency,  
Nutrition & Health Environment Section, Division of Human Health,  
Wagramer Strasse 5, A-1400 Vienna, Austria  
Tel.: +43 1 2600 21740  
Fax: +43 1 2600 7  
E-mail address: B.Smodis@iaea.org

- Tajani, A. International Atomic Energy Agency,  
Instrumentation Unit, Agency's Laboratories, Seibersdorf,  
A-2444 Seibersdorf, Austria  
Tel.: +43 1 2600 2891  
Fax: +43 1 2600 28222  
E-mail address: A.Tajani@iaea.org
- Vian, A. Division for Quality Control and Accountancy Analysis,  
COGEMA La Hague, F-50444 Beaumont-Hague Cedex, France  
Tel.: +33 2 3302 6798 or 6701  
Fax : +33 2 3302 7583  
E-mail address: Not available
- Walsh, M. International Atomic Energy Agency,  
Industr. Applications and Chemistry Section,  
Division of Physical and Chemical Sciences,  
Wagramer Strasse 5, A-1400 Vienna, Austria  
Tel.: +43 1 2600 21750  
Fax: +43 1 2600 7  
E-mail address: M.Walsh@iaea.org
- Williams, A. EURACHEM,  
19 Hamesmoor Way, Mytchett, GU16 6JG Camberley,  
United Kingdom  
Tel.: +44 1252 542 854  
Fax: +44 1252 542 854  
E-mail address: alex\_williams@camberley.demon.co.uk
- Zeiller, E. International Atomic Energy Agency,  
Chemistry Unit, Agency's Laboratories, Seibersdorf,  
A-2444 Seibersdorf, Austria  
Tel.: +43 1 2600 28220  
Fax: +43 1 2600 28222  
E-mail address: E.Zeiller@iaea.org

### **Observers**

- Bode, Dr. P. Delft University of Technology,  
Interfaculty Reactor Institute,  
Makelweg 15, 2629 JB Delft, Netherlands  
Tel.: +31 15 278 3530  
Fax: +31 15 278 3906  
E-mail address: bode@iri.tudelft.nl
- Stepanek, Dr. V. Nuclear Physics Institute,  
Academy of Sciences of the Czech Republic,  
CZ-250 68 Rez near Prague, Czech Republic  
Tel.: +420 2 7717 2268  
Fax: +420 2 685 7003  
E-mail address: stepanek@ujf.caz.cz